Universidade do Minho
Escola de Engenharia

Inês Alexandra Casaca Lage de Castro

Ohmic Heating as an alternative to conventional thermal treatment

Dissertation for PhD degree in
Chemical and Biological Engineering

Supervision
Doctor António A. Vicente

July 2007

Author: Inês Alexandra Casaca Lage de Castro

e-mail: icastro@cpc.com.pt

Phone: +351 22 995 2036

ID. 10797468

Title of Thesis

Ohmic Heating as an alternative to conventional thermal treatment

Supervision

Doctor António A. Vicente

Year of conclusion: 2007

Dissertation for PhD degree in Chemical and Biological Engineering

University of Minho, July, the 2nd 2007

Acknowledgements

"sempre que o Homem sonha o mundo pula e avança, como bola colorida nas mãos de uma criança"

Rómulo de Carvalho

Um Doutoramento não é mais do que um sonho de fazer o mundo avançar. Nem sempre os avanços mais significativos são os científicos..., são talvez a evolução como pessoa, como colega de trabalho como profissional. Mas nada nem ninguém evolui sozinho! A todos aqueles que me ajudaram nesta etapa o meu sincero agradecimento.

Destaco especialmente,

O meu Orientador e Amigo Doutor António Vicente pela orientação e pela paciência que demonstrou ao longo destes anos.

Ao Prof. Doutor José Teixeira pelo incentivo que sempre me deu.

To Dr. Sudhir Sastry who has kindly received me in his lab and always had time to guide me.

To Lalleg Loghavi who was a true friend during my stay in Ohio.

À Doutora Lucilia Dominues que gentilmente cedeu a estirpe para a realização das fermentações.

À Fundação para a Ciência e Tecnologia pelo financiamento da bolsa.

Aos meus amigos Miguel e Diogo.

E, finalmente, um agradecimento muito especial

Aos meus Pais por serem os melhores Pais do mundo.

Ao Daniel por todo o amor e amizade.

Ao meu filhote Francisco, simplesmente por existir.

À minha Madrinha Bébé e Tia Zim.

Sumário

Este trabalho pretende explorar os efeitos não térmicos relacionados com a tecnologia de aquecimento óhmico. Desta forma, foram abordados diversos temas na tentativa de obter resultados que conduzam, posteriormente, a diversas linhas de investigação relacionadas com a tecnologia de aquecimento óhmico (ou aplicação de campos eléctricos moderados). Os assuntos foram abordados de um ponto de vista essencialmente prático e agrupados em em cinco capítulos principais.

No primeiro capítulo é feita uma revisão bibliográfica genérica sobre a tecnologia de aquecimento óhmico indicando as suas vantagens e desvantagens, modelos matemáticos usados e tipos de equipamentos existentes. Adicionalmente, aborda-se a questão da viabilidade económica desta tecnologia consoante as suas potenciais aplicações e são descritas, com algum detalhe, as actuais aplicações na indústria alimentar já implementadas (ou em fase de teste).

No segundo capítulo, pretendeu-se determinar se existiam efeitos "não térmicos", relacionados com a presença de campos eléctricos moderados, que alterem as cinéticas de inactivação térmica de diversas enzimas. Para tal, foram escolhidas algumas enzimas relevantes na indústria alimentar quer por serem utilizadas como TTI's (*time temperature integrators*) quer por serem necessárias para a produção de alguns alimentos. Estudaram-se as cinéticas de inactivação da lipoxigenase (LOX), polifenoloxidase (PPO), fosfatase alcalina (ALP), pectinase (PEC) e β-galactosidase (β-Gal). Os resultados obtidos indicam que algumas das enzimas (LOX e PPO) são bastante afectadas pela presença de campos elétricos moderados enquanto que as restantes (ALP, PEC e β-Gal) apresentam um efeito menos significativo.

Na terceira secção deste trabalho foi realizado um estudo semelhante aos referido no segundo capítulo mas usando microrganismos alvo. Para tal foram seleccionados microrganismos representativos na indústria alimentar quer pela sua resistência térmica quer pela sua elevada probabilidade de aparecimento em alimentos: ascosporos de *Byssochlamys fulva*, células de *Escherichia coli* e esporos de *Bacillus licheniformis* em matrizes de alimentos, respectivamente, polpa de morango, leita de cabra e compota de cloudberry.

Em todos os microrganismos estudados a presença de um campo eléctrico tem um efeito adicional na perda de viabilidade microbiana, consequentemente, os valores do tempo de redução decimal obtidos (valores *D*) foram, em geral, inferiores quando existia um campo eléctrico. Em suma, a presença de um campo eléctrico diminui o tempo de

processamento térmico necessário à inactivação microbiana, nos alimentos e condições testadas. A extrapolação dos resultados obtidos para outras matrizes ou microrganismos deverá ser realizada com precaução para que a segurança alimentar não seja posta em causa.

A aplicação de campos eléctricos moderados a processos fermentativos constitui o tema sob investigação no quarto capitulo desta tese. Utilizou-se uma estirpe recombinante de levedura produtora de β-Gal extra-celular e com elevado rendimento de produção de etanol e aplicaram-se campos eléctricos (0 a 2 V/cm) continuos ou descontinuos em condições de aerobiose ou anaerobiose. Os resultados experimentais apontam para um efeito pouco significativo quando se trata de condições de anaerobiose mas, na presença de arejamento, obteve-se uma redução considerável da fase de latência (reduzindo o tempo total da fermentação) e um aumento do rendimento em biomassa (cujo aumento varia linearmente com o aumento do campo eléctrico). Por outro lado, e dado que se trata de uma estirpe recombinante, verificou-se uma perda de estabilidade plasmídica aquando do uso de campos eléctricos contínuos. Tal não se verificou quando o campo eléctrico era apenas aplicado na fase inicial da fermentação abrindo novas perspectivas para optimização de processos fermentativos usandos campos eléctricos contínuos ou descontínuos consoante a aplicação pretendida.

A avaliação do perfil óptimo de actividade da enzima excretada durante as fermentações foi igualmente estudado, conluindo-se que a presença do campo eléctrico não altera o perfil óptimo da enzima.

No quinto e último capítulo deste documento efectua-se a determinação do comportamento hidrodinâmico de um aquecedor óhmico à escala piloto e comparam-se os resultados obtidos usando a ferramenta de CFD (*computational fluid dynamics*) com os dados obtidos experimentalmente.

Conluindo, os temas abordados apesar de diversos, destinaram-se a reunir dados para a validação da tecnologia de processamento óhmico com alternativa processual aos tratamentos térmicos convencionais e abrem horizontes para novas aplicações desta tecnologia.

Abstract

This manuscript intends to address "non-thermal" effects associated with using electricity during a thermal process. Being so, a wide range of research areas were focused with the main objective of obtaining results which will be used to develop new research topics related to the use of moderate electric fields. The main themes were approached from a practical point of view and grouped into five main chapters.

The first chapter reviews the main research studies related to ohmic heating technology highlighting the most important vantages and disadvantages of the technology itself, mathematical modeling for process description and available equipments and configurations. Furthermore, the economical viability depending on the specific application is also addressed and actual applications of this technology to the food industry are described in detail.

The following chapter deals with the "non-thermal" effects of electricity in food enzymes, namely the inactivation kinetics of the enzymes when an electric field is present. Several food relevant enzymes were chosen, namely lipoxygenase (LOX), alkaline phosphatase (ALP), polyphenol oxidase (PPO), pectinase (PEC) and β-galactosidase (β-gal). Some of these enzyes are used as TTI's (time temperature integrators) in the food sector. The experimental results indicate that some of the enzymes (LOX and PPO) are significantly affected by the presence of electric fields while the others (PEC, ALP and β-gal) do not seem to be clearly affected.

The third chapter has the main goal of assessing the "electricity effect" on target microorganisms. Being so, microorganisms relevant to food safety (due to high thermal resistance or probability of occurrence) were chosen: *Byssochlamys fulva* ascospores, *Escherichia coli* vegetative cells and spores of *Bacillus licheniformis* and their inactivation kinetics determined in real food matrices, respectively strawberry pulp, goat milk and cloudberry jam.

For all the microorganisms tested the ohmic decimal reduction times (*D*-values) were lower than the ones obtained when using conventional heating. It was possible to conclude that the presence of a moderate electric field during a thermal process reduces the time needed to achieve microbial inactivation (in the conditions and for the microorganisms tested). Care should be taken when extrapolating the results to other food matrices or different microorganisms because food safety can be jeopardized.

The application of moderate electric fields to fermentative processes is the topic under research in the fourth chapter. A recombinant yeast strain with high yields of ethanol production and the ability to ferment lactose and excreting β-Gal was used. Moderate electric fields, ranging from 0 to 2 V/cm, were applied continuously or in specific stages of the fermentation. Aerobic and anaerobic conditions were tested. The results point out to a clear effect of the electric field under aerobic conditions namely in terms of reduction of the lag phase and the increase of biomass yields (which increases linearly with the electric field) thus considerably reducing the total fermentation time. However under anaerobic conditions the "electric" effect was not evident. On the other hand, plasmid stability was affected by the increase of the electric field value when using it continuously but if an electric field was used only during a limited time the results were quite encouraging. The results obtained in this section open a wide range of potential new applications of moderate electric fields technology (ohmic heating).

Furthermore, the temperature and pH profiles of the excreted enzyme were studied and it has been concluded that there were no effects of the electric field on the enzyme characteristics.

In the last chapter, the hydrodynamic behavior of a lab scale ohmic heater was determined and the results compared with the ones obtained from CFD (computational fluid dynamic) computer modelling.

Summing up, the themes addressed were quite wide and aimed at gathering data for the validation of the ohmic heating technology as an alternative processing technology. Moreover, news topics for further research were raised during this work.

Table of Contents

List of General Nomenclature

Symbol

A_{fP} - cross sectional area of parallel fluid [m^2]

A_{fS} - cross sectional area of serial fluid [m^2]

A_p - area of each solid particle [m^2]

A_{pP} - cross sectional area of parallel particles [m^2]

C_A – activity [U]

C_{A0} - initial activity [U]

C_{pf} - fluid specific heat [$J \cdot kg^{-1} \cdot K^{-1}$]

C_{pp} - particle specific heat [$J \cdot kg^{-1} \cdot K^{-1}$]

cp – Specific heat [$J \cdot kg^{-1}\ K^{-1}$]

D - decimal reduction time [s]

D_{conv} - decimal reduction time, under conventional heating conditions [s]

D_{oh} - decimal redution time, under ohmic heating conditions [s]

E_a - activation energy [$J \cdot mol^{-1}$]

F - electric field [$V \cdot m^{-1}$]

H – Hold back [-]

I - current intensity [A]

$\dot{Q}$ - heat generated [$J \cdot s^{-1}$]

$\dot{Q}_f$ - heat generated in the fluid [$J \cdot s^{-1}$]

$\dot{Q}_p$ - heat generated in the particle [$J \cdot s^{-1}$]

qs_{p1} – productivity in β-Gal [$U/g_{\ lactose}/h$]

R - electrical resistance [Ω]

R - radius of the heater tube [m]

Re - Reynolds number [-]

R_{fP} – parallel resistance of fluid [Ω]

R_{fS} - serial resistance of fluid [Ω]

R_{pP} - parallel resistance of particles [Ω]

s - dissolved solids content [$kg \cdot m^{-3}$]

S – Segregation [-]

t_{lag} – lag phase length [h]

t_D – generation time [h]

T_{0p} - initial temperature of the particle [K]

T_{air} - temperature of the air surrounding the walls of the heater [K]

T_f - fluid temperature [K]

T_p - particle temperature [K]

T_{ps} - temperature at the surface of the solid particle [K]

T_{ps} - temperature at the surface of the solid particle [K]

T_{ref} - reference temperature [K]

U - overall heat transfer coefficient [$W \cdot m^{-2} \cdot K^{-1}$]

V – voltage [V]

V_f - volume of the fluid [m^3]

V_p - volume of the particle [m^3]

V_{sys} - volume of the relevant part of the system [m^3]

V_{sys} - volume of the system between the electrodes [m^3]

∇V - voltage gradient [V]

Yx/s – biomassa yield in substrate [$g_{biomass}/g_{lactose}$]

$Yp1/s$ – product yield (ethanol) in substrate [$g_{ethanol}/g_{lactose}$]

$Yp2/s$ – product yield (β-Gal) in substrate [$U/g_{lactose}$]

$Yp1/x$ – product yield (ethanol) in biomass [$g_{ethanol}/g_{biomass}$]

$Yp2/x$ – product yield (β-Gal) in biomass [$U/g_{biomass}$]

Z - dependence on temperature of D value [K]

h_{fp} - fluid-particle heat transfer coefficient [$W \cdot m^{-2} \cdot K^{-1}$]

i - node number [-]

k- frequency constant [s^{-1}]

k_0 - pre-exponential factor [s^{-1}]

k_f - fluid thermal conductivity [$W \cdot m^{-1} \cdot K^{-1}$]

k_p - particle thermal conductivity [$W \cdot m^{-1} \cdot K^{-1}$]

k_x - thermal conductivity in the x direction [$W \cdot m^{-1} \cdot K^{-1}$]

k_y - thermal conductivity in the y direction [$W \cdot m^{-1} \cdot K^{-1}$]

K - a consistency index [$kg.sn^{-2}.m]^{-1}$

l_{fP} - length of parallel fluid [m]

l_{fS} - length of serial fluid [m]

l_{pP} - length of parallel particles [m]

m - temperature coefficient [$S \cdot m^{-1} \cdot K^{-1}$]

m_f - temperature coefficient of the fluid [S·m^{-1}·K^{-1}]

m_p - temperature coefficient of the particle [S·m^{-1}·K^{-1}]

n - flow behavior index [-]

n - time step index [-]

$\vec{n}$ - unit vector normal to the surface of the tube's wall [-]

n_p - number of solid particles in the considered volume [-]

r - radial coordinates [-]

t - time [s]

w - tube's wall [-]

x, y - space coordinates [-]

z - axial coordinates [-]

Greek Symbol

$\beta(\varepsilon_f)$ - fraction of heat transfer by conduction through the mixture in the fluid phase [-]

ε_f - fluid volume fraction in the heater [-]

ε_p - volume fraction [-]

η - ethanol yield expressed in percentage pf the theoretical value [%]

ρ_f - fluid density [kg·m^{-3}]

ρ_p - particle density [kg·m^{-3}]

σ_{0f} - electrical conductivity of the fluid before the heating takes place [S·m^{-1}]

σ_{0p} - electrical conductivity of the particle before the heating takes place [S·m^{-1}]

σ_{eff} - effective electrical conductivity [S·m^{-1}]

σ_{ref} - electrical conductivity at a reference temperature [S·m^{-1}]

σ_T - electrical conductivity at temperature T [S·m^{-1}]

σ_x - electrical conductivity in the x direction [S·m^{-1}]

σ_y – electrical conductivity in the y direction [S·m^{-1}]

σ - electrical conductivity [S·m^{-1}]

υ - kinematic viscosity [m^2 s]

τ_0 - yield stress [Pa]

ρ - density [Kg m^{-3}]

μ - specific growth rate [h^{-1}]

$\bar{v}_z$ - mean fluid velocity profile in the axial direction [m·s^{-1}]

$\bar{v}_z$ - mean fluid velocity profile in the axial direction [m·s^{-1}]

Abbreviations

ALP - alkaline phosphatase

β-GAL – β-galactosidase

CFD – Computational fluid dynamics

LOX - lipoxygenase

OH - ohmic heating

PEC - pectinase

PPO - polyphenoloxidase

List of Figures

List of Tables

List of Equations

Chapter 1.

GENERAL INTRODUCTION

1. Introduction

Heating is probably the oldest means of processing foods and has been used by Mankind for millennia. However, the technology used to heat foods in order to process them has had a spectacular evolution during the 20th century which has continued until now. Technologies such as ohmic heating, dielectric heating (which includes microwave heating and radio frequency heating) and inductive heating have been developed and can replace, at least partially, the traditional heating methods which rely essentially on conductive, convective and radiative heat transfer. They all have a common feature: heat is generated directly inside the food and this has direct implications in terms of both energetic and heating efficiency. Also infrared heating has been developed as a means of heat processing of foods. These are called novel thermal processing technologies, meaning that the change in temperature is the main processing factor, as opposed to the novel non-thermal processing technologies such as pulsed electric fields, high pressure, pulsed light, ultrasound, gamma radiation, among others, where temperature may also change but is not the main responsible for food processing.

However, despite the advantages claimed for each of these technologies, their industrial application is not yet widespread due to several factors:

- Lack of knowledge of: the process itself; the resistance of microorganisms, enzymes and nutrients
- Lack of legal approval
- The need to prove process safety in terms of operating procedures (working with radiation, magnetic or electric fields)
- Reluctance from the consumer
- Disadvantages inherent to the process: investment costs, productivity

Some additional research and development effort must be made in order to fully understand and validate these new technologies with regard to food safety and food quality.

2. Ohmic heating

Ohmic heating (OH) (also called Joule heating, electrical resistance heating, direct electrical resistance heating, electroheating or electroconductive heating) is defined as a process where electric currents are passed through foods to heat them (Figure 1.1). Heat is internally generated due to electrical resistance (Alwis and Fryer, 1990) OH is distinguished from other electrical heating methods by a) the presence of electrodes contacting the foods (in microwave and inductive heating electrodes are absent), b) the frequency applied (unrestricted, except for the specially assigned radio or microwave frequency range) and c) waveform (also unrestricted, although typically sinusoidal).

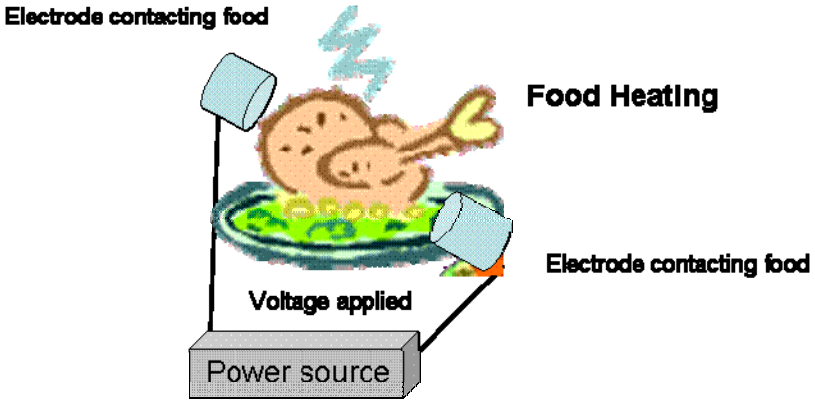

Figure 1.1: The principle of ohmic heating

The OH concept is well known and various attempts have been made to use it in food processing. A successful application of electricity in food processing was developed in the 19th century to pasteurize milk (Getchel, 1935). This pasteurization method was called "Electropure Process" and by 1938 it was used in approximately fifty milk pasteurizers in five US states and served about 50000 consumers (Getchel, 1938). This application was abandoned apparently due to high processing costs (Alwis and Fryer, 1990). Also, other applications were abandoned because of the short supply of inert materials needed for the electrodes, although electroconductive thawing was an exception (Mizrahi *et al*., 1975).

However, research on ohmic applications in fruits, vegetables, meat products and surimi has been more recently undertaken by several authors (Palaniappan and Sastry, 1991; Palaniappan and Sastry, 1991; Wang, Sastry, 1997; Castro *et al.*, 2003).

Aseptic processing is considerably developed in the food industry especially for liquid foods which are processed predominantly by heat exchangers. Food technologists and the food industry are interested in extending this technology to more complex foods such as

highly viscous, low acid and particulate containing foods. In fact, most of the technologies actually used rely on conductive, convective and radiative heat transfer. Their application to particulate foods is limited by the time required to ensure the sterilization of the centre of larger particles, often causing overcooking of the surrounding volume. Consequently, product safety is achieved at the expense of quality.

In order to maximize food quality High Temperature Short Time (HTST) processes have been used. Such processes are based on reactions that reduce the level of bacterial spores with lower activation energy than those responsible for the loss of quality (e.g. reduction in vitamins concentration and color degradation).

OH technology has gained interest recently because the products are of a superior quality than those processed by conventional technologies (Castro *et al.*, 2003; Parrott, 1992; Kim *et al*., 1996). Moreover, the ohmic heater assembly can be incorporated into a complete product sterilization or cooking process. Among the advantages claimed for this technology are uniformity of heating and improvements in quality with minimal structural, nutritional or organoleptic changes (Skuder, 1989). The potential applications are very wide and include e.g. blanching, evaporation, dehydration, fermentation (Cho *et al*., 1996), pasteurization and sterilization.

OH is currently used in Europe, Asia and North America to produce a variety of high-quality, low and high-acid products containing particulates. A large number of additional applications are being developed for this technology and will be discuss further ahead.

A consortium of 25 partners from industry (food processors, equipment manufacturers and ingredient suppliers), academia (food science, engineering, microbiology and economics) and government was formed in 1992 in the US in order to overcome the challenges still remaining about regulatory evaluation and formula optimization.

A 5 kW of pilot-scale continuous flow ohmic system (APV Baker, Ltd., Crawley, UK) was evaluated and a wide variety of shelf-stable (low and high acid) products were developed. These included broccoli and cheese (broccoli florets in Cheddar cheese sauce), shrimp gumbo (shrimp, okra and tomatoes in a savory sauce), strawberries in glaze, oriental chicken (chicken, waterchestnuts, corn, peapods, bamboo shoots, mushrooms, carrots and red peppers in Savoy sauce) and pasta primavera (shrimp, surimi, carrots, green beans and mushrooms in Alfredo sauce). These products were found to have equal to, or higher than, texture, color and nutrient retention compared to those processed by traditional methods such as freezing, retorting and aseptic processing. The consortium concluded that the technology was technically and economically viable (Parrott, 1992).

The OH system allows for the production of new, high-added-value, shelf-stable products with a quality previously unattainable with alternative sterilization techniques, especially for particulate foods. Its major advantages are (Parrott, 1992):

- continuous production without heat-transfer surfaces;
- rapid and uniform treatment of liquid and solid phases with minimal heat damages and nutrient losses (*e.g.* unlike microwave heating, which has a finite penetration depth into solid materials);
- ideal process for shear-sensitive products because of low flow velocity;
- optimization of capital investment and product safety as a result of high solids loading;
- reduced fouling when compared to conventional heating;
- better and simpler process control with reduced maintenance costs;
- environmentally friendly system.

Some of the disadvantages accounting for OH are the higher initial operational costs and the lack of information or validation procedures for this technology.

3. Modelling Ohmic heating

The main objective of OH is to increase the temperature of food materials to a point at which the food is considered adequately processed. Also, the so-called *cold spot* must be identified. The most effective manner requires the exact measurement of the temperature profile in the food material when heating is applied. Models describing the effect of the main operating parameters on temperature of food materials (and especially of the system's cold spot) are required because they are the best way (economical and fast) to study and validate a new process.

3.1. Basic principles

3.1.1. Electric Field

In order to generate heat in an OH system an electric field must be applied to the food. The electric field (voltage distribution) is a function of the electrode and system geometry, electrical conductivity and also of the applied voltage (Alwis and Fryer, 1990). The electric field is determined by the solution of Laplace's equation:

$$\nabla(\sigma \cdot \nabla V) = 0 \qquad \textbf{(Eq. 1.1)}$$

where σ is the electrical conductivity and ∇V is the voltage gradient. This equation has been obtained combining Ohm's law with the continuity equation for electric current (Hayt, 1981), and differs from the usual form of Laplace's equation:

$$\nabla^2 V = 0 \qquad \textbf{(Eq. 1.2)}$$

because σ is a function of both position and temperature, as mentioned before.

In order to solve Equation (1), boundary conditions specific for each case must be established. The solution has been obtained by de Alwis and Fryer (1990) for a static ohmic heater containing a single particle, using as boundary conditions: a) a uniform voltage on the electrodes or b) no current flux across the boundary elsewhere. For a more general case of many different particles flowing in a fluid composed of several liquid phases (*e.g.* vegetable soup, where different vegetable solid pieces are dip in a fluid broth with at least an aqueous and a lipid phase), the mathematical solution for Equation 1.1 is, to our knowledge, still unknown. In these cases, the prediction of the electric field has been based on semi-empirical models (Sastry *et al.*, 1992; Sastry, 1992).

The determination of the electric field is one of the most challenging subjects of the modeling effort in the OH technology.

3.1.2. Heat Generation

In order to ohmically heat a food it is necessary to pass electrical current through it. The heat generated in the food by that current ($\dot{Q}$) is proportional to the square of its intensity (I), the proportionality constant being the electrical resistance (R), thus yielding:

$$\dot{Q} = R \cdot I^2 \qquad \textbf{(Eq. 1.3)}$$

Alternatively, if both electrical conductivity (σ) and voltage gradient (∇V) are known, it is possible to write:

$$\dot{Q} = \left|\nabla V\right|^2 \cdot \sigma \qquad \textbf{(Eq. 1.4)}$$

where σ is a function of position and temperature. The dependence of position is because foods are not necessarily homogeneous materials; the limiting scenarios being foods containing particles (e.g. vegetables soup) and that of a reasonably homogeneous liquid (e.g. orange juice). The relation of σ with temperature is usually well described by a straight line of the type (Palaniappan and Sastry, 1991):

$$\sigma_T = \sigma_{ref} \cdot \left[1 + m \cdot \left(T - T_{ref}\right)\right] \qquad \textbf{(Eq. 1.5)}$$

where σ_T is the electrical conductivity at temperature T, σ_{ref} is the electrical conductivity at a reference temperature, T_{ref}, and m is the temperature coefficient.

3.1.3. Energy Balance

The next step for model is to determine the temperature distribution of the fluid and the solid phases (if present). This is done by establishing an energy balance for the fluid phase and solid phase (Orangi and Sastry, 1998). Both the equations for the fluid and solid phases are established based on the knowledge of the predominant energy (mainly heat) transfer phenomena occurring during OH. These are schematically outlined in Figure 1.2 together with the relevant mass and momentum transfer phenomena, z and r which are the axial and radial coordinates, respectively.

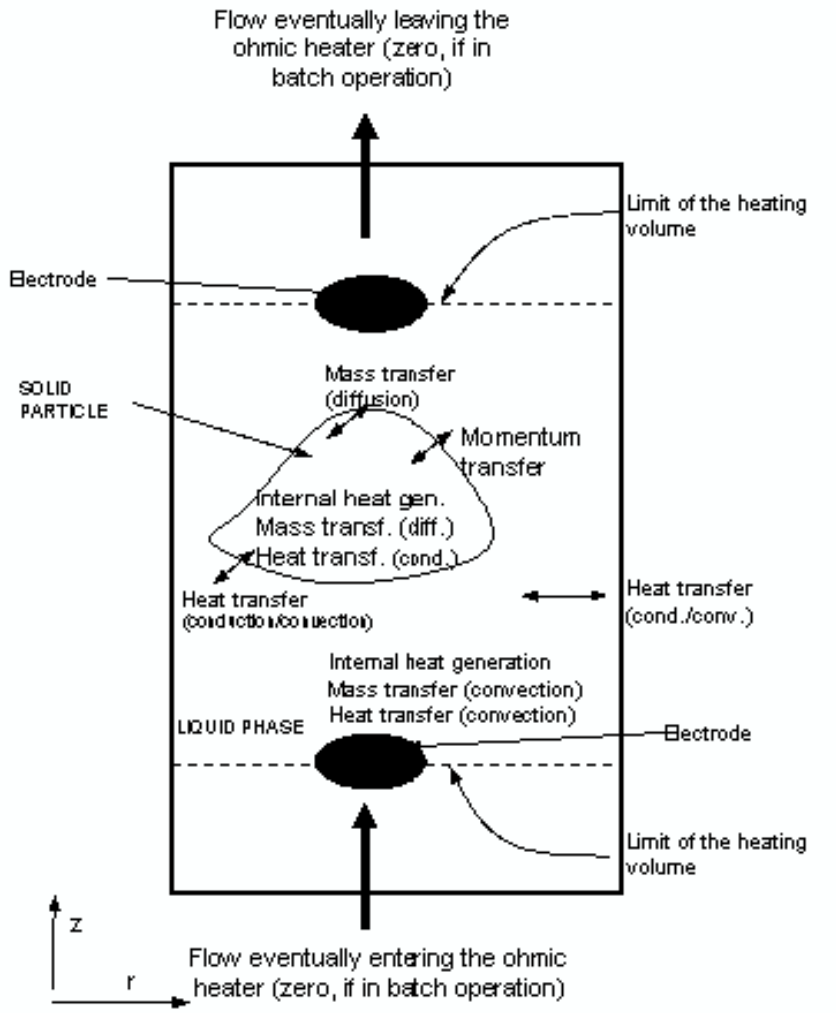

Figure 1.2: Main heat, mass and momentum transfer phenomena occurring during OH. The presence (continuous) or absence (batch) of a mass flow through the heater will alter the hydrodynamic conditions and thus the relative importance of the phenomena.

According to (Figure 1.2), for a continuous process (the more general case) and for the fluid phase (the system considered here is a tubular heater – which is the most common geometry – where the electrodes are placed along the heater, thus creating a longitudinal voltage field; in any case, the application of the following equation to the case of a radial voltage field – i.e., where the electrodes are placed on the walls of the tube – should be straightforward), the energy balance is:

$$\rho_f \cdot C_{pf} \cdot \bar{v}_z \cdot \varepsilon_f \cdot \frac{\partial T_f}{\partial z} = \beta(\varepsilon_f) \cdot \nabla(k_f \cdot \nabla T_f) - \frac{n_p \cdot A_p \cdot h_{fp}}{V_{sys}} \cdot (T_f - T_{ps}) + \frac{\dot{Q}_f}{V_{sys}} \quad \textbf{(Eq. 1.6)}$$

where ρ_f is the fluid density, C_{pf} is the fluid specific heat, $\bar{v}_z$ is the mean fluid velocity profile in the axial direction, ε_f is the fluid volume fraction in the heater, T_f is the fluid temperature, k_f is the fluid thermal conductivity, n_p is the number of solid particles in the considered volume, A_p is the area of each solid particle, h_{fp} is the fluid-particle heat transfer

coefficient, V_{sys} is the volume of the system between the electrodes, T_{ps} is the temperature at the surface of the solid particle, being also:

$$\nabla^2 = \frac{\partial^2}{\partial r^2} + \frac{1}{r}\frac{\partial}{\partial r} + \frac{\partial^2}{\partial z^2} \qquad \textbf{(Eq. 1.7)}$$

where r and z are the radial and axial coordinates, respectively, and $\dot{Q}_f$ being the heat generated in the fluid, given by the combination of Equations 1.4 and 1.5, yielding:

$$\dot{Q}_f = \left|\nabla V\right|^2 \cdot \sigma_{0f} \cdot \left(1 + m_f \cdot T_f\right) \qquad \textbf{(Eq. 1.8)}$$

where σ_{0f} is the electrical conductivity of the fluid before the heating takes place (initial value of σ_f) and m_f is the temperature coefficient of the fluid. Still in Equation 1.6, $\beta(\varepsilon_f)$ represents the fraction of heat transfer by conduction through the mixture in the fluid phase. The exact form of $\beta(\varepsilon_f)$ is unknown but, based on the Kopelman model (Kopelman, 1966), its expression can be given by:

$$\beta\left(\varepsilon_f\right) = 1 - \left(1 - \varepsilon_f\right)^{2/3} \qquad \textbf{(Eq. 1.9)}$$

In any case, Orangi *et al.* (1998) noted that the influence of this term on the result is marginal, as the conduction term is very small relative to other terms in Equation 1.6. Also, in this equation, the axial conduction term $\left(\partial^2/\partial z^2\right)$ is normally considered small when compared with the radial conduction term (this situation corresponds to a large Peclet number), and can be neglected.

For Equation 1.6, if no solids are present then np equals zero, thus canceling the term.

$$n_p \cdot A_p \cdot h_{fp} \cdot \left(T_f - T_{ps}\right). \qquad \textbf{(Eq. 1.10)}$$

Also for Equation 1.6, the value of $\bar{v}_z$ (the mean fluid velocity profile in the axial direction) can be obtained assuming plug flow (an assumption generally valid for high solids concentration) or considering the more general case of a flow with a velocity gradient (assuming a power law fluid behavior), which can be given by (Orangi *et al.*, 1998):

$$v_z = \left(\frac{3n+1}{n+1}\right) \cdot \bar{v}_z \cdot \left[1 - \left(\frac{r}{R}\right)^{n+1/n}\right] \qquad \textbf{(Eq. 1.11)}$$

where n is the flow behavior index. In this case, v_z will replace $\bar{v}_z$ in Equation 1.6.

In order to obtain the solution of Equation 1.6, initial and boundary conditions must now be established. As initial condition, the following applies:

$T_f = T_0$, at $z = 0$

For the boundary condition at $r = R$ (R being the radius of the heater tube), it is necessary to consider the balance between conductive and convective heat transfer on the outer surface of the tube:

$$-k_f \cdot \nabla T_f \cdot \vec{n}\Big|_w = U \cdot \left(T_f - T_{air}\right)\Big|_w \qquad \textbf{(Eq. 1.12)}$$

where $\vec{n}$ is the unit vector normal to the surface of the tube's wall (w), U the overall heat transfer coefficient and T_{air} the temperature of the air surrounding the walls of the heater. This balance must then be applied to Equation 1.6 to obtain the boundary condition at $r = R$.

Another boundary condition must be established on the axis ($r = 0$) which can be obtained by applying Equation 1.6 when $r \rightarrow 0$.

The energy balance for the solid phase is (assuming spherical particles, Figure 1.2):

$$\rho_p \cdot C_{pp} \cdot \frac{\partial T_p}{\partial t} = \nabla\left(k_p \cdot \nabla T_p\right) + \frac{\dot{Q}_p}{V_p} \qquad \textbf{(Eq. 1.13)}$$

where ρ_p is the particle density, C_{pp} is the particle specific heat, T_p is the particle temperature, t is the time, k_p is the particle thermal conductivity, V_p is the volume of the particle, T_{ps} is the temperature at the surface of the solid particle and $\dot{Q}_p$ is the heat generated in the particle, given by the combination of Equations (1.4) and (1.5), yielding:

$$\dot{Q}_p = \left|\nabla V\right|^2 \cdot \sigma_{0p} \cdot \left(1 + m_p \cdot T_p\right) \qquad \textbf{(Eq. 1.14)}$$

where σ_{0p} is the electrical conductivity of the particle before the heating takes place (initial value of σ_p) and m_p is the temperature coefficient of the particle.

Similarly to what has been made with Equation (1.6), initial and boundary conditions must now be established for Equation (1.13). As initial condition, the following holds:

$$\mathbf{T_p = T_{0p}, \text{ at } t = 0} \qquad \textbf{(Eq. 1.15)}$$

where T_{0p} is the initial temperature of the particle.

The boundary condition is established at the surface (s) of the particle, where it is again necessary to consider the balance between conductive and convective heat transfer, given by:

$$-k_p \cdot \nabla T_p \cdot \vec{n}\Big|_s = h_{fp} \cdot \left(T_{ps} - T_f\right)\Big|_s \qquad \textbf{(Eq. 1.16)}$$

If there are more than one solid phases present, this energy balance must be applied to each of them.

3.1.4. Mass and Momentum Balance

In order to completely describe the system it is necessary to solve mass and momentum balance equations in three dimensions. This includes the solutions of those balances for both the solid phase (or phases, if several are present) and the liquid phase (or phases, if several are present) and constitutes substantial modeling and computational efforts (Alwis and Fryer, 1990; Orangi *et al.*, 1998; Sastry and Li, 1996). The hydrodynamics of the overall system (batch or continuous) must be well characterized in order to define fully the velocity field of all phases present in the ohmic heater. This is related to the determination of the quickest particle (or portion of fluid) and is crucial in determining the safety of the heat treatment. There are commercial software programs, based on computational fluid dynamics, which are able to address these issues. These are being used to obtain the flow field in a continuous ohmic heater to use this information to obtain the temperature distribution of the solid and of the liquid phases in a two-phase flow.

The equations described above will form the basis for the development of models to predict the heating rate of fluids and fluids containing solid particles. According to Alwis *et al.* (1989) the heating rate is a function of a) electrical conductivity of the food constituents (of both fluid and solid phases); b) particle geometry and size; c) particle orientation; and d) thermal variation of physical properties. Sastry and Palaniappan (1992) added particle's volume fraction to this list. While the particles' size, geometry, orientation and volume fraction are parameters relatively easy to measure and control and there are extensive data available on the temperature dependence of the main physical property, electrical conductivity (especially particle's electrical conductivity) is a critical point (Sastry, 1992).

3.1.5. Electrical Conductivity

Probably the most important parameter in OH modeling is σ (Fryer and Li, 1993). Some of the characteristics of this property are summarized below:

- σ can be anisotropic (varies in different directions);
- changes in the value of σ reflect changes in the matrix structure, *e.g.* during starch gelatinization or cell lysis;
- the value of σ which is not suitable for ohmic processing can be suitably modified, *e.g.* by blanching.

However, perhaps the most striking feature of σ is its dependence of temperature, as it has been shown to increase with increasing *T*. This observation is due to a variable opposition (drag force) to the movement of the ions responsible for conducting the electricity in food materials: for higher temperatures, that opposition is less important than for lower temperatures (Anon, 1982).

For most solid foods, σ increases sharply with temperature at around 60ºC and this has been attributed to the breakdown of cell wall materials (Sastry and Palaniappan, 1992), releasing ionic compounds to the bulk medium. Figure 1.3a represents this dependence for several electric field (*F*) strength values, demonstrating that the relationship between σ and *T* becomes linear for increasing values of *F* (the lower limit of *F* – i.e. *F* = 0 $V \cdot m^{-1}$ – represents conventional heating). This effect has been demonstrated by, amongst others, Palaniappan and Sastry (1991), who suggested that it may be due to electro-osmotic effects which could increase the effective conductivity at low temperatures. This means that, for normal OH conditions, the relationship between σ and *T* can be represented by Equation (1.5).

For liquid foods, σ always has a linear relationship with *T*, however the value of σ decreases if non-polar (thus non-conductive) constituents are present (Figure 1.3b). If those constituents are generally regarded as the "solid content" of the liquid (e.g., the pulp content of juice), it is possible to write *e.g.* for tomato and orange juices (Palaniappan and Sastry, 1991):

$$\sigma_T = \sigma_{ref} \cdot \left[1 + K_1 \cdot \left(T - T_{ref}\right)\right] - K_2 \cdot S \qquad \textbf{(Eq. 1.17)}$$

where K_1 and K_2 are constants and *S* is the dissolved solids content.

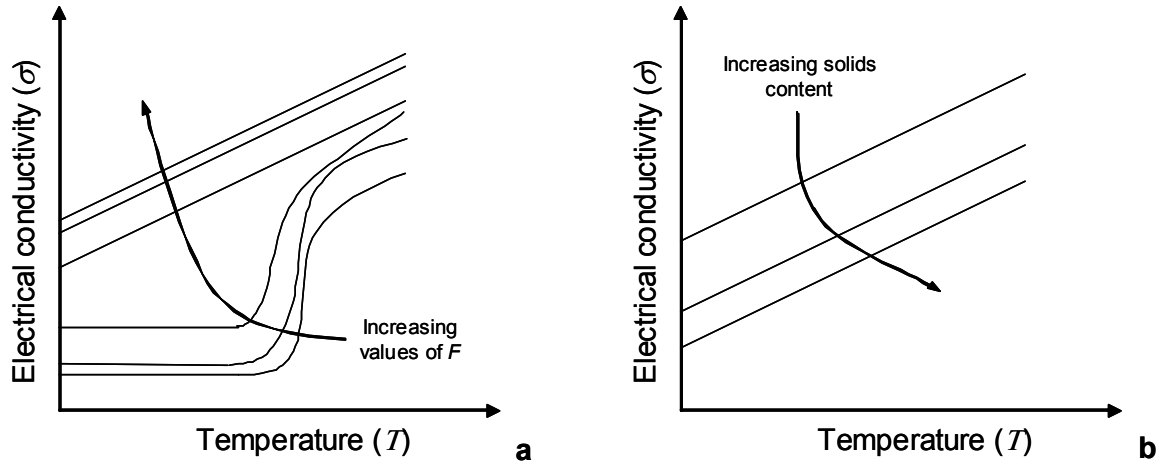

Figure 1.3: a) variation of σ with T for solids and for several electric field strength values (F), showing that the relationship between σ and T becomes linear for increasing values of F (the lower limit of F – i.e. $F = 0$ V·m^{-1} – represents conventional heating); b) variation of σ with T for liquids, showing that σ has always a linear relationship with T, with the value of σ decreasing for increasing concentration of non-polar (thus non-conductive) constituents (e.g. soluble solids) (adapted from Sastry and Palaniappan, 1992).

A similar influence of solids concentration on σ has also been reported by other authors (Castro *et al.*, 2003; Zareifard *et al.*, 2003), but in this cases the solids were particles of significant sizes suspended in a fluid. This situation differs from the above because the value of σ is not that of the fluid but a combined value for the mixture fluid + particles, the so-called *effective* electrical conductivity (σ_{eff}). In fact, not only solid content but also solid size will influence the mixture σ_{eff}.

Another major factor affecting σ is the ionic content of the food: the higher the ionic content, the higher the value of σ (Zareifard *et al.*, 2003). This has been demonstrated by several authors (Palaniappan and Sastry, 1991; Castro *et al.*, 2002; S Palaniappan *et al.*, 1991; Wang and Sastry, 1993).

σ is also a function of the frequency at which it is measured (Lima and Sastry, 1999) and evidence also shows that the value of σ of a food heated electrically is different from that cooked by conventional heating (Fryer and Li, 1993). In fact, Wang and Sastry (1997) demonstrated that samples pre-heated by either conventional or OH had a higher heating rate due to increased σ, and that the values found for σ were different in each case.

It has been mentioned that σ *versus* T is usually a linear relationship. However this is not always the case. Several examples exist where the curve became non-linear (Wang and Sastry, 1993; Castro *et al.*, 2004). This non-linearity has been attributed to the equilibration of solutes within the samples during heating, thus altering the value of the observed σ_{eff}.

3.1.6. Other Parameters: Particle Orientation, Geometry, Size and Concentration – the Effective Electrical Conductivity

Other parameters have been found to influence the values of OH rate of the constituents of a food as mentioned before. When more than one phase is present, these parameters can exert their influence *via* the effective conductivity of the mixture (σ_{eff}) which is the case of particle size and concentration, or they can directly influence the heating rate of the different constituents, which is the case of particle orientation and geometry.

Particle geometry was demonstrated to be of importance only when the aspect ratio of the solid particle is far from unity (Larkin and Spinak, 1996). If this is the case, and for a static OH system containing a fluid and a single elongated particle with a lower conductivity than the fluid, de Alwis *et al.* (1989) showed that when the particle was placed with its longer axis parallel to the electric field (Figure 1.4a), then it would heat slower than the fluid. However, if such a particle would be placed with its longer axis perpendicular to the electric field (see Figure 1.4b), then the particle would heat faster than the fluid. Exactly the reverse would occur if the particle had a higher conductivity than the fluid (Figure 1.4c and Figure 1.4d). This has been confirmed by mathematical (Alwis and Fryer, 1990; Fu and Hsieh, 1999). The cases documented by Figure 1.4a and d are referred by Sastry and Salengke (1998) as being worst-case scenarios. The particle will be under-heated compared to the fluid and it may be under-processed. In the case of Figure 1.4a, under-heating may result from the major part of the current bypassing the particle, thus heating more the surrounding fluid. Alternatively (Figure 1.4d), under-heating may result from the particle transmitting most of the current thus creating a low field gradient within the particle and low current densities in its vicinity. A similar situation will be that of a cluster of particles (more conductive than the fluid) blocking the cross section of the heater. However, the authors conclude that both the latter cases are avoidable in an industrial application (*e.g.* controlling particle size or on-line sensing the σ of the product to divert possible particle clumps from the product stream prior to heating), being the former the one which may cause greater concern. In practice, if a single low conductivity particle enters the system, there is potential for under-processing that particle, once its cold spot would have a significantly lower temperature than that of the fluid (Sastry, 1992). Such a particle might be a fat globule which, if carrying a microbial load, could present a serious risk for the safety of the product being processed.

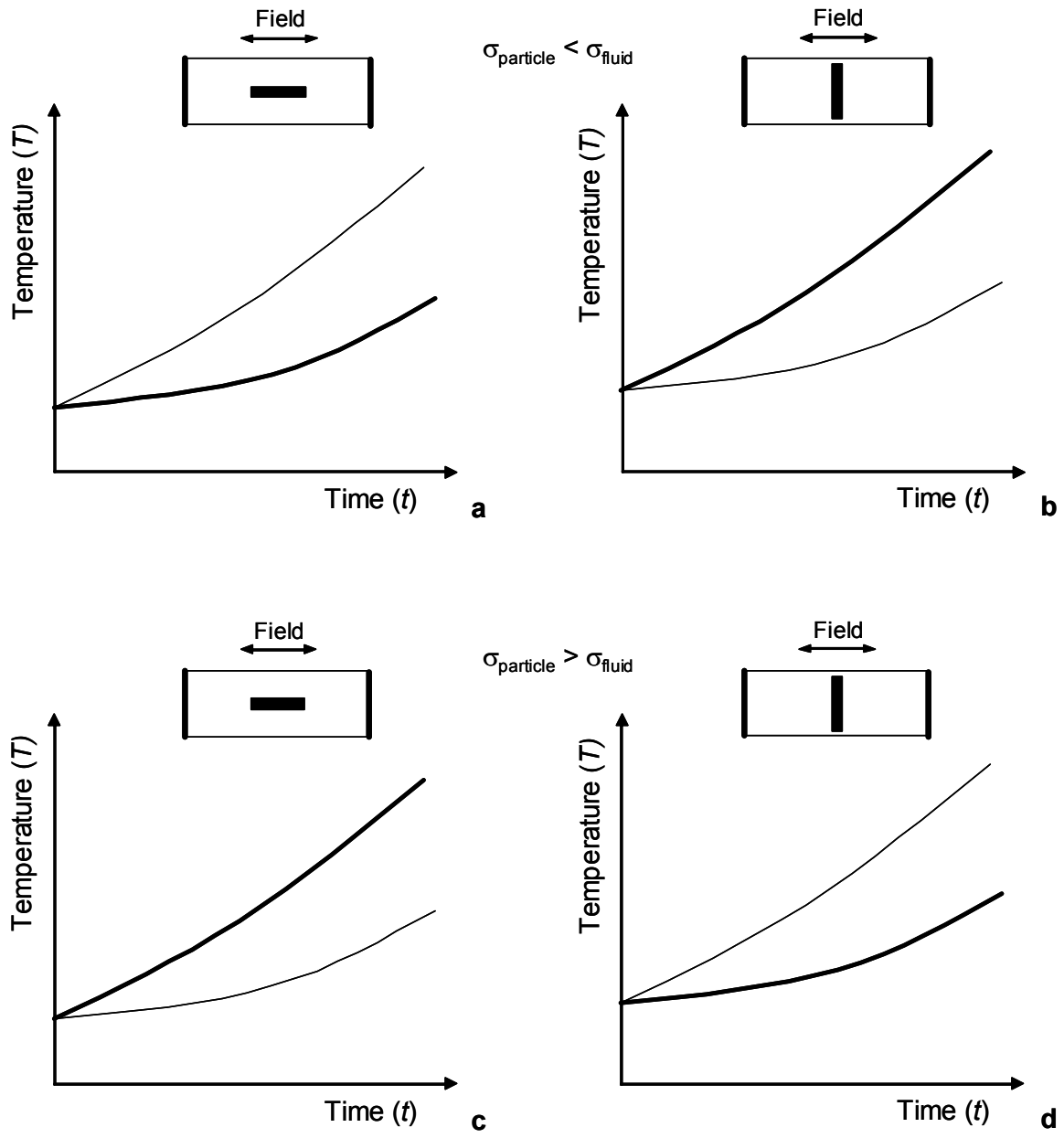

Figure 1.4: Heating curves of a single solid particle suspended in a fluid contained in a static ohmic heater (——— - particle; ——— - fluid): a) and b) when the particle has a lower electrical conductivity than the fluid and its longer axis is parallel to the electric field (a) or perpendicular to the electric field b); c) and d) when the particle has a higher electrical conductivity than the fluid and its longer axis is parallel to the electric field (c) or perpendicular to the electric field d).

Most of the conclusions presented above have been drawn for a static ohmic heater. In a continuous-flow ohmic heater, the fluid will be agitated and therefore the fluid-particle heat transfer will be higher than in the static situation. Sastry and Salengke (1998) have shown that the static situation is not always related to the worst-case scenario. In fact, when the solid is less conductive than the fluid the worst situation will be that of a mixed fluid (continuous situation). Nevertheless, if the solid is more conductive than the fluid, then the

worst case will be that of a static fluid (static situation). Evidently, none of the rheological properties of the fluid have great influence, and viscous fluids tend to make a continuous system behave as a static system (Khalaf and Sastry, 1996).

The concentration and size of the particles are also responsible for alterations of the heating rate of particle/fluid mixtures (Figure 1.4 a and b). In fact, the values of σ of orange and tomato juices decreased with solids content (Palaniappan and Sastry, 1991). The same observation has been made by other authors using other food systems (e.g. Zareifard *et al.* (Zareifard *et al.*, 2003) used carrot puree or cubes immersed in a starch solution and Castro *et al.* (2003) used strawberry cubes immersed in strawberry pulp (Figure 1.5). A possible explanation for this finding is given by Palaniappan and Sastry (1991) who establish a comparison with the case of a fluid without particles. In this case, the increase of σ with T is due to the reduced opposition (drag force) to the movement of ions. At constant T, this opposition is increased when solid particles are present (e.g. due to the increased tortuosity of the path that the ions have to follow, among other effects), and this may be the reason for the observed decreasing trend of σ with increasing particles content, which is in line with what happened with dissolved solids concentration. This same explanation may be applied to justify the decreasing of σ when particle size increases (Figure 1.5b). This effect has been observed by several authors in various systems (Palaniappan and Sastry, 1991; Castro *et al.*, 2003; Zareifard *et al.*, 2003).

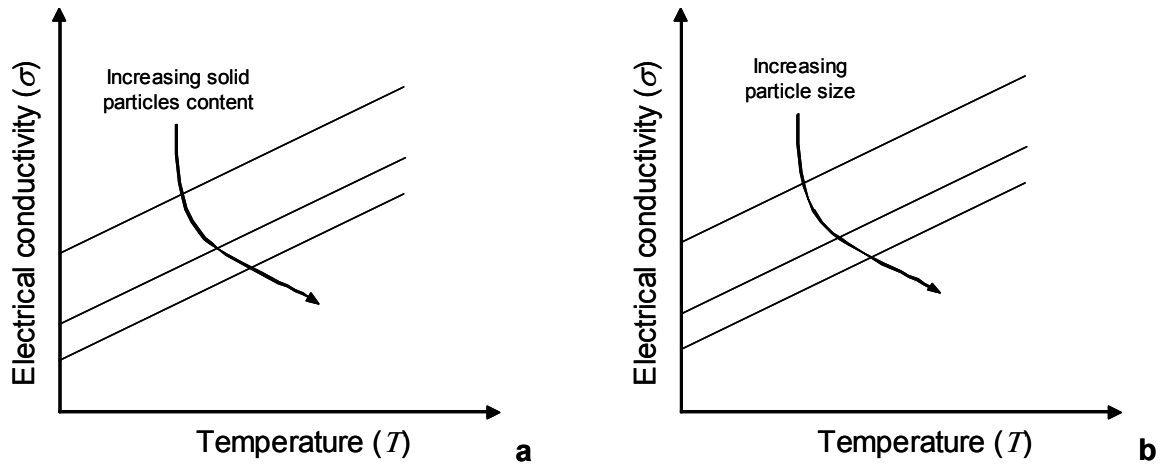

Figure 1.5: a) variation of σ with T for various particles contents, showing that σ has always a linear relationship with T, with the value of σ decreasing for increasing particles volume fraction; b) variation of σ with T for various particles sizes, showing that also in this case σ has always a linear relationship with T, with the value of σ decreasing for increasing particles size (adapted from Zareifard *et al.* (Zareifard *et al.*, 2003)).

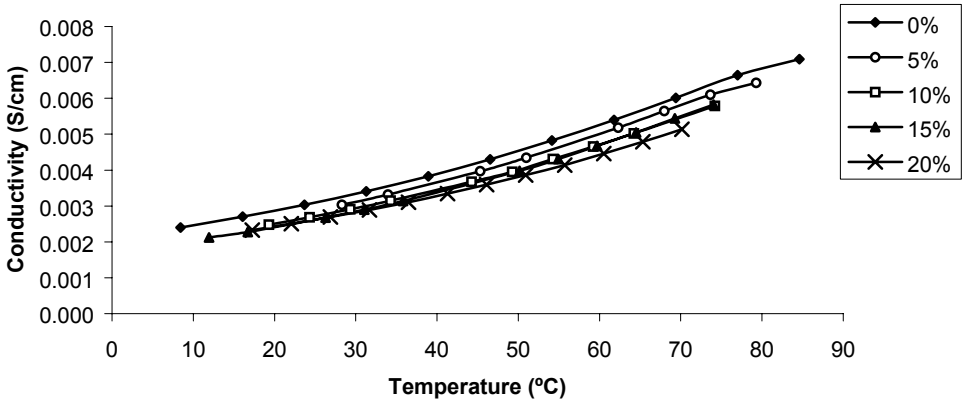

Figure 1.6: Electrical conductivity curves of strawberry pulp containing strawberry cubes (average size 6.4 mm), with different solids content, during ohmic heating (Castro *et al.*, 2003).

If a solid particle with a lower σ than the fluid, in which the particle is immersed, is subjected to OH, it will heat slower than the fluid (assuming a particle with an aspect ratio close to unity or aligned as in Figure 1.5a. However, if a number of such particles are present, simulations have shown and experiments have confirmed (Sastry and Palaniappan, 1992) that although the heating rate of the particles is initially lower than that of the fluid, heating rate of the particles overtakes that of the fluid. This can be explained in light of what has been represented in Figure 1.5b, where a particle with a lower σ blocking the current conduction would heat faster than the fluid; similarly, as the particles concentration increases, they will increasingly block the conduction paths forcing a greater proportion of the total current to flow through them, thus showing higher heat generation rates than those of the fluid. This means that the particle's σ, although lower than the fluid's σ at low temperatures, will increase faster (Figure 1.7b), overtaking the latter for higher temperatures therefore justifying the shape of the heating curves in Figure 1.7a.

These models (of which Equation 1.19 is an example) can be of use if they are representative in the conditions under which they are to be applied. If this is the case, then it is possible to use σ_{eff} to estimate the temperature increase of a mixture when it is subjected to OH by a very simple calculation.

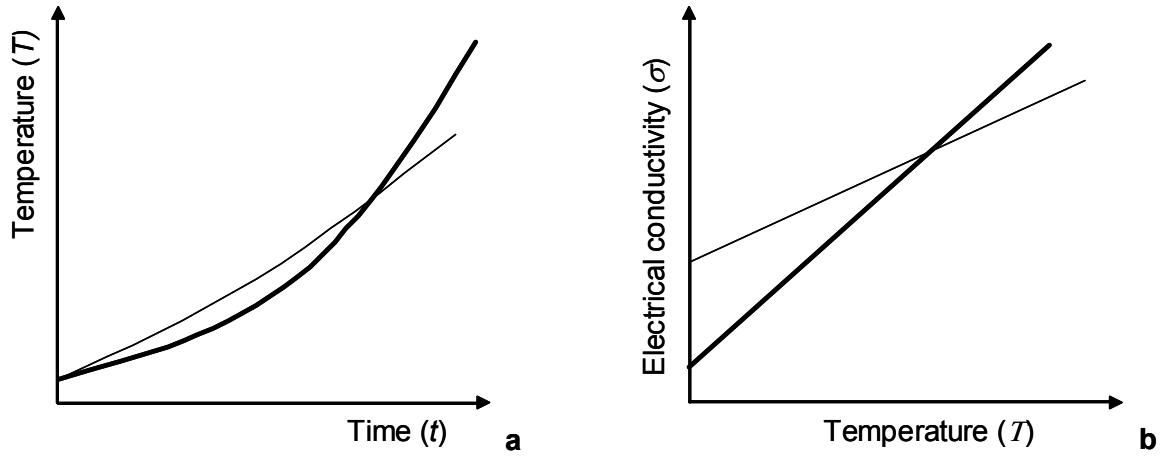

Figure 1.7: Behavior of a mixture of a fluid with a high concentration of particles (these having a value of σ lower than that of the fluid) (——— - particles; ——— - fluid); a) heating of particles and fluid (adapted from Sastry and Palaniappan (Sastry and Palaniappan, 1992) and b) corresponding variation of σ with T (adapted from Zareifard *et al.* (Zareifard *et al.*, 2003)).

3.2. Models

The models described constitute important landmarks in the modeling effort in OH. Generally speaking, all assume that the physical properties of the phases in presence are constant with respect to the temperature, with the obvious exception being electrical conductivity. Considering the coexistence of several solid particles immersed in a fluid, it is also generally assumed that the particles have short interaction times with the surrounding particles and with the walls of the heater.

3.2.1. Model for a Single Particle in a Static Heater Containing a Fluid

A model for a single solid particle in a static heater containing a fluid has been developed initially by de Alwis and Fryer (Alwis and Fryer, 1990) and further enhanced by de Alwis and Fryer (1990) for a two-dimensional system. The main purpose of the model is to predict the sterilization effect in a practical situation, where complex food shapes are heated. It is a finite-element model which has been designed to simulate three types of situations:

- *zero convection.* This is the case of highly viscous and gel-forming foods, where convective processes are less significant.
- *enhanced conduction*. When convection cannot be neglected, one of the convenient ways of treating the problem is to consider the existence of an *effective* conductivity value (σ_{eff}), which can be determined empirically and approximately to replace the effects of both convection and conduction.
- *well-stirred liquid*. In previous work (Alwis *et al.*, 1989), where an unstirred fluid was used, no hot spots were noticed when very low viscosity mixtures were heated, indicating that rapid convective mixing was taking place. In this case, a well-stirred liquid condition can be applied.

To obtain the electric field distribution Equation (1) was written for a 2-D situation, yielding:

$$\frac{\partial}{\partial x}\left(\sigma_x \cdot \frac{\partial V}{dx}\right)+\frac{\partial}{\partial y}\left(\sigma_y \cdot \frac{\partial V}{dy}\right)=0 \qquad \textbf{(Eq. 1.18)}$$

where x and y are the space coordinates of the system and σ_x and σ_y the values of the σ in the x and y direction, respectively. The solution of this equation was obtained using boundary conditions of a) a uniform voltage on the electrodes, or b) no current flux elsewhere across the boundary.

For heat generation, a network theory approach was used in which each triangular element was considered an isolated network, with nodal voltages known by solution of Equation (1.18). Heat generation in the particle was thus found by:

$$\dot{Q}=\sum_{i=1}^{i=3} V_i \cdot I_i \qquad \textbf{(Eq. 1.19)}$$

where i is the node number.

Finally, the temperature distribution has been found by means of an energy balance, similar to that presented in Equation (1.13):

$$\rho \cdot C_p \cdot \frac{\partial T}{\partial t} = \frac{\partial}{\partial x}\left(k_x \cdot \frac{\partial T}{\partial x}\right) + \frac{\partial}{\partial y}\left(k_y \cdot \frac{\partial T}{\partial y}\right) + \frac{\dot{Q}}{V_{sys}} \qquad \textbf{(Eq. 1.20)}$$

where k_x and k_y are the values for the thermal conductivity in the x and y directions and V_{sys} is the volume of the relevant part of the system (either solid or liquid).

The model was validated by comparing the results of the simulations to those from pieces of lamb. The model has also been used to simulate the heating of particles with different shapes and under different orientations, the results of which have been presented previously.

Later on, Zhang and Fryer (1993) extended the work subsequently by using commercial software to simulate the behavior of a two-phase system containing different numbers of particles. The same commercial software was also used by Fu and Hsieh (1999) to simulate the temperature distribution in a two-dimensional OH system. The simulation results were compared with experiments made in an ohmic heater that was especially designed to meet the main assumptions of the model (a two-dimensional heating system containing a fluid and a single solid particle). They concluded that the boundary conditions and physical property values were crucial to obtain a reliable simulation.

3.2.2. Model for Multi-particle Mixtures in a Static Heater Containing a Fluid

The case of a mixture of particles in a static heater containing a fluid was studied (Sastry, Palaniappan, 1992). This is a three-dimensional finite element model aiming at predicting the temperature of the mixture of a liquid in which various particles are suspended. The most accurate solution has to be obtained considering the existence of a particle size distribution, having the heat transfer problem to be solved for each particle. Such solution is unlikely to be applied in practice due to the extreme computational effort needed. Instead, an "average size" particle can be assumed, with cubic geometry.

Again, the electric field problem has to be solved. A solution for Equation (1.1), which would be difficult for a mixture of several particles since it would need knowledge of the location and properties of every particle at all points in time instead, the authors obtained a estimation of the electric field distribution using a circuit theory-based approach. Two cases were analyzed:

- *mixtures of several particles involving large particle populations*. Such a mixture is considered to be composed of a continuous (fluid) and a discrete (particles) phase. The equivalent electrical circuit is that of parallel fluid (R_{fP}) and particles (R_{pP}) resistances, and in series with a liquid resistance (R_{fS}) therefore, the total resistance (R) is:

$$R = R_{fS} + \frac{R_{fP} \cdot R_{pP}}{R_{fP} + R_{pP}} \qquad \textbf{(Eq. 1.21)}$$

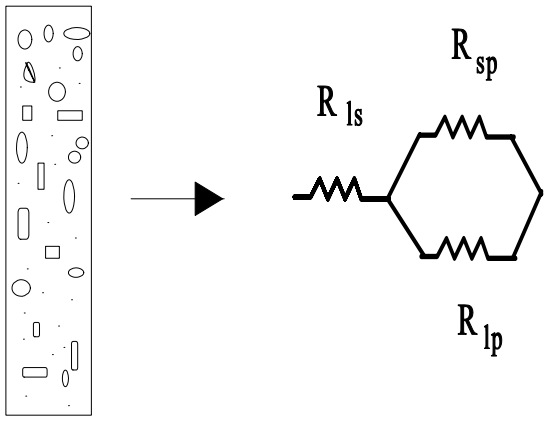

and:

$$R_{fS} = \frac{l_{fS}}{A_{fS} \cdot \sigma_f} \qquad \textbf{(Eq. 1.22)}$$

$$R_{pP} = \frac{l_{pP}}{A_{pP} \cdot \sigma_p} \qquad \textbf{(Eq. 1.23)}$$

$$R_{fP} = \frac{l_{fP}}{A_{fP} \cdot \sigma_f} \qquad \textbf{(Eq. 1.24)}$$

where l_{fS}, l_{fP} and l_{pP} are the lengths of each phase respectively, which are related to the length of the heater (l) and to each other by

$$l = l_{fS} + l_{fP} \qquad \textbf{(Eq. 1.25)}$$

and by

$$l_{pP} = l_{fP} \qquad \textbf{(Eq. 1.26)}$$

and for A_{fS}, A_{fP} and A_{pP} (the cross sectional areas of each phase), they are related to the cross sectional area of the heater (A) and to each other by

$$A = A_{fS} = A_{pP} + A_{fP} \quad \textbf{(Eq. 1.27)}$$

In a similar way to Kopelman (1966), it was assumed that the cross sectional area and length of the discrete phase (particles) could be estimated from the volume fraction of that phase (ε_p) by

$$A_{pP} = A \cdot \varepsilon_p^{2/3} \quad \textbf{(Eq. 1.28)}$$

and

$$l_{pP} = l \cdot \varepsilon_p^{1/3} \quad \textbf{(Eq. 1.29)}$$

Finally, the electric field was calculated using

$$V = I \cdot R(x) \quad \textbf{(Eq. 1.30)}$$

where *R(x)* is the resistance as calculated by Equation (21) up to position *x*, where the voltage (*V*) is to be calculated.

- *mixtures with relatively small numbers of particles*. In this situation the orientation and location of the particles are easily known, thus the equivalent resistance can be calculated separately for zones with or without particles. For the former, the equivalent resistance (*R*) can be calculated as in Equation (1.21) while for the latter, the equivalent resistance simply equals R_{fS}, as in Equation (1.22). The electric field can then be calculated using Equation (1.30).

The next problem is the one of heat generation. This has been solved for this model as explained previously by using Equations (1.3) to (1.5).

Finally, the energy balance must be established for the fluid phase and the particles, to allow the determination of temperatures of each phase during the heating process. For the fluid phase, Equation (1.6) was slightly modified (Equation (1.6) is valid for the more general case of a continuous ohmic heater) for usage in a static (batch) ohmic heater, which yields:

$$\rho_f \cdot V_f \cdot C_{pf} \cdot \frac{T_f^{n+1} - T_f^n}{\Delta t} = -U \cdot A_w \cdot \left(\overline{T}_f - \overline{T}_{air}\right) - n_p \cdot A_p \cdot h_{fp} \cdot \left(\overline{T}_f - \overline{T}_{ps}\right) + \dot{Q}_f \quad \textbf{(Eq. 1.31)}$$

where V_f is the volume of the fluid, *n* is the time step index, $\overline{T}_{air}$ is the average temperature of the air surrounding the heater and

$$\overline{T}_f = \frac{T_f^{n+1} - T_f^n}{2} \qquad \textbf{(Eq. 1.32)}$$

$$\overline{T}_{ps} = \frac{T_{ps}^{n+1} - T_{ps}^n}{2} \qquad \textbf{(Eq. 1.33)}$$

For the particles, Equation (1.13) holds with Equation (1.16) as the boundary condition.

The simulations were carried out and compared to the experimental results obtained with potato cubes of various sizes heated in a static ohmic heater containing phosphate solutions of various concentrations to simulate fluid phases with different electrical conductivities. This mathematical model was considered to be in agreement with the experiments. Critical parameters were found to be the a) conductivities of liquid and solid phases and b) volume fraction of each phase. This model has been compared with the one presented in the previous section in terms of their capability of predicting the behavior of the static ohmic heater in a worst-case scenario (Sastry and Salengke, 1998). The assessment of which model is more conservative depends on whether the particles are more or less conductive than the fluid.

1. Model for Multi-particle Mixtures in a Continuous Flow Heater Containing a Fluid

The model described in previous section for a static heater has been extended to the situation of a continuous flow heater by Sastry (Sastry, 1992). Equations and assumptions were essentially the same [Equations (1.23) to (1.33)], in the introduction of fluid and particle flow in and out of the system. Both fluid and particles will increase in temperature (and thus conductivity) during their path through the heater and therefore the voltage drop must be calculated not for the whole heater but separately for each of the incremental sections into which the heater must be divided for the calculations. As a consequence of this, Equations (1.23) to (1.30) have to be applied separately for each of those sections, in order to determine the electric field. Subsequently, Equations (1.3) to (1.5) need to be applied for the heat generation and finally Equations (1.31) to (1.33) are applied to resolve the thermal problem.

The simulations performed with this model allowed several important aspects of continuous processing with OH technology, to be emphasized

- although when a multi-particle mixture of low conductivity is present these particles tend to heat faster than the fluid, if an isolated low conductivity particle crosses the system it can be underprocessed;

- the residence time distribution and the fluid-particle heat transfer coefficient are crucial aspects to consider when designing a continuous heater.

These results were confirmed and extended by Orangi *et al.* (1966), who studied a similar problem when investigating the continuous flow sterilization of solid-liquid food mixtures by OH.

2. Other Models

Other models of the behavior of particle/fluid mixtures subjected to OH have been developed. Benabderrahmane and Pain (2000) presented a model based on the principle of a mean slip velocity between the fluid and the particles in plug flow (the Slip Phase Model). The existence of a difference between the velocity of the fluid and that of the particles has been demonstrated by Lareo *et al.* (1994, 1995), Liu *et al.* (1993), Fairhurst (1998), and Fairhurst and Pain (1999) and therefore is considered in this model. It also takes into consideration internal heat generation, convective heat transfer and heat conduction within the solid particles, although the heater walls are assumed to be adiabatic. One of the main contributions of this model is that it demonstrates the importance of the temperature gradient inside the particles. It also confirmed results obtained earlier by other authors (see, e.g., Sastry) showing that for a mixture of particles in a fluid, the process critical point is situated in the fluid and not in the particles. For conventional heating processes the critical point is in the particles.

Other in depth problems have been addressed that arose during the modeling effort during the previous two decades. Lacey (1995 a,b) and Lacey *et al.* (1999), who studied the problem of thermal runaway while modeling OH, firstly by considering only heat transfer by conduction and secondly including heat convection, which was found to dominate heat conduction (Please *et al.*, 1994). In the same line, a diffusion-convection problem was addressed by Kavallaris and Tzanetis (2002), having the Heaviside function representing the food resistivity (which is the inverse of the conductivity).

4. Basic ohmic heater configurations

Basic configurations for ohmic heaters will be presented but it does not imply that these are the only ones available. In fact, other possibilities exist, including some under development, which are not considered here. The fundamental requirements for OH equipment for food processing are a pair of electrodes, a container for the food to be processed and an alternating power supply.

The ohmic heater can be integrated into a batch or continuous process. The most typical configuration for the ohmic heater is that of a horizontal cylinder with one electrode placed in each extremity for a batch process (Figure 1.8a). For a continuous process the design of the ohmic heater can be more variable, depending on the manufacturer. It can range from a simple tube with pairs of opposing electrodes mounted on the tube walls opposite to each other (Figure 1.8b), to coaxial tubes acting as electrodes with the food flowing between (Figure 1.8c), or a vertical tube with the electrodes embodied at regular intervals (Figure 1.8d). As the electric field is perpendicular to the food flow for the equipment represented in Figure 1.8b and c, these configurations are often called *cross-field*. If the electric field is parallel to the food flow in the (Figure 1.8d) the configuration obtained is termed *in-field*.

Ideally, it is possible to consider that in the cross-field configuration the electric field strength is constant. For the in-field configuration, σ will increase and therefore the field strength experienced by the product will increase as it approaches the outlet. The product will heat during its path through the heater. To minimize this effect, when multiple electrodes are used in series (Figure 1.8d) they are spaced to account for the increase of σ of food with temperature. Therefore, as the product approaches the outlet of the heater a lower value of the electric field strength is needed and this is accomplished by increasing the spacing between each pair of electrodes.

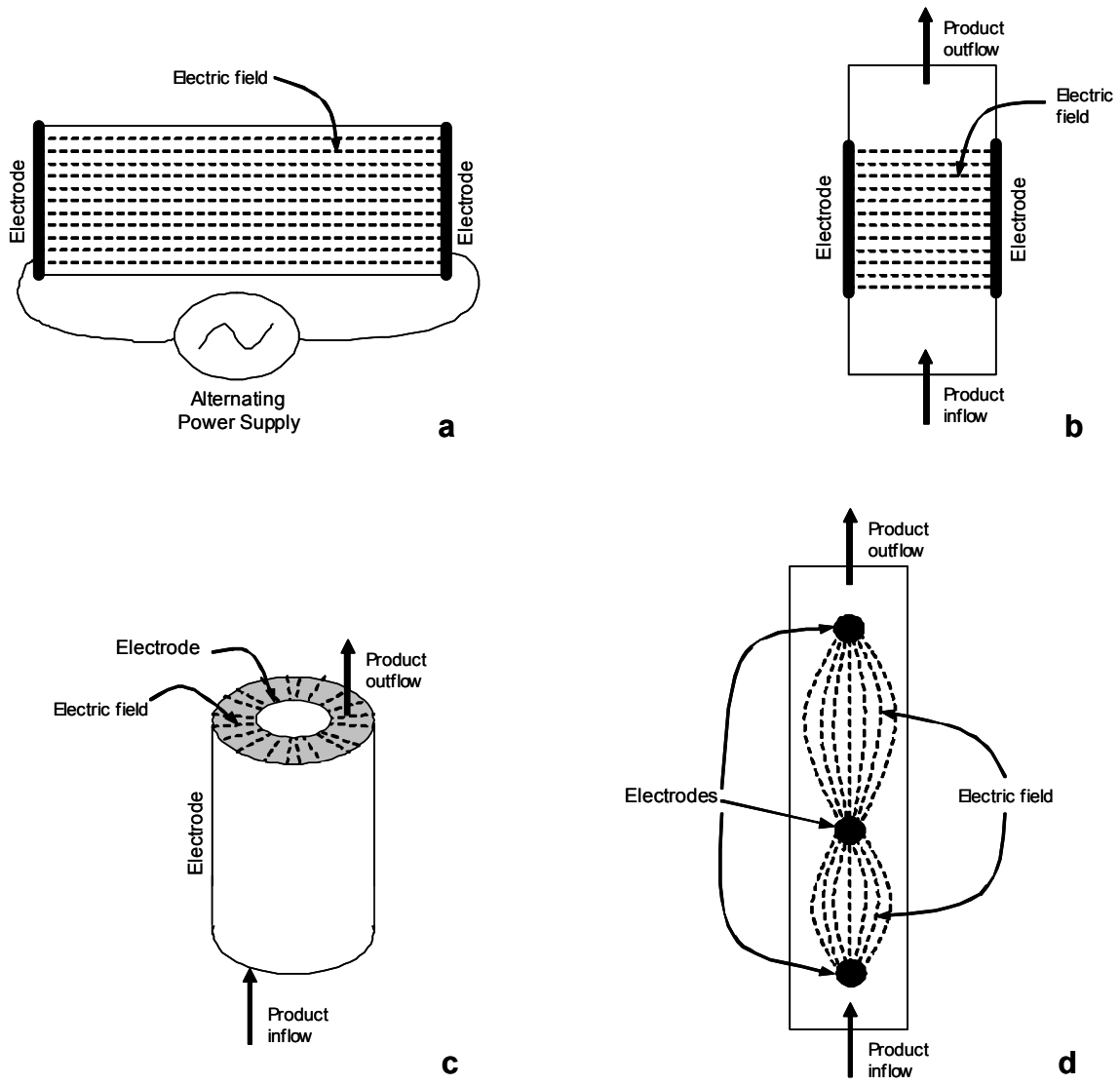

Figure 1.8: Basic configurations for ohmic heaters: a) batch; b-d) continuous. b) and c) correspond to the cross-field configuration while d) corresponds to the in-field configuration, depending on if the electric field lines are perpendicular or parallel to the direction of the flow of the food, respectively.

The choice of the best configuration will obviously depend on the food being processed and the objectives of the process (*e.g.* cooking, pasteurization, sterilization).

Batch processes are typically used to cook e.g. meat products (Piette and Brodeur, 2001), while continuous processes are more appropriate for viscous fluids or fluids with particulates.

5. Applications

The OH technology provides new, high-added-value, shelf-stable products with a quality unachievable by the traditional processing technologies. The process can be used in a) the thermal processing of high-acid food products such as tomato-based sauces, b) pasteurization of whole liquid egg (Parrott, 1992) c) fish pastes, d) on meat products processing as an alternative cooking to the traditional smokehouse.

5.1. Meat Products

The first experiments using OH in meat products were made in Finland in the 1970's, but operational difficulties led to the abortion of the project. Later on, in the 1990's a project for cooking liver pâté and hams was carried out in France by the Meat Institute Development Association (ADIV) and Électricité de France (EDF).

One OH application is thawing process, when the traditional thawing methods cannot provide high quality products. Wang *et al.* (2002) applied the technology to frozen meat samples, in a liquid-contact thawing method. The results demonstrated a uniform and quicker thawing process. Also, meat properties such as color and pH were not changed significantly and the final products achieved a good thawing quality. These results demonstrate the potential uses of OH in contact thawing, especially for meat products. Although the initial batch results were very promising, the attempts to develop a prototype version for a continuous cooking process were unsuccessful.

Canadian scientists (Piette and Brodeur, 2001) have been working on the ohmic cooking of meat products (sausages and ham) with promising results in batch operations. Brine-cured meat products were found to be admirably suited to OH having extremely reduced cooking times (*e.g.* a ham weighing one kilogram was cooked in less than two minutes). However, these flash cooking times did not reduce the bacterial load to levels that guaranteed product safety. Pasteurization had to be taken into consideration and a time-temperature profile was established. However, under these conditions, no noticeable changes were reported in the products' taste, texture or shelf-life.

Combined ohmic and conventional cooking of hamburger patties has recently been patented as a new method of cooking (Farid, 2001). The method is based on passing electric current through the meat patties causing internal heat generation. It has been found to reduce cooking time up to half the time usually required in conventional cooking. It was also

concluded that ohmic heating has no effect on the quality of the ohmically-cooked hamburger (Ozkan *et al.*, 2004). However, it is noteworthy that this quality related conclusion may not be true when ohmic heating is applied to other food products.

5.2. Fruit and Vegetable Products

Strawberry fruit jams are extremely important for the Portuguese fruit jams industry because they account for most of its sales (around 90%). The search for alternative processing technologies leading to higher quality products is one of the main goals and the economic viability of this technology depends on the possibility of applying it to most of the products processed by this industry (Castro *et al.*, 2003). In the study by Castro *et al.* (2003), several strawberry based products were tested by OH. The obtained results showed that, for most of the products, high heating rates could be achieved, despite the significant differences of σ between the products stet test. Also, the increase of the applied electric field could increase the heating rate (Figure 1.9 a and b).

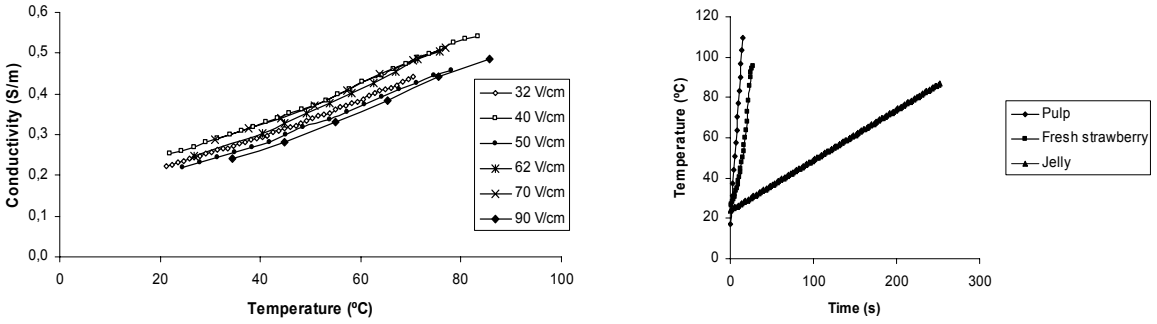

Figure 1.9: a) The influence of electric field on electrical conductivity of strawberry pulp; b) differences in heating rates of three strawberry based products (Castro *et al.*, 2003).

The suitability of OH for strawberry products having different solids concentrations, or Brix values, was also tested (Castro *et al.*, 2003). σ was shown to decrease with the increase of solids content in a mixture of particles with a bi-modal particle size distribution, but the decrease was more significant for the bigger particles tested (Figure 1.10a). The results also suggest that for higher solids content (> 20 % w/w) and sugar contents over 40.0 ºBrix, σ is too low to use in the conventional ohmic heaters and a new design is required (Figure 1.10b).

Most of the commercially available vegetables are submitted to more than one thermal treatment (*e.g.* blanching, sterilization). Wang and Sastry (1997) studied the effects of an

ohmic pre-treatment and found no significant changes in the moisture content of the final products. This technology might be an alternative to conventional blanching treatments.

It has already been demonstrated that the texture of fruits and vegetables is greatly influenced by temperature and thermal processing (Hoogzand and Doesburg, 1961; Bartolome and Hoff, 1972). The firmness of processed vegetables (*e.g.* canned cauliflower, asparagus) can be improved by low-temperature, long-time pre-treatments. Eliot *et al.* (1999) studied the influence of precooking by OH on the firmness of cauliflower. The experimental data showed that OH combined with low-temperature precooking in saline solutions offers a viable solution to HTST sterilization of cauliflower florets. A similar study was also performed with potato cubes (Eliot *et al.*, 1999; Eliot and Goullieux, 2000), and concluded that an ohmic pre-treatment prevented loss of firmness when compared to a conventional pre-treatment (50 % in some cases).

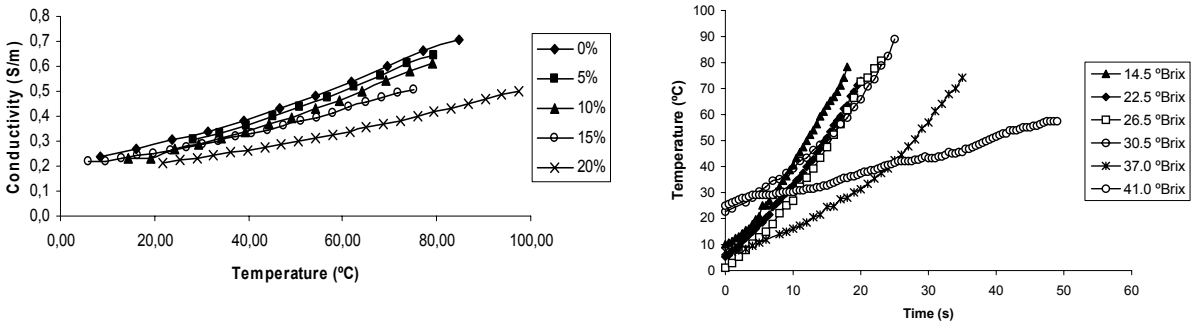

a **b**

Figure 1.10: a) The influence of solid particles concentration on electrical conductivity of strawberry pulp; b) differences in heating rates of strawberry pulps with different Brix values (Castro *et al.*, 2004).

5.3. Seafood products

Most of the scientific literature concerning seafood products deals with surimi. Surimi is stabilized myofibrillar proteins from fish muscle, which is used in several Japanese food products. The textural properties of the products treated by OH were found to be superior to those heated in a 90 ºC water bath. Also, an increase in shear stress and shear strain of surimi gels was found when ohmic technology was applied (Yongsawatdigul *et al.*, 1995) and, in addition, a superior gel quality was achieved. Higher heating rates are not beneficial to surimi manufacture (Yongsawatdigul and Park, 1996). Instead, slow heating rates produce stronger gels. Ohmic processing of surimi is very effective in obtaining a wide range of linear heating rates which plays an important role in the study of surimi gelation.

It is expected that with the continuous research and development of new electrode materials and of equipment with innovative design, several other food applications using OH will soon be possible.

5.4. Other applications

The use of an OH microreactor (Figure 1.11) for biological sample processing for the purpose of genetic analysis was reported by Cordero *et al.* (2003). The rapid and uniform heating capabilities of OH are further enhanced when conducted on a miniature scale, thereby promoting this heating strategy for cell lysis in a microsystem. Biological cells suspended in an electrolyte can be exposed to OH-mediated thermal treatment optimized for metabolite release.

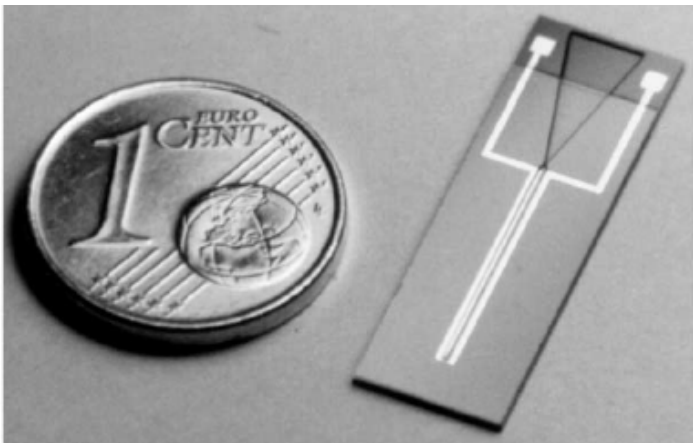

Figure 1.11: Silicon ohmic heater micro-reactor

6. Economics

Although data on commercial OH operations are scarce there are several OH facilities in operation around the world. Furthermore, several applications of OH are still under study and various products are being processed in pilot scale equipment, but not at industrial scale. As a consequence, processing costs were not yet fully assessed.

With the objective of determining the economic viability of this technology, a comparison of OH with other food processing methods was made by Allen *et al.* (1996). In their study, several assumptions were made about the products, facilities, and components of costs. Estimated values for labor, energy, quality control, packing, maintenance and equipment depreciation were provided by well trained food technologists and researchers. The product and production characteristics of the food products under analysis are summarized in Table 1.1 and Table 1.2.

Table 1.1: Low-acid formulated products: product and production characteristics for various processing technologies.

	Processing technology		
	Retorting	**Freezing**	**Continuous-flow OH**
Studied products	Fresh or frozen meat and vegetables	Fresh or frozen meat and vegetables	Fresh or frozen meat and vegetables
Carrier	Gravy or sauce	Gravy or sauce	Gravy or sauce
Package	Microwavable tray	Microwavable tray	Microwavable tray
Product storage	Shelf-stable	Frozen	Shelf-stable
Product shelf life	About 1 year	About 1 year	About 1 year
Annual production	5.44 million Kg	5.44 million Kg	OH 75: 3.18 million kg[1] OH 300: 12.70 million kg[1]

[1] – per main ohmic heaterSource: Allen *et al.* (1996)

Table 1.2: High-acid formulated products: product and production characteristics for various processing technologies.

	Processing technology		
	Freezing	**Conventional thermal heating (tubular heat exchanger)**	**Continuous-flow ohmic eating**
Studied products	Fresh fruit	Fresh fruit	Fresh or frozen fruit
Carrier	Sugar syrup	Sugar syrup	Sugar and starch syrup
Package	Plastic tubs	Bag-in-box	Bag-in-box
Product storage	Frozen	Shelf-stable	Shelf-stable
Product shelf life	About 1 year	1 year	1 year
Annual production	15.88 million kg	15.88 million kg	OH 75: 1.58 million kg[1] OH 300: 6.3 million kg[1]

[1] – per main ohmic heater

Source: Allen *et al.* (1996)

The main difference between the two types of ohmic heaters used in this study, OH 75 and OH 300, as their power is 75 and 300 kW, respectively.

The conclusions withdrawn from this study show the importance of the type of product and of the power of the ohmic heater on the economics of the process. The OH 300 appears to be a viable alternative to conventional processing technologies when processing low-acid foods. It may also be a useful technology for high-acid foods, but only if high quality products are required.

Studies conducted at the Agri-Food Canada's Food Research and Development Centre (FRDC) with meat products, where the traditional smokehouse cooking was replaced by an ohmic process, indicated that energy savings of at least 70% could be achieved. In fact, the specific energy consumption required to cook a brine-cured meat product was of the order of 210 and 258 $kJ \cdot kg^{-1}$, compared to 859 $kJ \cdot kg^{-1}$ for conventional cooking (Piette and Brodeur, 2001). In an industrial production context, energy savings would undoubtedly be even greater, as considerably less energy would be lost because of optimally designed equipment. Also, time savings would probably be considerable (a few minutes with ohmic cooking as opposed to a week with the traditional smoking house) indicating that ohmic cooking is an economic method for making excellent meat products.

To obtain more accurate results on the profitability of this technology when applied to specific facilities, it is necessary to consider full production schedules, startup costs, as well as considerations on product type (Allen *et al.*, 1996). Such actions must be taken in order to establish the commercial feasibility in this technology.

7. Future Challenges

OH is a food processing technology that presents several advantages when compared to existing technologies. It can improve food quality and is a clean technology. Also the economic advantages of its use have been demonstrated.

The application of OH for food processing is not well characterized and not all its potentialities have been fully exploited due to the complexity of the phenomena occurring during OH processing and the complexity of food materials.

In conclusion, if attention is paid to the phenomena occurring during OH there is a) electrical current generation and transport, b) heat generation and transport and c) eventually mass and momentum transport. These phenomena are intimately associated and interact with each other. Also, there are several consequences occurring as a result of the electrical current passage and heat being generated because of the electrical current. These reactions include thermal and electrical microbial killing, nutrients modification and enzyme inactivation.

Various reactions must be considered to occur in a food matrix that includes in its composition several components with different electrical, heat, mass and momentum transfer properties. Obviously, each individual component and their interactions will play a decisive role in the efficiency of the OH process. Such a role may be played on the thermal killing of the microbial population or on the modification of the functional, nutritional and organoleptic properties of foods. This reasoning clearly points out the complexity associated with thermal processing of foods and in particular with OH thermal processing.

Several additional points associated with the fundamentals of ohmic processing must be addressed. In the particular case of a continuous flow ohmic heater, the flow properties of the food components must be fully characterized and related to the temperature profiles of those components. These phenomena may be considered from a macroscopic point of view. However, microscopic phenomena also take place. At this level, disruption of cell membranes, structural changes in food components (including enzyme inactivation) and mass transfer phenomena must be considered.

Also, novel applications and a deeper knowledge of current applications must be obtained. There is lack of information on metabolic and morpho-physiological effects of ohmic heating (or electric field).

Research is required in the following areas:

- to asses the effect of OH on microbial structures such as spores namely in terms of activation;
- to evaluate the effect of OH on metabolic pathways that lead to the production of toxins (e.g. micotoxins, antimicrobials);
- to evaluate the effect of OH on genetic reproductive structures namely DNA damage, DNA repair enzymes, cell cycle;
- to evaluate the effect of OH on cell to cell communication and signal transduction;
- to assess the risk of the electric field as a potential mutagenic for biological cells (virus, bacteria and eukaryotic cells);
- to understand transport phenomena and pore formation of biological membranes when a low electric field is present ;
- to study the use of an electrical field on purification and extraction processes in order to improve the yields and purification of biological macromolecules;
- to study and optimize the use of continuous or intermittent electric field on batch and continuous fermentative processes, tissue cells production and other biomedical applications;
- to study the applicability of OH for different product formulations (a wide range of sugar or fat concentrations) and to determine its economical viability;
- to characterize the flow of the food components when being processed in an ohmic heater by developing adequate hydrodynamic models;
- to develop methods and models that will allow a more precise mapping of temperatures on foods submitted to OH;
- to develop general models that can adequately describe ohmic processing of foods;
- to implement these models so that an adequate control of the rate of heating can be achieved, thus minimizing the thermal degradation effects on desirable product attributes but maintaining a safe product;
- to study if electrical conductivity measurements can be used as a rapid method to determine food authenticity.

In terms of process development, the more relevant points to be addressed are:

- food preservation (with respect to spores and filamentous fungi);

- food processing – application of OH to particulate foods (food purees containing particles, food suspensions, etc.) and foods with a non-Newtonian rheological behavior; to combine OH with other processing techniques such as high pressures or irradiation.
- food processing – integration of OH in existing food industries as an alternative to conventional pre-heating, in those cases where higher quality products and more efficient processing are to be obtained;
- food thawing and water removal processes (evaporation and dehydration);
- to develop alternative designs for ohmic heaters, adapted to specific food processes (e.*g.* to efficiently heat low electrical conductivity foodstuffs);
- to develop new packages in which foods can be ohmically heated
- to study the application of OH on controlled drug release systems
- to design new bio-reactors for ohmically assisted biological processes

This technology will gain an increasing importance in food processing as a deeper understanding of the fundamental science is achieved.

8. References

Allen, K., Eidman, V., Kinsey, J., (1996). An economic-engineering study of ohmic food processing. Food Technology 50:269-273.

Alvarado, D., Viteri, N.P., (1989). Efecto de la temperatura sobre la degradación aerobica de vitamina C en jugos de frutas cítricas. Archivo Latinoamericano de Nutricion 39(4):601-612.

Alwis, A.A.P., Fryer, P.J., (1990). A finite-element analysis of heat generation and transfer during OH of food. Chemical Engineering Science 45 (6):1547-1559.

Alwis, A.A.P., Fryer, P.J., (1990). The use of network theory in the finite-element analysis of coupled thermo-electric fields. Communications of Applied Numerical Methods 6:61-66.

Alwis, A.A.P., Halden, K., Fryer, P.J., (1989). Shape and conductivity effects in the ohmic heating of foods. Chemical Engineering Research and Design 67: 159-168.

Anon, (1982). Theory and application of electrolytic conductivity measurement. The Foxboro Company, Foxboro, MA (unpublished).

Barbosa-Cánovas, G.V., Pothakamury, U.R., Palou, E., Swanson, B.G., (1998). Biological effects and applications of pulsed electric fields for the preservation of foods. In: Barbosa-Cánovas, G.V., Pothakamury, U.R., Palou, E., Swanson, B.G., eds. Nonthermal Preservation of Foods. New York: Marcel Dekker.

Bartolome, L.G., Hoff, J.H., (1972). Firming of potatoes: biochemical effects of pre-heating. Journal of Agriculture and Food Chemistry 20:266-270.

Benabderrahmane, Y., Pain, J.P.. Thermal behaviour of a solid/liquid mixture in an ohmic heating sterilizer - slip phase model. Chemical Engineering Science 55:1371-1384, 2000.

Castro, A.J. Swanson, B.G., Barbosa-Cánovas, G.V., Meyer, R., (2001). Pulsed electric field modification of milk alkaline phosphatase activity. In: Barbosa-Cánovas, G.V., QH Zhang, eds. Pulsed Electric Fields in Food Processing: Fundamental Aspects and Applications (Vol. 3). Lancaster, PA: Technomic Publishing Co., pp 65-83.

Castro, I., Teixeira, J.A. , Salengke, S., Sastry S.K., Vicente, A.A., (2004). Ohmic heating of strawberry products: electrical conductivity measurements and degradation kinetics. Innovative Food Science and Emerging Technologies.

Castro, I., Teixeira, J.A. , Vicente, A.A., (2002). The influence of food additives on the electrical conductivity of a strawberry pulp. Proceedings of the 32nd Annual Food Science and Technology Research Conference, University College Cork, Cork, Ireland.

Castro, I., Teixeira, J.A. , Vicente, A.A., (2003). The influence of the presence of an electric field on lipoxygenase and β-galactosidase inactivation kinetics. Proceedings of NFIF 2003 – New Functional Ingredients and Foods – Safety, Health and Convenience, Copenhagen, Denmark.

Castro, I., Teixeira, J.A., Vicente, A.A., (2003). The influence of field strength, sugar and solid content on electrical conductivity of strawberry products. Journal of Food Process Engineering 26:17-29.

Cho, H.Y., Yousef, A.E., Sastry S.K., (1999). Kinetics of inactivation of *Bacillus subtilis* by continuous or intermittent ohmic and conventional heating. Biotechnology and Bioengineering 62:368-372.

Cho, H.Y., Yousef, A.E., Sastry, S.K., (1996). Growth kinetics of *Lactobacillus acidophilus* under ohmic heating. Biotechnology and Bioengineering 49:334-340.

Denys, S., Loey, A.M., Hendrickx, M.E., (2000). A modelling approach for evaluating process uniformity during batch high hydrostatic pressure processing: combination of a numerical heat transfer model and enzyme inactivation kinetics. Innovative Food Science and Emerging Technologies 1:5-19.

Eliot, S.C., Goullieux, A., (2000). Application of the firming effect of low-temperature long-time pre-cooking to ohmic heating of potatoes. Science des Aliments 20:265-280.

Eliot, S.C., Goullieux, A., Pain, J.P., (1999). Combined effects of blanching pretreatments and ohmic heating on the texture of potato cubes. Science des Aliments 19:111-117.

Eliot, S.C., Goullieux, A., Pain, J.P., (1999). Processing of cauliflower by ohmic heating: influence of precooking on firmness. Journal of the Science of Food and Agriculture 79:1406-1412.

Fairhurst, P.G., (1998). Contribution to the study of the flow behaviour of large nearly neutrally buoyant spheres in non-newtonian media: Application to HTST processing. PhD dissertation, Département de Génie Chimique, Université de Technologie de Compiègne, Compiègne, France.

Fairhurst, P.G., Pain, J.P., (1999). Passage time distributions for high solid fraction solid-liquid food mixtures in horizontal flow: unimodal size particle distributions. Journal of Food Engineering 39:345-357.

Fryer, P.J., Li, Z., (1993). Electrical resistance heating of foods. Journal of Food Science and Technology 4:364-369.

Fu, W.R., Hsieh, C.C., (1999). Simulation and verification of two-dimensional ohmic heating in static system. Journal of Food Science 64:946-949.

Garotte, R.L., Silva, E.R., Bertone, R.A., (2003). Kinetic parameters for thermal inactivation of cut green beans lipoxygenase using unsteady-state methods. Latin American Applied Research 33:87-90.

Getchel, B.E., (1935). Electric pasteurization of milk. Agriculture Engineering 16(10): 408-410.

Grahl, T., Markl, H., (1996). Killing of microorganisms by pulsed electric fields. Applied Microbiology and Biotechnology, 45:148-157.

Hayt, W.H., (1981). Engineering Electromagnetics. 4th ed. New York: McGraw-Hill.

Ho, S.Y., Mittal, G.S., Cross, J.D., (1997). Effects of high field electric pulses on the activity of selected enzymes. Journal of Food Engineering 31:69-84.

Hoogzand, C., Doesburg, J.J., (1961). Effect of blanching on texture and pectin of canned cauliflower. Food Technology 15:160-163.

Johnson, J.R., Braddock, R.J., Chen, C.S., (1995). Kinetics of ascorbic acid loss and nonenzymatic browning in orange juice serum: experimental rate constants. Journal of Food Science 60(3):502-505.

Kavallaris, N.I., Tzanetis, D.E., (2002). An ohmic heating non-local diffusion-convection problem for the Heaviside function. ANZIAM Journal 44(E): E114-E142.

Khalaf, W.G., Sastry S.K., (1996). Effect of fluid viscosity on the ohmic heating rate of solid-liquid mixtures. Journal of Food Engineering 27:145-158.

Kim, H.J., Choi, Y.M., Yang, T.C.S., Taub, I.A., Tempest, P., Skudder, P., Tucker, G., Parrott, D.L., (1996). Validation of OH for quality enhancement of food products. Food Technology 50:253-261.

Kim, L., Hwang, M.S., Kim, E.S., 1995). Extraction, partial characterization, and inhibition patterns of polyphenol oxidase from burdock (*Arctium lappa*). In: CY Lee, JR Whitaker, eds. Enzymatic Browning and It's Prevention. Washington, D. C.: American Chemical Society Symposium Series 600, pp 267-276.

Kopelman, I.J., (1966). Transient heat transfer and thermal properties in food systems. PhD dissertation, Michigan State University, East Lansing, MI.

Lacey, A.A., (1995). Thermal runaway in a non-local problem modelling ohmic heating. Part I: Model derivation and some special cases. European Journal of Applied Mathematics 6: 127-144 (a).

Lacey, A.A., (1995). Thermal runaway in a non-local problem modelling ohmic heating. Part II: General proof of blow-up and asymptotes of runaway. European Journal of Applied Mathematics 6: 201-224, (b).

Lacey, A.A., Tzanetis, D.E., Vlamos, P.M.. Behaviour of a non-local reactive convection problem modelling ohmic heating of food. The Quarterly Journal of Mechanics and Applied Mathematics 52:623-644, 1999.

Lareo, C., (1995). The vertical flow of solid-liquid food mixtures. PhD dissertation, Department of Chemical Engineering, University of Cambridge, Cambridge, UK.

Lareo, C., Branch, C.A., Fryer, P.J., (2004). The flow behaviour of solid-liquid food mixtures. Proceedings of Institute of Chemical Engineers Symposium: Food Process Engineering, 1994, pp203-210.

Larkin, J.W., Spinak, S.H., (1996). Safety considerations for ohmically heated, aseptically processed, multiphase low-acid food products. Food Technology 50(5):242-245.

Lima, M., (2001). Ascorbic acid degradation kinetics and mass transfer effects in biological tissue during ohmic heating. PhD dissertation, Ohio State University, Columbus, OH, 1996.

Lima, M., Sastry S.K., (1999). The effects of ohmic frequency on hot-air drying and juice yield. Journal of Food Engineering 41:115-119.

Liu, S., Pain, J.P., Procter, J., Alwis, A.A.P., Fryer, P.J., (1993). An experimental study of particle flow velocities in solid-liquid food mixtures. Chemical Engineering Communications 124:97-114.

Loey, A., Verachtert, B., Hendrickx, M., (2002). Effects of high electric field pulses on enzymes. Trends in Food Science & Technology 12:94-102.

Ludikhuyze, L., (1998). High pressure technology in food processing and preservation: a kinetic case study on the combined effect of pressure and temperature on enzymes. PhD dissertation. Katholieke Universiteit Leuven, Leuven, Belgium.

Mizrahi, S., Kopelman, I., Perlaman, J., (1975). Blanching by electroconductive heating. Journal of Food Technology 10:281-288.

Moses, B.D., (1938). Electric pasteurization of milk. Agriculture Engineering 19: 525-526.

Orangi, S., Sastry, S.K., Li, Q., (1998). A numerical investigation of electroconductive heating in solid-liquid mixtures. International Journal of Heat and Mass Transfer 41:2211-2220.

Ózkan, N., Ho, I., Farid, M., (2004). Combined ohmic and plate heating of hamburgerpatties: quality of cooked patties, Journal of Food Engineering 63:141–145

Palaniappan, S., Sastry S.K., (1991). Modelling of electrical conductivity of liquid-particle mixtures. Food and Bioproducts Processing, Part C, Transactions of the Institution of Chemical Engineers 69:167-174.

Palaniappan, S., Sastry S.K., Richter, E.R., (1992). Effects of electroconductive heat treatment and electrical pretreatment on thermal death kinetics of selected microorganisms. Biotechnology and Bioengineering 39:225-232.

Palaniappan, S., Sastry, S.K, (1991). Electrical conductivities of selected solid foods during OH. Journal of Food Process Engineering 14:221-236.

Palaniappan, S., Sastry, S.K., (1991). Electrical conductivity of selected juices: influences of temperature, solids content, applied voltage, and particle size. Journal of Food Processing Engineering 14:247-260.

Parrott, D.L., (1992). Use of OH for aseptic processing of food particulates. Food Technology 45(12):68-72.

Piette, G., Brodeur, C., Ohmic cooking for meat products: The heat is on! Le Monde Alimentaire (2001). 5(6):22-24.

Please, C.P., Schwendeman, D.W., Hagan, P.S., (1994). Ohmic heating of foods during aseptic processing. IMA Journal of Mathematics for Business and Industry 5: 283-301.

Saguy, I., Kopelman, I.J., Mizrah, S., (1978). Simulation of ascorbic acid stability during heat processing and concentration of grapefruit juice. Journal of Food Process Engineering 2:213-225.

Sastry S.K., Barach, J.T., (2000). Ohmic and inductive heating. Journal of Food Science 65:42-46.

Sastry S.K., Palaniappan, S., (1992). Ohmic heating of liquid-particle mixtures. Food Technology 45(12):64-67.

Sastry S.K., Salengke, S., (1998). Ohmic heating of solid-liquid mixtures: a comparison of mathematical models under worst-case heating conditions. Journal of Food Process Engineering 29:441-458.

Sastry, S.K., (1992). A model for heating of liquid-particle mixtures in a continuous flow ohmic heater. Journal of Food Process Engineering 15:263-278.

Sastry, S.K., Li, Q., (1996). Modelling the ohmic heating of foods. Food Technology 50(5):246-249.

Sastry, S.K., Palaniappan, S., (1992). Mathematical modelling and experimental studies on ohmic heating of liquid-particle mixtures in a static heater. Journal of Food Engineering 15:241-261.

Skuder, P.J., (1989). OH in food processing. Asian Food Journal 4(4):10-11, 1989.

Somogyi, L.P., Ramaswamy, H.S., Hui, Y.H.. Biology, principles and applications. In: Somogyi, L.P., Ramaswamy, H.S., Hui, Y.H., (1996), eds. Processing Fruits: Science and Technology. Vol. 1. Lancaster, PA: Technomic Publishing Co.

Tannenbaum, S., (1976). Ascorbic acid. In: O Fennema, ed. Principles of Food Science. Part I. Food Chemistry, 2nd ed. New York: Marcel Dekker, 1976.

Tetra Pak. The Orange Book. Lund, Sweden: Tetra Pak Processing Systems AB, 1998.

Trammell, D.J., Dalsis, D.E., Malone, R.T., (1986). Effect of oxygen on taste, ascorbic acid loss and browning for HTST-pasteurized, single strength orange juice. Journal of Food Science 61(3):477-489.

Villota, R., Hawkes, J.G., (1992). Reaction kinetics in food systems. In: D Heldman, D Lund, eds. Handbook of Engineering. New York: Marcel Dekker.

Wang, W.C., Chen, J.I., Hua, H.H., (2002). Study of liquid-contact thawing by ohmic heating. Proceedings of IFT Annual Meeting and Food Expo, Anaheim, California.

Wang, W.C., Sastry S.K., (1993). Salt diffusion into vegetable tissue as a pretreatment for ohmic heating: electrical conductivity profiles and vacuum infusion studies. Journal of Food Engineering 20:299-309.

Wang, W.C., Sastry, S.K., (1997). Changes in electrical conductivity of selected vegetables during multiple thermal treatments. Journal of Food Process Engineering 20:499-516.

Yongsawatdigul, J., Park, J.W., (1996). Linear heating rate affects gelation of Alaska pollock and pacific whiting surimi. Journal of Food Science 61(1): 149-153.

Yongsawatdigul, J., Park, J.W., Kolbe, E., (1995). Electric conductivity of Pacific whiting surimi paste during ohmic heating. Journal of Food Science 60(5):922-935.

Yongsawatdigul, J., Park, J.W., Kolbe, E., (1997). Degradation kinetics of myosin heavy chain of pacific whiting surimi. Journal of Food Science 62(4):724-728.

Zareifard, M.R., Ramaswamy, H.S., Trigui, M., Marcotte, M., (2003). Ohmic heating behaviour and electrical conductivity of two-phase food systems. Innovative Food Science and Emerging Technologies 4:45-55.

Zhang, L., Fryer, P.J. (1993). Models for the electrical heating of solid-liquid food mixtures. Chemical Engineering Science 48:633-642.

Chapter 2.

THE EFFECT OF THE ELECTRIC FIELD ON IMPORTANT FOOD PROCESSING ENZYMES: COMPARISON OF INACTIVATION KINETICS UNDER CONVENTIONAL AND OHMIC HEATING

Abstract

The validation of industrial processes in terms of food safety and quality is an extremely relevant issue. This is generally made through the use of biological indicators such as enzymes or microorganisms.

This chapter deals with the determination of the inactivation kinetics of several enzymes, some of them used as time temperature integrators, others affecting quality issues in the food industry. The tested enzymes were polyphenoloxidase, lipoxygenase, pectinase, alkaline phosphatase and β-galactosidase and the inactivation assays were performed under conventional and ohmic heating conditions. The thermal history of the samples (conventionally and ohmically processed) was made equal in order to determine if there was an additional inactivation caused by the presence of an electric field, thus eliminating temperature as a variable. All the enzymes followed first order inactivation kinetics for both conventional and ohmic heating treatments. The presence of an electric field does not cause an enhanced inactivation to alkaline phosphatase, pectinase and β- galactosidase. However, lipoxygenase and polyphenoloxidase kinetics were significantly affected by the electric field, reducing the time needed for inactivation. This effect may be attributed to conformational changes in the protein structure or in the active binding site or loss of prosthetic metal group thus affecting enzyme activity.

Industrial relevance: When an emerging technology is about to be used the validation process has to be performed from the start and no data extrapolation should be made. The hypothesis advanced for the existence of non thermal effects reinforced the need to verify those effects on important food enzymes which is the case of the present research.

1. Introduction

The increased interest of consumers both for healthy and high quality foods has prompted producers to develop new products and new processing technologies. The industrial application of the OH technology is fully dependent on its validation with experimental data in order to evaluate the effects of the electric field on microorganisms, enzymes, toxins and biological tissues.

Several enzymes are used in the food industry aiming at improving food quality (*e.g.* texture and flavor), recovering by-products and achieving higher rates of extraction (Somogyi, 1996; Van Loey, 2002). On the other hand, enzymes may also have negative effects on food quality such as production of off-odors and tastes and altering textural properties. Therefore, control of enzymatic activity is required in many food processing steps in order to promote/inhibit enzymatic activity during processing. Studies on the degradation kinetics of various enzymes were conducted by several authors in order to determine the effects of pulse electric fields on enzymes' inactivation (Barbosa-Canovas *et al.*, 1998; Castro *et al.*, 1994; Ho *et al.*, 1997; Grahl and Markl, 1996). Also, the effects of high hydrostatic pressure processing on enzyme inactivation kinetics were assessed e.g. by Ludikhuyze (1998) and Denys *et al.* (2000).

There is only limited information available concerning the effects of ohmic heating on enzyme activity.

1.1. Process evaluation

The thermal treatment of foods is one of the oldest and more widely used methods to increase shelf-life of foodstuffs. Technological developments such as treatments with high temperatures and short times (HTST) or ultra high temperature (UHT) and the aseptic processing of particulate foods are very interesting from an industrial point of view because they have several advantages related to nutritional and organoleptic aspects. Apart from the heating system used and the way in which heat is generated, it is fundamental to evaluate the impact of the thermal (and also of the non-thermal) effects on microbiological safety (inactivation of microorganisms or reduction of their numbers to acceptable levels) and on quality issues (e.g. texture, flavor).

The validation of a process is not straightforward and most of the times the industrial processes and equipments make it a hard task. The time-temperature integrators (TTIs) offer

an alternative to the thermocouples and the conventional microbiological methods used to quantify the impact of a given thermal treatment. This evaluation is traditionally done by four distinct methods briefly described in the next paragraphs.

1.2. In situ

This method is based on the measurement of some parameters or quality attributes such as vitamins content (Mulley *et al.*, 1975), texture, taste or even color (Hayakawa and Timbers, 1977).

These thermal inactivation values are established using the decimal reduction time (*D*) of the target property in the food while considering first order degradation kinetics.

The main advantage of this method is the possibility of performing direct measurements (in some cases even *on-line*) of the parameter with acceptable accuracy. However, in several situations, the concentration of the naturally occurring element is either far below the detection limit of the analytical method or the analytical method is laborious and expensive.

1.3. Physical-mathematics approach

This method is based on mathematical modeling of the thermal process under well-known sterilization conditions. Several models were proposed for canned foods and particulate foods (Stoforos and Merson, 1990; Larkin, 1989; Skjoldebrand, 1993). One of the major drawbacks of this method is the difficulty of measuring the physical parameters required for the model of which viscosity and heat transfer coefficients are representative examples. Moreover, these models must be microbiologically validated (Martínez and Ocio, 2005).

1.4. Inoculated experimental packs

Another way to validate thermal processes is through the use of inoculated experimental packs. This methodology is normally used to evaluate mathematical models and consists of 3 main steps: 1) inoculating containers with the reference microorganism; 2) submitting them to different thermal treatments; 3) incubating at optimal growth conditions. The containers are regularly inspected for spoilage signs thus validating the model (Martínez, 1988). A modification of this methodology was developed by Yawger (1978,

1979). It differs from the previous method because it measures the lethality of the process and not the percentage of spoiled containers.

1.5. Time-temperature integrators (TTI)

The driving force for the development of TTIs was the demand for high quality foods and also the need of the industry to attain better process control and, simultaneously, to reduce energy consumption. Consequently, several new technologies have been developed which required validation in order to guarantee the same level of safety. Furthermore, the TTIs must be capable not only of measuring the impact of thermal treatments but also of assessing other additional affects (e.g. that of electricity).

These devices are generally microorganisms or enzymes (either in suspension or immobilized in/on a carrier such as e.g. alginate beads) which have a proportional response to the intensity of the treatment. One definition for a TTI is *a small device that shows some irreversible changes with the time-temperature, which is measurable easily and accurately, and mimics the changes produced in a temperature sensible factor contained in a foodstuff that suffers the same treatment at a variable temperature* (Martínez *et al.*, 2005). The main advantage of a TTI is its ability to quantify the integrated impact of both the time and the temperature in the target parameter without requiring data on the thermal history of the product (Van Loey *et al.*, 1999). Consequently, a potential candidate to be a TTI for thermal processes has to fulfill the following requirements (Martínez *et al.*, 2005):

- The TTI should include a calibrated and resistant sensor element for the thermal process and should experience the same evolution of temperature as the food matrix;
- The size and shape should be as identical as possible to the food matrix in order to follow the same flow patterns and to distribute homogeneously;
- The sensor element should not be lost during the process;
- The integrator should be cheap, stable, easy to recover and capable of long time storage without any loss of functionality;

There are also kinetic aspects that a TTI must fulfill:

$$\left(F^{z}_{Tref}\right)_{indicator} = \left(F^{z}_{Tref}\right)_{TTI} \quad \textbf{(Eq. 2.1)}$$

Equation 2.1 means that the lethality achieved in the integrator should be similar to the lethality of the factor used as the indicator (microorganism, enzyme, etc).

According to the type of sensor element the TTIs can be classified into 3 main groups: chemical, physical and biological (Van Loey *et al.*, 1999).

1.5.1. Chemical TTIs

These TTIs relate the extent of a chemical reaction with a thermal process. Several systems are available in the literature such as thiamine heat inactivation (Mulley *et al.*, 1975a,b,c), color changes (Favetto *et al.*, 1989), sugar hydrolysis (Kim and Taub, 1993), amongst others.

Although they play an important role, they present a major disadvantage: the high value of z (20 to 50 ºC) or the low value of activation energy (60-160 kJ/mol) make them unable to guarantee microbiological safety in the interval of sterilization temperatures (Martínez *et al.*, 2005).

1.5.2. Physical TTIs

Physical time-temperature integrators are based on diffusion phenomena. Witousky (1997) proposed a system using a colored compound that can melt and be absorbed in wick paper in the presence of steam. The TTI response is calculated by measuring the distance migrated by the melted element. This TTI has obvious limitations due to the toxicity of the element, differences in the food matrix which will make difficult to find "universal" TTI's, among others. Swartzel *et al.*, (1991), presented a TTI based on the ionic diffusion and capacity of a semi-conductor metal; and some other solutions exist.

1.5.3. Biological TTIs

1.5.3.1. Protein-based TTI: enzymatic and non-enzimatic (immunochemical)

Heat can cause irreversible changes in the tertiary structure of proteins which, in the particular case of enzymes, affects their activity. This activity loss can be correlated to the

thermal process. The wide range of proteins with different thermo-stability and activation energies is very useful to cover a broad interval of food quality and safety attributes.

A TTI is called enzymatic TTI when the residual activity of the enzyme is a direct response of the thermal impact. Several TTIs have been reported for enzymes such as peroxidase, galactosidase, lipase and nitrate reductase encapsulated in alginate (Mulley *et al.*, 1975; Hendrickx *et al.*, 1992, Cordt *et al.*, 1992 a,b).

One of the major drawbacks of using enzymes is their low thermal stability, especially for HTST processes in which they are inactivated long before reaching the treatment temperature.

Immunochemical methods are based on the antibody-antigen response. The thermal treatment can affect binding sites thus preventing the binding.

1.5.3.2. Microbiological TTIs

A microbiological TTI consists of a carrier system inoculated with a microorganism of well-known thermal resistance and concentration, under the specific sterilization to assess. The level of microbial inactivation can, therefore, be related to the magnitude of the thermal process. To become a microbiological integrator a number of requirements must be fulfilled:

- The microorganism should have low variability in number and thermal resistance;
- The system must be calibrated under the exact conditions one whishes to assess;
- The relation between the microbiological integrator and the natural microbial load of the product should be known;

The selection of the microorganism to be used as TTI will depend on the sterilization treatment and also on the specific application for which it will be used.

1.6. Lipoxygenase (LOX)

Lipoxygenase (EC 1.13.1.13) was first reported as a carotene-destroying enzyme in soy beans. This enzyme is found in alfalfa, various legumes, radishes and potato but the highest activity is found in soy beans. LOX is widely distributed in vegetables and evidence is mounting to support its involvement in off-flavor development and color loss (Garotte, 2003). This enzyme is active at low temperatures which makes it a serious problem in

unblanched peas and beans. It catalyzes the oxidation of polyunsaturated fatty acids containing a cis,cis-1,4-pentadiene group (e.g. linoleic acid) by molecular oxygen.

Garotte (2003) evaluated the sensory character of blanched vegetable purées to which isolated enzymes had been added and found that LOX was the enzyme most active in aroma deterioration in English green peas and green beans. In order to optimize the blanching process of vegetables, it is essential to establish the kinetic model of the inactivation of this indicator enzyme.

LOX is extensively used in bread production because of its bleaching effect, which changes the natural yellow pigments of the flour and results in bread with a very white crumb. In contrast to bread, the production of macaroni and other pasta products requires retention of the yellow pigment thus low enzimatic activity is preferred. Moreover, it interacts with the gluten side chain, making the gluten more hydrophobic and, subsequently, stronger. With stronger gluten, the dough will have better gas retention properties and increased tolerance to mixing.

Several authors recommend the use of LOX activity to estimate blanching adequacy (Barett and Theerakulkait, 1995; Romero and Barrett, 1997).

1.7. Pectinase (PEC)

Pectinase is a general term for enzymes that break down pectin, a polysaccharide substrate that is found in the cell walls of plants. One of the most studied and widely used commercial pectinases is polygalacturonase. It is useful because pectin is the jelly-like matrixes which helps cement plant cells together and in which other cell wall components, such as cellulose fibrils, are embedded.

Like all enzymes, pectinases have an optimum temperature and pH at which they are most active. Typically, commercial pectinases might be activated at 45 to 55 °C and work well at a pH of 4.8 to 5. A higher temperature will increase the reaction rate. However, the higher temperature will eventually denature the enzyme, ultimately destroying the enzymatic action. The value of pH also plays a role, and having it too high or too low would also result in the enzyme inactivation.

Polygalacturonase E.C. 3.2.1.15 hydrolyzes the linkages that hold the small building blocks of galacturonic acid together in the pectic substances, producing smaller molecules (Figure 2.1). One of the major problems in the preparation of fruit juices and wine is cloudiness due primarily to the presence of pectins. These consist primarily of a-1,4-

anhydrogalacturonic acid polymers, with varying degrees of methyl esterification. They are associated with other plant polymers and, after homogenisation, with the cell debris. The cloudiness that they cause is difficult to remove except by enzymatic hydrolysis. Such treatment has the additional benefits of reducing the solution viscosity, increasing the volume of juice produced (e.g. the yield of juice from white grapes can be raised by 15 %), subtle but generally beneficial changes in the flavour and, in the case of wine-making, shorter fermentation times. Insoluble plant material is easily removed by filtration, or settling and decantation, once the stabilising effect of the pectins on the colloidal haze has been removed.

In short, the main functions of pectinases in foods are: to clarify juices and wines, to reduce viscosity by hydrolyzing the pectin, to accelerate the rate of filtration, to prevent pectin gel formation and to improve color extraction from grape skin (Somogyi, 1996).

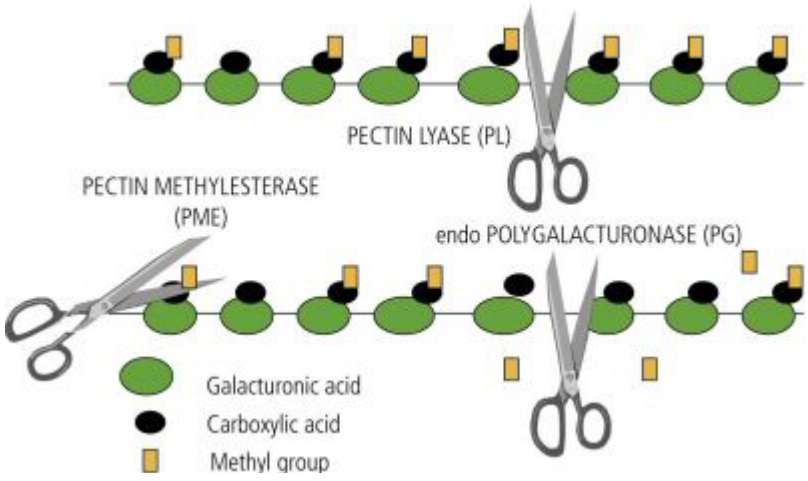

Figure 2.1: Mode of action of the main pectinolytic enzymes

1.8. Polyphenoloxidase (PPO)

The official name of the enzyme responsible for enzymatic browning is ortho-diphenol oxygen oxidoreductase (EC 1.10.3.1), also known as catecholase, tyrosinase, phenolase, and polyphenol oxidase. (Kim, 1995, Somogyi, 1996). There are different phenols present in fruits and vegetables at the same time used as substrates for PPO. The reactions involve hydroxylation of monophenols to give o-phenols and the removal of hydrogens from o-diphenol to give an o-quinone. Another possible reaction is the oxidation of an o-diphenol to a benzoquinone. PPO from banana, tea leaf, tobacco leaf and peach have been reported to act only on o-diphenols and not to hydroxylate monophenols. Polyphenol oxidases from potato, apple, sugar beet leaf and broad bean leaf have both types of activity. The enzyme contains 1 atom of copper per molecule (Kertesz and Zito, 1957). The Cu^{2+} may be removed and the enzyme inactivated in this manner, but it may be reactivated by adding Cu^{2+}.

Browning occurs only when the tissues are disrupted or destroyed and the compounds come into contact with air and with each other. The browning of fruits and vegetables is undesirable and so these are handled carefully to avoid tissue injury. In some cases, however (*e.g.* cocoa and tea), browning is important to flavor and color development and so the tissues of these plants are deliberately damaged

Polyphenol oxidase activity is important in some fermentation processes like in tea, coffee and tobacco curing and the enzyme itself may find application in the food industry for the production of colored end products and of particular flavors associated with the browning reaction.

1.9. Alkaline phosphatase (ALP)

Alkaline phosphatase (ALP) E.C. 3.1.3.1 is the name given to a group of isoenzymes which catalyze the hydrolysis of organic phosphates at alkaline pH. It is involved in several physiological processes apparently connected to membrane transport phenomena and is used in biomedical research. It can be found principally in bone, liver, kidney, intestinal wall and placenta. Different isoenzymes are associated with each of these locations.

In the food industry, ALP is an enzyme used as an indicator of the effectiveness of the milk thermal processing, because it exhibits a greater thermal resistance than that of pathogens in the pasteurization temperature range.

1.10. β -Galactosidase (β -Gal)

A β-D-galactoside galactohidrolase, E.C. 3.2.1.23, usually designated by β-galactosidase or lactase, it is an enzyme that catalyzes the hydrolysis reaction of lactose into glucose and galactose.

This enzyme is of particular importance for people that are lactose-intolerant. This is an inborn error and ingested lactose (in milk or dairy products) cannot be broken down to glucose and galactose resulting is severe discomforts. The main applications of this enzyme are to produce dairy products with low lactose content. The production and applications of this enzyme are discussed in more detail in another chapter of this thesis.

2. Materials and Methods

2.1. Heating phase

2.1.1. Conventional thermal degradation

For each enzyme tested, samples of 0.2 ml in 2 mL Eppendorf tubes (9 mm of internal diameter and 40 mm of height) were placed in a temperature controlled water bath at the desired temperature. Samples were taken at regular time intervals and placed immediately into ice to stop the thermal degradation effect. The dimensions of the Eppendorf tubes minimize temperature gradients due to heat transfer resistance. Temperature raise was measured by placing a thermocouple in the geometric centre of the tubes and comparing the temperature evolution with that of the external water bath; Such thermocouple, connected to the data acquisition system previously described (Castro *et al.*, 2003), was also used to monitor the thermal history of the samples, until temperature stabilization.

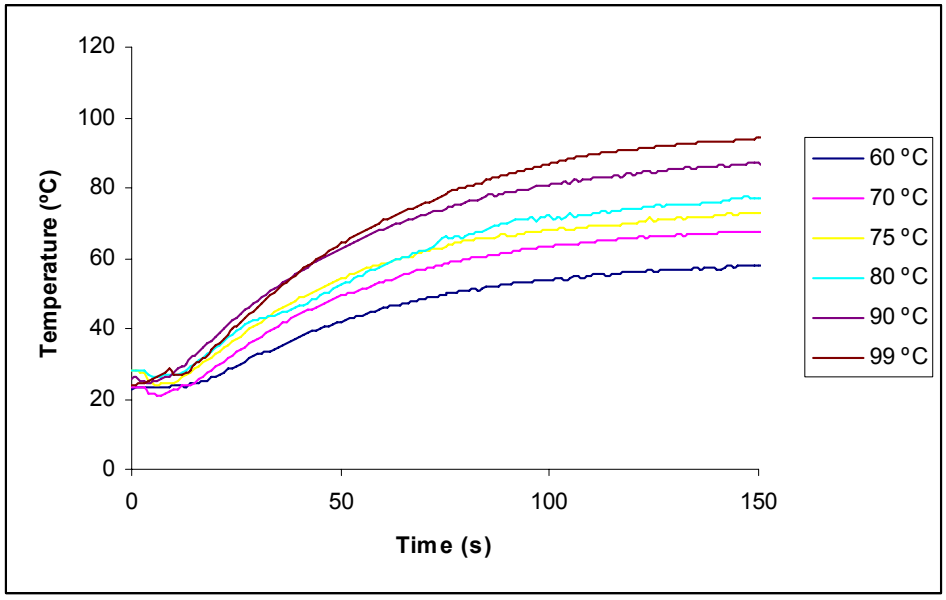

Figure 2.2: Temperature rise of the samples inside the eppendorfs

2.1.2. Ohmic thermal degradation

The ohmic heater used consisted of a cylindrical glass tube of 30 cm total length and 2.3 cm inside diameter (Figure 2.3). Three thermocouple openings were provided: two at equal distance of the centre of the tube and one at the centre, where the thermocouple was placed. Two Titanium electrodes with Teflon pressure caps were placed at each top of the tube.

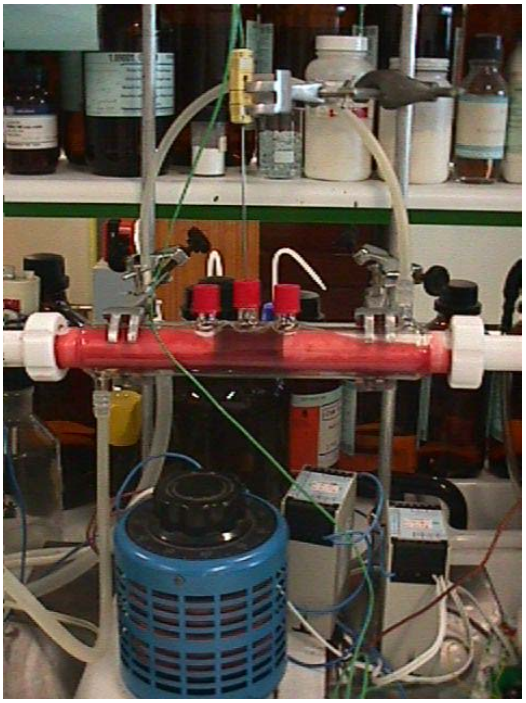

Figure 2.3: Ohmic heater

For each enzyme, samples of approximately 25 ml were heated using an alternating current source, of 50 Hz frequency and variable amplitude. Temperature was continuously monitored using type-K thermocouples, set at the geometrical centre of the chamber.

The power source was turned on and the electric field was varied through the use of a rheostat in order to simulate the conventional thermal history of the samples. An example of comparison of the thermal history of the samples is presented further ahead in the chapter (Figure 2.5). It is very important to have a coincidence in the heating phase of both processes because the objective is to evaluate the non thermal effects of the ohmic processing, thus the thermal effects should be made equal. Samples were taken and placed immediately into ice to stop the thermal degradation effect.

It should be stressed that the electric field strength used during the holding phase of the experiments is low (in every case approximately equal to 20 V/cm) when compared to the ones used in the heating phase of the samples (50 V/cm < E < 90 V/cm).

Each experiment was conducted in duplicate.

For each of the enzymes tested the temperature range used was specified in order to match their different inactivation temperatures.

2.2. Modeling

Thermal process characteristics for enzymatic reactions are described in accordance with kinetic parameters such as decimal reduction times (D), inactivation rate constant (k), z-values (z), and activation energies (Ea). The D value is defined as the time required to inactivate 90 percent of the original enzyme activity at a given temperature (Equation 2.2). An inactivation reaction, which follows first-order kinetics, has a D value equivalent to 2.303/k. The temperature dependence of the D-value is given by the z-value, which represents the temperature increase required in order to obtain a ten-fold (1-log cycle) decrease in D-value (Equation 2.3). Corresponding to the z-value is the activation energy (Ea), which expresses the temperature dependence of the k-value as indicated in the Arrhenius relationship (Equation 2.4).

$$\frac{\log C_A - \log C_{Ao}}{t} = \frac{1}{D} \qquad \textbf{(Eq. 2.2)}$$

$$\frac{\log D_2 - \log D_1}{T_2 - T_1} = \frac{1}{z} \qquad \textbf{(Eq. 2.3)}$$

$$k(t) = k_0 \exp^{\left(-\frac{E_a}{RT}\right)} \qquad \textbf{(Eq. 2.4)}$$

Where,

C_A – *activity (U)*

C_{A0} – *initial activity (U)*

D - Decimal reduction time (min)

z - Temperature sensitivity indicator (ºC)

E_a – Activation energy (kJ·mol^{-1})

k - Frequency constant (s^{-1})

k_0 - Pre-exponential factor (s^{-1})

The kinetic parameters (D, z, E_a and K) were calculated for all the experiments.

2.3. Enzyme activity measurements

2.3.1. LOX

LOX type IB from soybeans was purchased as a lyophilized powder, (Sigma L7395) and was dissolved, without further purification, in Tris-HCl buffer (0.01 M; pH 9). One unit of enzyme causes an increase in the absorption at 234 nm of 0.001 *per* minute at pH 9 and 25 ºC, when linoleic acid is used as substrate. Such unit is equivalent to the oxidation of 0.12 µmol of linoleic acid (Kruger *et al.,* 1991). The absorption at 234 nm was recorded during 3 min and the activity was determined from the slope of the linear zone of the curve.

The inactivation kinetics was determined in the range of 60 to 78 ºC for both types of treatments.

2.3.2. PEC

PEC (Novo Enzymes) activity was determined spectrophotometrically at 276 nm and 40 ºC, using polygalacturonic acid (citrate buffer, pH 4.5) as substrate. One unit is equivalent to the oxidation of 0.1 µmol of polygalacturonic acid. The activity was determined from the slope of the curve during 20 min (Honda *et al*, 1982).

A temperature interval from 60 to 75 ºC was used to calculate the inactivation kinetics.

2.3.3. PPO

PPO was extracted from apples (cv *Golden delicious*). Apples were blended with a solution of phosphate buffer (pH 7) containing 1 % (w/v) polyvinylpirrolidine. The mixture was filtered and the liquid extract was recovered. The extract was then centrifuged for 10 min at 10000 rpm, at 4 ºC. The activity was determined spectrophotometrically at 395 nm (30 ºC) using catechol (in phosphate buffer, pH 6) as the substrate (Robinson, 1991).

Temperatures ranging from 70 to 95 ºC were used to determine the inactivation kinetics.

2.3.4. ALP

The determination of ALP activity was performed directly in milk. The activity was expressed in terms of nmol of p-nitrophenilphosphate (pNPP) /mL per minute. The activity was measured as the release of p-nitrophenil (pNP) from pNPP. Samples were incubated with 47 mg p-NPP/25 mL Tris buffer, pH 10.4 at 37 ºC. The reaction was stopped with 0.02 M NaOH and the activity was measured spectrophotometrically at 410 nm (Williams *et al* 1990). For this enzyme the inactivation temperatures used varied from 55 to 70 ºC.

2.3.5. β-GAL

β-Gal was obtained by fermentation of lactose by a genetically modified strain of *Saccharomyces cerevisiae*, containing a plasmid carrying the β-Gal gene of *Aspergillus niger* (Domingues *et al.*, 2000). It is an extracelullar enzyme and therefore it was used without further purification. One unit of activity was defined as the amount of enzyme that hydrolyses 1 nmol of p-nitrophenil β-D-galactopyranoside (pNPG) per minute, at 65 °C. The activity was measured as the amount of p-nitrophenol released from pNPG per minute. Samples were incubated with 1.7 mM substrate in 0.075 M Na-acetate buffer, pH 4.5. The pH was raised to 10 with 1 M of Na_2CO_3 and the activity was measured spectrophotometrically at 405 nm (Bailey and Linko, 1990).

The *D*-values were calculated for a temperature range of 65 to 80 ºC.

Table 2.1: Overview of enzymatic systems tested, media used and activity measuring methods.

Enzyme	Origin	Medium	Activity assay
Lipoxygenase (LOX)	Soybean (Sigma)	Tris-HCl buffer (pH 9)	Spectrophotometric at 234 nm and 25 ºC; Substrate: linoleic acid
Polyphenoloxidase (PPO)	Apples (cv. Golden delicious)	Phosphate buffer (pH 6)	Spectrophotometric at 395 nm and 30 ºC; Substrate: catechol
Pectinase (PEC)	Fermentation (Novo enzymes)	Citrate buffer (pH 4.5)	Spectrophotometric at 276 nm and 40 ºC; Substrate: polygalaturonic acid
Alkaline phosphatase (ALP)	Raw milk	Milk	Spectrophotometric at 410 nm and 37 ºC; Substrate: p-Nitrophenylphosphate
β-galactosidase (β-GAL)	Fermentation broth	Fermentation broth	Spectrophotometric at 405 nm and 65 ºC; Substrate: p-Nitrophenylgalactopiranosyde (pNPG)

2.4. Reducing SDS-PAGE electrophoresis (SDS-PAGE)

The electrophoretic apparatus was carefully cleaned with isopropanol and the separation gel was applied, using a Pasteur pipette, immediately after preparation. Gel was poured until 1 cm to the top of the chamber. The composition of the solutions used is described in Table 2.2.

Table 2.2: Solution used for SDS-PAGE

Solutions	Composition
Separation gel 5%	2.5 ml 30% (w/v) Acrylamide /0.8% Bis-acrylamide 3.75 ml 1.5M Tris/HCl/SDS pH 8.8 8.75 ml dH_2O 50 µl 10% (w/v) APS 10 µl TEMED
Separation gel 15%	7.5 ml 30% (w/v) Acrylamide /0.8% Bis-acrylamide 3.75 ml 1.5M Tris/HCl/SDS pH 8.8 3.75 ml dH2O 50 µl 10% (w/v) APS 10 µl TEMED
1,5M Tris/HCl/SDS pH 8,8	91 g Base Tris 300 ml dH2O Set pH to 8.8 using 1N HCl 10 ml 20% (w/v) SDS Add dH2O until obtaining a final volume of 500 ml

The separation gel was allowed to polymerize with its top covered by a layer of isopropanol. After polymerization, the isopropanol was removed and the top washed with a solution of 1.5M Tris/HCl/SDS pH 8.8. The packing gel (see Table 2.3 for composition of the solutions used) was prepared and placed on the top layer avoiding the formation of gas bubbles. A Teflon comb of 0.75 mm was gently placed on the top of the gel until complete polymerization was achieved.

Table 2.3: Packing gel composition

Solutions	Composition
Packing gel	650 µl 30% (w/v) Acrylamide/0.8% Bis-acrylamide 1.25 ml 0,5M Tris/HCl/SDS pH 6.8 3.05 ml dH_2O 25 µl 10% (p/v) APS 5 µl TEMED
0,5M Tris/HCl/SDS pH 6,8	6.05 g Base Tris 40 ml dH_2O Set pH to 6.8 using 1 N HCl 2 ml 20% (w/v) SDS Add dH_2O until obtaining a final volume of 100 ml

The electrophoretic chamber containing the gel was placed inside the apparatus and completely covered with SDS-PAGE electrolyte (Table 2.4). The comb was carefully withdrawn and the wells rinsed with SDS-PAGE electrolyte.

Samples were applied in the wells and the power was turned on.

Table 2.4: SDS-PAGE electrolyte

Solutions	Composition
SDS-PAGE electrolyte	6.04 g Base Tris 28.8 g Glycine 10 ml 20% (w/v) SDS Add dH_2O until obtaining a final volume of 2 l

Samples were stained by adding equal volumes of sample and buffer A (10 µl) (see composition in Table 2.5).

Table 2.5: Composition of the buffer solution

Solutions	Composition
Buffer A	25 ml 0.5M Tris/HCl/SDS pH 6.8 4 ml 20% (w/v) SDS 10 ml 2-Mercaptoethanol 20 ml Glycerol 5 mg Bromophenol blue Add dH_2O until obtaining a final volume of 100 ml

2.5. Native-PAGE electrophoresis

The experimental procedure is similar to the previously described for SDS-PAGE having some changes only in the composition of the solutions that do not contain SDS (Table 2.6).

Table 2.6: Composition of the solutions used for native-PAGE

Solutions	Composition
Separation gel 5%	2.5 ml 30% (w/v) Acrylamide /0.8% Bis-acrylamide 3.75 ml 1.5M Tris-HCl pH 8.8 8.75 ml dH_2O 50 µl 10% (w/v) APS 10 µl TEMED
Packing gel	650 µl 30% (w/v) Acrylamide/0.8% Bis-acrylamide 1.25 ml 0.5M Tris/HCl pH 6.8 3.05 ml dH_2O 25 µl 10% (w/v) APS 5 µl TEMED
1,5M Tris/HCl pH 8,8	91 g Base Tris 300 ml dH_2O Set pH to 8.8 using 1N HCl Add dH_2O until obtaining a final value of 500 ml
0,5M Tris-HCl pH 6,8	6.05 g Base Tris 40 ml dH_2O Set pH to 6.8 using 1N HCl Add dH_2O until obtaining a final value of 100 ml
PAGE - electrolyte	6.04 g Base Tris 28.8 g Glicine Add dH_2O until obtaining a final value of 2 l
Buffer B	25 ml 0.5M Tris/HCl pH 6.8 20 ml Glicerol 5 mg Bromophenol Blue Add dH_2O until obtaining a final value of 100 ml

2.6. Coomassie blue staining

The most common method for visualizing proteins within the gel itself is staining with Coomassie Brilliant Blue Dye. The mechanism of Coomassie dye binding to proteins is not completely understood, however it depends in part on basic and hydrophobic residues. For this reason, binding varies widely among proteins. Coomassie staining turns the entire gel

blue and to see the protein bands, the gel must be de-stained with a methanol/acetic acid mixture to remove background stain.

Figure 2.4: Coomassie staining protocol

The gel was placed in a glass vessel containing the Coomassie blue dye and it was allowed to incubate for 2 hours at room temperature with slow agitation (Figure 2.4.) To de-stain, the Coomassie solution was removed, the gel was rinsed with de-ionized water followed by sinking in de-staining solution, with agitation, at room temperature, until only the protein bands were visible. See Table 2.7 for solution composition details.

Table 2.7: Solutions used for Coomassie staining protocol

Solutions	Composition
Coomassie blue	25% (w/v) Coomassie blue R-250 91 ml EtOH 91 ml dH_2O 18 ml Acetic acid
De-staining	200 ml Methanol 152 ml dH_2O 48 ml Acetic acid

2.7. Statistical analysis

In order to evaluate whether the differences found in the kinetic parameters determined, under conventional and ohmic heating treatments, were significant or not, two-way analysis of variance (ANOVA) was performed at a significance level of 5 %. The results of this analysis were expressed in terms of the probability of the samples being equal (if lower than 5 %, they were considered different).

3. Results and Discussion

The application of ohmic heating technology in food processing offers potential both as a preservation technology and as an adjunct to other processes such as drying or extraction. Regarding the use of ohmic heating as a preservation technology, its impact on enzymes is of particular importance. Because of the beneficial and /or detrimental effects of enzymes, the control of enzymatic activity is required in many processing steps. When the maintenance of enzymatic activity is desirable, the knowledge of enzyme stability under the relevant processing conditions is required for process design. Alternatively, in case of detrimental enzymatic action, the knowledge of inactivation kinetics under processing conditions is of prime significance. Enzyme denaturation is caused by rearrangement and/or destruction of non-covalent bonds such as hydrogen bonds, hydrophobic interactions and ionic bonds of the tertiary protein structure. The presence of an electric field can influence biochemical reactions by changing molecular spacing and increasing interchain reactions. In this study, the temperature as a variable was eliminated by simulating the conventional heating profile during the ohmic heating phase (Figure 2.5); being so, the possible differences in the results obtained must be related to the effects of the applied electric field.

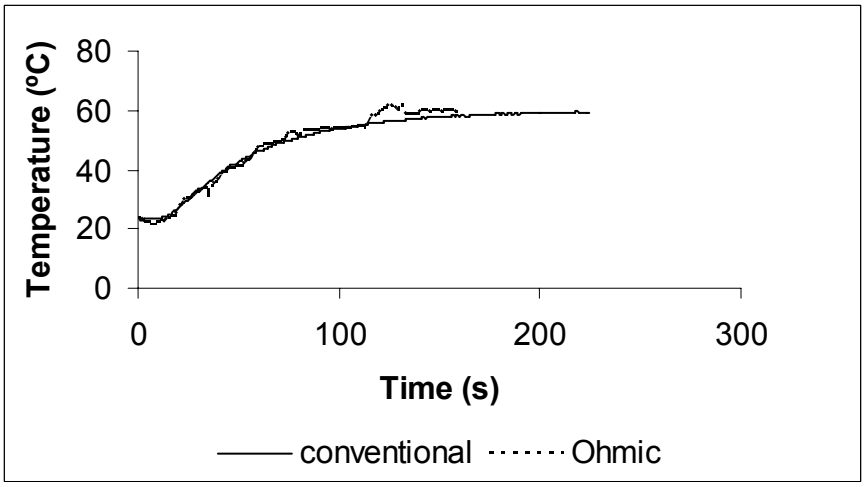

Figure 2.5: Example of a conventional and ohmic heating profile.

The following results correspond to the determination of the non-thermal effects (if any) of ohmic heating in five different enzymes: lipoxygenase, pectinase, polyphenoloxidase, alkaline phosphatase and β-galactosidase.

3.1. LOX

Lipoxygenases (LOX) are non-heme but iron-containing dioxygenases which catalyze the dioxygenation of polyunsaturated fatty acids containing a cis,cis-1,4-pentadiene-conjugated double bond system such as linoleate and linolenate, to yield hydroperoxides.

Table 2.8 presents the kinetic parameters obtained for the thermal degradation of LOX. The obtained results show that the electric field has an additional effect on the LOX inactivation with approximately five times lower *D* values (Figure 2.6). The results of analysis of variance show that the differences found were significant at a 95 % significance level for all of the *D* values ($p < 0.05$) as well as in for *z* values ($p = 0.047$). This means that for the same inactivation degree, the time required for thermal treatment (e.g. blanching of vegetables) is much lower (Figure 2.6), when an ohmic heating process is applied, thus reducing negative thermal effects in the other food components.

Table 2.8: Kinetic parameters of thermal degradation of LOX

Temperature (ºC)	60	62	65	68	70	75	78
$D_{conventional}$ (min)	117.80 ± 5.88	20.44 ± -	10.03 ± 1.15	5.43 ± 0.01	3.76 ± 0.10	0.99 ± 0.07	0.77 ± 0.04
D_{ohmic} (min)	6.92 ± 0.47	5.38 ± 0.11	-	1.57 ± 0.07	-	0.58 ± 0.00	0.47 ± 0.00
$z_{conventional}$ (ºC)	11.10 ± 0.35 ($r^2 = 0.99$)						
z_{ohmic} (ºC)	15.04 ± 0.38 ($r^2 = 0.98$)						
$E_{a\_conventional}$ (kJ·mol^{-1})	275 ± 1.89						
E_{a_ohmic} (kJ·mol^{-1})	148 ± 3.71						

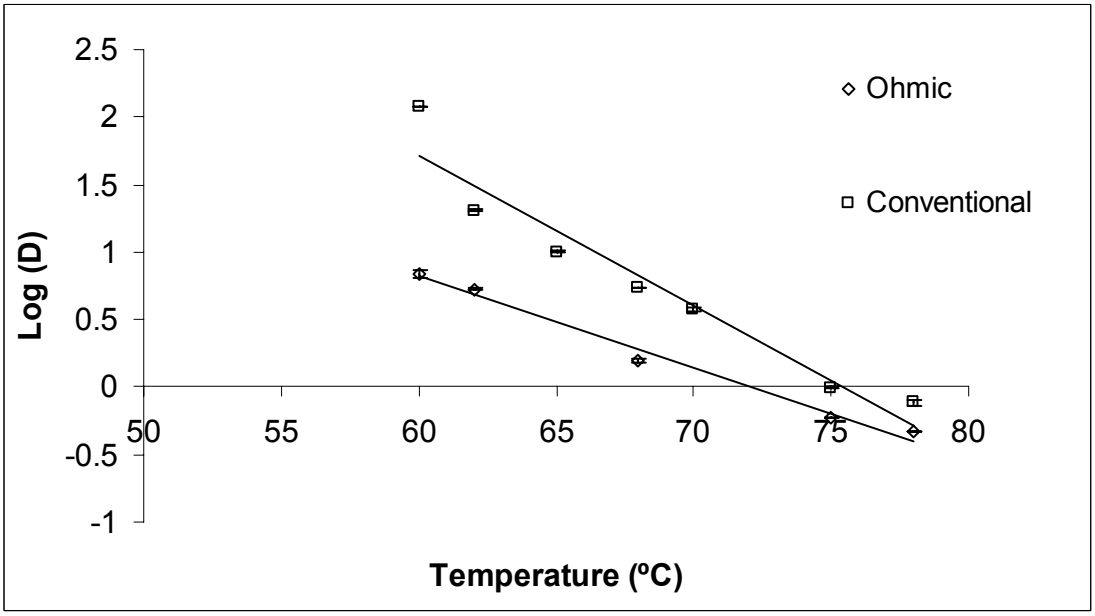

Figure 2.6: Degradation kinetics of LOX when submitted to conventional or ohmic heating.

The hypothesis of the additional effect of the electric field being due to the separation of the subunits or breakage of the enzyme molecule was raised. This hypothesis was checked by polyacrylamide gel electrophoresis – PAGE. When the PAGE system is run with proteins under their native form (native PAGE), these proteins move through the gel when an electric field is applied and each band on the gel represents a different protein (or a protein sub-unit). If there was a sub-unit separation due to heating/electric field, different bands would appear in the gel, corresponding to different sub-units. Nevertheless, both the non-treated enzyme and the heat treated enzyme (both conventionally and ohmically treated) presented the same number and position of bands in the gel, leading to the conclusion that before and after the thermal treatments (conventional or ohmic) the enzyme had the same molecular weight and no sub-unit separation occurred.

The same PAGE can be performed when proteins are previously treated with Sodium dodecyl sulphate (SDS – PAGE). The SDS is an anionic detergent which denatures proteins and induces a negative charge cloud on the surface of the denatured molecules, so that they acquire equal charge densities per unit length. This makes them migrate through the gel according to their molecular weight and was used to verify differences in the protein's size. Also, in this electrophoresis both proteins (conventionally or ohmic heated) and the native enzyme had the same profile on the gel. Although further investigation is needed, the differences between both treatments seem to be related to the binding capacity (due to

conformational changes of the active binding site or cofactor absence) and not directly to structural damage such as cleavage or separation of subunits as could initially be supposed. These results are in accordance with those of Ludikhuyze *et al.* (1998). These authors reported that the kinetic parameters describing denaturation (as determined by changes in native conformation, measured using gel electrophoresis) were not in agreement with those describing inactivation (as determined by spectrophotometrically measured changes in residual activity). In general, inactivation seemed to occur more readily than denaturation, indicating that only minor changes in the tertiary structure are responsible for the loss of enzyme activity.

The structure of soybean lipoxygenase-1, determined by X-ray diffraction methods, revealed that the 839 amino acids in the protein are organized in two domains: a β-sheet N-terminal domain and a large, mostly helical C-terminal domain. The iron is present in the C-terminal domain facing two internal cavities that are probably the conduits through which the fatty acid and molecular oxygen gain access to the metal (Skrzypczak-Jankun *et al.*, 1996). The iron cation is buried inside the protein molecule. The active site shows three oxygen atoms and three nitrogen atoms as possible iron ligands ((Skrzypczak-Jankun *et al.*, 1996). The iron content in soybean lipoxygenase-1 is important for enzyme activity. If the iron is removed e.g. by a chelating agent, the activity of the enzyme will decrease. The active center includes the iron ligands and the surrounding environment, and any conformational change in the active center may affect the activity of the enzyme (Wu, 1996). Ohmic heating affects the ionic movement in the media thus the removal of the iron from the active binding site and consequent decrease of activity may help to explain the enhanced lost of activity.

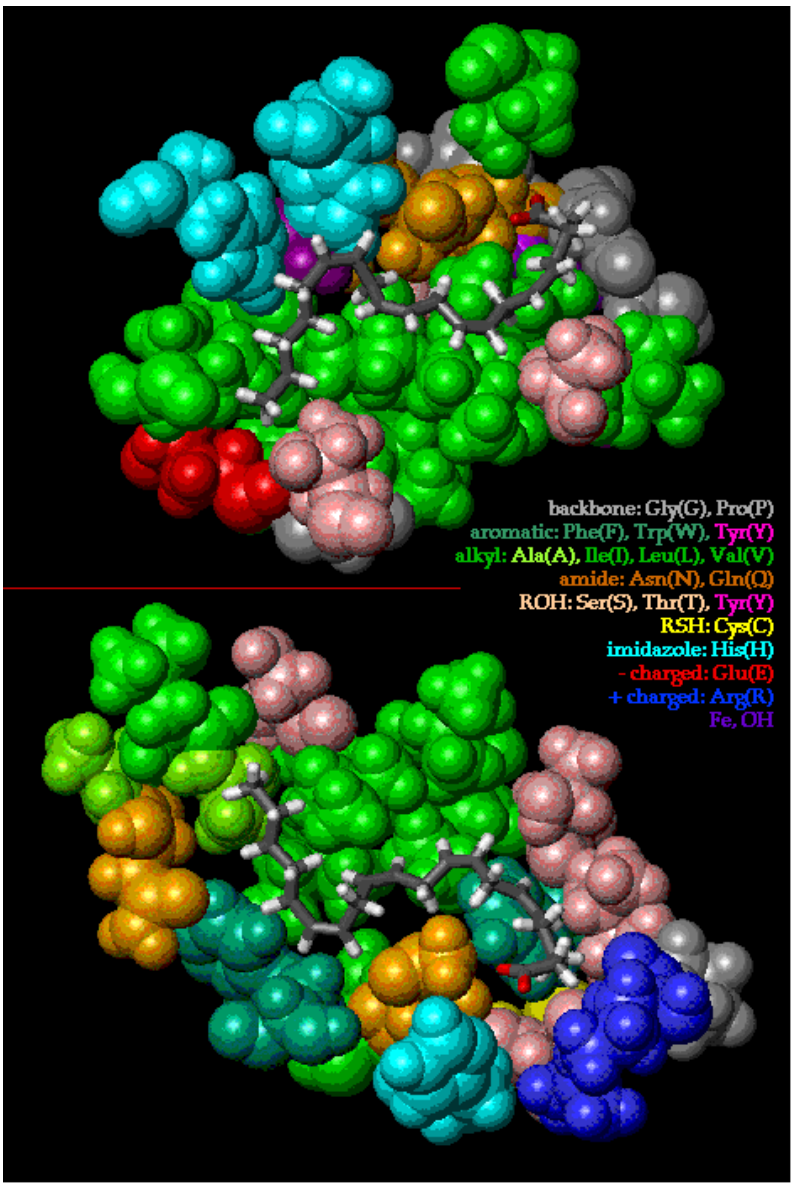

Figure 2.7: Structure of soybean lipoxygenase (from http://www.haverford.edu/chem/Scarrow/SLO)

3.2. PEC

Pectinolytic enzymes are especially important for fruit and vegetable juice technology. Common uses include clarification, pulp treatment, tissue maceration, liquefaction and other specialty functions. A common component of commercial pectinases is endo-polygalacturonase. This enzyme is used industrially e.g. to avoid fruit peeps in several products namely strawberry pulps and jams. The enzyme is added to the pulps at approximately 40 ºC and inactivated afterwards during the pasteurization process. The incomplete or inactivation may cause textural losses leading to products out of specification limits. The possible interest in using ohmic heating technology to process this products as an alternative e.g. to the traditional scrapped surface heat exchangers drove the need to investigate the effects of this new technology on this enzyme.

The kinetic inactivation parameters were calculated for both conventional and ohmic heating, in citrate buffer, using temperatures from 60 to 75 ºC. Although during the heating phase there were slight differences (± 3 V/cm) between the applied electric fields, during the holding phase the electric field remained constant in order to address mainly the non-thermal effects.

The kinetic parameters for PEC inactivation are presented in Table 2.9 where, together with Figure 2.8, it is clear that the electric field does not have a significant influence in the inactivation kinetic parameters. The results of the ANOVA test show that, for both conventional and ohmic processing, D and z values can be considered identical ($p > 0.05$). PEC has no prosthetic group (Table 2.15) and the hypothesis that relates the loss of activity to the loss of the metallic prosthetic group caused by the electric field (posed in the previous section) can be maintained given the data obtained for this enzyme.

Table 2.9: Kinetic parameters of thermal degradation of PEC.

Temperature (ºC)	60	62	65	68	70	75
$D_{conventional}$ (min)	14.66 ± 0.01	8.70 ± 0.01	3.57 ± 0.23	1.68 ± 0.01	0.83 ± 0.00	0.52 ± 0.00
D_{ohmic}(min)	14.19 ± 0.01	9.80 ± 0.01	4.08 ± 0.01	1.56 ± 0.00	0.74 ± 0.00	-
$z_{conventional}$ (ºC)	8.12 ± 0.01 (r^2 = 0.99)					
z_{ohmic} (ºC)	7.72 ± 0.00(r^2 = 0.99)					
$E_{a\_conventional}$ (kJ·mol^{-1})	226.59 ± 0.14					
E_{a_ohmic} (kJ·mol^{-1})	282.59 ± 0.60					

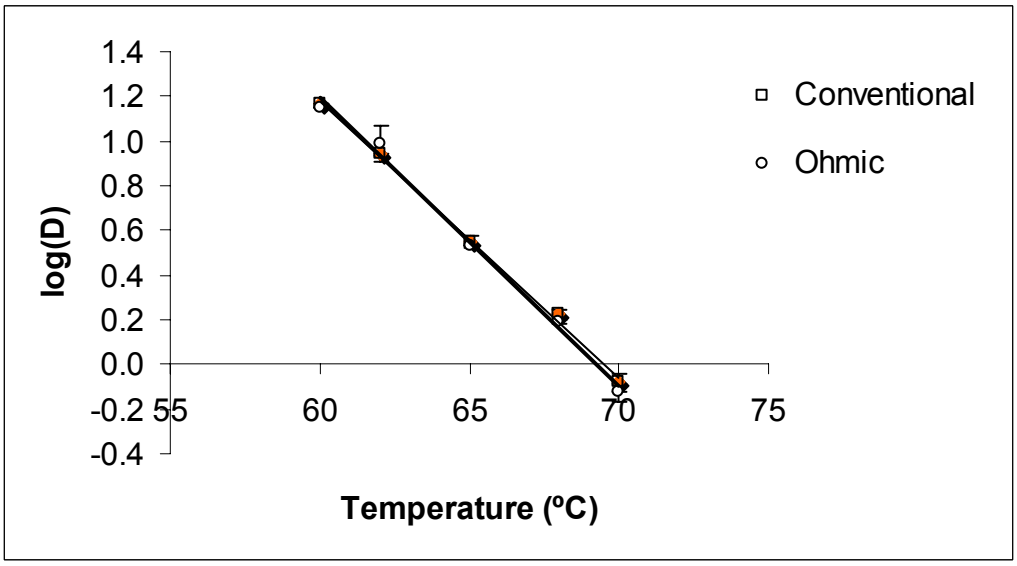

Figure 2.8: Degradation kinetics of PEC when submitted to conventional or ohmic heating.

Bonnin *et al.* (2001) carried out a study on the endopolygalacturonase from the phytopathogenic fungus *Fusarium moniliforme*. Mass spectrometry on hydrolysis products allowed to show that this enzyme is able to bind methyl as well as acetyl groups in its active site. Molecular modeling was then used to come closer to the structural reasons of this tolerance, reporting slightly different conformational structures of the enzyme. In a second step, oligomers methylated in one or more positions were built and the enzyme was docked on them. Docking energies of these complexes were very slightly affected by substrate methylesterification, explaining the mode of action observed on methylated substrates. Moreover, Sicilia *et al.* (2005) studied the docking mechanism of several polygalacturonases excreted from several fungi. A homology model shows that BcPG1

(*Botrytis cinerea* polygalacturonase), like AnPGII (*Aspergillus niger* polygalacturonase) and FmPG (*Fusarium moniliforme* polygalacturonase), folds as a parallel right-ended *β*-helix. A deep cleft on one side of the *β*-helix contains the residues involved in catalysis and substrate binding (Figure 2.9). The electrostatic potential surfaces and also the conformation of the binding site present some differences between the three isoenzymes studied (Figure 2.10). These variations may play a role in defining the specific activities and also on the effect of the electric field in each particular enzyme. Being so, the conclusion taken for the particular enzyme under study may not be extrapolated to other similar enzymes which can possibly be more affected by the electric field, thus causing changes in the activation or inactivation kinetics.

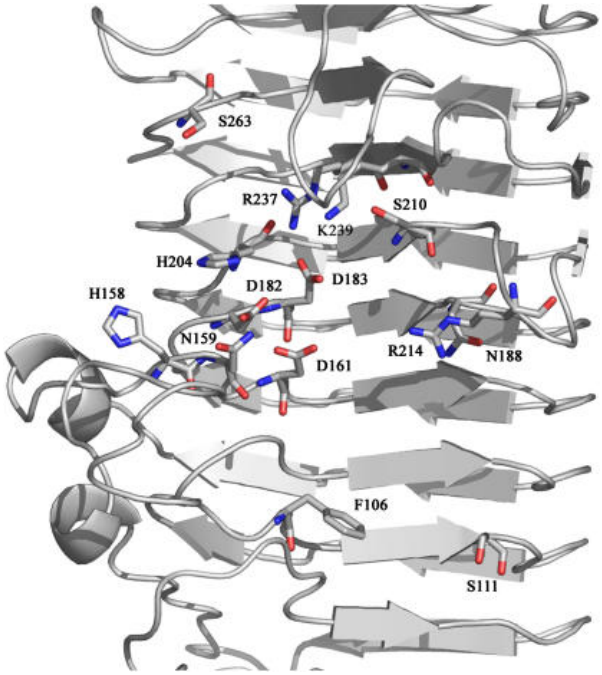

Figure 2.9: Ribbon representation of the homology-modeled BcPG1 oriented as to highlight the active site cleft. The reaction is catalyzed by residues D161, D182, D183, and H204. Residues important for substrate binding, based on experimental data and predictions obtained from various PGs, are shown. Their correspondence to predicted substrate binding subsites is shown in Table 2.10 Sicilia *et al.* (2005)

Table 2.10: Residues at predicted substrate binding subsites in different polygalacturonases - Sicilia *et al.* (2005)

Subsite	AnPGII	FmPG	BcPG1
−4	His-132	Gln-133	Ser-111
−3	Arg-223	Lys-244	Arg-214
	Lys-127	His-128	Phe-106
−2	Lys-127	His-128	Phe-106
	Asn-207	Thr-218	Asn-188
−1	Lys-258	Lys-269	Lys-239
	Ser-229	Ser-240	Ser-210
	Tyr-291	Tyr-302	Tyr-272
	Asn-178	Asn-189	Asn-159
+1	Arg-256	Arg-267	Arg-237
	Lys-258	Lys-269	Lys-239
	His-223	His-234	His-204
+2	His-177	His-188	His-158
	Asp-282	Thr-293	Ser-263
+3	Asp-282	Thr-293	Ser-263

FmPG*- Fusarium moniliforme *polygalacturonase; AnPGII* - Aspergillus niger *polygalacturonase; BcPG1* - Botrytis cinerea *polygalacturonase

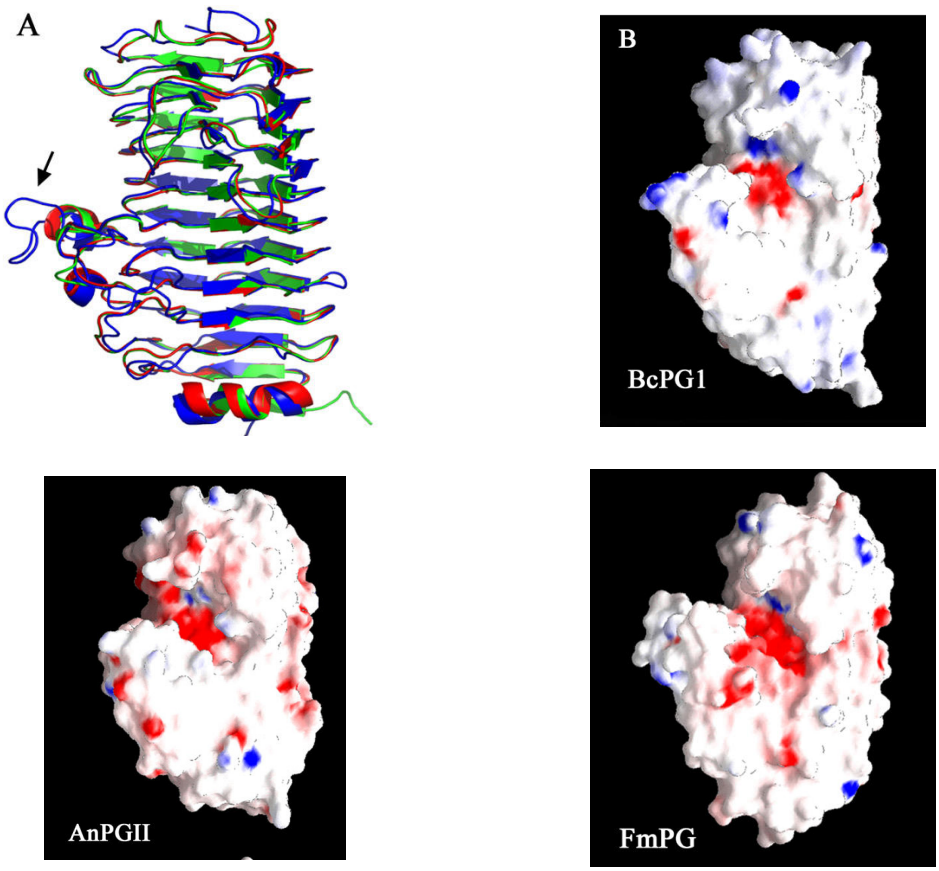

Figure 2.10: Conservation of the PG fold; structural superposition among AnPGII (red), FmPG (blue), and BcPG1 (green). The arrow indicates a variable loop at the crevice of the active site where a seven-residue insertion is found in FmPG. B, Electrostatic potential surfaces of BcPG1, AnPGII, and FmPG. Positive charges are shown in blue, and negative charges are shown in red. Differences can be seen, around the active site cleft, in both molecular shapes and charge distributions.

Giner-Seguí *et al.* (2006) investigated the effect of pulsed electric fields (PEF) on polygalacturonase activity in an aqueous solution of a commercial enzyme preparation. The experimentally determined kinetic mechanism was in accordance to the model proposed by Giner *et al.* (2005). This model is hypothesized to proceed by two consecutive irreversible first-order steps with the presence of intermediate active forms of the enzyme (I) between the native and the completely inactivated enzyme (D) (Equation 2.5).

$$N \xrightarrow{k2} I \xrightarrow{k1} D \qquad \textbf{(Eq. 2.5)}$$

The results obtained by these authors indicate that when using electric fields between 15 and 35 kV.cm^{-1} the intermediate forms (I) are up to 25 % more active than the initial

native forms of the enzyme. The overall effect of PEF treatments on activation, inactivation, or unchanged activity will depend on the quantity of intermediates that are produced in step 1 by PEF and remain not consumed in the subsequent step 2, which yields final products with null PG activity (Figure 2.11). However, in case of PEF at E = 38 kV cm^{-1}, the reaction intermediates that were generated in the first step already had less activity. The explanation for this data, given by the authors, was that PEF treatments promote shifts on the molecular structure of the enzyme. In the first stage, the PEF treatments have shifted the structure of the native molecules into a number of intermediate forms with enzyme activity. A fraction of these forms may have structures that favor the catalytic reaction (enhancement of the enzyme activity). The increase of the electric field leads to an increase in the fraction of intermediates with enzyme activity lower than the native forms of the enzyme.

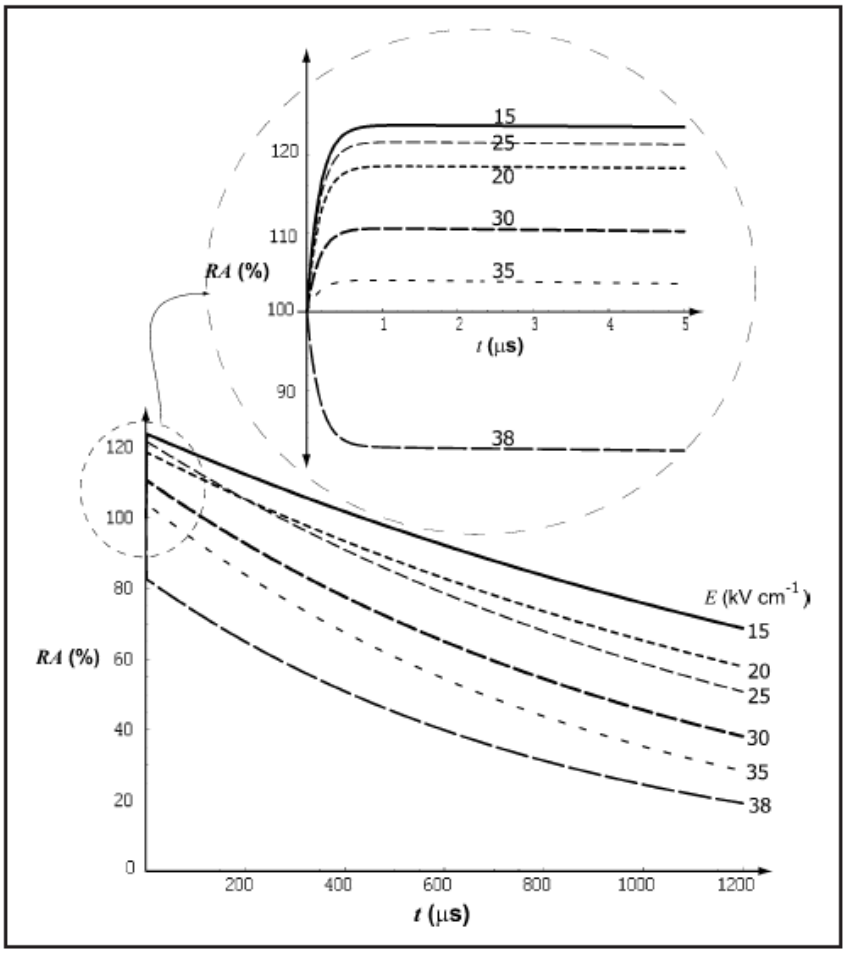

Figure 2.11: Residual activity (RA) of polygalacturonase as a function of time and applied electric field (from Giner-Seguí *et al.*, 2006)

In the case of ohmic heating the electric field was three orders of magnitude lower (20 V/cm) though the time was significantly higher (over 6 orders of magnitude). No similar effect (activity enhancement) was observed in our assays. One may advance two hypotheses: 1) the electric field was not strong enough to cause additional (to the thermal) conformational changes in the enzyme; 2) the intermediates formed had the same activity as the enzyme in the native form. The use of different electric field intensities in the holding phase (keeping temperature constant) may help to clarify the existence of an inactivation mechanism caused by moderated electric fields applied continuously.

The potential applications of this enzyme remain valid if ohmic heating technology is used for processing foods. In fact, the color extraction from grapes is improved by the use of pectinases and also by the increase of temperature (Somogyi, 1996). Ohmic heating has been reported to enhance beet dye extraction (de Alwis and Fryer, 1990) and to improve apple juice yield (Lima and Sastry, 1999). The combination of pectinases with ohmic heating may enhance the improvement of the quality of wines and other beverages. The use of ohmic heating to increase the temperature, during the color extraction phase of a vinification process, may be an interesting industrial application of this technology, and these results show clearly that it can be applied together with pectinases, which activity is not affected, or may be even enhanced, by the electric field.

3.3. PPO

Natural phenolic compounds in fruit and vegetables in the presence of PPO and oxygen are oxidized to o-quinone that subsequently polymerizes nonenzymatically to brown pigments (Golan-Goldhirsh & Whitaker, 1984; Sapers, 1993). This browning process leads also to a change in flavor and a reduction in nutritional quality, especially ascorbic acid (Vamos-Vigyazo, 1981; Golan-Goldhirsh & Whitaker, 1984). The most important factors that determine the rate of the enzymatic browning of fruit and vegetables are the concentrations of both active PPO and phenolic compounds present, the pH, the temperature and the oxygen availability of the tissue. pH and oxygen also influence subsequent nonenzymatic browning (Martinez & Whitaker,1995). In general, exposure of PPO to temperatures of 70–90 ºC destroys their catalytic activity (Vamos-Vigyazo, 1981). Thermal inactivation profiles of PPO in fruit and vegetable processing follow first-order reaction kinetics with the time required varying with the product. The potential use of ohmic heating technology for processing fruits purées and juices has been reported in the literature to be advantageous especially for highly viscous or particulate products.

The effect of the electric field on the thermal inactivation kinetics of PPO extracted from apples was investigated in the temperature range of 70 to 95 ºC. The kinetic parameters obtained are presented in Table 2.12 and Figure 2.12. For both types of treatments the extent of PPO denaturation increased with temperature and treatment time following a first order inactivation kinetics. This fact is consistent with several studies found on the literature.

The time required for complete inactivation of the enzyme depends on the amount of enzyme found in the fruit and also on the presence or absence of fruit pulp during the heat treatment. Some available data on inactivation parameters of this enzyme is presented in Table 2.11. The inactivation time is extremely variable but the decimal reduction time obtained for both conventional and ohmic heating is in the range reported for apples (Table 2.11).

Table 2.11: Heat inactivation of PPO in natural fruit juices

Fruit juice	pH	Time required for complete inactivation at 75 ºC (min)
Peach cloudy	4.03	3.41
Peach clear	4.07	0.83
Pear cloudy	4.40	60
Pear clear	4.02	10.5
Plum cloudy	3.69	> 100
Grape clear	3.56	6.0
Grape clear	3.08	0.77
Apple cloudy	3.40	14
Apple clear	3.35	0.29
Apple cloudy	4.20	> 100
Apple clear	4.26	7.17

Adapted from Jankov, 1962

Table 2.12: Kinetic parameters of thermal degradation of PPO.

Temperature (ºC)	70	75	80	85	90	95
$D_{conventional}$ (min)	193.0 ± -	61.61 ± 3.14	23.74 ± 2.50	10.30 ± 0.05	3.15± 0.42	1.51± 0.00
D_{ohmic} (min)	-	19.37± 0.01	6.79 ± 0.00	3.52± 0.00	0.92± 0.00	0.58± 0.04
$z_{conventional}$ (ºC)	12,20 ± 0.08 (r^2 = 0.99)					
z_{ohmic} (ºC)	12.97 ± 0.24 (r^2 = 0.98)					
$E_{a\_conventional}$ (kJ·mol^{-1})	201.02 ± 2.87					
E_{a_ohmic} (kJ·mol^{-1})	189.46 ± 3.81					

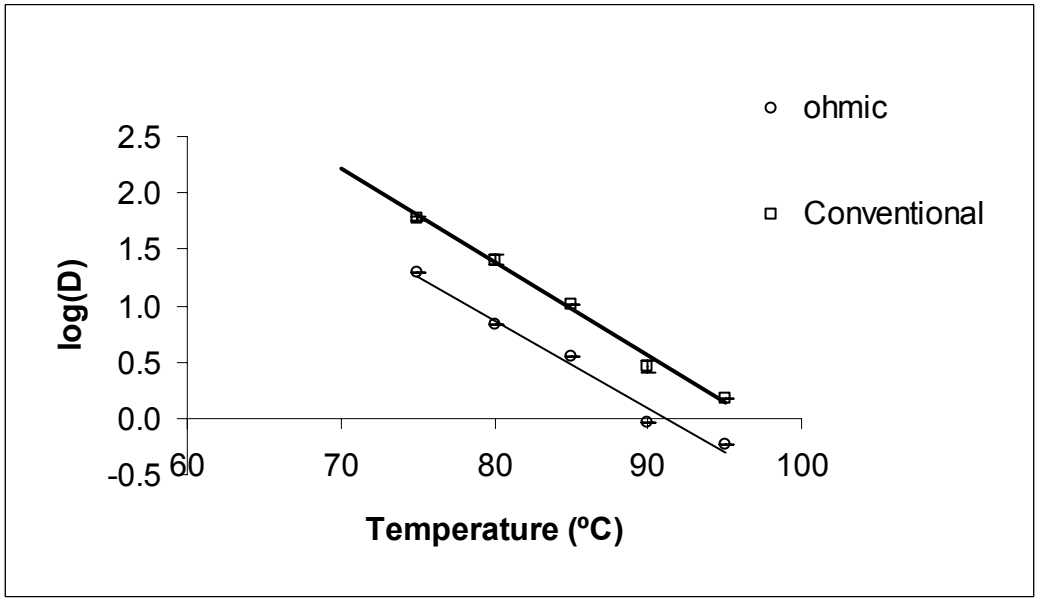

Figure 2.12: Degradation kinetics of PPO when submitted to conventional or ohmic heating.

Enhanced enzyme inactivation is obtained when an electric field is present, thus reducing inactivation time. Statistical significant differences were found between *z* values ($p = 0.02$, see Table 2.15).

Plant PPOs are ubiquitous plant enzymes containing a dinuclear copper center (metalloproteins). The secondary structure is primarily α-helical with the core of the enzyme formed by a four-helix-bundle composed of α-helices α2, α3, α6 and α7. The helical bundle accommodates the catalytic dinuclear copper center and is surrounded by helices, a 1 and a 4, and several short β-strands. Two disulfide bridges (Cys 11–Cys 28 and Cys 27–Cys 89) help to anchor the loop rich N-terminal region of the protein (residues 1–50) to helix α2. Each of the two active site coppers is coordinated by three histidine residues contributed from the four helices of the α-bundle (Figure 2.13). CuA is coordinated by His 88, His 109, and His 118. His 88 is located in the middle of helix α2, His 109 and His 118 are at the beginning and in the middle of helix α3 (Figure 2.13).The second catalytic copper, the CuB site, is coordinated by His 240, His 244 and His 274. These residues are found at the middle of helices α6 and α7. A four-coordinate trigonal pyramidal coordination sphere for both cupric metal ions with His was determined for sweet potato enzyme (Klabunde *et al.*, 1998). This author also proposed a catalytic mechanism in which 2 atoms of oxygen bind to the dicuprous metal center replacing the solvent molecule bonded to CuA in the reduced enzyme form. The active binding site of the enzyme is a hydrophobic cavity whose conformation is mainly determined by van-der-Waals forces and the binding of the substrate

causes an increase in the Cu-N distance. The presence of electric interactions caused by the presence of the electric field may be hypothesis to: affect van-der-Waals forces thus causing conformational changes of the binding site; remove copper from the enzyme and consequently the ability to catalyze the reaction, prevent the binding of oxygen atoms to the cupric metal center. It is well established that the ionic movement is significantly affected by the electric field thus the above hypothesis should be tested to clarify the additional inactivation mechanism caused by electricity.

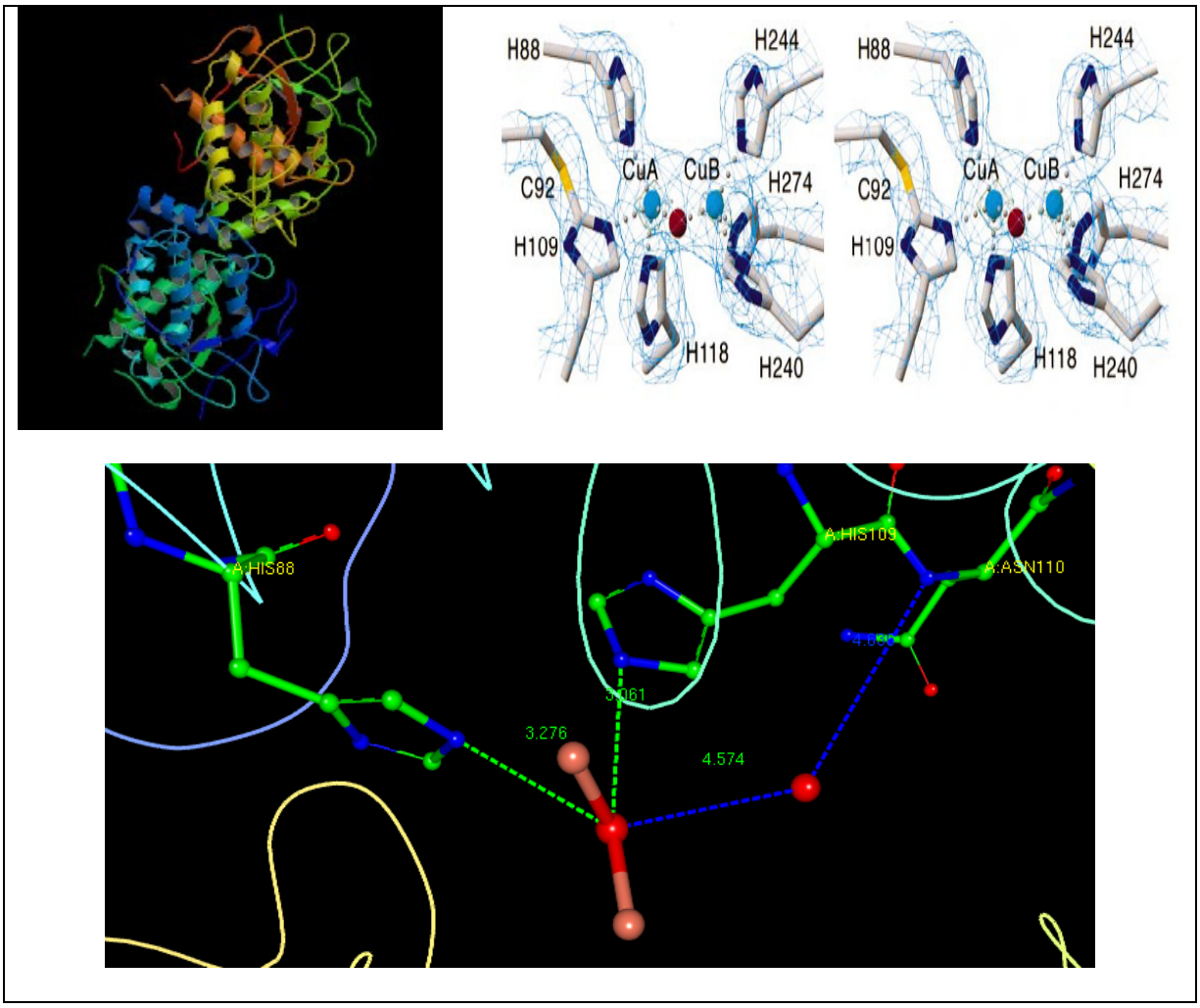

Figure 2.13: Crystal structure of sweet potato polyphenol oxidase (adapted from Klabunde *et al.*, 1998)

These results are encouraging to use ohmic heating in blanching of fruits, for example, in order to obtain the same level of PPO inactivation, a less aggressive thermal treatment is needed. Consequently, the thermal destruction of nutrients (e.g. vitamins and pigments) and fruit texture (a quality parameter) will be obviously reduced, thus increasing the final quality of the products.

3.4. ALP

Heat treatment of milk should meet the minimally required time/temperature to obtain the desired food safety and extend the shelf-life of products without significant heat-induced damage (organoleptic and nutritional). The sensitivity to heat of some indigenous enzymes makes them good indicators for the severity or effectiveness of heat treatment of milk and milk products, because they possess a thermal resistance higher than that of the most heat-resistant, non-spore-forming pathogens found in milk (Andrews, Anderson, & Goodnough, 1987; Griffiths, 1986; McKellar & Emmons, 1991). The determination of alkaline phosphatase (ALP) activity in milk is commonly used as a standard test for the determination of proper pasteurization of milk (Painter & Bradley, 1997). It is accepted that during pasteurization, the ALP activity should decrease about 500-fold. A higher ALP activity level may indicate serious deficiencies in the pasteurization process (Sharma, Sehgal, & Kumar, 2003).

The potential application of ohmic heating technology to the pasteurization of milk leads to the need of understanding if the traditional process indicators (ALP activity) remain valid or if new indicative process parameters have to be searched for and their values determined.

In the present work, the thermal inactivation of ALP in raw milk was investigated in the temperature range of 55 to 70 ºC, using conventional and ohmic heating.

For ALP both conventional and ohmic inactivation kinetics are similar (Table 2.13, Figure 2.12: Degradation kinetics of PPO when submitted to conventional or ohmic heating.Figure 2.12) and the results of the z values obtained do not show a clear additional effect of the electric field on the enzyme inactivation ($p > 0.05$, see Table 2.15). However, for lower temperatures, D values are significantly different ($p < 0.05$). This result may suggest that the continuous application of an electric field may have a “delaying” effect on this enzyme at lower temperatures.

Table 2.13: Kinetic parameters of thermal degradation of ALP.

Temperature (ºC)	55	60	62	65	67	70
$D_{conventional}$ (min)	35.46± 0.00	18.66 ± 0.01	4.41 ± 0.01	3.54 ± 0.01	1.96 ± 0.08	0.91 ± 0.01
D_{ohmic} (min)	31.75 ± 0.01	10.51 ± 0.01	4.06 ± 0.01	2.89 ± 0.01	1.28 ± 0.01	0.89 ± 0.02
$z_{conventional}$ (ºC)				9.05 ± 0.13(r^2 = 0.98)		
z_{ohmic} (ºC)				9.30 ± 0.05 (r^2 = 0.99)		
$E_{a\_conventional}$ (kJ·mol^{-1})				234.98 ± 0.00		
E_{a_ohmic} (kJ·mol^{-1})				225.71 ± 2.78		

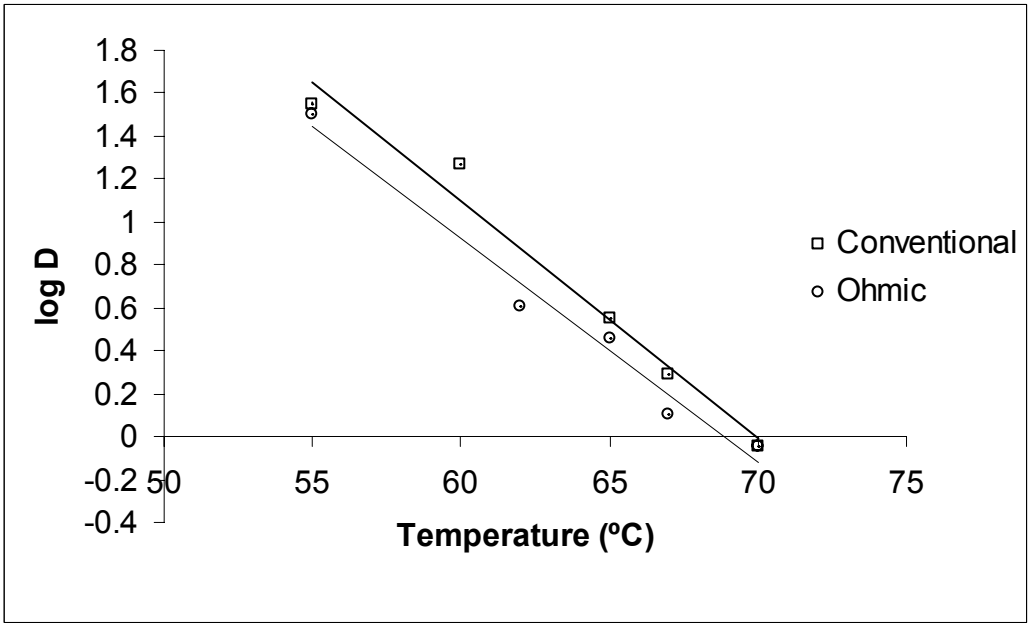

Figure 2.14: Degradation kinetics of ALP when submitted to conventional or ohmic heating.

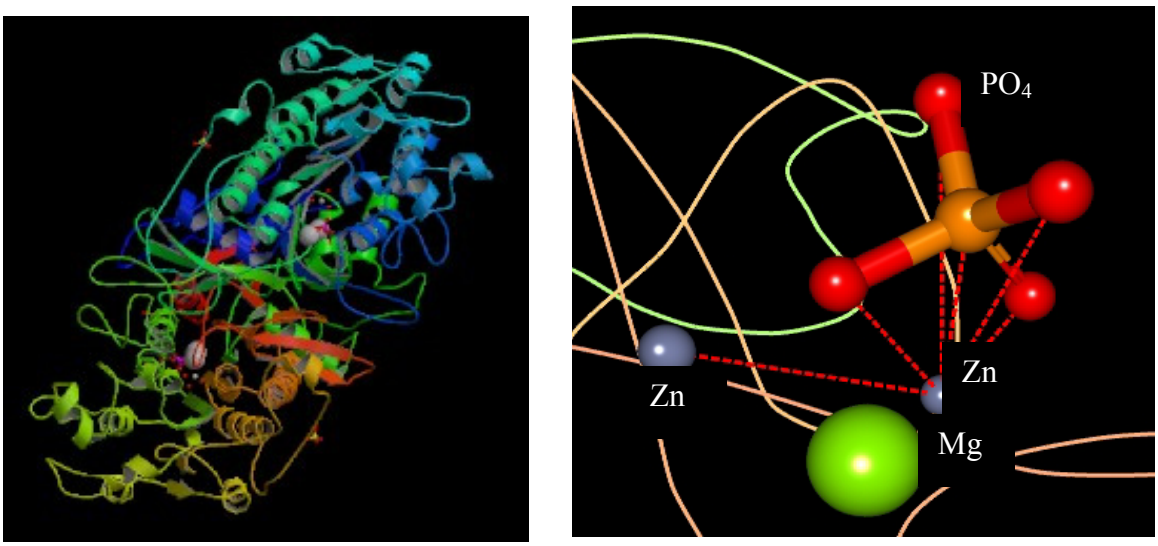

Figure 2.15: Cristal structure of ALP and disposition of the metallic atoms in nucleus

Alkaline phosphatases are dimeric metalloenzymes having two Zn^{2+} and one Mg^{2+} ions at the catalytic site and these elements are fundamental for enzymatic activity (Kim and Wyckoff, 1991). The ligand combination at the catalytic site of alkaline phosphatases is largely conserved from *Escherichia coli* to humans, being the bacterial enzyme the most studied. In *E. coli* the Zn^{2+} ion at metal-binding site 2 activates the hydroxyl group of Ser102, which performs a nucleophilic attack on the phosphate moiety of the substrate, resulting in a covalent phosphoseryl intermediate (Gettins and Coleman, 1983). A water molecule, activated by the Zn^{2+} ion at metal-binding site 1 hydrolyzes this intermediate via a non-covalent enzyme–phosphate complex. This phosphate moiety is then released from the complex and the enzyme returns to its free state. Thus, of the three metal ions found at the active site, the two Zn2+ ions are thought to play important roles in catalysis. A recent study indicated that the Mg2+ ion affects the orientation of Ser102, which alters the protein conformation near the Zn2+ ion at M2 (Holtz and Kantrowitz, 2000) Moreover, bovine milk ALP activity markedly decreased when the Mg2+ ion at its active site was replaced by Zn2+, and a number of APLs require the addition of Mg2+ to achieve maximum activity (Chappelet-Tordo and Lazdunski, 1983).

The electric field did not show a clear additional effect on enzyme loss of activity in the tested conditions. In fact, D-values are statistically different for 3 of the tested temperatures (55, 60 and 65 ºC) but statistically identical for the other 3 temperatures tested at a 5 % significance level; however the presence of metallic cofactors would point out to a different result once the loss of this metallic cofactors were advanced as a possible explanation for

the results obtained for PPO and LOX (see above). This result may be explained by differences in the intramolecular forces (between the amino-acid residues and the amino-acids and metallic ions), being this forces stronger in the case of milk APL when compared to the other enzymes. This would prevent conformational changes (additional to the thermal) and/or the loss of metallic ions, both responsible for inactivation of the enzyme.

Considering that milk thermal processing effectiveness is often determined based in the measurement of this enzyme's activity, the results point out to the conclusion that even if milk is ohmically pasteurized this enzyme may continue to be used as a time-temperature indicator (TTI) by the dairy industry. In fact, if there was activity loss caused by the presence of the electric field, the risk of accepting under-processed milk was high, thus affecting food safety.

3.5. β-Gal

The potential use of β-galactosidase in the food industry for the production of lactose-free products is gaining importance because the number of lactose intolerant individuals has been increasing in the last years (Gonzalez and Monsan, 1991). Furthermore, the use of alternative processing technologies, either thermal or non-thermal (e.g. ohmic heating, pulsed electric fields, high pressure) to process products with heat sensitive components (e.g. most of vitamins are included in the heat sensitive group, integrating higher nutritional value products or even functional food products or ingredients) has been gaining more and more attention from food technologists in the last decade. This is mainly due to the ever increasing consumer demand for healthier foods.

β-gal activity needs to be maintained or even enhanced during the industrial production process which justifies the need for verifying if the presence of a moderate electric field will have any influence on the enzyme's activity. The enzyme used in the work presented here was obtained by a fermentative process as described earlier in the chapter and the process temperature was varied from 65 to 80 ºC.

The inactivation parameters, expressed in terms of *D* and *z*-values are presented in Table 2.14 and Figure 2.16.

Table 2.14: Kinetic parameters of thermal degradation of β-GAL

Temperature (ºC)	65	70	72	75	78	80
$D_{conventional}$ (min)	182.0 ± 0.13	33.90 ± 0.49	12.89 ± 0.81	2.99 ± 0.18	0.52 ± 0.05	0.50 ± 0.03
D_{ohmic} (min)	-	-	9.70 ± 0.01	2.77 ± 0.06	0.64 ± 0.06	0.28 ± 0.00
$z_{conventional}$ (ºC)	5.12 ± 0.08 (r^2 = 0.99)					
z_{ohmic} (ºC)	5.08 ± 0.17 (r^2 = 0.98)					
$E_{a\ conventional}$ (kJ·mol^{-1})	399.39 ± 2.51					
E_{a_ohmic} (kJ·mol^{-1})	354.28 ± 9.65					

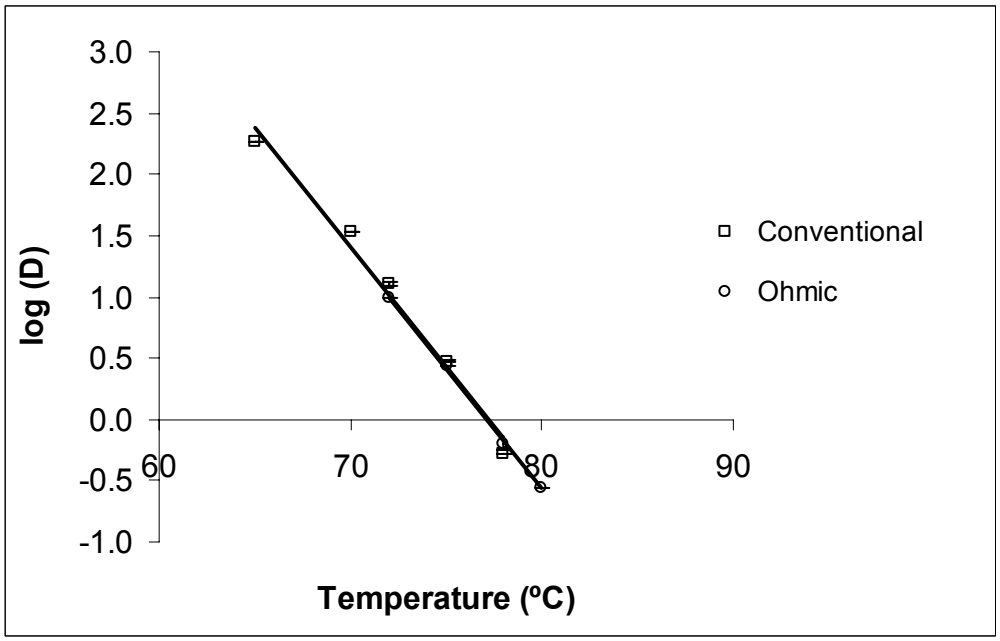

Figure 2.16: Degradation kinetics of β-Gal when submitted to conventional or ohmic heating.

For β-GAL, as already reported for PEC, both conventional and ohmic inactivation mechanisms are similar and the results obtained do not show an additional effect of the electric field on the enzyme inactivation ($p > 0.05$, see Table 2.15).

The enzyme from *Escherichia coli*, a very large protein with a tetrameric molecular mass of about 465 kDa, is active in the tetrameric form. Each monomer folds into five

compact sequential domains, plus an extended segment of about 50 residues at the N-terminus, and contains 23 tryptophan residues. The domains are packed very tightly to give a compact monomer. The residues at the N-terminus of each monomer are required for formation of the active tetrameric enzyme (D'Auria *et al.*, 2001). The β-galactosidase from an extreme thermophile, *Thermus thermophilus* A4, is thermostable and forms a homotrimeric structure resembling a flowerpot (Hidaka *et al.* 2002). The environment around the catalytic nucleophile (Glu312) is similar to that in the case of *E. coli* β-galactosidase, but the recognition mechanism for a substrate is different. Trp182 of the next subunit of the trimer constitutes a part of the active-site pocket, indicating that the trimeric structure is essential for the enzyme activity. Rojas *et al.* (2004) stated that the significant sequence similarity with β-galactosidases from *Aspergillus candidus*, *A. niger* and *Talaromyces emersonii* allows to conclude that these proteins should share significant structural homology with the enzyme produced by *Penicillium* spp. Their structure can be divided into five domains.

Amino acid sequence comparison between β-galactosidases from fungi shows that all the nine residues involved in galactose binding are well conserved among the different species. However for the *E. coli* enzyme the catalytic activity is only possible when a quaternary structure exists while for fungal enzymes the entire of the catalytic machinery would appear to be provided by a single subunit and are therefore compatible with being catalytically active as monomers (Rojas *et al.*, 2004). Being so, and considering that the β-gal from different sources have different structural conformations (Figure 2.17: Stereo view of the structural superposition of Psp-□-gal (in cyan), Ec-□-gal (in orange) and A4-□-gal (in brown) (adapted from Rojas *et al.,* 2004). and catalytic mechanisms, as explained above in the text, it is noteworthy that the results obtained for this particular enzyme should not be extrapolated to other enzymes produced by different microorganisms. It is likely that e.g. the *E. coli* enzyme would be more affected by the electric field then the enzymes from other sources once these may display catalytic activity as monomers.

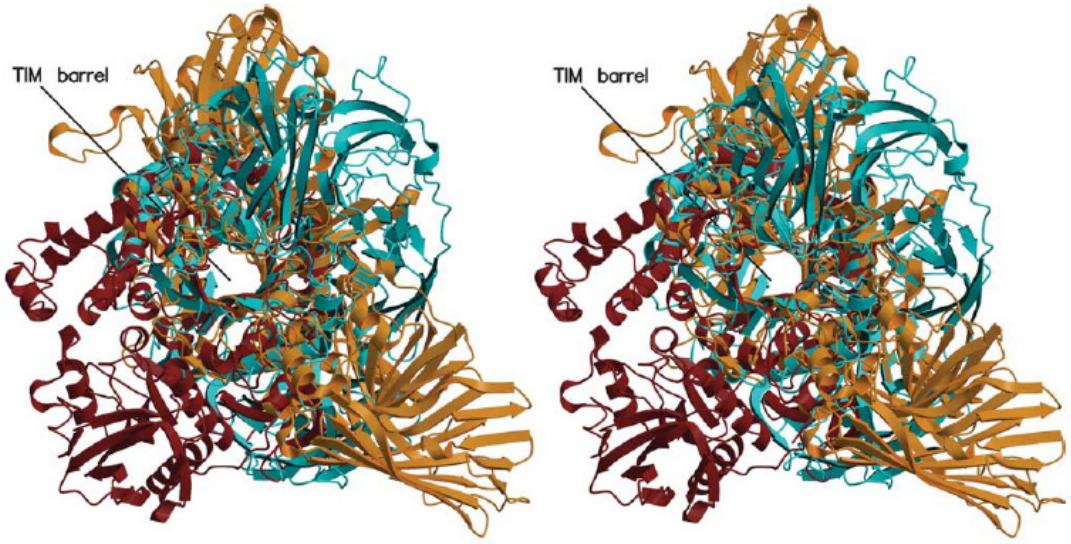

Figure 2.17: Stereo view of the structural superposition of Psp-β-gal (in cyan), Ec-β-gal (in orange) and A4-β-gal (in brown) (adapted from Rojas *et al.*, 2004).

4. Conclusions

The obtained results regarding enzyme degradation kinetics in the presence of an electric field suggest that the "electric effect" is enzyme-dependant. This means that some important enzymes (e.g. PEC, β-GAL) will not have enhanced inactivation kinetics in the presence of a moderate electric field while others will be easily destroyed under such conditions (e.g. LOX).

In general, the enzymes having a metal prosthetic group (Table 2.15) are more affected by the presence of a moderate electric field. This was hypothesized to be due to the loss of the metal ion which is attracted to one of the electrical poles.

Table 2.15: LSD test for *z* values determined under ohmic and conventional heating conditions, for all the enzymes tested.

Enzyme	Prosthetic group	$z_{conventional}$	z_{ohmic}	*p*
LOX	Fe	11.10	15.04	0.047
PEC	-	8.12	7.72	0.075
PPO	Cu	12.20	12.80	0.02
ALP	Zn, Mg	9.05	9.30	0.145
β-GAL	Zn	5.12	5.08	0.437

In terms of activation energy (Figure 2.18) all the enzymes assayed had values in the same order of magnitude and in general only slight differences exist between conventional or ohmic heating. However, in the case of LOX, which is the enzyme most affected by the electric field, the activation energy for the ohmic process is significantly lower. On the contrary, for PEC (not affected by the electric field) this parameter is slightly higher in the ohmic process. The activation energy of a reaction is the amount of energy needed to start the reaction. Considering this definition, the values of this parameter obtained in the present work seem to indicate that it can be of use when predicting if an enzyme will be affected by the electric field and what is the extent of that influence.

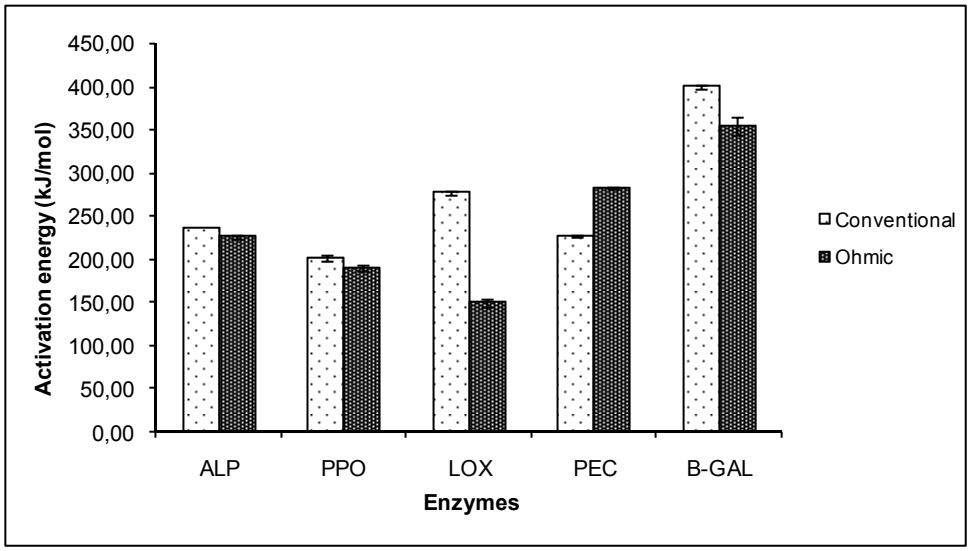

Figure 2.18: Comparison of activation energy for all the enzymes tested, for both conventional and ohmic heating

The effect of the electrical field on enzymes has to be assessed before the ohmic heating technology is fully implanted for the continuous processing of foods.

The obtained data, using target enzymes from different sectors of the food industry, show that the use of ohmic heating as an alternative to conventional heating can be beneficial in terms of enzyme inactivation when that is the main purpose (cases of LOX and PPO) because the electric field reduces the *D*-values for those enzymes when compared to conventional heating. The activity of PEC, ALP and β-GAL seems not to be more affected by ohmic heating than by conventional heating. This result is quite encouraging because PEC and β-GAL are process enzymes that should not be inactivated. However, care should be taken on extrapolating the results once these conclusions may not be verified in other food matrixs or other food enzymes. On the other hand, the use of ohmic heating technology implies that process effectiveness criteria (TTIs such as enzymes and target microorganisms) must be validated. The kinetic parameters obtained show that ALP may continue to be used as a TTI, in the dairy industry, without further adaptations. On the contrary, for PPO and LOX the traditionally used inactivation kinetics will have to be replaced by the ones obtained in the present work, if ohmic heating technology is to be applied.

The effect of ohmic heating on enzymes structure needs to be further assessed.

5. Future chanllenges

Recently, several thermal and non-thermal technologies have been proposed for food processing, having as their main objective to contribute to the production of safer and higher quality food products. Ohmic heating is one of these technologies presenting as its main advantage that heat generation occurs inside the material being processed. It is emphasized here that the internal heat generation induced by ohmic heating eliminates the problems associated with heat conduction in food materials, preventing the over-cooking typical of conventional thermal food processing. Enzymes are of extreme importance in the food processing industry either because they are necessary or need to be inactivated since they can cause detrimental effects on foodstuffs.

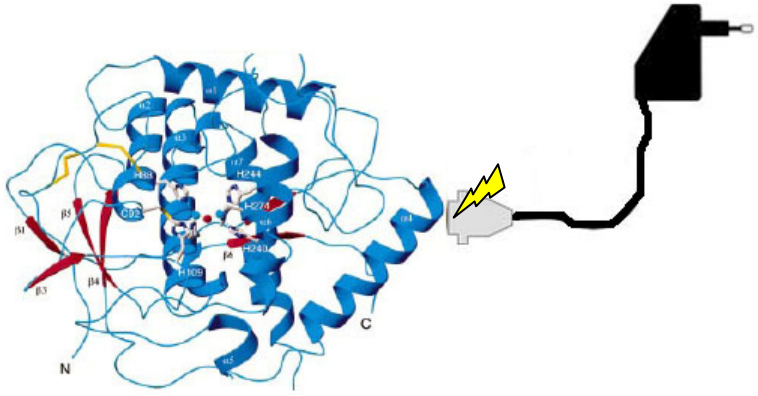

Figure 2.19: Does electricity change protein structure ?

Fundamental research must be conducted regarding enzymatic technology applied to food, pharmaceutical or medical industry in order to fully address possible electric effects on the bio-molecules thus contributing to improve and optimize processes. It is then important:

- to understand deeply the effect of electricity on proteins structure (Figure 2.19);
- to attend to the effect of electricity on protein-ligand interactions;
- to address the impact of the electric field on metallic and non-metallic cofactors

Furthermore, the influence of electricity on DNA repair enzymes or oxidative stress enzymes must also be investigated since it may lead to important conclusions to be used in the medical or pharmaceutical industries.

6. References

Bailey M., Linko M., (1990). Production of B- galactosidase by Aspergillus oryzae in submerged biorector cultivation. J. Biotecnol. 16: 57-66.

Barbosa-Cánovas, G.V., Pothakamury U.R., Palou E., Swanson B.G., (1998). Biological effects and applications of pulsed electric fields for the preservation of foods. In: Barbosa-Cánovas, G.V., Pothakamury, U.R., Palou, E., Swanson, B.G., eds. Nonthermal Preservation of Foods. New York: Marcel Dekker

Bonnin, E., Le Goff, A., Korner, R., Van Alebeek, G., Christensen, T., Voragen, A.G.J., Roepstorff, P., Caprari, C., Thibault, J.F., (2001). Study of the mode of action of endopolygalacturonase from Fusarium moniliforme. Biochimica Et Biophysica Acta-General Subjects, 1526 (3): 301-309.

Castro A.J., Swanson B.G., Barbosa-Cánovas G.V., Meyer R., (2001). Pulsed electric field modification of milk alkaline phosphatase activity. In: Barbosa-Cánovas, G.V., QH Zhang, eds. Pulsed Electric Fields in Food Processing: Fundamental Aspects and Applications (Vol. 3). Lancaster, PA: Technomic Publishing Co., pp 65-83.

Castro, I., Teixeira, J. A., Salengke, S., Sastry, S. K., Vicente, A. A., (2004). Ohmic heating of strawberry products: electrical conductivity measurements and degradation kinetics; Inn Food Sci Emerg Technol., 5, 27-36.

Claeys, Wendie L. Indrawati, Van Loey, A. M., Hendrickx, M. E., (2003). Review: are intrinsic TTIs for thermally processed milk applicable for high-pressure processing assessment? Innovative Food Science and Emerging Technologies 4, 1–14

D'Auria, S., Di Cesare, N., Gryczynski, I., Rossi, M, Lakowicz, J. R., (2001). On the Effect of Sodium Dodecyl Sulfate on the Structure of □-Galactosidase from Escherichia coli. A Fluorescence Study. J. Biochem. Vol. 130, pp. 13-18.

De Alwis A.A.P., Fryer P.J., (1990). The use of network theory in the finite-element analysis of coupled thermo-electric fields. Com Appl Num Meth 6:61-66.

Denys S., Van Loey A.M., Hendrickx M.E., (2000). A modelling approach for evaluating process uniformity during batch high hydrostatic pressure processing: combination of a numerical heat transfer model and enzyme inactivation kinetics. Inn Food Sci Emerg Technol 1:5-19.

Domingues, L; Vicente, A.A.; Lima, N.; Teixeira, J.A., (2000). Applications of Yeast Flocculation in Biotechnological Processes; Biotech Biop Eng, 5, 288-305.

Garotte R.L., Silva E.R., Bertone R.A., (2003). Kinetic parameters for thermal inactivation of cut green beans lipoxygenase using unsteady-state methods. Latin Amer Appl Res 33:87-90.

Gettins, P., Coleman, J.E., (1983). 31P nuclear magnetic resonance of phosphoenzyme intermediates of alkaline phosphatase. J Biol Chem 258, 408–416.

Giner-Seguí, J., Bailo-Ballarín, E., Gorinstein, S., Martín-Belloso, O., (2006). New Kinetic Approach to the Evolution of Polygalacturonase (EC 3.2.1.15) Activity in a Commercial Enzyme Preparation Under Pulsed Electric Fields Journal of Food Science 71 (6), E262–E269.

Golan-Goldhirsh, A., Whitaker, J. R., (1984). Effect of ascorbic acid, sodium bisulfite and thiol compounds on mushroom polyphenol oxidase. Journal of Agricultural and Food Chemistry, 32,1003–1009.

Gonzalez R.R., Monsan P., (1991) Purification and some characteristics of β-galactosidase from Aspergillus fonsecaeus. Enzyme Microb Technol 13: 349-352.

Grahl T., Markl H., (1996). Killing of microorganisms by pulsed electric fields. Appl Micro Biotech, 45:148-157.

Hidaka, M., Fushinobu, S., Ohtsu, N., Motoshima, H., Matsuzawa, H., Shoun, H., Wakagi, T., (2002). Trimeric Crystal Structure of the Glycoside Hydrolase Family 42 beta-Galactosidase from Thermus thermophilus A4 and the Structure of its Complex with Galactose J.MOL.BIOL. v322 pp.79-91.

Ho S.Y., Mittal G.S., Cross J.D., (1997). Effects of high field electric pulses on the activity of selected enzymes. J Food Eng 31:69-84.

Honda S., Nishimura Y., Takahashi M., Chiba H., Kakehi K., (1982). Anal Biochem, 119- 194.

Jankov, S. (1962). Fruchtsaft-Ind. 7,12.

Kim L., Hwang M.S., Kim E.S, (1995). Extraction, partial characterization, and inhibition patterns of polyphenol oxidase from burdock (Arctium lappa). In: CY Lee, JR Whitaker, eds. Enzymatic Browning and It's Prevention. Washington, D. C.: American Chemical Society Symposium Series 600.

Kim, E.E., Wyckoff, H.W., (1991). Reaction mechanism of alkaline phosphatase based on crystal structures. Twometal ion catalysis. J Mol Biol 218, 449–464.

Klabunde, T., Eicken, B., Sacchettini, J. C., Krebs, B., (1998) Crystal structure of a plant catechol oxidase containing a dicopper center. Nature structural biology • volume 5 number 12 • december.

Kruger J.E., MacGregor A.W., Marchylo B, (1991). Endodenous cereal enzymes. In Food Enzymology, Vol. 2, Chapter 17 pp 1-46, P.F. Fox, ed. Elsevier Applied Sci., London and New York.

Lima M., Sastry S.K., (1999). The effects of ohmic heating frequency on hot-air drying rate and juice yield. J Food Sci 41:115-119.

Linden, G., Chappelet-Tordo, D., Lazdunski, M., (1977). Milk alkaline phosphatase. Stimulation by Mg2+ and properties of the Mg2+ site. Biochim Biophys Acta 483, 100–106.

Ludikhuyze L., (1998). High pressure technology in food processing and preservation: a kinetic case study on the combined effect of pressure and temperature on enzymes. PhD dissertation. Katholieke Universiteit Leuven, Leuven, Belgium.

Ludikhuyze, L. R., Indrawati, I. Van den Broeck, C. A. Weemaes and Hendrickx, M. E., (1998). High Pressure and Thermal Denaturation Kinetics of Soybean Lipoxygenase: a Study based on Gel Electrophoresis Lebensmittel-Wissenschaft und-Technologie Volume 31, Issues 7-8 , November 1998, Pages 680-686

Martinez, M. V., & Whitaker, J. R. (1995). The biochemistry and control of enzymatic browning. Trends in Food Science and Technology, 6, 195–200.

Robinson D.S., (1991). Peroxidases and their significance in fruits and vegetables. In Food Enzymology, Vol. 1, Chapter 10 pp 399-426, P.F. Fox, ed. Elsevier Applied Sci., London and New York.

Rojas, A. L., Nagem, R. A. P., Neustroev, K. N., Adamska, M. A. M., Eneyskaya, E. V., Kulminskaya, A. A., Garratt, R. C., Golubev, A. M., Polikarpov, I., (2004). Crystal Structures of b-Galactosidase from Penicilliumsp. and its Complex with Galactose. J. Mol. Biol. 343, 1281–1292.

Sapers, G. M. (1993). Browning of foods: Control by sulfites, antioxidants and other means. Food Technology, 47, 75–84.

Sicilia, F., Fernandez-Recio, J., Caprari, C., De Lorenzo, G., Tsernoglou, D., Cervone, F., Federici, L., (2005). The Polygalacturonase-Inhibiting Protein PGIP2 of Phaseolus vulgaris Has Evolved a Mixed Mode of Inhibition of Endopolygalacturonase PG1 of Botrytis cinerea1. Plant Physiol. 2005 November; 139(3): 1380–1388. v.139(3).

Ska, A.W., Bryjak, J, Illeova, V., (2006). Milan Polakovic. Kinetics of thermal inactivation of alkaline phosphatase in bovine and caprine milk and buffer, International Dairy Journal.

Somogyi L.P., Ramaswamy H.S., Hui Y.H., (1996). Biology, principles and applications In: Processing fruits: science and technology. Vol. 1. Technomic Publishing Co., Inc. Lancaster, Pensylvania.

Stec, B., Holtz K.M., Kantrowitz, E.R., (2000). A revised mechanism for the alkaline phosphatase reaction involving three metal ions. J Mol Biol 299, 1303–1311.

Skrzypczak-Jankun, E., Funk, M. O., Boyington, J. C. Amzel, L. M. (1996). Lipoxygenase: a molecular complex with a non-heme iron Journal of Molecular Structure, Volume 374, Issues 1-3, Pages 47-52.

Vamos-Vigyazo, L. (1981). Polyphenol oxidase and peroxidase in fruits and vegetables. CRC Critical Reviews in Food Science and Nutrition, 15, 49– 127.

Van Loey, A., Verachtert, B., Hendrickx, M., (2002). Effects of high electric field pulses on enzymes. Trends Food Sci Technol 12:94-102.

Williams, D.J., Nottingham, S.M., (1990). Suitability of a modification to the Aschattenburg and Mullen alkaline phosphatase test for goast's milk: collaborative study. Aust J Dairy Technol.

Chapter 3.

THE EFFECT OF MODERATE ELECTRIC FIELDS ON IMPORTANT FOOD SPOILAGE MICROORGANISMS: COMPARISON OF INACTIVATION KINETICS UNDER CONVENTIONAL AND OHMIC HEATING

Abstract

Although electricity has been widely used in biological systems, there is lack of information regarding the effects of alternating electric current on microbial growth. Moreover, the published results are controverse and sometimes thermal effects cannot be effectively eliminated as a process variable making difficult the assessment of electrical effects *per se*.

This part of the work aimed at determining the existence of a non-thermal effect of electricity in the inactivation of different food spoilage microorganisms. The chosen microorganisms were ascospores of *Byssochlamys fulva*, *Escherichia coli* (a gram negative bacterium) and spores of *Bacillus licheniformis*. The inactivation kinetics for each microorganism was performed in several food products, namely strawberry pulps (with different ºBrix values), goat milk and cloudberry jam. The temperature range of the assays was dependent on the microorganism being studied.

In every case, the inactivation kinetics followed a first order kinetics and *D* and *z* values were calculated. The *D*-values obtained when using ohmic heating were always lower than the ones calculated from conventional treatment experiments pointing out to a non-thermal effect of electricity in the different microorganisms or spores. *z*-values were similar for both types of treatments in all cases.

The results obtained lead to the formulation of the hypotheses that the electric field generates changes in the cells micro-environment namely in terms of the ionic strength (ions concentration), induces irreversible pore formation and also affects proteins involved in the ascospore germination mechanism or in the active transport of molecules into the cell thus interfering not only in the membrane barrier capacity but also in some physiological functions, leading to the loss of viability.

Industrial relevance: The validation and industrial implementation of ohmic heating technology is highly dependent on the existence of data reporting the efficiency of the process for microbial inactivation and its advantages regarding the conventional or other innovative technologies. Some of the advantages can be the inactivation of spores and the requirements for less aggressive heat treatments which may improve the final quality of the food products or ingredients.

Keywords: microorganisms inactivation kinetics, food spoilage microorganisms, moderate electric field

1. Introduction

1.1. Microbial kinetics

Microbial inactivation in foodstuffs is predominantly carried out by thermal processes and the thermal inactivation kinetics of most of the target microorganisms is well studied. The need to reduce processing time and the increasing interest in using OH as an alternative heating technology to conventional heat transfer during commercial processes was the drive for the study of non-thermal mechanisms of microbial inactivation.

The destruction of microorganisms by non-thermal effects such as electricity is still not well understood and generates some controversy. Little work has been done in this field. Moreover, most of the published results do not refer to the sample temperature, or cannot eliminate temperature as a variable parameter leading to a strong motivation to try new approaches leading to more consistent conclusions about this subject.

The kinetics of inactivation of *Bacillus subtilis* spores by continuous or intermittent ohmic and conventional heating were studied by Cho *et al.* (1999) to determine if electricity had an additional effect on the killing of this microorganism during single and double-stage heating treatments. Experiments were conducted in an ohmic fermentor for temperatures ranging from 88 to 99.1 ºC (see Table 3.1). Spores heated at 92.3 ºC had significantly lower decimal reduction time *(D)* values when using ohmic rather than conventional heating. These results indicate that electricity has an additional killing effect against bacterial spores. The dependence on temperature of the *D* value (*z* value) and the activation energy (E_a) were not significantly affected indicating that electricity affects the death rate but not the temperature dependency of the spore inactivation process.

Table 3.1: Kinetic constants and thermal inactivation parameters for *Bacillus subtilis* spores under conventional and ohmic heating.

Temperature (ºC)	D_{conv} (min^{-1})	D_{oh} (min^{-1})	k_{0conv} (s^{-1})	k_{0oh} (s^{-1})
88.0	32.8	30.2	0.00117	0.001271
92.3	9.87	8.55	0.003889	0.004489
95.0	5.06	-	0.007586	-
95.5	-	4.38	-	0.008763
97.0	3.05	-	0.012585	-
99.1	-	1.76	-	0.021809
z (ºC)	8.74	9.16	-	-
E_a (kJ.mol^{-1})	-	-	292.88	282.42

Source: adapted from Cho *et al.* (1999)

Palaniappan *et al.* (1992) indicated that electricity did not influence inactivation kinetics but the application of a non-lethal electric field reduces the intensity of the subsequent thermal treatment. This implies that the electric field lowers the heat resistance of microorganisms. Microbial death during OH was mainly attributed to thermal effects, while the non-thermal effects were found to be insignificant (Table 3.2)

Table 3.2: Kinetic constants and thermal inactivation parameters for *Zygosaccharomyces bailii* under conventional and ohmic heating.

Temperature (ºC)	D_{conv} (min^{-1})	D_{oh} (min^{-1})	$k_{0conv.}$ (s^{-1})	k_{0oh} (s^{-1})
49.8	294.6	274.0	0.008	0.009
52.3	149.7	113.0	0.016	0.021
55.8	47.21	43.11	0.049	0.054
58.8	16.88	17.84	0.137	0.130
z (ºC)	7.19	7.68	-	-
E_a (kJ.mol^{-1})	-	-	123.97	116.19

Source: Palaniappan *et al.* (1992)

Yildiz and Baysal (2006) studied the effects of alternative current heating treatment on *Aspergillus niger*, pectin methylesterase and pectin content in tomato. These authors

concluded that the critical treatment time for *A. niger* decreased as the electric field strength increased. However, the temperature profile was different between the assays and therefore the effect of electricity *per se* was not proved. The enhanced inactivation could be due either to higher electric field or simply higher temperature. To date, no more studies on fungal inactivation using electricity (ohmic or pulsed electric fields) were found on the available literature.

Data on non-thermal effects are scarce and more studies are needed to determine the effect of electricity on the physiological characteristics of microbes, changes in glycosylation degree of proteins and lipids, DNA damages, mutagenic effects and other factors that may affect the heat resistance of microorganisms.

The influence of the electric field in different microorganisms, having diverse morpho-physiological characteristics, such as bacteria, filamentous fungi and yeast need to be fully recognized because all of these can either be food spoilage microorganisms or helpful in food production processes. Being so, one may need to inactivate them or keep them in foods (e.g. fermented foods) thus data on non-thermal effects can be used to optimize processes.

1.2. Fundamental Effects and Mechanisms of Electropermeabilization

Following the first empirical descriptions of Gossling (1960) and Doevenspeck (1960, 1961), it was not until the 1980s that the interest to use electroporation in medical science and genetic engineering emerged. Whereas the basis of the disruptive effect of electric fields on biological cells has already been discussed empirically in the 1960s, only later on the dielectric rupture theory was introduced by Neumann and Rosenheck (1972) and Zimmermann *et al.* (1974). Subsequently, the electrical breakdown of cellular membranes has been explored based on model systems as phospholipid vesicles and planar bilayers as well as microorganisms (Zimmermann *et al.* 1974; Chernomordik *et al.* 1987; Chang *et al.* 1992; Wouters and Smelt 1997; Barsotti *et al.* 1999; Ho and Mittal 2000). However, until the present moment there is no clear evidence of the underlying mechanisms at the cellular level. Elucidation of membrane permeabilization is a difficult task as the time sequence of formation of pores is in the sub-microsecond range and the area of pore formation is only in the range of 0.1 % of the total membrane surface. The permeabilization of a cell membrane requires two key steps: firstly, the formation of a pore has to be induced by the electric field applied and, secondly, this pore has to be stable enough to allow interaction of the intra- and extracellular media. The available information regarding the time sequence and the

dynamics of the electroporation process as well as on reversible-irreversible structural changes of cells during and after ohmic or pulsed electric field (PEF) treatments is scarce. Two effects have been described to be triggered by the electric field, the ionic punch-through effect (Coster 1965) and the dielectrical breakdown of the membrane (Zimmermann *et al.* 1973). Currently, it is generally accepted that the primary effect of electric field on biological cells is related to local structural changes and breakdown of the cell membrane. This organelle is a highly important component of the biological cell as it acts as semipermeable barrier responsible for mass transfer and plays an important role in synthesis of RNA and DNA, protein and cell wall components as well as many other complex metabolic activities (Rogers *et al.* 1980). In addition, the disruption of intracellular organelles and other structural changes have been described (Harrison *et al.* 1997). The cell membrane of biological cells can be considered as a capacitor filled with dielectric material of low electrical conductance, and a dielectric constant in the range of 2 (Zimmermann *et al.* 1974). Accumulation of charges with opposite polarity on both sides of the membrane leads to a naturally occurring, perpendicular transmembrane potential of about 10 mV. In an electrically conductive media placed between a high voltage and a grounded electrode the resulting electrical field can be predicted from the Laplace equation. By exposure to an external electrical field an additional potential is induced by movement of charges along the electric field lines. A schematic depiction of impact of external electric field on cell membranes is shown in Figure 3.1.

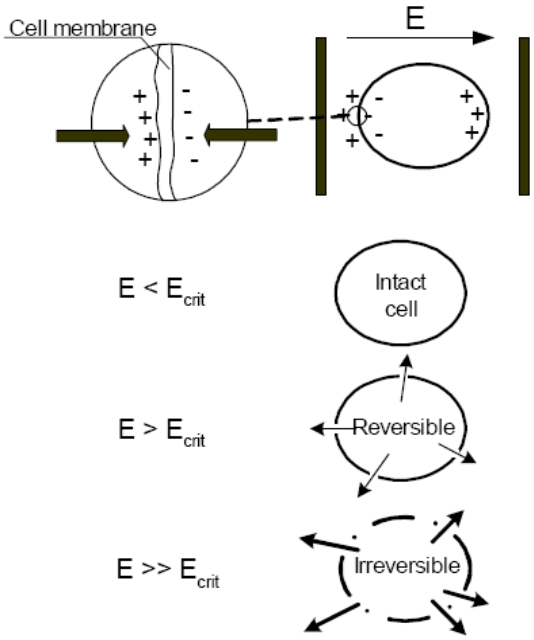

Figure 3.1: Schematic depiction of mechanism of membrane permeabilization by electro-compressive forces induced by an external electrical field. Increasing treatment intensity will lead to formation of large, irreversible membrane pores.

When the overall voltage exceeds a critical value of about 1 V, depending upon the compressibility, the permittivity, and the initial thickness of the membrane (Crowley 1973; Zimmermann 1996) the electro-compressive force causes a local dielectric rupture of the membrane inducing the formation of a pore, acting as a conductive channel (Schoenbach *et al.* 1997). Taking into account a membrane thickness of 5 nm this translates to a dielectric strength (electrical field) of 2000 kV/cm. A drastic increase in permeability re-establishes the equilibrium of the electrochemical and electric potential differences of the cell plasma and the extracellular medium forming a Donnan-equilibrium (Glaser, 1998). This phenomenon was termed dielectric breakdown, borrowing the expression from solid state physics (Zimmermann *et al.* 1976). An electro-mechanical model was developed, implying that the presence of an electrical field across the membrane results in a mechanical compression. The cell membrane was considered as a capacitor, containing a perfectly elastic dielectric. Compressive forces are balanced by the restoring mechanical force, increasing the compression by increasing the transmembrane potential a mechanical instability can occur. Crowley (1973) reported a good agreement between predicted breakdown voltage and assumed elastic parameters for a model system of phosphatidylcholin bimolecular lipid layers. Electrical breakdown has been shown for algal cells as well as for bacteria and human red blood cells measuring size distribution with a

Coulter counter, concluding that probably the most important application will be to load cells with substances the cell membrane is normally impermeable to (Zimmermann *et al.* 1976).

Up to now the electro-mechanical instability is still being used to explain the effect of external electrical fields on biological cells and is one of the most accepted theories. The electric breakdown is reversible if the pores induced are small in comparison to the membrane area. Increase of electric field strength and treatment intensity by increasing pulse width and/or number will promote formation of large pores and the reversible damage will turn into irreversible breakdown. Experimental evidence is supporting this electro-mechanical compression model: a critic electric field strength was found and was dependent on the size and geometry of a cell in the range of 1 – 2 kV/cm for plant cells and 10 - 14 V/cm for microbial cells as *E. coli*. However, as subsequent phenomena such as resealing of pores, membrane conductance course and transport phenomena are not taken into account, several other models have been proposed to predict the mechanisms at a molecular level, as the fluid mosaic model of a lipid bilayer with embedded protein units (Jacob *et al.* 1981).

In contrast to the electric compressive forces, other theories include the occurrence of membrane deteriorations and reorientations on the lipid bilayer and the protein channels as cause of increase in permeability. Dimitrov (1984) presented an extension of the electromechanical model taking into account the viscoelastic properties of the membrane, membrane surface tension and molecular rearrangements as well as pore expansion to describe the time course of field-induced breakdown of membranes. Other alternative concepts are based on molecular reorientation and localized defects within the cell membrane which are expanded and destabilized by exposure to an electric field. The presence of small fluctuating hydrophobic pores in the lipid matrix was suggested to be the initial structural basis of electroporation (Chernomordik 1992). By external electrical stress these may be transformed into hydrophilic pores by reorientation if the pore radius is increased above the value where the pore energies of both orientations coincide. The pore energy is the change of free energy resulting from the formation of a pore within the lipid bilayer. As long as the pore radius is small the formation of hydrophobic pores is more favorable, but at a range of 0.5 nm the pore energies of hydrophobic and hydrophilic pores become equal and pore inversion may occur (Glaser *et al.* 1998). Dipolar reorientation of phospholipids and transition from hydrophobic to hydrophilic pores has been described by Tsong (1991), assuming a change in membrane structure by Joule heating within a conductive pore. These pores might also cause a loss of ability to regulate the intracellular

pH (Simpson *et al.* 1999) and short circuit of protein-pumps (Chernomordik 1992). Membrane rupture was related to osmotic imbalances and cell swelling after opening of pores, and defined a two-step mechanism (Tsong 1990): an initial perforation of the cell membrane after a dielectric breakdown is followed by a time-dependent pore expansion.

Electroporation could take place both in lipid domains and protein channels, in particular as their functionality is influenced by the transmembrane potential. The gating potential for protein channels is in the 50 mV range, considerably smaller than the dielectric strength of a phospholipid bilayer. However, though opening of protein channels is induced it may not be sufficient to prevent the development of a transmembrane potential above the breakdown potential of the lipid bilayer. Based on experiments with model systems such as liposomes or protoplasts large eukaryotic cells and microbes several theories have been developed or proposed to explain the underlying mechanism of pore formation and resealing (Neumann and Rosenheck 1972; Zimmermann *et al.* 1974; Sugar and Neumann 1984; Weaver and Powell 1989; Chang *et al.* 1992; Ho and Mittal 1996; Kinosita and Tsong 1997; Neumann *et al.* 1998; Weaver 2000). Pore formation might also occur as a consequence of structural defects within the cell membrane, expanding spontaneously formed pores in the presence of an electric field (Tsong 1991). An unprecedented amount of research work has been published in the field of genetic- and bio-engineering (Prasanna and Panda 1997; Pavlin *et al.* 2002; Valic *et al.* 2003; Puc *et al.* 2004), a comprehensive review on the (lack of) knowledge regarding cell permeabilization mechanisms has been published by Teissie *et al.* (2005). Even if underlying mechanisms of action are the same and micro-fluidic units are very helpful for mechanism elucidation, in contrast to food application, treatment intensity is much lower and in most cases a very small volume (in the range of μl to ml) is treated.

1.2.1. Effect of size, shape and morfology

Accurate modelling of the effect of electric filed on microorganisms is extremely difficult and it is microorganism- and population-dependent. The variability of one population in terms of size and even in shape can be significant and the shape factor affects the membrane critical potential and thus the critical potential necessary to induce irreversible electroporation. Being so, data to validate inactivation kinetics has to be experimentally obtained.

The potential difference ΔV_M at the membrane of a biological cell with spherical shape and a radius R induced by the electric field can be calculated by the following equation which is derived from solving several simplifying restrictions (Neumann, 1996):

$$\Delta\varphi_M = -\frac{3}{2} E \cdot f(k) \cdot R \cdot \cos(\alpha) \qquad \textbf{(Eq. 3.1)}$$

For the calculation of ΔV_M at a particular location at the membrane, the angle α of the radial direction vector has to be specified. By definition α is zero (and cos(α)=1) when the vector coincides with the direction of the electric field. Hence, the highest membrane potential differences are assumed to occur at the two poles of the cell in field direction.

The factor *f(k)* is an explicit function of the electrical conductivities of the suspending medium *k*, the plasma *ki*, the cell membrane *kM* and the ratio of the membrane thickness and the cell radius (Neumann, 1989).

For cells with non-spherical shape an estimate for membrane potential is given by (Zimmermann, Pilwat & Riemann, 1974)

$$\Delta V_M = -f(A) A_f E \qquad \textbf{(Eq. 3.2)}$$

This equation yields the local membrane potential difference at the distance *AF* from the centre in direction of the external electrical field. The shape factor *f(A)* is a function of the three semi-axis of elliptical cells.

Using experimental results for *ΔVM* the equation can be solved to determine the critical field strength (*E*) that leads to electroporation.

The impact of cell size and geometry on *E* can be visualized in Figure 3.2. A summary of data on cell size and shape is presented on Table 3.3.

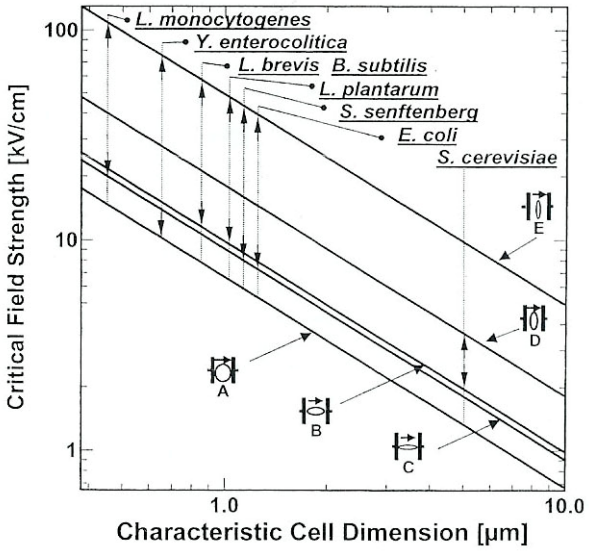

Figure 3.2: Critical electroporative field strength (*E*) as a function of cell dimensions and assuming *ΔVM* equal to 1 (Heinz et al, 2002)

Table 3.3: Geometry and mean size distribution of selected microorganisms (Heinz *et al.*, 2002)

Microorganism	Shape	Size (μm)
Listeria monocytogenes	Short rods	0.4-0.5 x 0.5-2
Yersinia enterocolitica	Straight rods to cocobacilli	0.5-0.8 x 1-3
Lactobacillus brevis	Rods with rounded ends	0.7-1.0 x 2-4
Bacillus subtilis	Rods with rounded or square ends	Small: 0.5 x 1.2 Large: 2.5 x 10
Lactobacillus plantarum	Rods with rounded ends	0.9-1.2 x 3-8
Salmonella senftenberg	Straight rods	0.7-1.5 2-5
Escherichia coli	Straight rods	1.0-1.5 x 2-6
Saccharomyces cerevisiae	Ellipsoidal shape	3.0-15 x 2-8

It is evident that the critical field strength sharply increases when the characteristic dimension of the cell decreases. It is also noteworthy that variations in cell shape produce a considerable raise of *E*. A rod-shaped cell requires an electrical field more than 5 times higher to the one required for a spherical cell with the same characteristic dimension.

In bacteria, the rigid cell wall is a single bag-shaped structure composed of a network of repeating, cross-linked peptidoglycan, also called murein (Figure 3.3). Thus, the cell wall can be several layers thick, each layer being a sheet of linked peptidoglycan units. The Gram-positive bacterial cell wall is distinguished by having multiple layers of peptidoglycan sheets and is thus up to ten times the thickness of a Gram-negative bacterial cell wall. In contrast to the Gram-positive bacterial cell wall, the Gram-negative bacterial cell wall is much more complex. It consists of a rigid peptidoglycan layer, which is much thinner than that found in the Gram-positive cells, overlaid by an outer membrane containing a diversity of structures. Between the cytoplasmic membrane and the outer membrane is the periplasmic space containing a gel-like periplasm in which resides the cell wall peptidoglycan as well as various enzymes. In addition to phospholipids, the outer membrane contains unique Gram-negative lipopolysaccharides (LPS) and various proteins (porins) and lipoproteins. In general, Gram-positive organisms seem to be less sensitive to heat which may be due, not only but also, to these morphological differences between the bacteria.

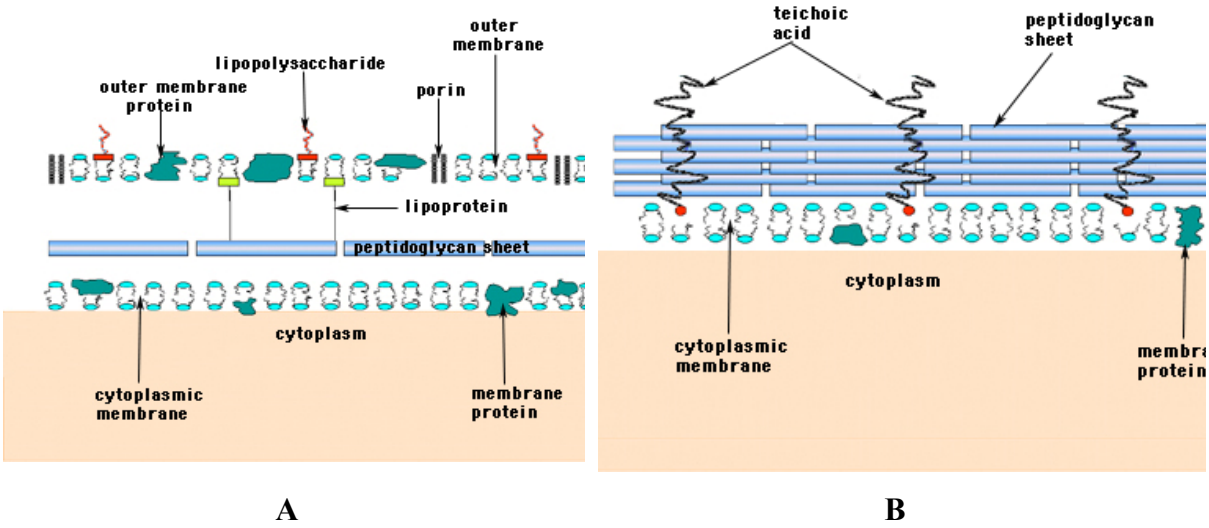

Figure 3.3: Cell wall composition of Gram negative (A) and Gram positive (B) bacteria

It should be stressed that, due to the large diversity in cell size and shape of a microbial population, the prediction of the critical field strength for a number of microorganisms has to be regarded only as an estimate.

1.3. Heat Resistant Food spoilage Fungi: Byssochlamys fulva

Spoilage of thermally processed fruits and fruit products by heat resistant molds has been recognized in several countries (Beuchat *et al.*, 1979; Fravel, and Adams 1986; Hocking, A. D., and J. I. Pitt. 1984., amongst others). *Byssochlamys fulva*, *B. nivea*, *Neosartorya fischeri*, *Talaromyces macrosporus*, *T. bacillisporus*, and *Eupenicillium brefeldianum* have been most frequently encountered. Ten *Byssochlamys* species have been recognized as spoilage molds in canned fruit since the early 1930's (Hull, 1933, 1938) and have been extensively studied (Beuchat *et al.*, 1979; Jesenska *et al.* 1984; King *et al.* 1969; Put, 1964). First noticed in England in the early 1930s, these fungi have since caused spoilage outbreaks in Europe, Africa, North America, and Australia.

Spoilage by other heat-resistant molds is a less serious problem and only recently was recognized. Consequently, less information is available concerning the behavior of these other genera in thermally processed fruit products.

Heat-resistant molds are characterized by the production of ascospores, in some instances comparable to bacterial spores. This enables them to survive the thermal processes given to some fruit products (Table 3.4).

Byssochlamys fulva (Figure 3.4) is distinguished by rapidly growing brown colonies with areas of fine white hyphae in which asci are produced in open clusters, at 30 ºC. However, at 25 ºC colonies may not produce the white hyphae resembling Paecilomyces variotii and only microscopic observation may help to distinguish them. Perhaps the most important physiological characteristic that makes this species significant in food mycology is the heat resistance of its ascospores. Many variables can affect the heat resistance of the ascospores namely intraspecies variations, pH, water activity and presence of preservatives (Bayne and Michener, 1979; Hatcher *et al.* 1979; Beuchat and Rice, 1979). Another distinctive feature of this fungus is the ability to grow at very low oxygen tensions, not common to other heat resistant fungi, providing a selective advantage in products such as canned, bottled or cartooned fruits and fruit juices (Pitt & Hockin, 1985). The small oxygen concentration present in the headspace is sufficient for growth and production of pectic enzymes which can result in complete breakdown of texture in fruits and also can result in off-flavor development (Hull, 1939; Beuchat and Rice, 1979).

Some *Byssochlamys* species produce mycotoxins such as patulin, byssotoxin A, and byssochlamic acid which have impact on food safety (King, 1972; Pieckova, 1997; Rice *et al.*, 1977). Heat-resistant molds, therefore, may constitute a public health hazard as well as a quality problem.

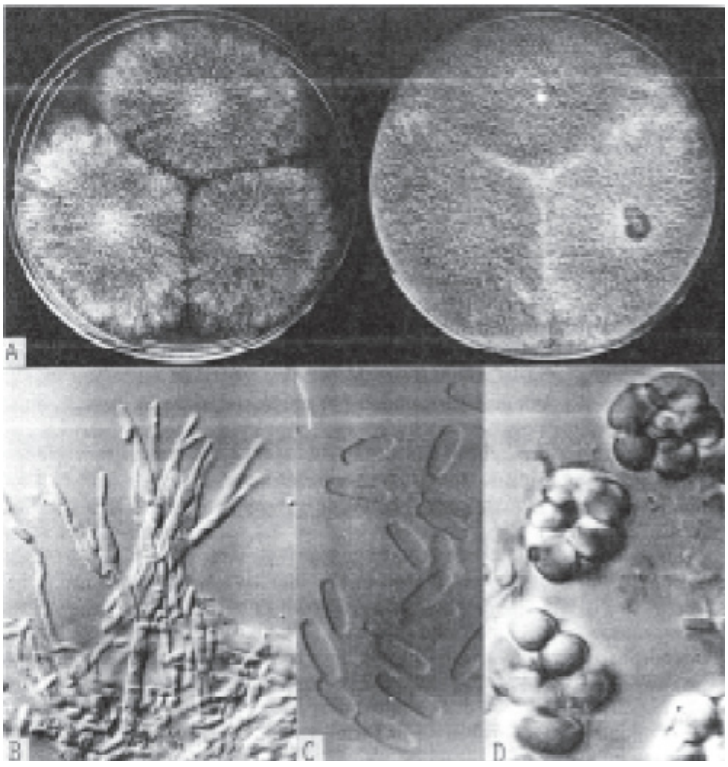

Figure 3.4 - *Byssochlamys fulva*: (A) colonies on CYA and MEA, 7 days, 25°C; (B) penicillus, x 750; (C) conidia, x 1875; (D) asci and ascospores, x 1875.

Table 3.4: Tolerance of heat-resistant molds isolated from foods (adapted from Splittstoesser and King, 1984).

Mold	Heat-resistant Structure	Heating Medium	Heat Resistance
Byssochlamys fulva	Ascospores	Glucose-tartaric acid, pH 3.6	90°C, 51 min, 1000-fold reduction
		Grape juice, 26 °Brix	85 °C, 150 min, 100-fold
Byssochlamys nivea	Ascospores	Grape juice	88°C, survived 60 min
		Apple Juice	99°C, survived in juice
Eupenicillium lapidosum	Ascospores	Blueberry juice	81°C, 10 min, survival; 81°C,
			15 min, death
			z = 10.3°F
	Cleistothecia	Blueberry juice	93.3°C, 9 min, growth; 93.3°C,
			10 min, death
			z = 10.6°F
Eupenicillium brefeldianum	Ascopores	Apple juice	90°C, 1 min, death
			z = 7.2°C
	Cleistothecia	Apple juice	90°C, 220 min, death z = 11.7°C
Talaromyces macrosporus	Ascospores	Apple juice	90°C, 2 min, death
			z = 7.8°C

Table 3.5: Tolerance of heat-resistant molds isolated from foods (adapted from Splittstoesser and King, 1984). (cont)

Mold	Heat-resistant Structure	Heating Medium	Heat Resistance
	(3 isolates)	Fruit-based fillings	D91°C = 2.9 to 5.4 min z = 9.4 to 23.3°F
		Apple juice	D90.6°C = 1.4 min z = 9.5°F
		Apple juice	D90.6°C = 2.2 min z =5.2°C
	Cleistothecia	Apple juice	90°C, 80 min, death z = 11.7°C
Monascus purpureus	Whole culture	Grape juice	Survival several min 100°C
Humicola fuscoatra	Chlamydospores	Water	80°C, 101 min, 10-fold inactivation
Phialophora sp.	Chlamydospores	Apple juice	80°C, 2.3 min, 10-fold
			inactivation
Neosartorya fischeri	Ascospores	Water	100°C, 60 min, survival
	(3 isolates)	Fruit-based fillings	D91°C = <2.0 min;
			D88°C = 4.2–16.2 min
			z = 5.4 = 11°F
		Apple juice	87.8°C, 1.4 min33 z = 5.6°C
Neosartorya fischeri var. glaber	Ascospores	Water	90°C, 60 min, survival
		Grape juice	85°C, 10 min, 10% survival
Thermoascus auranthiacum	Whole culture	Grape juice	88°C, 60 min, survival

Note: Once these results were gathered from different sources care must be taken in comparing the results of different authors.

1.4. Food spoilage bacteria: Escherichia coli

Escherichia coli, originally known as Bacterium coli commune, was identified in 1885 by the German pediatrician, Theodor Escherich (Neill *et al.*, 1994). It is a typical Gram negative bacterium, possessing an inner membrane (cytoplasmic membrane) surrounded by a murein wall and by an outer membrane. The space between both membranes is called periplasm and significantly differs from the cytosol in terms of composition (Figure 3.5). It is a facultative anaerobic, short, and straight bacillus. As a mesophile it can grow at temperatures ranging from 8 to 48°C with a maximum growth rate at 39ºC at a minimum water activity of 0.95. It is fairly acid tolerant and can grow at pH values ranging from 4.4 to 10.

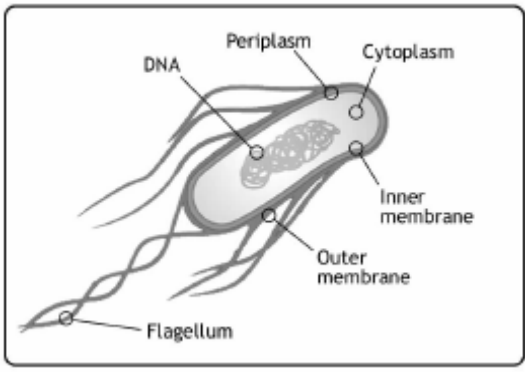

Figure 3.5: *E. coli* schematic representation

E. coli is widely distributed in the intestine of humans and warm-blooded animals and is the predominant facultative anaerobe in the bowel and part of the essential intestinal flora that maintains the physiology of the healthy host (Conway, 1995). *E. coli* is a member of the family *Enterobacteriaceae* (Ewing, 1986.), which includes many genera, including known pathogens such as *Salmonella*, *Shigella*, and *Yersini*a. Although most strains of *E. coli* are not regarded as pathogens, they can be opportunistic pathogens that cause infections in immunocompromised hosts. There are also pathogenic strains of *E. coli* that, when ingested, cause gastrointestinal illness in healthy humans which will be discussed further ahead in the text.

In 1892, Shardinger proposed the use of *E. coli* as an indicator of fecal contamination. Although the concept of using *E. coli* as an indirect indicator of health risk was sound, it was complicated in practice, due to the presence of other enteric bacteria like *Citrobacter*, *Klebsiella* and *Enterobacter* that can also ferment lactose and are similar to *E. coli* in phenotypic characteristics, so that they are not easily distinguished. As a result, the term

"coliform" was coined to describe this group of enteric bacteria. Coliform is not a taxonomic classification but rather a working definition used to describe a group of Gram-negative, facultative anaerobic rod-shaped bacteria that ferment lactose to produce acid and gas within 48 h at 35 °C. In 1914, the U.S. Public Health Service adopted the enumeration of coliforms as a more convenient standard of sanitary significance.

Referred to as Diarrheagenic *E. coli* (Nataro, and Kaper, 1998) or commonly as pathogenic *E. coli*, this group are classified based on their unique virulence factors and can only be identified by these traits. Hence, analysis for pathogenic *E. coli* often requires that the isolates be first identified as *E. coli* before testing for virulence markers. The pathogenic groups includes enterotoxigenic *E. coli* (ETEC), enteropathogenic *E. coli* (EPEC), enterohemorrhagic *E. coli* (EHEC), enteroinvasive *E. coli* (EIEC), enteroaggregative *E. coli* (EAEC), diffusely adherent *E. coli* (DAEC) and perhaps others that are not yet well characterized (Levine, 1987; Nataro, and Kaper, 1998). Of these, only the first 4 groups have been implicated in food or water borne illness.

ETEC is recognized as the causative agent of travelers' diarrhea, being this illness is characterized by watery diarrhea with little or no fever. ETEC infections occur commonly in under-developed countries but, in the U.S., it has been implicated in sporadic waterborne outbreaks as well as due to the consumption of soft cheeses, Mexican-style foods and raw vegetables. Pathogenesis of ETEC is due to the production of any of several enterotoxins. Because of its high infectious dose, analysis for ETEC is usually not performed unless high levels of *E. coli* have been found in a food. Also, if ETEC is detected, levels should also be enumerated to assess the potential hazard of the contaminated food.

EIEC closely resembles *Shigella* and causes an invasive, dysenteric form of diarrhea in humans (DuPont *et al.*, 1971). Like *Shigella*, there are no known animal reservoirs; hence the primary source for EIEC appears to be infected humans. Although the infective dose of *Shigella* is low and in the range of 10 to few hundred cells, volunteer feeding studies showed that at least 106 EIEC organisms are required to cause illness in healthy adults. Unlike typical *E. coli*, EIEC are non-motile, do not decarboxylate lysine and do not ferment lactose. Pathogenicity of EIEC is primarily due its ability to invade and destroy colonic tissue.

EPEC causes a profuse watery diarrheal disease and it is a leading cause of infantile diarrhea in developing countries. EPEC outbreaks have been linked to the consumption of contaminated drinking water as well as some meat products. Through volunteer feeding studies the infectious dose of EPEC in healthy adults has been estimated to be 106

organisms. Pathogenesis of EPEC involves intimin protein that causes attachment and effacing lesions (Hicks *et al.*, 1998); but it also involves a plasmid-encoded protein referred to as EPEC adherence factor (EAF) that enables localized adherence of bacteria to intestinal cells.

EHEC are recognized as the primary cause of hemorrhagic colitis (HC) or bloody diarrhea, which can progress to the potentially fatal hemolytic uremic syndrome (HUS). EHEC are typified by the production of verotoxin or Shiga toxins (Stx). There are many serotypes of Stx-producing *E. coli* (STEC), but only those that have been clinically associated with HC are designated as EHEC. Of these, O157:H7 is the prototypic EHEC and most often implicated in illness worldwide (CDC, 1993; Griffin and Tauxe, 1991; Karmali, 1989). The infectious dose for O157:H7 is estimated to be 10 - 100 cells; but no information is available for other EHEC serotypes. EHEC infections are mostly food or water borne and have implicated undercooked ground beef (CDC, 1993; Griffin and Tauxe, 1991), raw milk (Riley *et al.*, 1983), cold sandwiches, water (Swerdlow *et al.*, 1992), unpasteurized apple juice (CDC, 1996), among other food products.

1.5. Food spoilage bacteria: Bacillus licheniformis

Heat resistance is an important characteristic of *Bacillus* genus spores, which are highly resistant to HTST (high temperatures short time) treatments.

Bacillus licheniformis is a Gram positive bacteria commonly found in the soil. Recently, studies have also shown that it is found on bird feathers, especially chest and back plumage, and most often in ground dwelling birds (like sparrows) and aquatic species (like ducks). It is a gram positive, thermophillic bacterium. Optimal growth temperature is around 50 °C, though it can survive at much higher temperatures. Optimal temperature for enzyme secretion is 37 °C. It can exist in spore form to resist harsh environs or in a vegetative state when conditions are good.

Currently, scientists are exploring its ability to degrade feathers for agricultural purposes. Feathers contain high amounts of non digestible proteins, but researchers hope that by fermentation with *B. licheniformis*, they can use waste feathers to produce cheap and nutritious feather meal to feed to livestock. Moreover, it is used in the biotechnology industry to manufacture enzymes, antibiotics, biochemicals and consumer products. However, species such as *B. licheniformis* are also commonly isolated from fruit preparations that have been associated with food poisoning (Iurlina *et al.*, 2006, Salkinoja-

Salonen *et al.*, 19) (Table 3.6, Table 3.7, Table 3.8). Different foods, infecting doses and symptoms weree found in food spoilage by *Bacillus licheniformis* (Table 3.6, Table 3.7, Table 3.8), having serious consequences such as death. *Bacillus licheniformis* is one of the microorganisms most frequently involved in the spoilage of canned vegetables (Fields *et al.*, 1977). Its ability to grow in very acidic media and its reported capability of neutralising its growth medium to pH values in which *C. botulinum* would be able to grow and produce its toxin (Fields *et al.*, 1977; Rodriguez *et al.*, 1993), has made it important in acidified canned vegetables as its survival from heat processes may increase the risk of botulinic intoxication. It has been long known that pH of heat treatment medium influences heat resistance of bacteria. Most authors agree that heat resistance is higher at pH close to neutrality decreasing, with acidification (Xezones and Hutchings, 1965; Lowick and Anema, 1972; Mazokhina *et al.*, 1973; Brown and Thorpe, 1978; Cameron *et al.*, 1980; Cerny, 1980). The magnitude of this effect and the range of pH's where this is biggest seems to vary, not only among species (Cerny, 1980) but also among different strains of the same species (Brown and Thorpe, 1978).

Mature spores have no detectable metabolism, a state that is described as cryptobiotic. They are highly resistant to environmental stresses such as high temperature (some endospores can be boiled for several hours and retain their viability), irradiation, strong acids, disinfectants, etc. Although cryptobiotic, they retain viability indefinitely such that under appropriate environmental conditions, they germinate into vegetative cells. Endospores are formed by vegetative cells in response to environmental signals that indicate a limiting factor for vegetative growth, such as exhaustion of an essential nutrient. They germinate and become vegetative cells when the environmental stress is relieved. Hence, endospore-formation is a mechanism of survival rather than a mechanism of reproduction. *Bacillus* spores show a more complex ultrastructure than that seen in vegetative cells (Figure 3.6). The spore protoplast (core) is surrounded by the core (cell) wall, the cortex, and then the spore coat. Depending on the species, an exosporium may be present. The core wall is composed of the same type of peptidoglycan as the vegetative cell wall. The cortex is composed of a unique peptidoglycan that bears three repeat subunits, always contains DPA (Dipicolinic acid**)**, and has very little cross-linking between tetrapeptide chains. The outer spore coat represents 30-60 percent of the dry weight of the spore. The spore coat proteins have an unusually high content of cysteine and of hydrophobic amino acids, and are highly resistant to treatments that solubilize most proteins.

-

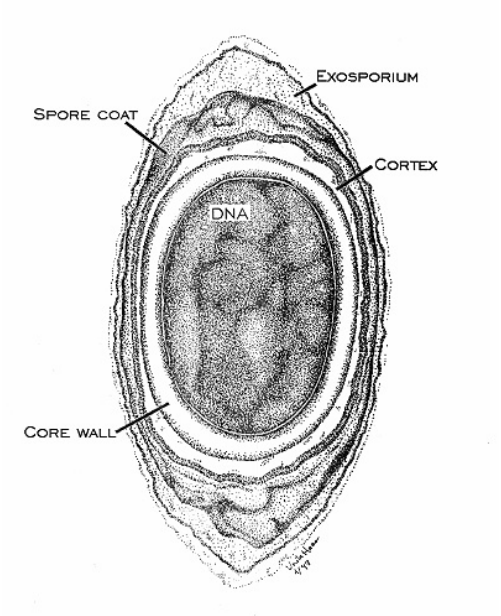

Figure 3.6: Schematic representation of a *Bacillus ssp* endospore

Table 3.6 Origins and toxicities of *B. licheniformis* isolates (Salkinoja-Salonen *et al.*, 1999)

Source of isolate	Country	Description of illness			CFU g of food^{-1}	Toxic properties of the *B. licheniformis* isolates		
		Onset (h) or phase	Symptom(s)	No. ill/no. risk		Hemolysis	Toxicity to boar sperm	Inhibition zone (mm) of *C. renale*
Ice cream	UK	Acute	SC, V, D	2/2		Beta	−	<2
Feces of food poisoning patient	UK	Acute	N, V, D, AP	1/1		Beta	++	>20
Curried chicken and mayonnaise sandwich	UK	5	N, SC, D	1/1	3×10^6	Beta	+	>20
Minced beef pie	UK	12	AP, D	1/1	1×10^8		−	<2
Tandoori king prawn	UK					Beta	−	<2
Blue cheese, salad dressing	UK	12	N, AP, D	6/9		Beta	−	<2
Pancake	UK		N, V	1/?	1.1×10^8	Beta	−	>10
Curry rice	UK		V	1/1	1.1×10^6	Beta	+	>10
Profiteroles	UK	7		3/?	3.1×10^5		++	>10
Vanilla sauce	Norway		N, V, B	>2			−	<2
Vanilla pudding (reconstituted)	Finland	6-8	SC, V, D	111/124 (6 hospitalized, 1 fatal)		ND	−	>20

Table 3.7 Origins and toxicities of *B. licheniformis* isolates (Salkinoja-Salonen *et al.*, 1999) (cont.)

Error! Reference source not found.

Source of isolate	Country	Description of illness			CFU g of food^{-1}	Toxic properties of the *B. licheniformis* isolates		
		Onset (h) or phase	Symptom(s)	No. ill/no. risk		Hemolysis	Toxicity to boar sperm	Inhibition zone (mm) of *C. renale*
Infant feed (formula)	Finland			1/1 (fatal)		Alpha, beta	++	>10
Infant feed (formula)	Finland			1/1 (fatal)		Alpha, beta	++	>10
Infant feed formula, unused package	Finland					Beta	++	>10
Infant feed formula, unused package	Finland					Beta	+	>10
Milk from postmastitic cow, 1st quarter	Finland					Beta	++	>10
Milk from postmastitic cow, 2nd quarter	Finland					Beta	−	>10
Milk from postmastitic cow, 3rd quarter	Finland					Beta	++	>10
Unused food packaging paperboard	Finland						−	<2

Table 3.8 Origins and toxicities of *B. licheniformis* isolates (Salkinoja-Salonen *et al.*, 1999) (cont.)Error! Reference source not found.

Source of isolate	Country	Description of illness			CFU g of food^{-1}	Toxic properties of the *B. licheniformis* isolates		
		Onset (h) or phase	Symptom(s)	No. ill/no. risk		Hemolysis	Toxicity to boar sperm	Inhibition zone (mm) of *C. renale*
Unused food packaging paperboard	Finland						–	>10
Air (garbage dump)	Finland					Beta	–	<2
Type strain, culture collection							–	<2

2. Materials and Methods

2.1. Food products

In the present study three different food products were analyzed: strawberry pulp, goat milk and cloudberry jam, obtained directly from jam and goat cheese producers.

Milk (pH 6.59 ± 0.04) was collected immediately before industrial pasteurisation and was transported under refrigerated conditions to the laboratory. Experiments were conducted promptly in order to avoid microbiological deterioration of the products, which might affect the results.

The cloudberry jam had an initial pH value of 3.83 ± 0.03. Further preparation was necessary for the samples of cloudberry jam, which were homogenized and smashed using a Moulinex Commercial Turbo Blender. The seeds present in the jam were drained off and the remnant was centrifuged (5 minutes at 3000 g). This procedure was necessary to liquefy the sample. The homogenates were sterilized (121 ºC, 15 min.) in order to eliminate contaminations during sample preparation stages.

Strawberry pulp was collected immediately before industrial pasteurisation and was transported under refrigerated conditions to the University of Minho. Experiments were conducted immediately to avoid microbiological deterioration, which might affect the results mainly due to the generation of carbon dioxide originating from the product's fermentation. Gas content has been described in the literature to have a strong influence on the electrical properties of fluids, namely on its electrical conductivity (Castro *et al.*, 2002). The pulp used had an initial pH value of 4.0, a Brix value of 14.5º and 2.5 % (w/w) of starch content. Brix was adjusted to different concentrations (from 14.5º to 37.0º) by adding sucrose. Brix was measured with a thermostated refractometer (Abbe Schmidt Haench – Elaptron, Germany) at 20 ºC. No further preparation steps were necessary prior to assays.

2.2. Microorganisms

2.2.1. *Byssochlamys fulva*

The strain of *B. fulva* DSM nº1808 was purchased from DSM (Deutsche Sammlung von Mikroorganismen und Zellkulturen GmbH, Braunschweig) and was maintained through monthly transfers and storage at 4 ºC. One loop of the plates was transferred to potato dextrose agar (PDA, pH 5.6) and allowed to grow at 32 ºC for 20 days until asci maturation

occurred. Cultivation at a temperature higher then 30 ºC is essential because this species may lose its ability to produce ascospores when propagated at 25 ºC (Beauchat, 1987).

The asci were recovered by flooding the culture with sterile peptone water and gently agitating. Ascospores were separated from myceliar fragments by filtration through sterile glass wool (Beauchat, 1987). To break asci and recover single ascospores the peptone water suspension was submitted to pressure and breakage was monitored by microscopy. The ascospores solution was centrifuged at 2500 g for 10 min, the supernatant was discarded and the ascospores were added to the strawberry pulp (pH 4.02).

Ascospores were activated by heating the solution to 80 ºC during 20 min (Splittstoesser *et al.*, 1972; Splittstoesser, 1977). This activation step eliminates background contaminants and also some mycelia or conidiospores still present in the samples.

2.2.2. *Escherchia coli*

The strain of *E. coli* ATCC® 25922 used in this work was purchased from Oxoid (Basingstoke, U.K.) as a Culti-loop®. For the preparation of a suspension of cells, a 1 mL loop of stock culture was transferred to 10 mL of Tryptic Soy Broth (TSB) (ref 211825, Becton, Dickinson and Company, Sparks, USA) and aerobically incubated a 37 ºC for 18 h. Cells were at exponential growth phase. The population density in each inoculum was evaluated using the pour plate procedure.

2.2.3. *Bacillus licheniformis*

The strain of *B. licheniformis* ATCC® 14580 (Spanish Type Culture Collection 20) was maintained through monthly transfers on Plate Count Agar (PCA) (ref 247940, Becton, Dickinson and Company, Sparks, USA) slants and stored at 4 ºC. Cultures were then transferred and spread on the surface of PCA and incubated at 35 ºC for 14 days. Sporulation was checked by phase contrast microscopy and green malachite staining technique. The spores (Figure 3.7) were harvested with a glass spatula and sterile peptone water and then washed and concentrated by centrifugation four times at 2500 g for 15 min with sterile peptone water (Mazas *et al.*, 1995). After the last centrifugation and re-suspension in sterile distilled water, the spore suspension was heated (80 ºC for 10 min) to kill vegetative cells and stored at 4 ºC until use.

A

B

Figure 3.7: A) Sporulating cells of *B. licheniformis*; B) Cells of *E. coli*;

A summary of the main characteristics of the microorganisms used in this work is presented in Table 3.9.

Table 3.9: Geometry and mean size distribution of selected microorganisms

Microorganism	Gram staining	Shape	Size (μm)
B. fulva ascospores	-	Ellipsoidal shape	5.5-7 x 3.5-4.5
E. coli	Negative	Straight rods	1.0-1.5 x 2-6
B. licheniformis spores	-	Ellipsoidal shape	

2.3. Heat treatments

The heat treatments were made in duplicate (two replicates) for each temperature and type of treatment. The time zero was considered when the sample reached the desired temperature. The thermal history of the samples was monitored by the introduction of a type-K thermocouple connected to a data acquisition system and made equal for both heating treatments with the purpose of eliminating thermal effects as a variable (Figure 3.8).

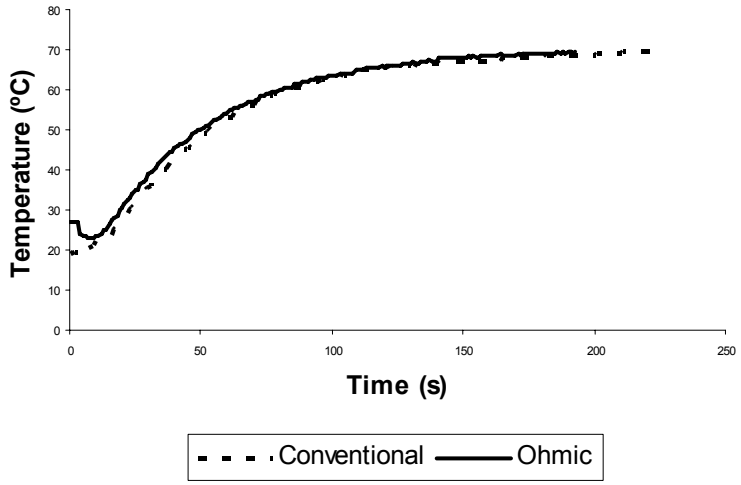

Figure 3.8: Example of a conventional and ohmic heating profile. Note the coincidence of both curves, sign of an identical thermal history.

2.3.1. Conventional heating

The thermal inactivation kinetics using conventional heating was performed in Eppendorf tubes (9 mm of internal diameter and 40 mm height) containing the inoculated sample. These tubes were completely immersed in a temperature-controlled bath during the heating cycle. For *Byssochlamys fulva* some of the assays were performed at temperatures above 100 ºC, so the water bath was replaced by an oil bath.

Pairs of tubes were subsequently removed from the bath at appropriate time intervals. All tubes containing the samples were immediately transferred to an ice bath until further analyses were performed, to stop the thermal degradation effect. This procedure was repeated for all temperatures. Eppendorf tubes were chosen because their dimensions minimize temperature gradients due to heat transfer resistance.

2.3.2. Ohmic heating

The ohmic heater consisted of a jacketed cylindrical glass tube of 30 cm total length and 2.3 cm inside diameter (Figure 3.9). Three thermocouple openings were provided; two at an equal distance of the centre of the tube and one at the centre, where a thermocouple type-K was placed. Two platinized Titanium electrodes with Teflon pressure caps were placed at each end of the tube. For each type of microorganism, samples of approximately 25 mL were heated using an alternating current source of 50 Hz frequency and variable amplitude. For the ohmic heating treatment the inoculated sample was transferred to the ohmic chamber. As in conventional inactivation, timing was started and two samples were

removed when the sample reached the desired test temperature. Each test temperature was maintained constant, during the prescribed time interval, by the control of the voltage applied to the ohmic heating unit and circulation of water. It should be stressed that the electric field strength used during the holding phase of the experiments was very low (in every case approximately equal 20 V/cm) when compared to the ones used in the heating phase of the samples.

Pairs of samples were subsequently collected with a micropipette at the established time intervals. All the samples were immediately transferred to an ice bath until further analyses were performed.

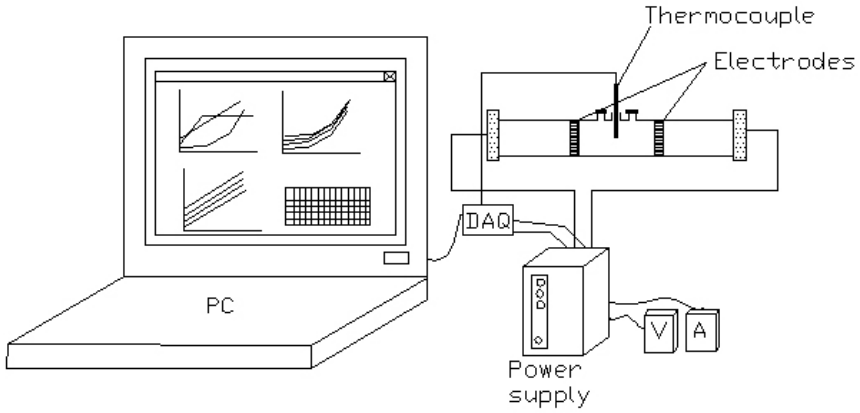

Figure 3.9: Schematic represantatin of the experimental set-up and data acquisition system

2.4. Electrical conductivity measurements and field strength experiments

A set of experiments was conducted to measure and determine the effect of field strength on the electrical conductivity changes during ohmic heating. The goat milk and strawberry pulp samples were heated up to 90 ºC using different field strengths. The strawberry pulp having different º Brix was also tested using a constant electric field of 60 V/cm. During the experiments the electric field was varied through the use of a rheostat to adjust the voltage supplied. A data-logger was employed to record continuously and simultaneously, current intensity, voltage and temperature. In order to measure voltage across and current through the samples, voltage and current transducers (Fema electronics, Portugal) were used. Electrical conductivity was determined by the following equation.

$$\sigma = \frac{L}{AR} \qquad \textbf{(Eq. 3.3)}$$

A - Inner cross sectional area of ohmic heater (m^2)

L - Interval between electrodes (m)

R - Resistance (Ω)

σ - Electrical conductivity (S/m)

2.5. Determination of water activity (aw)

Water activity was determined at 25 ºC with a AW Sprint TH500 (Novasina, Switzerland) apparatus and measured in duplicate for each sample.

2.6. Determination of thermal resistance

2.6.1. *Byssochlamys fulva*

Ascospores were activated by heating the strawberry pulps (with different values of ºBrix) to 80 ºC during 20 min and the assays where made immediately after activation at temperatures of 85 ºC, 90 ºC, 100ºC and 105 ºC for both types of heating treatments. For enumeration purposes appropriate serial dilutions (1:10) were made with sterile peptone water (0.1 %) and plated in triplicate in DRCB agar (Oxoid) for 48 h at 30 ºC (Figure 3.10).

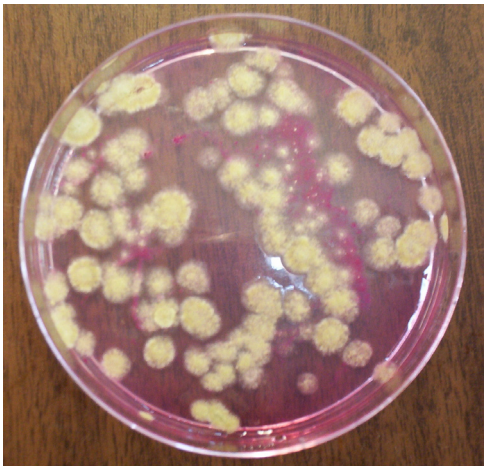

Figure 3.10: Colonies of *Byssochlamys Fulva* on DRBC agar.

2.6.2. *Escherichia coli*

For each experiment, 50 mL of goat milk were homogenized and pasteurized (60 ºC, 10 min) to eliminate background microflora. The *E. coli* inoculum (1 mL) was added to the goat milk in order to achieve a final concentration of approximately 108–109 CFU/mL. For conventional heating experiments the inoculated samples were again homogenized, placed in sterile Eppendorf tubes (1 mL) and subjected to test temperatures of 55 ºC, 60 ºC; 63 ºC, 65 ºC, 67 ºC and 70 ºC in a temperature-controlled water bath. For ohmic heating experiments, approximately 25 mL of inoculated sample was placed in the ohmic heater and heated at 55 ºC, 63 ºC, 65 ºC and 67 ºC. The number of viable colonies of *E. coli* was counted in MacConkey agar No.3 (Oxoid) after incubation at 36 ºC for 18-24h.

2.6.3. *Bacillus licheniformis*

The suspension of spores was diluted before the experiments using the extract of cloudberry jam that was previously sterilized (121 ºC for 15 min). Initial concentrations of spores in suspension varied from 104 to 107 cfu/ml. Volumes of 2 ml of the inoculated cloudberry jam were placed in sterile Eppendorf tubes and heated at 70 ºC, 75 ºC, 80 ºC, 85 ºC and 90 ºC in a temperature-controlled water bath. In the ohmic heater, 25 mL of inoculated cloudberry jam were heated at 70 ºC, 75 ºC, 80 ºC and 90 ºC. The number of surviving spores of *B. licheniformis* was determined using PCA (OXOID) and incubation at 37 ºC for 24 h.

.

2.7. Determination of heat resistance parameters (D and z)

For each temperature, media, and strain, *D* values (in minutes) were determined by regression:

$$\mathbf{Log\ N = Log\ No - t/D} \qquad \textbf{(Eq. 3.4)}$$

Where *N* is the experimental count value at time *t* and *No* is the initial count value. *D*-values were derived by plotting the logarithm of the number of survivors versus time. The number of survivors was determined by plate counts done at intervals during exposure to the

heat treatment. For each temperature the logarithm of the colony forming units was plotted against time and a linear regression line was calculated from the data using least squares minimization. The *z* values were determined from the slope of the regression line obtained by plotting log *D* versus the corresponding heating temperatures.

$$\frac{\log D_2 - \log D_1}{T_2 - T_1} = \frac{1}{Z} \qquad \textbf{(Eq. 3.5)}$$

Furthermore, whenever necessary, data was analyzed statistically using an Analysis of Variance approach (ANOVA). When treatment factors were significant, Student's t-statistics were used for multiple comparisons of means.

3. Results and Discussion

Although the effects of electricity in cells have been widely studied, very few inactivation kinetics of microorganism in food matrices, using electricity, are available in the literature. Most of the data found regarded the use of the PEF technology, which is a non-thermal process and therefore cannot be compared to ohmic heating, where there is a potential synergy between thermal and nonthermal effects on microbes.

However, the increasing interest of food industry in ohmic heating (or moderate electric fields) technology drove the need to address the thermal and non-thermal effects of low intensity continuous electric fields on inactivation kinetics of microorganisms. The production of high quality or high value food products or ingredients using this technology is a real possibility, owing both to the less aggressive thermal treatments (due to uniform heating) and to the possible enhanced effect on microbial inactivation caused by electricity. The first factor has been exhaustively reported in the literature but the second has been more controversial, essentially due to the lack of authoritative works on the subject where temperature would not influence the reported results and where real food matrices would be used instead of model systems.

The aim of this work was to eliminate the temperature as a process variable in order to observe the effect of low intensity continuous electric fields in different types of food spoilage microorganisms in complex food products.

The microorganisms chosen for this work are relevant in the food safety area either because they are considered hygiene indicators having high levels of occurrence (*E. coli*); or due to their enhanced thermal resistance which renders them difficult to eliminate using other non-conventional technologies such as high pressure processing (*B. licheniformis* endospores and *B. fulva* ascospores). It is noteworthy that all the microorganisms used are relevant in the food product they were tested in. This fact is of extreme importance because the composition of the heating matrix has a significant influence on the heat resistance of the microorganisms and the obtained results, considering the technology used, should not be extrapolated to other food products. As previously mentioned, the heating rates of both types of treatments (conventional or ohmic) were made similar by controlling the applied voltage. The applied voltage during the heating phase is extremely variable between the several products and depends essentially on their electrical conductivity. During the holding phase the electric field was constant for every temperature and microorganism and equal to 20 V/cm. Moreover, if the electrical conductivity value is very low, the application of ohmic

heating would be compromised because either the heating rate would be too slow or high voltage inputs would be needed.

To predict the electric field strength required to simulate the heating phase the electrical conductivities of the samples using a wide range of field strengths were measured, whenever possible, and the results are presented in each of the sections corresponding to the microorganism used to inoculate the respective food product.

Possible non-thermal effects in ohmic heating promoted by chemical reactions at the surface of the electrodes were avoided by the use of platinized-Titanium electrodes. Results of recent studies (Chaminda *et al.*, 2005) suggest the potential use of platinized-Titanium electrodes for ohmic heating of foods with commonly available low-frequency alternating currents due to their relatively inert electrochemical behaviour at all the pH values.

3.1. B. fulva

Strawberry fruit jams are extremely important for the Portuguese fruit jams industry because they account for most of the sales (around 90 %). The search for alternative processing technologies leading to higher quality products is, therefore, one of the main goals and the economic viability of this technology depends on the possibility of applying it to most of the products processed by this industry. The influence of different values of ºBrix and solids content on electrical conductivity of strawberry pulps and also the effect on ascorbic acid degradation kinetics were previously reported (Castro *et al.*, 2003) and favorable conclusions about the use of this technology were drawn. However, no microbial studies were conducted at the time.

The mold *B. fulva* has been documented for the spoilage of canned and bottled fruits, especially in strawberries (Beauchat and Rice, 1979). This species produces ascospores capable of withstanding thermal processing treatments given to fruit jams and thus represent a potential problem to the preservation of products during the shelf-life of the product. This mold was identified several times in the industry from which the samples were obtained, however no viable culture isolated industrially and capable of producing ascospores was available at the time of the assays.

Initially, the electrical conductivity was determined as a function of the field strength and the results are shown in Figure 3.11. As reported by Castro *et al.* (2003), there is a linear relation between electrical conductivity and temperature in this case. Moreover, the

effect of field strength is not as evident as in other products reported in the literature. This behaviour may be due to the presence of texturizing agents (such as starch and pectin) which change their properties (namely, the viscosity) during heating, therefore increasing the drag forces of the medium, reducing the mobility of the fluid and of the ionic components present (Castro *et al.*, 2003).

The results in Figure 3.12 indicate that the electrical conductivity of strawberry pulp is suppressed (up to 60 % decrease) by the presence of sugar. This was expected to happen because non-ionic constituents such as fat, oil and sugar cause a decrease in electrical conductivity (Sastry, 1991). The values of the electrical conductivity of all the pulp formulations tested show that they are suitable to be ohmically heated and the assays using contaminated pulp (with ascospores) were performed. Special care was taken to avoid the formation of air bubbles.

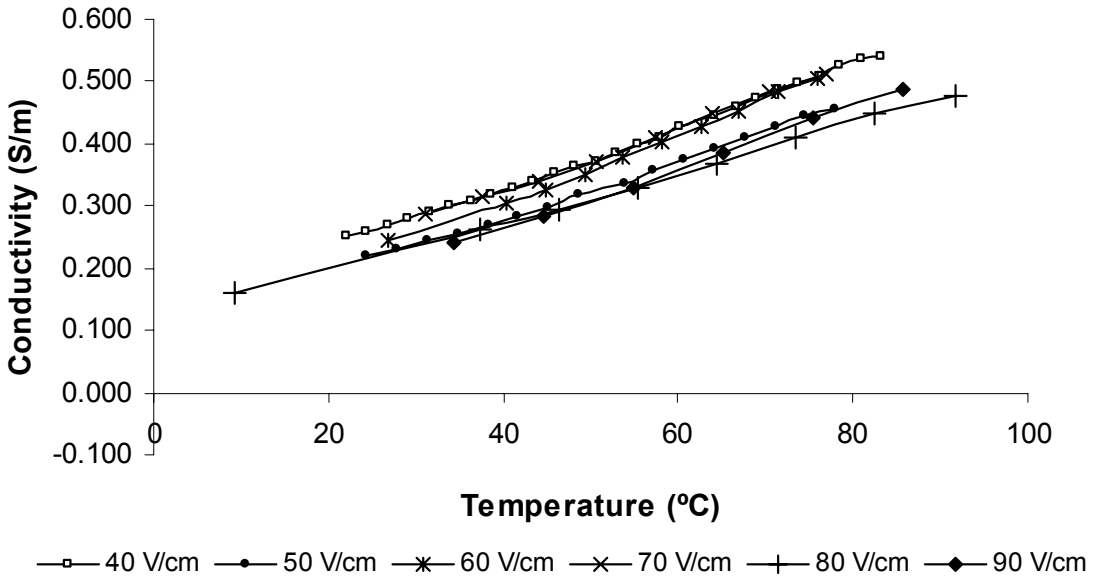

Figure 3.11: Electrical conductivity curves of strawberry pulp, when submitted to different field strengths

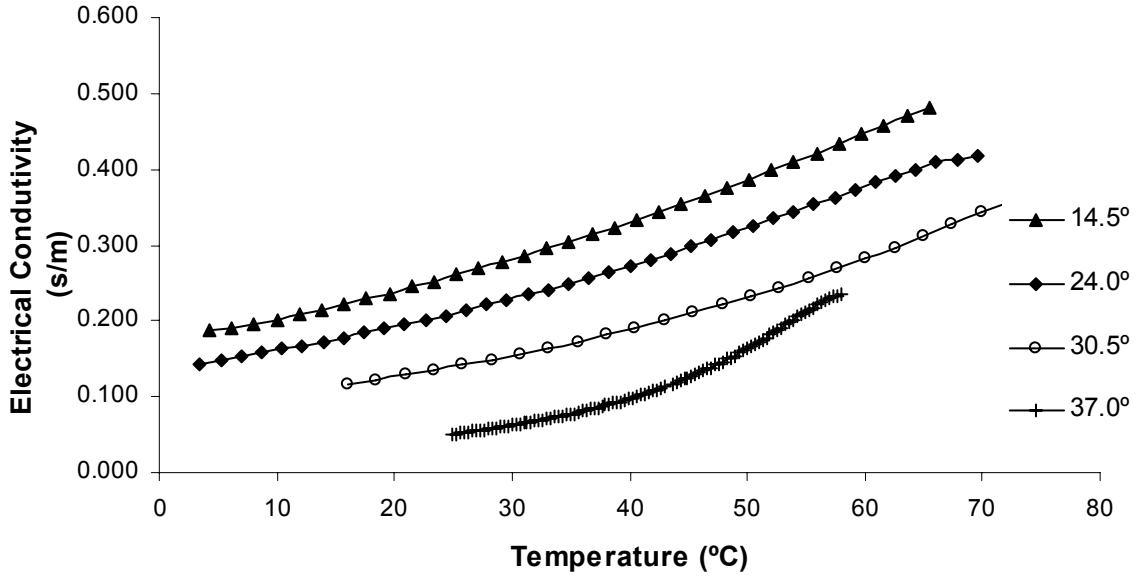

Figure 3.12: Electrical conductivity curves of strawberry pulp, with different values of ºBrix, during ohmic heating, using 60 V/cm

The experimental results of the ascospores inactivation as well as the corresponding values of the inactivation parameters (*D* and *Z* values) are shown in Figures 3.13 to 3.21 and Tables 3.10 to 3.14, respectively. Strawberry pulps with different values of ºBrix were used.

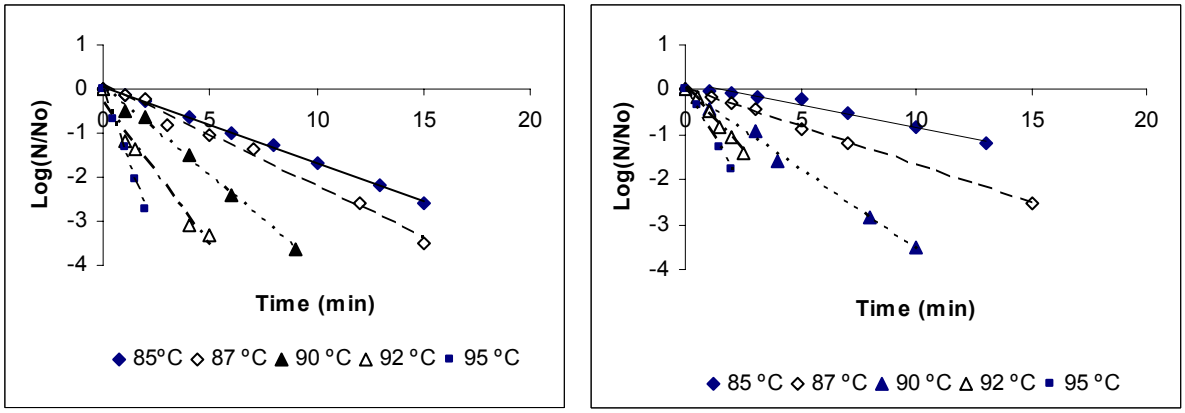

Figure 3.13: *D*-values for *B. fulva* ascospores in strawberry pulp (14.5 ºBrix) when submitted to conventional (A) and ohmic (B) heating treatments.

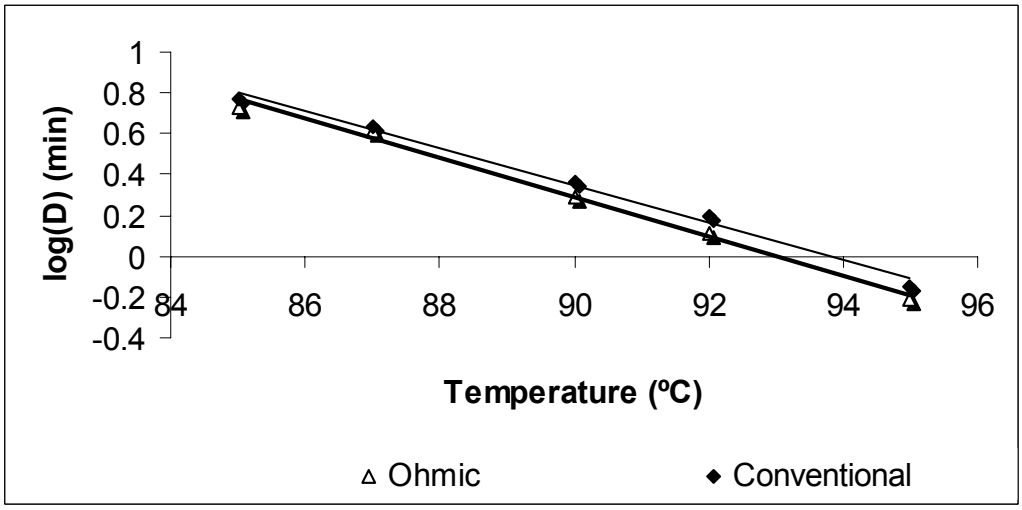

Figure 3.14: Death kinetics of *B. fulva* ascospores in strawberry pulp (14.5 ºBrix) when submitted to conventional and ohmic heating; determination of the *z* values

Table 3.10: Kinetic parameters of thermal degradation of *B. fulva* in strawberry pulp (14.5 ºBrix).

Temperature (ºC)	85	87	90	92	95
$D_{conventional}$ (min)	5.85 ±0.10	4.31±0.04	2.28±0.25	1.58±0.01	0.71±0.02
% Cv	1.70	1.01	11.05	0.82	3.24
D_{ohmic} (min)	5.41 ±0.06	4.10±0.03	1.93±0.06	1.29±0.11	0.61±0.05
% Cv	1.18	0.69	2.93	8.77	4.64
$z_{conventional}$ (ºC)	10.99± 0.23 (r^2 = 0.99)				
z_{ohmic} (ºC)	10.36±0.38 (r^2 = 0.98)				

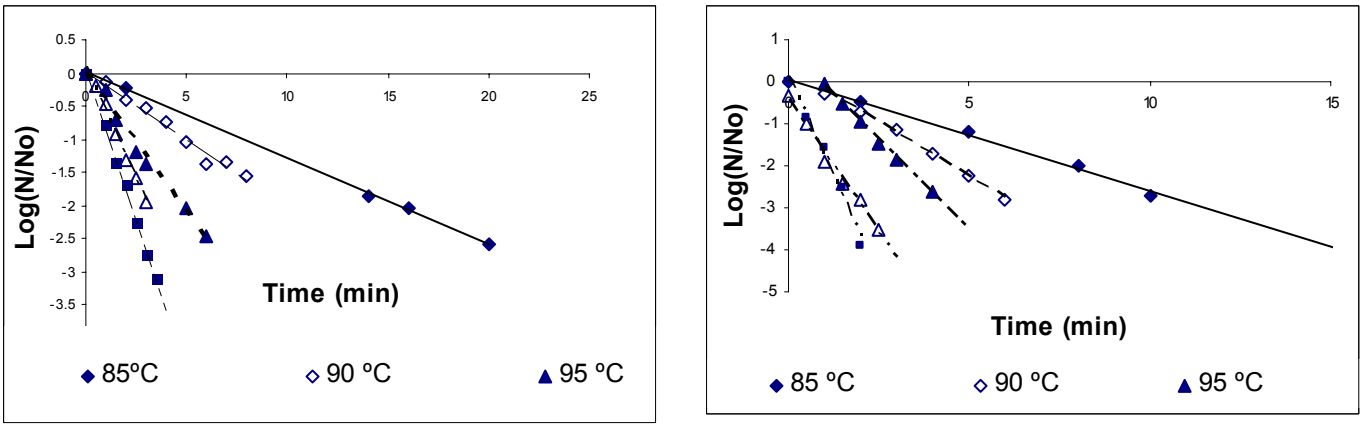

Figure 3.15: *D*-values for *B. fulva* ascospores in strawberry pulp (24 ºBrix) when submitted to conventional (A) and ohmic (B) heating treatments.

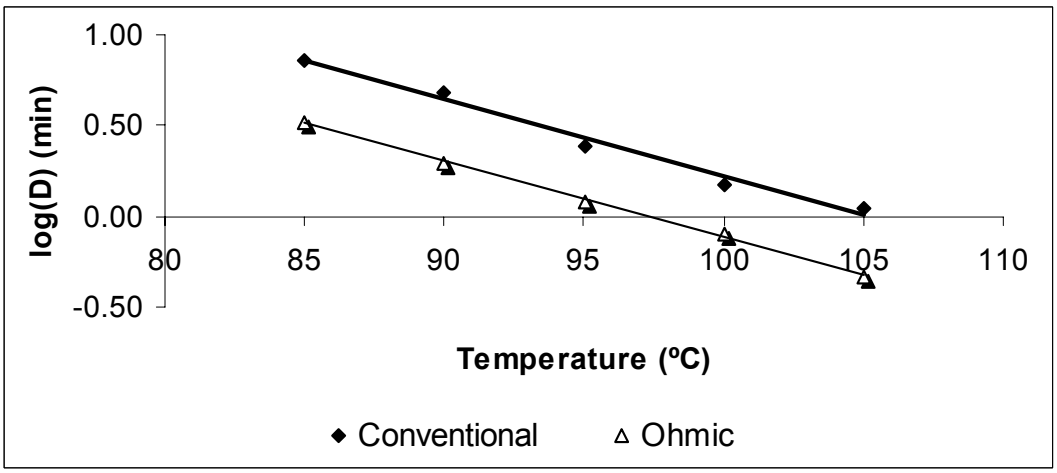

Figure 3.16: Death kinetics of *B. fulva* ascospores in strawberry pulp (24 ºBrix) when submitted to conventional and ohmic heating; determination of the *z* values

Table 3.11: Kinetic parameters of thermal degradation of *B. fulva* in strawberry pulp (24 ºBrix).

Temperature (ºC)	85	90	95	100	105
$D_{conventional}$ (min)	7.23 ±0.65	4.84±0.05	2.41±0.01	1.51±0.03	1.12±0.02
% Cv	9.01	0.99	0.34	1.89	1.41
D_{ohmic} (min)	3.31±0.06	1.97±0.00	1.20±0.05	0.80±0.01	0.47±0.04
% Cv	1.78	0.22	4.20	1.32	8.86
$z_{conventional}$ (ºC)	23.51±0.59 (r^2 = 0.98)				
z_{ohmic} (ºC)	23.88±0.64(r^2 = 0.98)				

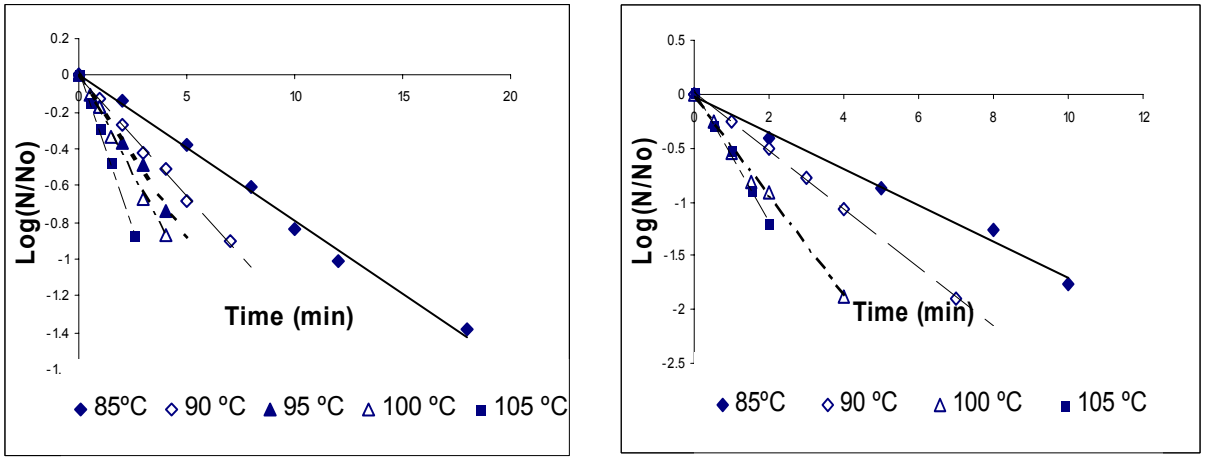

A **B**

Figure 3.17: *D*-values for *B. fulva* ascospores in strawberry pulp (30.5 ºBrix) when submitted to conventional (A) and ohmic (B) heating treatments.

Figure 3.18: Death kinetics of *B. fulva* ascospores in strawberry pulp (30.5 ºBrix) when submitted to conventional and ohmic heating; determination of the *z* values

Table 3.12: Kinetic parameters of thermal degradation of *B. fulva* in strawberry pulp (30.5 ºBrix).

Temperature (ºC)	85	90	95	100	105
$D_{conventional}$ (min)	12.16±0.59	7.83±0.19	5.79±0.37	4.17±0.45	2.86±0.01
% Cv	4.81	2.38	6.42	10.81	0.51
D_{ohmic} (min)	6.00±0.08	3.70±0.01	-	2.10±0.03	1.65±0.01
% Cv	1.40	0.23	-	1.52	0.44
$z_{conventional}$ (ºC)	33.46±1.11 (r^2 = 0.99)				
z_{ohmic} (ºC)	36.30±0.28(r^2 = 0.98)				

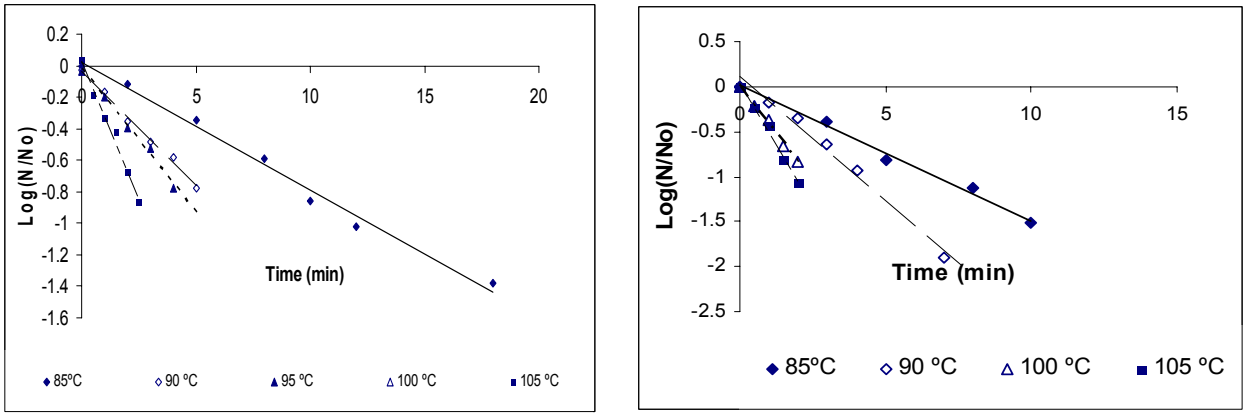

Figure 3.19: *D*-values for *B. fulva* ascospores in strawberry pulp (37.0 ºBrix) when submitted to conventional (A) and ohmic (B) heating treatments.

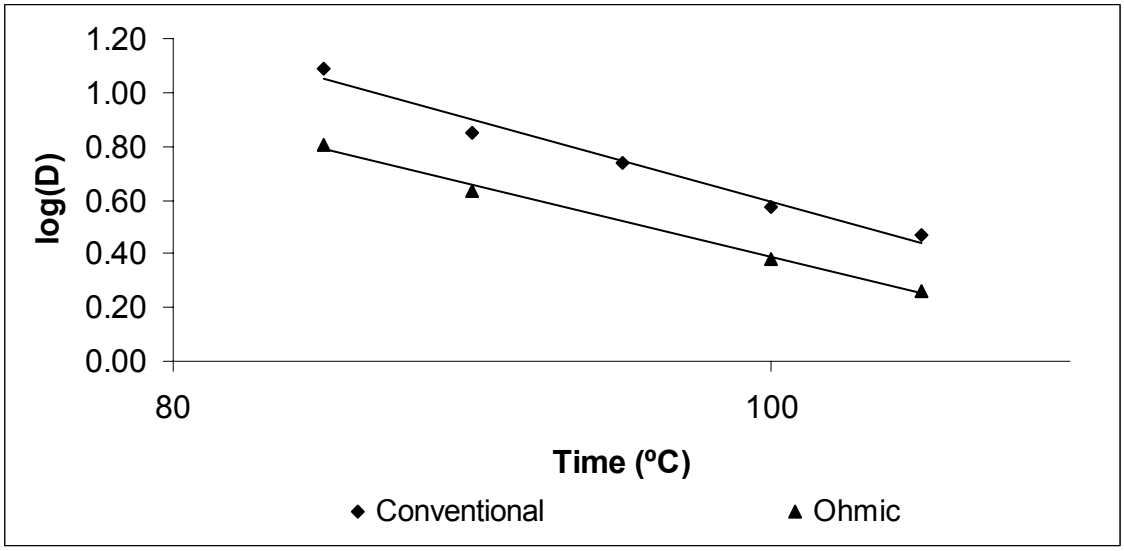

Figure 3.20: Death kinetics of *B. fulva* ascospores in strawberry pulp (37.0 ºBrix) when submitted to conventional and ohmic heating; determination of the *z* values

Table 3.13: Kinetic parameters of thermal degradation of *B. fulva* in strawberry pulp (37.0 ºBrix).

Temperature (ºC)	85	90	95	100	105
$D_{conventional}$ (min)	12.31±0.10	7.37±0.73	5.47±0.37	3.73±-	3.08±0.29
% Cv	0.78	9.95	1.55	-	9.49
D_{ohmic} (min)	6.50±0.22	4.27±0.09	-	2.41±0.04	1.83±0.01
% Cv	3.31	2.12	-	1.79	0.25
$z_{conventional}$ (ºC)	33.28±0.80 (r^2 = 0.97)				
z_{ohmic} (ºC)	37.24±0.10(r^2 = 0.99)				

The results show that thermal degradation of *B. fulva* ascospores follows first order degradation kinetics for both conventional and ohmic heating, in the temperature (95 ºC to 105 ºC) and ºBrix values (14.5 to 37) range. Most studies on heat resistance of *Byssochamys* ssp have been carried out using asci (and not free ascospores as in the present work). Therefore, the observed inactivation rates were not linear, at least in the early stages of the inactivation process (Bayne and Michener, 1979), possibly due to the extra thermal resistance provided by the asci structure. Gillespy (1946) stated that when less than 10 % of the asci survive, the probability is that only one ascospore per ascus survives. It was further theorized, based on experimental data obtained for asci inactivation, that inactivation curves would be straight lines as for bacteria.

Heat resistance is influenced by many factors including species, nature of the heating matrix and, of course, treatment temperature (Beachat and Rice, 1979). Additionally Banner (1979) reported that long-chained fatty acids in spores and also the thickness of the wall may enhance heat resistance.

The measured kinetic parameters are, apparently, within the range of the values found in published literature for other food systems under conventional heating conditions (see Table 3.14) although no completely comparable data (in terms of food matrix characteristics) could be found. Also, no references were found where kinetic parameters under ohmic heating conditions were determined.

Table 3.14: Heat resistance data of *B. fulva* ascospores in different food matrix

Temperature (ºC)	Food Matrix	Available heat resistance data
85	Grape juice, 5º Brix	< 0.001to 50 % resistance after 60 minutes, depending on the strain
		8.4 % after 60 minutes, 2.1% after 75 minutes
		Survival after 60 minutes: 0.21% survival pH 1.4; 4.7 % pH 2.3; 36% pH 3 and 6
	Glucose solution	Survival after 75 minutes: 21% in 40 % solution 2.3 % in 10 % solution
86	Grape juice	D = 14 min
87.7	Grape drink	D = 10.32 min
87.8	Grape juice	D = 4.8 to 11.3 min, depending on the strain
88	Plum, strawberry, gooseberry and raspberry syrups	Survived for 30 minutes

Adapted from Beuchat and Rice, 1979

The calculated *D*-values were, in every case, lower for ohmic heating, meaning that the time required to inactivate ascospores, at a given temperature, is lower when electricity is present. In fact, this data corroborate the hypothesis that electricity has an additional effect on microbial inactivation, namely in ascospores. Statistical results showed that for the conditions tested the conventional *D*-values are significantly different from the ones obtained when using ohmic heating ($p < 0.05$). The exception is the 14.5 ºBrix experiment where for the temperatures of 87 ºC and 95 ºC the conventional and ohmic *D*-values are identical at a 5 % significance level.

Regarding the temperature dependence (*z*-value), this parameter is similar for both types of treatments when using 14.5 and 24 ºBrix samples but the raise of the ºBrix values to 30.5 and 37.0 led to a significant difference between the two types of treatments ($p < 0.05$, both cases) (Figure 3.21). In fact, when using ohmic heating the temperature interval needed to reduce 10 fold the inactivation time is approximately 10 % higher.

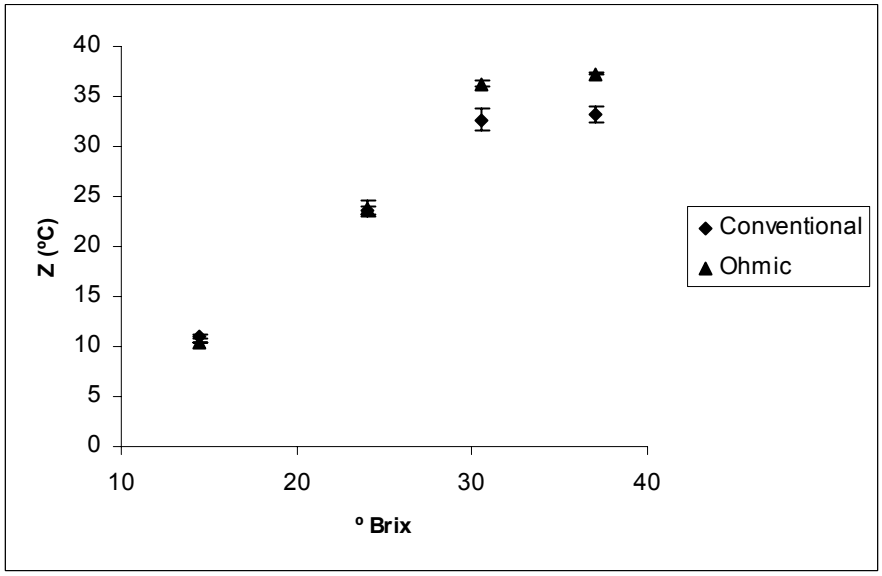

Figure 3.21: Variation of *z*-values as a function of the strawberry pulp ºBrix

Moreover, the protective effect against heat of sucrose is also confirmed by the obtained data: below 30 ºBrix, there is a linear increase of *z* with the sugar concentration (measured in terms of ºBrix). It is noteworthy that this effect is even more pronounced for the ohmic treatments. The protective action of sucrose against heat inactivation has been reported by several researchers. This fact is directly related to the water activity of the food matrix. The decrease of free water in the medium due to the addition of salts or sugars reduces the influence of inactivating agents on vital biochemical systems (Butz *et al.*, 1996). Additionally, the electrical conductivity is also lower (Figure 3.12), thus implying a lower electric current passing through the sample for the same electric field value. The water activity was measured to confirm the expected results and data are presented in

Table 3.15.

Table 3.15: Water activity of the strawberry pulps with different values of ºBrix.

ºBrix	Water activity
14.5	0.972
24.0	0.961
30.5	0.954
37.0	0.946

Considering that the ascospores were activated prior to inactivation treatment, the enzymes and other biochemical reactions involved in the germination process were triggered. It is well known that cells with higher activity are more affected by inactivation treatments than the ones with low metabolism (Beuchat and Rice, 1979). The decrease in water activity probably slows down the germination process (lower biological activity) thus cells are more heat resistant, and this fact is common to both treatments. Regarding ohmic heating, when a sample's electrical conductivity is lower the intensity of current passing thought the medium will also be lower when the electric field value is kept constant (which is the case here). It has been determined that samples with higher values of ºBrix were less conductive. Therefore, if the non-thermal effect is due to the passage of electrical current, it is expectable that a lower current intensity will provoke a lower non-thermal killing efficiency. In the present case, this justifies the observation that samples with higher values of ºBrix need a higher temperature increase (higher z) to cause a similar reduction in the values of D for the ohmic heating when compared to conventional heating.

3.2. E. coli

E. coli is one the more studied microorganisms in the fields of food processing, molecular biology and biochemistry and it is often regarded as a model microorganism. Pathogenic strains of *E. coli* are responsible for several foodborn outbreaks with significant social and economical consequences. Furthermore, this microorganism is also considered an indicator of poor post-processing sanitation and several microbiological criteria are defined world wide and also by EC (Reg. EC 2073/2005) for *E. coli* in a wide range of food products (e.g. cheese, shelfish, meat). The number of *Enterobacteria* (which includes *E. coli*) and *E. coli* are defined by an EC microbiological criteria to indicate process hygiene of pasteurized milk and dairy products and cheeses and butter produced from raw milk.

Pasteurized goat milk is used in Portugal mainly to produce several types of traditional cheeses and *E. coli* was considered relevant in this industry as an indicator of correct processing and handling of pasteurized milk.

Figure 3.22 presents the electrical conductivity of goat milk as a function of the electric field. The results confirm the linearity of electrical conductivity with temperature and indicate that for temperatures higher than 50 ºC the field strength has little or no effect on this parameter. These results were important to simulate the heating rate of the conventional heating. All the experiments were performed at constant electric field for the range of temperatures tested, so the results of the different assays can be compared in terms of the presence of an electric field without any additional effect of intensity.

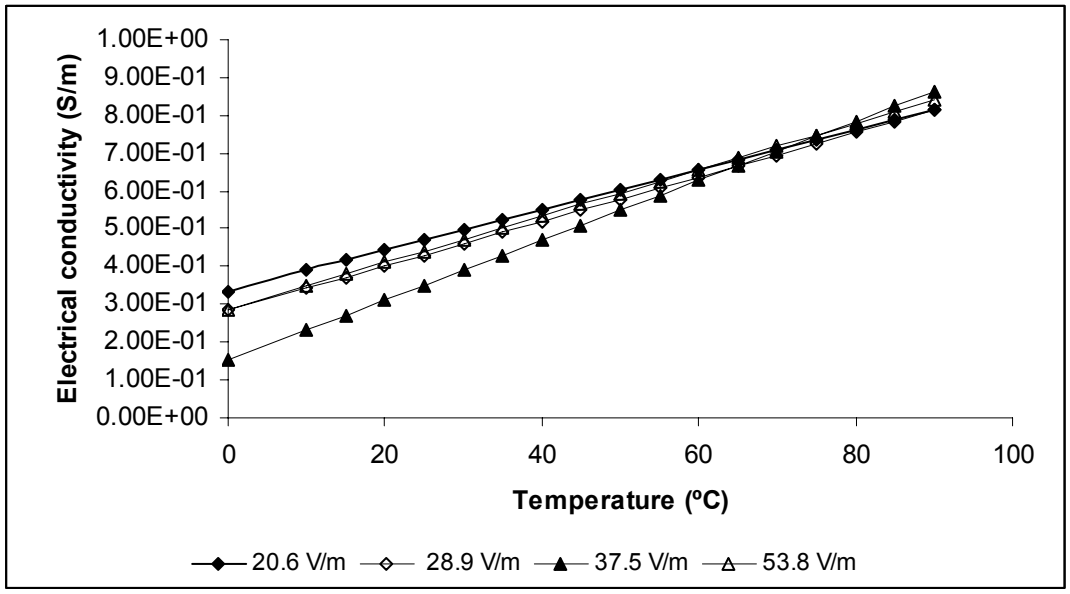

Figure 3.22: Electrical conductivity of goat milk as a function of the electric field strength

The heat resistance and the influence of the electric field (non-thermal effects) of this strain were tested and the inactivation parameters were calculated, as shown in Figure 3.23 and Figure 3.24 and

Table 3.16, respectively.

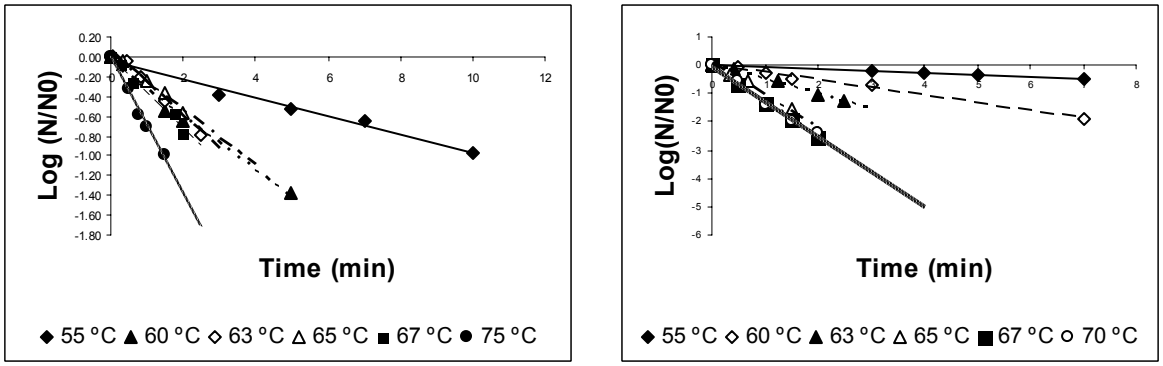

A **B**

Figure 3.23: *D*-values for *E. coli* in goat milk when submitted to conventional (A) and ohmic (B) heating treatments.

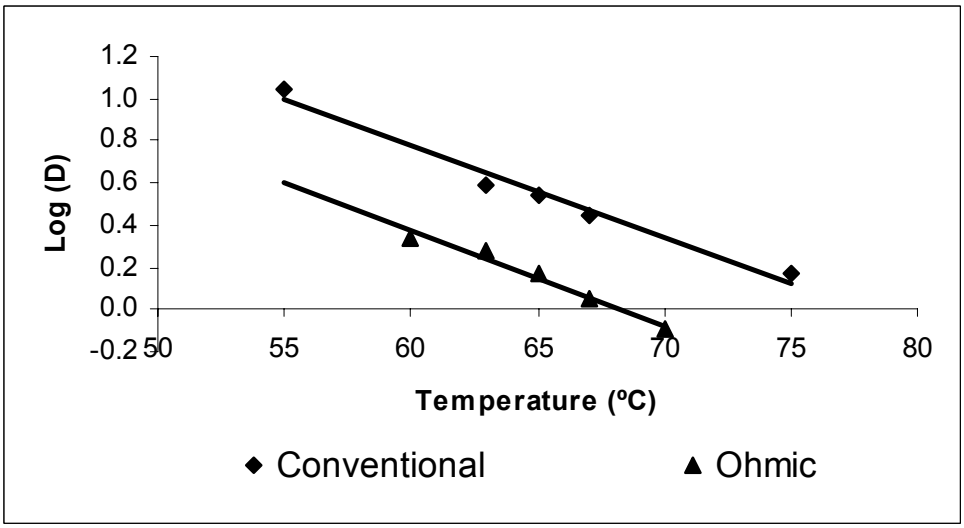

Figure 3.24: Death kinetics of *E. coli* in goat milk when submitted to conventional and ohmic heating; determination of the *z* values.

Table 3.16: Kinetic parameters of thermal degradation of *E. coli* in goat milk

Temperature (ºC)	55	60	63	65	67	70	75
$D_{conventional}$ (min)	10.94 ± 1.47	3.70 ±	3.29 ± 0.37	3.48 ± 0.17	2.84 ± 0.04	-	1.47 ± -
% Cv	13.44	-	11.41	4.88	1.47	-	-
D_{ohmic} (min)	14.18 ± 0.20	2.29 ± 0.17	1.92 ± 0.04	1.49 ± 0.01	1.09 ± 0.03	0.82 ± 0.03	-
% Cv	1.40	7.41	1.85	0.95	2.59	3.27	-
$Z_{conventional}$ (ºC)	21.39±0.03 (r^2 = 0.99)						
Z_{ohmic} (ºC)	21.49± 1.11(r^2 = 0.98)						

As observed for *B. fulva* ascospores in strawberry pulp, the *z*-value for both treatments is similar but the *D*-values are lower when an electric field is applied, thus reducing the time needed for microbial inactivation at a given temperature.

Damage to bacterial membranes by heat has been confirmed by evidence of the leakage of intracellular substances such as DNA, proteins, and cations into a heating matrix (Hurst *et al.*, 1974, Iandolo *et al.*, 1966, Shibasaki, and Tsuchido, 1973, Strange *et al.*, 1964), the loss of lipopolysaccharide (LPS) (Hitchener and Egan, 1977, Katsui *et al.* 1981) and reduction in substrate transporting ability (Grau, 1978).

The outer membrane of gram-negative bacteria, including *E. coli*, provides diffusion channels for low-molecular weight hydrophilic substances and forms a permeability barrier for hydrophobic compounds (Coleman *et al.*, 1979, Costerton *et al.*, 1974). In particular, the outer surface of the outer membrane consists of proteins and a specific component, lipopolysaccharide (LPS), which contributes substantially to the exclusion of exterior hydrophobic compounds from cells (Costerton *et al.*, 1974, Leive, L. 1974, Sheu, and Freese, 1973). Heat treatment of a wild-type *E. coli* caused an increase in cell surface hydrophobicity and release of some of the lipopolysaccharide molecules from the outer membrane (Tsuchido *et al.*, 1985). The release of part of the outer membrane by heat treatment appeared to bring about the disorganization of the outer membrane structure and, as a consequence, to result in the partial disruption of the permeability barrier function of the outer membrane (Tsuchido *et al.*, 1985). *E. coli* heat injury and loss of viability was associated primarily with ribosome denaturation (Mackey *et al.*, 1991). The ribosomal

stability is influenced when the intracellular cation concentration is altered; in particular, Mg^{2+} is required for ribosome integrity (Hurst and Hughes**,** 1978).

Considering all the above injuries caused by heat, the enhanced effect of electrical current on loss of viability of *E.coli* cells can be, as an hypothesis, attributed to: the contribution to the electroporation mechanisms that will aid to disrupt the heat fragilized outer membrane; the interference in the cell micro-environment change of the ionic strength, together with the increase of ionic leakage thus increasing ribosomal instability; the interaction and consequent alteration of the diffusion channels (Figure 3.25) for low-molecular weight hydrophilic substances present in the outer membrane.

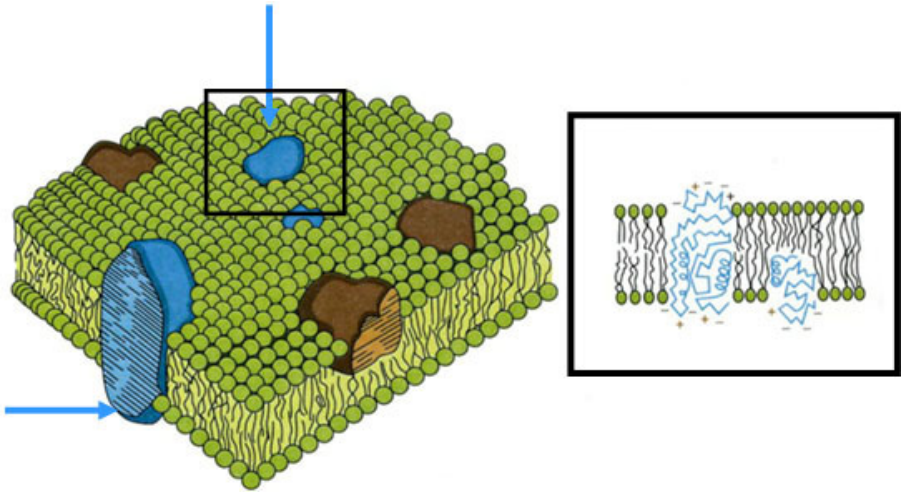

Figure 3.25: Fluid mosaic model of a biological membrane. In aqueous environments membrane phospholipids arrange themselves in such a way that they spontaneously form a fluid bilayer. Membrane protein may be either structural or functional. Proteins may be permanently or transiently associated with one side or the other of the membrane or built into the bilayer, or they may span the bilayer forming transport channels through the membrane

3.3. B. licheniformis

B. licheniformis spores in cloudberry jam were subjected to different treatments to determine the inactivation parameters and to asses if the presence of a moderate electric field (20 V/cm) plays a role in the spore inactivation mechanism.

The heat resistance of bacterial spores is influenced by several environmental factors (Faille *et al.* 1997). The major targets for heat inactivation or injury of spores are considered to be proteins and enzymes (Marquis *et al.* 1994). Nevertheless, in many spores it is not clear which enzymes or other proteins are the critical targets for killing, and it is likely that functional proteins in both the germination and outgrowth system are injured at the same time.

Cazemaier *et al.* (2001) attribute heat resistance of bacterial spores to three main factors: protoplast dehydration, mineralization and thermal adaptation. Since both protoplast mineralization and a higher sporulation temperature result in more dehydrated spore protoplasts, it is assumed that protoplast water content is the primary component determining spore heat resistance (Beaman *et al.* 1984; Bender and Marquis 1985; Marquis and Bender 1985; Nakashio and Gerhardt 1985; Beaman and Gerhardt 1986). The same author reported that *Bacillus* spores prepared on nutrient agar with a mix of metal ions (Ca^{2+}, Mn^{2+}, Mg^{2+}, Fe^{2+} and K^{+}) were more heat-resistant and had a lower protoplast water content than *Bacillus* spores prepared on nutrient agar only with Mn^{2+}. Although the mineral content in the spore protoplasts was not determined, it is assumed that the spores prepared on nutrient agar with a mix of metal ions are more mineralized than the spores prepared on nutrient agar with only Mn^{2+} (Beaman and Gerhardt 1986).

As previously mentioned for the other microorganisms, the temperature was eliminated as a variable (coincident heating phases) and different electrics fields were applied to heat the cloudberry jam to the desired temperature. During the holding phase a constant electric field was used for all the assays. The non-thermal effects were address by comparing the survival of the bacterial spores in the presence or absence of an electric field. The experimental results are shown in Figure 3.26, Figure 3.27 and

Table 3.17 and are expressed in terms of *D* and *z*-values.

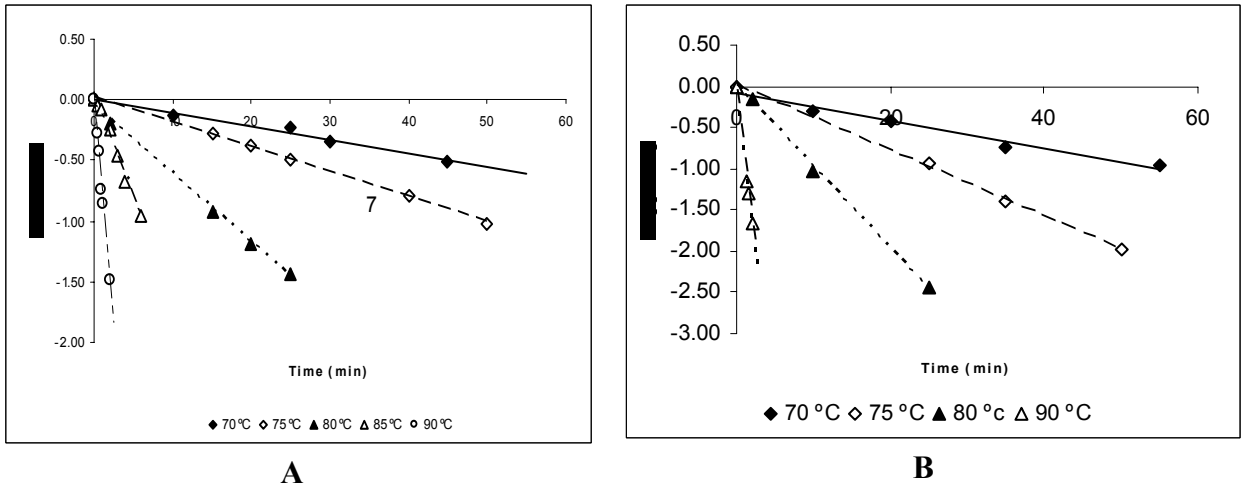

Figure 3.26: *D*-values for *B. licheniformis* in cloudberry jam when submitted to conventional (A) and ohmic (B) heating treatments.

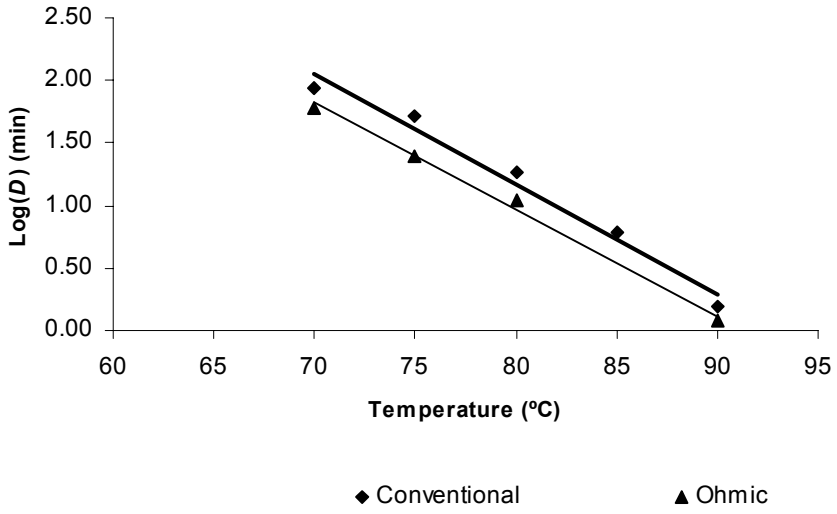

Figure 3.27: Death kinetics of *B. licheniformis* in cloudberry jam when submitted to conventional and ohmic heating; determination of the *z* values.

Table 3.17: Kinetic parameters of thermal degradation of *B. licheniformis* in cloudberry jam

Temperature (ºC)	70	75	80	85	90
$D_{conventional}$ (min)	85.3 ± 6.8	51.0 ± 2.3	18.1 ± 1.1	6.02 ± 0.11	1.57 ± 0.36
% Cv	7.9	4.6	6.3	1.7	22.7
D_{ohmic} (min)	60.8 ± 1.8	25.2 ± 1.2	11.1 ± 1.3	-	1.19 ± 0.01
% Cv	3.0	4.6	11.9	-	1.1
$Z_{conventional}$ (ºC)	11.31±0.49 (r^2 = 0.98)				
Z_{ohmic} (ºC)	11.70±0.03 (r^2 = 0.99)				

In agreement with the results of the previous sections, also in the present case the results show an enhanced effect of electricity in inactivation. For each of the studied temperatures the ohmic *D*-value is lower than the conventional *D*-value but the temperature dependence (*z*-value) remains the same for both treatments. This means that at a given temperature less time is needed to inactivate the microorganism when using ohmic heating however the temperature increase necessary to reduce 10 fold the inactivation time remains the same for both types of treatments.

In this particular case, the more probable effect of electricity is not expected to be on the spore wall due to its more resistant structure but possibly in the enzymes responsible for the activation and germination mechanism. In fact, electric fields of the same order of magnitude as those employed in this study were shown to affect some enzymes' activity (Castro *et al.*, 2004). This opens a whole new field of research and is out of the scope of the present work, but it is a very pertinent subject that deserves to be further explored.

3.4. Comparison of the effects of electrical field on the different microorganisms

The enhanced effect of electricity on the inactivation kinetics of microorganisms and spores was statistically significant in every case studied. Moreover, exception made for *B. fulva* ascospores (14.5 º Brix), the effect on the *D*-value (calculated as the percentage of decrease in this value for the ohmic treatment when compared to the conventional treatment, being in all cases $D_{oh}>D_{conv}$) was similar for the whole range of experiments and the average diminution was of ca. 60 % (Figure 3.28). Industrially, this is an extremely important result meaning that to obtain the same inactivation it will be possible to decrease in 60 % the treatment time with evident and extremely important economical and quality advantages.

The advantages of using this technology to produce high quality / high value foods, namely the ones containing thermolabile components should be reinforced here.

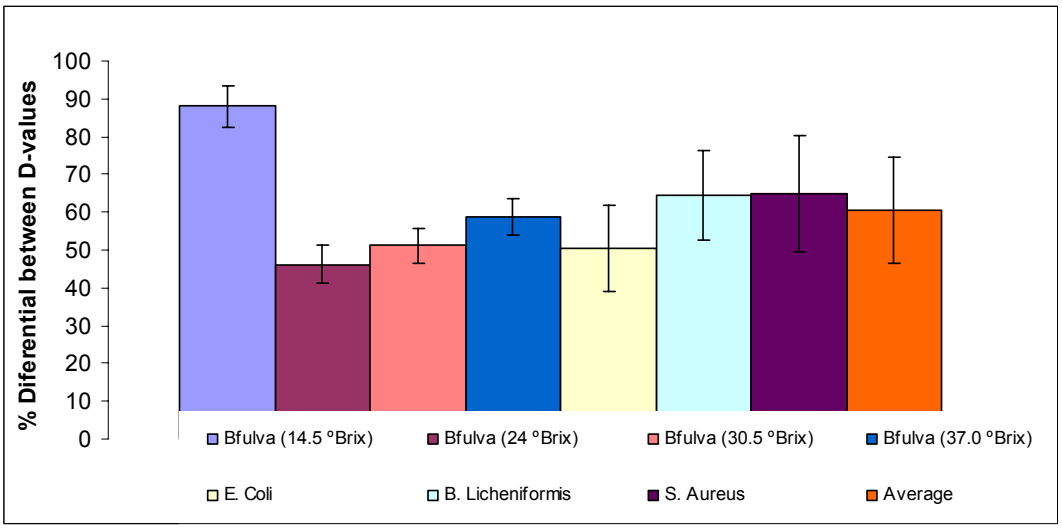

Figure 3.28: Comparison of the different between *D*-values for ohmic and conventional treatment, considering all the microorganisms tested

Furthermore, the results are not in accordance to the currently accepted theory regarding the effect of cell size and shape on the electrical effect. In fact, those theories were tested for high voltage pulsed electric fields (> 20 KV/cm), and this is clearly not the case of this research (in this work averaged in 20 V/cm). Apparently, from the results shown above, when using moderate electric fields the size and shape seem not to play a significant role otherwise the electricity effect on microbial cells and spores would be distinguishable for each organism.

4. Conclusions

The data presented in this chapter point out to significant effects of electricity in terms of microbial inactivation, in different types of microorganisms (Gram positive and Gram negative bacteria) and spores (fungal ascospores and bacterial endospores).

The inactivation profile (first order kinetics) remained when applying an electric field to the food matrix contaminated with the test organisms and the temperature dependence (*z*-values) also showed similar values in both types of treatments, except for strawberry pulps having higher ºBrix values (> 30 ºBrix), where significantly different *z*-values were found.

The basic effects of enhanced inactivation caused by electricity seem to be common to the several situations tested and may help to reinforce the most well accepted theory of pore formation and membrane destabilization. The possible interference of specific ionic and organic compounds concentration in proteins' activity and active transport phenomena associated to micro-environments around the cells due to changes in cell surface hydrophobicity were also hypothesized to partially explain some of the observed electrical effects. Such hypotheses still need further fundamental research and experimental validation.

Finally, these results could be the base for the industrial implementation of this technology assuring that food safety requirements are fulfilled. Moreover, it is also important to note that pasteurization / sterilization processes are critical control points (CCP) in HACCP systems. The monitoring and control of such CCP are based on the achievement of the required time/temperature binomium. However, when using ohmic heating, care must be taken because the applied electrical field is a new parameter to monitor and to control. The absence, even for a small period, of electrical current may allow cells to reestablish membrane pores, equilibrate electrical charges thus reducing or eliminating the electrical effect in inactivation which can, consequently, affect food safety.

5. Future chanllenges: Electrical effects on biological cells or systems

Little attention has been paid concerning the use of moderate electric fields in biological cells and systems and most of the literature only refers the effects of pulsed electric fields in microorganisms or biological cells (e.g. tumoral cell lines). The use of ohmic heating or moderate electric fields needs a deeper understanding in terms of morpho-physiological effects on living cells. Some of the aspects that should be considered are as follows:

- Physiological effects of electricity during microbial inactivation: metabolic pathways, active transport phenomena, membrane integrity, permeability and selectivity. Of prime importance should be the inactivation of microorganisms such as HIV virus in biological fluids without compromising their basic biological function.
- Mutagenic effects caused (if any) when applied either on inactivation or during the growth phases
- Cellular responses to electrical stress: metabolic pathways triggered, activated enzymes
- Gene activation and or inactivation (Figure 3.29)
- Gene therapy
- Microbial transformation (introduction or deletion of genes)
- Activation of bacterial and fungal spores
- Cell-to-cell signaling and *Quorum sensu*
- Possible applications in tissue organization growth namely for the production of organs
- Drug delivery systems (eg. Electrochemotherapy)

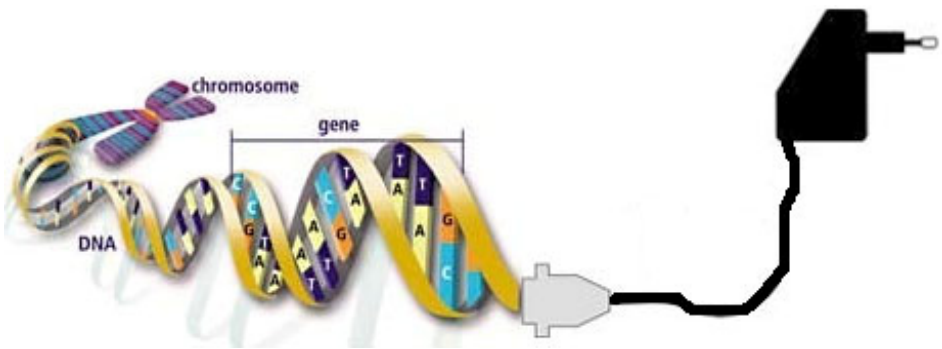

Figure 3.29: Does electricity activate genes?

The effects of electricity on cells or biological systems, when fully understood, can be possibly used to:

- Optimize food processes in terms of nutritional, organoleptic and food safety parameters;
- Develop new strategies for tissue engineering;
- Develop new strategies for drug delivery;

These studies must be made systematically and consider several parameters namely: voltage applied and also current intensity, waveform and frequency, time of voltage input (continuum or pulsed) reversible or irreversible mechanisms.

Fundamental research in this field may lead to an exciting new world of discoveries and manipulations in several areas of science.

6. References

Beaman, T.C. and Gerhardt, P., (1986) Heat resistance of bacterial spores correlated with protoplast dehydration, mineralisation, and thermal adaptation. Applied and Environmental Microbiology 52, 1242±1246.

Beaman, T.C., Koshikawa, T., Pankratz, H.S. and Gerhardt, P., (1984) Dehydration partitioned within core protoplast accounts for heat resistance of bacterial spores. FEMS Microbiology Letters 24, 47±51.

Bender, G.R., Marquis, R.E., (1985) Spore heat resistance and speci®c mineralisation. Applied and Environmental Microbiology 50, 1414±1421.

Butz, P., Funtenberger, S., Haberditzl, T., Tauscher, B., (1996). High pressure inactivation of Byssochlamys nivea ascospores and other heat resistant moulds. Lebensm. Wiss. U-Technol, 29 , 404-410.

Cazemier, A.E., Wagenaars, S.F.M., Ter Steeg, P.F., (2001). Effect of sporulation and recovery medium on the heat resistance and amount of injury of spores from spoilage bacilli. Journal of Applied Microbiology 2001, 90, 761±770

Centers for Disease Control and Prevention. 1993. Update: Multistate outbreak of *Escherichia coli* O157:H7 infections from hamburgers-Western United States, 1992-1993. Morbid. Mortal. Weekly Rep. 42:258-263.

Centers for Disease Control and Prevention. 1996. Outbreak of *Escherichia coli* O157:H7 infections associated with drinking unpasteurized commercial apple juice. Morbid. Mortal. Weekly Rep. 45:44.

Coleman, W. G., Jr., and Leive, L., (1979). Two mutations which affect the barrier function of the Escherichia coli K-12 outer membrane. J. Bacteriol. 139:899-910.

Conway, P.L., (1995). Microbial ecology of the human large intestine. In: G.R. Gibson and G.T. Macfarlane, eds. p.1-24. Human colonic bacteria: role in nutrition, physiology, and pathology. CRC Press, Boca Raton, FL.

Costerton, J. W., Ingram, J. M., and Cheng, K. J., (1974). Structure and function of the cell envelope of gram-negative bacteria. Bacteriol. Rev. 38:87-110.

DuPont H.L., Formal, S.B., Hornick, R.B., Snyder, M.J., Libonati, J.P., Sheahan, D.G., LaBrec, E.H. Kalas, J.P., (1971). Pathogenesis of *Escherichia coli* diarrhea. N. Engl. J. Med. 285:1-9.

Ewing, W.H., (1986). Edwards and Ewing's Identification of *Enterobacteriaceae*, 4th ed. Elsevier, New York.

Faille, C., Lebret, V., Gavini, F. and Maingonnat, J.F., (1997) Injury and lethality of heat treatment of Bacillus cereus spores suspended in buffer and in poultry meat. Journal of Food Protection 60, 544±547.

Grau, F. H., (1978). Significance of the inactivation of transport in thermal death of *Escherichia coli*. Appi. Environ. Microbiol. 36:230-236.

Griffin, P.M., Tauxe, R.V., (1991). The epidemiology of infections caused by *Escherichia coli* O157:H7, other enterohemorrhagic *E. coli* and the associated hemolytic uremic syndrome. Epidemiol. Rev. 13:60-98.

Hicks, S., Frankel, G., Kaper, J. B., Dougan, G., Phillips, A. D., (1998). Role of intimin and bundle-forming pili in enteropathogenic *Escherichia coli* adhesion to pediatric intestinal tissue in vitro. Infect. Immun. 66:1570-1578.

Hitchener, B. J., Egan, A. F., (1977). Outer-membrane damage in sublethally heated Escherichia coli K-12. Can. J. Microbiol. 23:311-318.

Hurst, A., Hughes, A., (1978). Stability of ribosomes of *Staphylococcus aureus*Staphylococcus aureus S6 sublethally heated in different buffers. J. Bacteriol. 133:564-568.

Hurst, A., Hughes, A., Collins-Thompson, D. L., Shah, B. G., (1974). Relationship between loss of magnesium and loss of salt tolerance after sublethal heating of Staphylococcus aureus.

Iandolo, J. J., Ordal, Z. J., (1966). Repair of thermal injury of Staphylococcus aureus. J. Bacteriol. 91:134-142.

Karmali, M. A. (1989). Infection by verotoxin-producing *Escherichia coli*. Clin Microbiol. Rev. 2:15-38.

Katsui, N., Tsuchido, T., Takano, M., Shibasaki, I., (1981). Effect of preincubation temperature on the heat resistance of Escherichia coli having different fatty acid compositions. J. Gen. Microbiol. 122:357-361.

Leive, L., (1974). The barrier function of the gram-negative envelope. Ann. N.Y. Acad. Sci. 235:109-129.

Levine, M. M., (1987). *Escherichia coli* that cause diarrhea: enterotoxigenic, enteroinvasive, enterohemorrhagic, and enteroadherent. J. Infect. Dis. 155:377-389.13.

Mackey, B. M., Miles, C. A., Parsons, S. E., Seymour, D. A., (1991). Thermal denaturation of whole cells and cell components of *Escherichia coli*Escherichia coli examined by differential scanning calorimetry. J. Gen. Microbiol. **137:**2361-2374.

Marquis, R.E., Bender, G.R., (1985). Mineralisation and heat resistance of bacterial spores. Journal of Bacteriology 161, 789±791.

Nakashio, S. and Gerhardt, P., (1985). Protoplast dehydration correlated with heat resistance of bacterial spores. Journal of Bacteriology 162, 571±578.

Nataro, J. P., Kaper, J. B., (1998). Diarrheagenic *Escherichia coli*. Clin. Microbiol. Rev. 11:132-201.

Neill, M. A., Tarr, P. I., Taylor, D. N., Trofa, A. F.. (1994). *Escherichia coli*. In Foodborne Disease Handbook, Y. H. Hui, J. R. Gorham, K. D. Murell, and D. O. Cliver, eds. Marcel Decker, Inc. New York. pp. 169-213.

Pitt, J. I. & Hocking, A. D., (1985). Fungi and Food Spoilage. Sydney: Academic Press, 413p.

Riley, L.W., Remis, R. S., Helgerson, S.D., McGee, H.B., Wells, J.G., Davis, B. R., Herbert, R. J., Olcott, G.S., Johnson, L.M., Hargett, N. T., Blake, P.A., Cohen, M. L., (1983). Hemorrhagic colitis associated with a rare Escherichia coli serotype O157:H7. N. Engl. J. Med. 308:681-685.

Salkinoja-Salonen, M. S., Vuorio, R., Andersson, M. A., Kämpfer, P., Andersson, M. C., Honkanen-Buzalski, T. and Scoging, A. C.

Samaranayake, C.P., Sastry, S. K., (2005). Electrode and pH effects on electrochemical reactions during ohmic heating. Journal of Electroanalytical Chemistry 577 125–135.

Sheu, C. W., and Freese, E.. (1973). Lipopolysaccharide layer protection of gram-negative bacteria against inhibition by longchain fatty acids. J. Bacteriol. 115:869-875.

Shibasaki, I., and Tsuchido, T., (1973). Enhancing effect of chemicals on the thermal injury of microorganisms. Acta Aliment. Acad. Sci. Hung. 2:327-349.

Strange, R. E., and Shon, M., (1964). Effects of thermal stress on viability and ribonucleic acid of Aerobacter aerogenes in aqueous suspension. J. Gen. Microbiol. 34:99-114.

Swerdlow, D. L., Woodruff, B. A., Brady, R. C., Griffin, P. M., Tippen, S.,H. D. Donnell Jr., P. M., Geldreich, E., Payne, B. J., Neyer, A., Wells, J. G., Greene, K. D., Bright, M., Bean, N., Blake, P. A., (1992). A waterborne outbreak in Missouri of *Escherichia coli* O157:H7 associated with bloody diarrhea and death. Ann. Intern. Med. 117:812-819.

Toxigenic Strains of Bacillus licheniformis Related to Food Poisoning, (1999). Applied and Environmental Microbiology, p. 4637-4645, Vol. 65, No. 10

Tsuchido, T., Katsui, N., Takeuchi, A., Takano, M., Shibasaki, I., (1985). Destruction of the Outer Membrane Permeability Barrier of Escherichia coli by Heat treatment. Aplied and environmental microbiology, p. 298-303.

Chapter 4.

FERMENTATIVE PROCESSES

Abstract

The production of ethanol and β-galactosidase from cheese whey and other sub-products from industries can be a good way of minimizing environmental problems and producing valuable products from low-cost raw materials. A recombinant S. cerevisiae NCYC869-A3/pVK1.1 flocculent strain expressing the lacA gene (coding for β-galactosidase) of Aspergillus niger was used in the experiments. Batch culture experiments were performed in SSlactose medium with 50 g/L lactose in a 2 dm^3 bioreactor with agitation, temperature and pH measurement and control. Continuous or discontinuous MEF's were applied with an intensity ranging from 0 to 2 V/cm under aerobic and anaerobic conditions. For all the experiments the biomass, β-galactosidase activity, lactose, glucose, galactose and ethanol were measured.

The lag phase, specific growth rate and biomass and product yields were calculated. Significant changes in lag phase and biomass yields were found, having a linear reaction with the increase of the electric field applied (in aerobic experiments).

Plasmid stability was affected when using higher electric fields in continuous, however if only used in the early stages it can be advantageous.

The results show that ohmic heating enhances early stages of the fermentation, and biomass productivity indicating that ohmically assisted fermentations may be extremely useful in food industry, biomedical and other industries.

Industrial Relevance: The optimization of fermentative processes namely reducing the lag phase or the increase of biomass production can have significant implications in industrial economics. If these applications are in the biomedical area, consequences as lowering drug price should be expected, having a social impact as well.

Keywords: MEF, fermentation, plasmid stability, biomass yield, optimization, β-galactosidase, ethanol

1. Introduction

Fermentation technology is a very promising and fast growing area of Biotechnology, absorbing an ever increasing range of processes and products. With a longer history than any area of biological sciences, fermentation technology spans important areas such as food and medicine.

Systems engineering approaches are increasingly applied in the bioprocess industries (i.e., biotechnological, food, pharmaceutical, environmental, etc.). In order to increase the productivity, profitability and/or efficiency of bioprocesses, considerable research effort has been devoted to their improvement via creation of genetically modified strains with high productivity, optimization of environmental and nutritional parameters, optimization and design of novel bioreactors and computer-aided process engineering methods.

One of the possible strategies to improve productivity is the use of continuous high-cell-density systems. Among these, the use of flocculating microorganisms is very attractive since there is no need of mechanical devices or supports (Kida *et al.* 1989). This is a huge advantage since it is well known that the support represents a major cost in immobilization procedures.

1.1. The use of moderate electric fields

The application of electricity to biological cells or systems, although being an old technology, has been gaining more and more interest in different areas of application namely, gene therapy, genetic studies, drug delivery systems and fermentative processes.

Carlson (1954) reported that alternating current causes an increase in enzymatic activity of living cells. Rowley (1972) presented results showing that alternating current had little or no effect on the growth rate of microorganisms in the frequency range of 1 - 60 Hz and current range of 15 and 30 mA. Shimada and Shimahara (1977) have reported that alternating current of 50 Hz influenced the growth lag phase of *E. coli* but it depends on the inoculum size, shaking rate during cultivation, and composition of the medium.

Various physical techniques, including electrical (Alp *et al.* 2002 ; Verduzco-Luque *et al.,* 2003 ; Ozkan, *et al.,* 2003 ; Poortinga, *et al.,* 2000 ; Pohl, 1972), ultrasonic (Spengler *et al.* 2000) and optical (Ozkan, *et al.* 2003; Grier, 2003) techniques have been used to pattern both animal and microbial cells. Poortinga and co-workers (2000) have described the use of DC and low-frequency AC electric fields to create patterned bacterial biofilms. Pohl (1972) has described the use of dielectrophoresis, the movement of particles in non-uniform AC electric fields, to create tissue-like materials from bacterial suspensions. Cells are suspended above the electrodes, and drawn towards the high electric field regions between the electrodes in the same way as iron filings are attracted to high magnetic field regions around the poles of a magnet. In principle, it is possible to create microbial biofilms with this method that consists of 3D colonies of different shapes, containing any type of microbe in any location on a surface. Limitations are set only by the sophistication of the facilities available for microelectrode fabrication. Interestingly, the electric field also orients the cells. Oriented cell growth has been reported during bacterial colony development (Shapiro, 1995,1997,1998), in microbial anaerobic aggregates, and during different developmental stages in *Myxococcus* (Kim and Kaiser, 1990).

The application of OH in the fermentation by *Lactobacillus acidophilus*, a lactic acid bacterium used in the dairy industry and with human health implications was studied by Cho *et al.* (1996). The lid of the fermentation vessel was equipped with ports for thermocouple, pH probe, inoculation, water circulation coil, medium circulation, and two stainless steel plate electrodes. Metal surfaces were coated with epoxylite for electrical insulation and inertness. Temperature control was carried out either under conventional (by

continuous water circulation) or OH (a constant voltage of 15 V – low voltage – or 40 V – high voltage – was applied), at different temperatures (30, 35 and 40ºC). The results indicated that the lag phase for fermentations at 30 ºC was significantly lower (18 fold) under low voltage ohmic conditions, which was also the lowest lag period of all the conditions tested. Although additional investigation is needed to explain the shortening of lag phase, this may be due to the improvement of absorption of nutrients and minimization of the inhibitory action of fresh medium. The application of an electrical field may induce pore formation in membranes (similar to the electroporation mechanism used to transform cells in molecular biology studies) allowing a faster and efficient transport of the nutrients into the cells thus decreasing lag phase. The minimum generation time for *L. acidophilus* was not affected by the heating method. Small differences in the final pH of the fermentation between the two methods were also reported. The consumption of glucose and the release of lactic acid were not significantly affected by the heating method. On the other hand, the production of lacidin A, an antimicrobial protein (bacteriocin) by the bacterium, decreased when fermentation occurred under ohmic conditions. The electrical current measurements follow approximately the changes in growth of *L. acidophilus* during the fermentation, and these changes in electrical conductivity could, perhaps, be used to monitor fermentations. This study provides evidence that OH in the food industry may be useful to shorten the time for e.g. yogurt and cheese production (Cho *et al.*, 1996), among other applications. Later on, Loghavi *et al.* (2005) examined the influence of MEF on the early, exponential and stationary phase of the fermentation and its impact on bacteriocin (lacidin A) production using different types of treatments: conventional (for 40 hrs), MEF (1 V/cm, 60 Hz, for 40 hrs), and combinations of MEF (1 V/cm, 60 Hz, for first 5 hrs) and conventional (for 35 hrs) fermentation. There was no significant change in the maximum specific growth rate, biomass production and pH change under the different experimental conditions, however the lacidin A production was lower when electric field was present at the later stages of fermentation. The reduction of lag phase was observed when a mild electric field was applied and these results were in accordance with the ones previously obtained by Cho *et al.* (1996).

The effect of the electric field frequency on growth parameters of *L. acidophilus* was investigated by Loghavi *et al.* (2006). A MEF of 1V/cm and frequencies of 45 Hz, 60 Hz, and 90 Hz were used. There was a significant increase in the bacteriocin production under ohmic (early stage of the fermentation) and conventional heating combination at 60 Hz. However no effect on growth kinetics was observed.

1.2. The enzyme β-Galactosidase

β-Galactosidase (EC 3.2.1.23) is able to cleave β-linked galactose residues from various compounds and is commonly used to cleave lactose into galactose and glucose.

People that are lactose-intolerant cannot drink milk or eat most of the dairy products. When the intestine produces little or no lactase, lactose (the milk sugar) is not digested and moves into the colon, where bacteria ferment it, producing hydrogen, carbon dioxide and organic acids. The results of this fermentation are diarrhea, flatulence (gas) and abdominal discomfort. The treatment of lactose containing foodstuffs with the enzyme β-galactosidase allows the production of dairy products for lactose-intolerant individuals and that is why several β-galactosidase preparations are commercially available (Godfrey, 2000).

Regarding food technology, products such as ice-cream and condensed milk, can lead to excessive lactose crystallisation resulting in products with a mealy, sandy or gritty texture if there is a high content of lactose in the milk (Neelakantan, 1999). The use of this enzyme as a processing aid for these industries is another example of a possible application of β-galactosidase.

New applications for β-galactosidase such as the recovery of biologically active oligosaccharides from milk have also been described in literature (Sarney *et al.*, 2000).

Table 4.1 - Main biotechnological applications of β-galactosidase

Biotechnological aplications of β-galactosidase
Lactose-free milk
Dairy products with low contents of lactose
Production of concentrates with low contents of lactose for ice-cream industry
Production of sweet yogurts
Production of foos syrups
Enzymatic treatment of cheese
Cheese whey processing for further industrial uses
Incorporation in medicines to lactose intolerant patients

2. Materials and Methods

2.1. Sterilization procedures

The materials, solutions and culture media were sterilized at 121 ºC for 20 minutes. The thermo-labile solutions were sterilized by filtration using a 0.2 μm filter.

2.2. Strain

The microorganism used in this work was a recombinant *Saccharomyces cerevisiae* NCYC869-A3/pVK1.1. This is a flocculent strain expressing the lacA gene (coding for β-galactosidase) of *Aspergillus niger* under ADHI promotor and terminator (Domingues *et al.*, 2002).

2.3. Culture Media and Inocula preparation

The recombinant yeast was maintained at 4 ºC on slants or at –80 ºC in permanent culture of YNB selective medium. For inocula and fermentation SSLactose liquid medium was used, using 20 g/l or 50 g/l of lactose, respectively (Table 4.2).
The solid media used was YNB and SS Lactose containing 2 % (w/v) agar.

Table 4.2: Culture media used in the experiments

YNB	6.7 g/l yeast nitrogen base (w/o amino acids) 20 g/l lactose
SSLactose	5 g/l KH_2PO_4 2 g/l $(NH_4)_2SO_4$ 0.4 g/l $MgSO_4.7H_2O$ 2.0 g/l Yeast extract 20 - 50 g/l Lactose

2.4. Biomass determination

Biomass concentrations were measured as dry weight (DW) and/or using absorbance methods. The DW was determined by filtering the sample through 0.2-μm filter-paper and then drying at 105 ºC for 24 h. The absorbance was measured at 620 nm using a Jasco's V-560 spectrometer (Jasco, Tokyo, Japan) and compared to a standard curve for absorbance versus DW previously constructed (Figure 4.1). Prior to absorbance readings cells were deflocculated with a solution of NaCl (1.5 % w/v, pH 3.0).

The construction of the calibration curve was made by making several dilutions of a cell culture suspension in order to obtain optical densities between 0.1 and 1.0. Each of these solutions was filtered, in triplicate, through a 0.45 μm filter and placed into an oven at 105 ºC during 24 h. Filters were cooled down and weighted. The weight difference divided by the sample volume returns the biomass concentration in g/l.

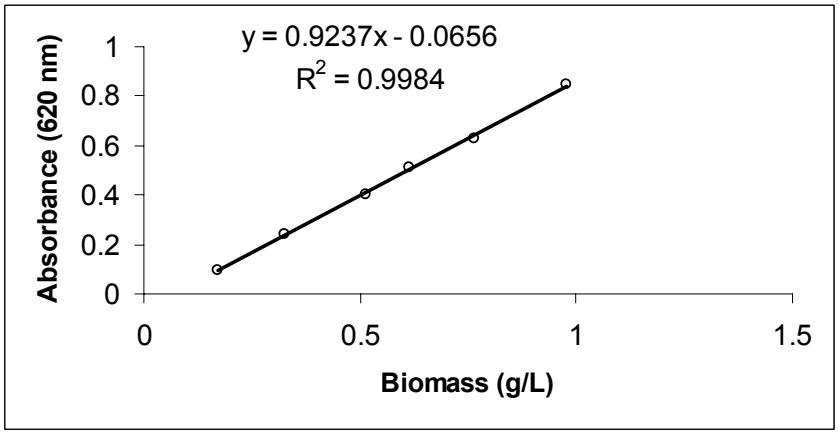

Figure 4.1: Correlation between dry weight and absorbance.

2.5. Biomass viability

An important parameter for monitoring a fermentative process is the presence of viable yeasts. A common method used to assess the degree of yeast viability is the use of a vital dye and the hemacytometer. Viable yeast does not stain; whereas non-viable, non-metabolizing cells stain with the color of the selected dye. The most common yeast viability stain is methylene blue. This stain has blue color in the oxidized form becoming colorless in the reduced form. One explanation to the fact that viable cells do not stain blue is advanced by Postgate (1967), quoted by Belo (1999), and hypothesizes that when the stain enters the cell is reduced by a dehidrogenase, which is not active in the dead cells.

Another theory is that the stain only enters the cells in which selective permeability is seriously compromised (Bonara and Mares, 1982, quoted by Belo, 1999).

The cell suspension was deflocculated and mixed with an equal volume of methylene blue solution (0.1 g/l methylene blue in ultrapure water) and incubated for 5 min at room temperature. Dead, blue-coloured cells were scored, in a Neubauer chamber, using a light microscope. The ratio of stained cells to the total number counted was calculated and the results expressed as percent viability.

Simultaneously the cells were plated in plate count agar and the number of colony forming units was evaluated.

2.6. Flocculation assays

After deflocculating the yeast cells (see the section "Biomass determination"), 24 ml of a cell suspension (within the concentration used in the calibration curve) was transferred to a 25 ml graduated cylinder to which 1 ml of calcium chloride was added. The volume of 25 ml was fulfilled using deflocculating solution. The solution was homogenized by inverting the graduated cylinder several times. In the control assay no calcium chloride was added. At defined time intervals (every 10 s for the first minute and every 20 s afterwards) 300 µL samples were collected at a depth corresponding to the 20 ml point and the corresponding optical density was read in a micro-plate. The cell concentration results were normalized by division by the initial cell concentration. The settling profile was represented as a percentage of suspended biomass as a function of time (adapted from Soares, 1995).

2.7. Plasmid stability

Plasmid stability is the relative amount of cells containing the plasmid after several generations. This stability was determined by platting the biomass samples into Petri dishes containing SSgalactose-X-GAL agar. The colonies stained blue still contain the plasmid while the colonies stained white lost the plasmid. It is then possible to estimate the plasmid stability by dividing the number of blue colonies by the total number of colonies.

Table 4.3: Media and solutions used for determining plasmid stability

SSglucose – X-GAL agar	5 g/l KH_2PO_4 2 g/l $(NH_4)_2SO_4$ 0.4 g/l $MgSO_4.7H_2O$ 2.0 g/l yeast extract 20 - 50 g/l glucose 2 % (p/v) agar X-GAL (1X)
1 % X-GAL dimethylformamide 2 ml Xgal/L	
X-Gal (1000X)	20 mg/ml N,N-Dimethylformamide

2.8. β-galactosidase activity measurements

β-GAL, in this case, is an extracelullar enzyme and it was used directly from fermentation broth without further purification. One unit of activity was defined as the amount of enzyme that hydrolyses 1 nmol of p-nitrophenil β-D-galactopyranoside (pNPG) per minute, at 65 °C. The activity was measured as the amount of p-nitrophenol released from pNPG per minute (Figure 4.2). The quantification was made in micro-plate wells, adapting the method described by Bailey and Linko (1990).

Initially, 180 µL of pPNG solution was placed into the micro-plate wells and incubated at 65 ºC for 4 minutes to achieve the desired temperature. A 20 µL sample is then added to the previous solution, mixed and incubated for 10 minutes. The reaction was stopped by adding 100 µL of stop solution (see Table 4.3). The absorbance readings were made spectrophotometrically at 405 nm, using acetate buffer as blank and converted into activity units using a calibration curve (Figure 4.3)

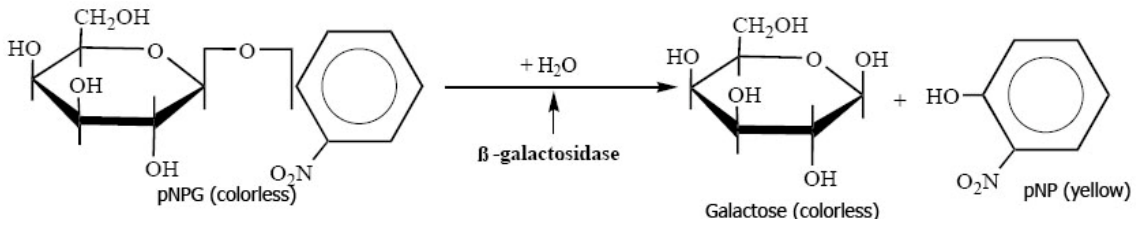

Figure 4.2: Reaction catalyzed by β-Galactosidase

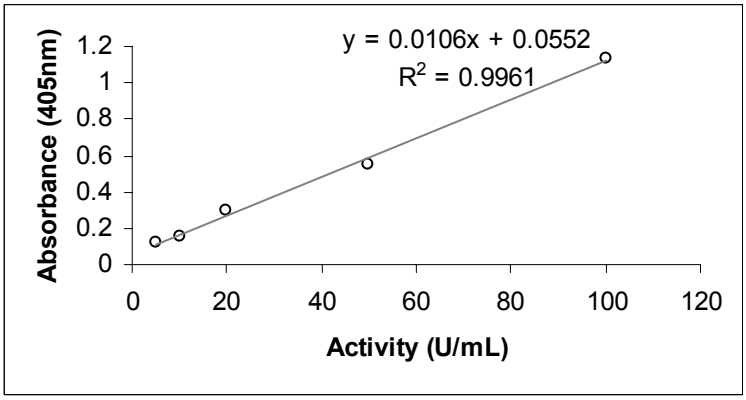

Figure 4.3: Calibration curve for β-Galactosidase activity.

Table 4.4: Solutions for activity measurement

pNPG Solution	1.7 mM pNPG Acetate buffer 0.075M
Acetate buffer 0.075M (pH = 4.5)	22,65 g/l Acetic acid Set pH to 4.5 with 10 M NaOH
Stop Solution	1 M Na_2CO_3

In order to characterize the excreted enzyme regarding optimal temperature and pH for maximum activity the assay temperature was varied from 30 to 100 ºC and pH ranged from 3.5 to 6.0. For each pH a calibration curve was constructed in a similar way as described above, replacing the acetate buffer in order to mach the desired pH.

2.9. Reducing Sugars

The total reducing sugar (RS) concentration was determined by the dinitrosalicilic (DNS - 10 g/l di-nitrosalicylic acid; 300 g/l potassium sodium tartarate-4-hydrate; 0.4 mol.L-1 NaOH) acid method described elsewhere (Miller, 1959).

For each sample, 500 µL of the DNS reagent were added to 500 µL of sample and placed in a boiling water bath during 5 minutes. Afterwards, 5 mL of deionised water were added and the absorbance of 300 µL of the resulting solution was measured at 540 nm in the microplate reader (Synergy HT HT, BIO-TEK, EUA. Calibration was performed with lactose standards within the range 0.1-1.25 g/l (Figure 4.4).

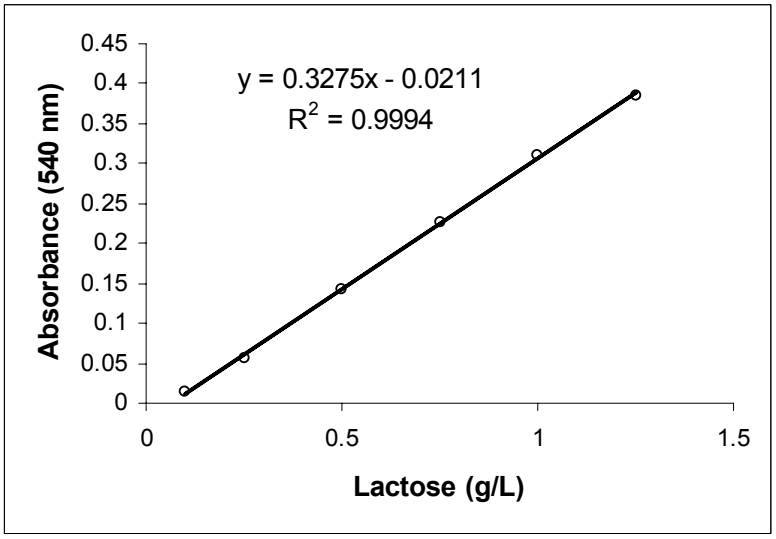

Figure 4.4: Calibration curve for reducing sugars quantification

2.10. Lactose, glucose, galactose and ethanol measurements

Sugars (lactose, glucose and galactose) and ethanol were quantified by HPLC (Chrompack, Middleburg, The Netherlands) using a refractive index (RI) detector (JASCO 830-RI Intelligent RI Detector, Jasco, Tokyo, Japan) and a column for organic acids. The eluent was 0.005 mol/l H_2SO_4. The analyses were made at an elution rate of 0.5 ml/min and an oven temperature of 35 ºC. The retention times of lactose, glucose, galactose and ethanol were, respectively, 12.2, 14.3, 15.4 and 31.1 min.

2.11. Total protein quantification

The quantification of the total protein was made using a commercially available kit (Pierce) based on Bradford's method (1976).

150 μL of each sample was pipetted into the microtiter wells, added another 150 μl of Coomassie Plus reagent to each well, mixed and wait for 2 minutes before reading absorbance at 595 nm. The blank was made with water.

The standard curve was prepared using bovine serum albumine standards within the range 2.5-25 mg/l (Figure 4.5).

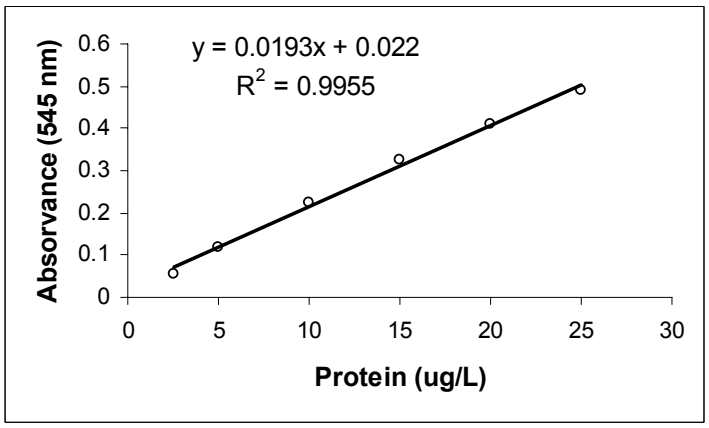

Figure 4.5: Calibration curve for total protein quantification

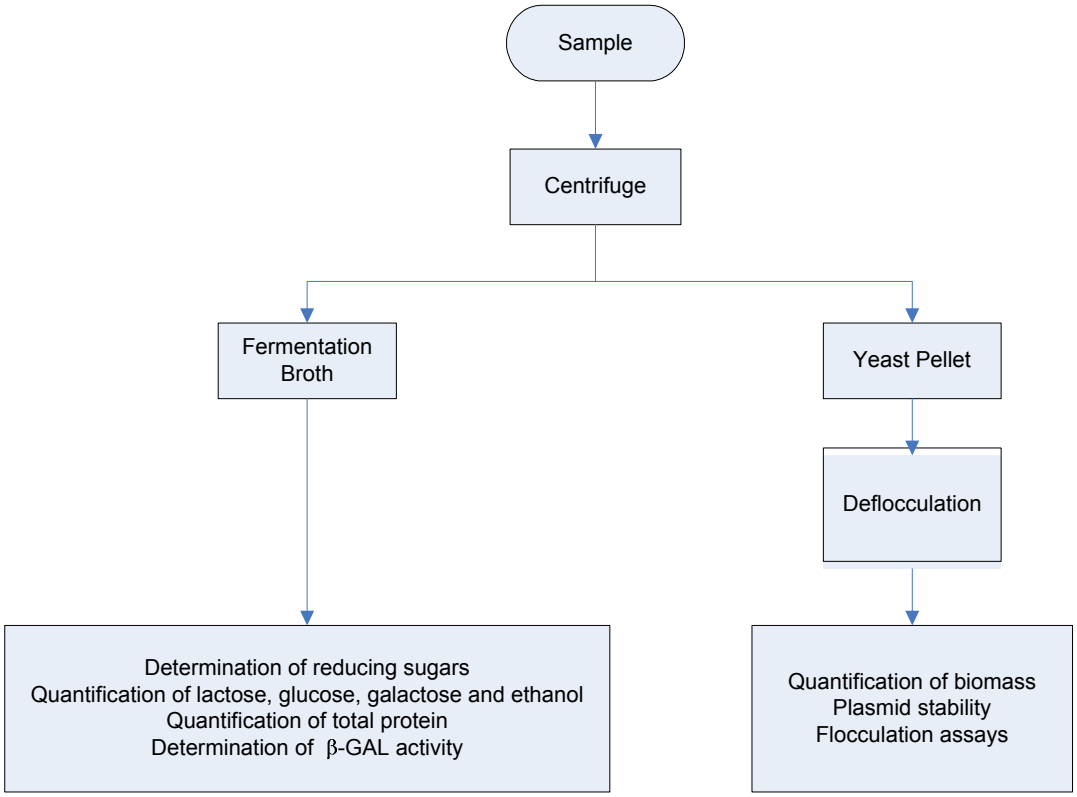

Figure 4.6: Summary of the analytical methods applied to the fermentation samples

2.12. Bioreactor operation

Batch culture experiments were performed using a 2 L bioreactor (Figure 4.7). All the experiments were conducted with agitation, temperature and pH measurement and control. Temperature was monitored using type-K thermocouples, with Teflon coating, placed inside the reactor. The temperature was kept at 30 ± 1 ºC by developing a control program in Labview 7.0 Express (National Instruments, U.S.A.). The initial pH was 5.4, which was allowed to drop to 4.0 during the fermentation and then kept at 4.0 ± 0.15 by automatic addition of ammonia solution (30 % v/v). The agitation at 150 r.p.m. was made by a magnetic stirrer and the bioreactor was aerated with filtered air at a flow rate of 0.25 vvm, when aerobic conditions were tested. These conditions guarantee a minimum of 20 % of dissolved oxygen during all stages of the fermentation. Anaerobic conditions were attained by an initial sparging of filtered air (during 15 min prior to the inoculation in order to have some dissolved oxygen available for the beginning of the fermentation) and then suppressing the air supply. The vessel and tubing were autoclaved for 30 min at 121 ºC.

Two stainless steel electrodes were placed symmetrically inside the bioreactor with a distance of 7.5 cm between them. Each electrode has a surface area of 65 cm^2.

The electric field, ranging from 0 to 2 V/cm, was generated by an alternating current source of 50 Hz.

A data-logger was employed to record continuously and simultaneously current intensity, voltage and temperature.

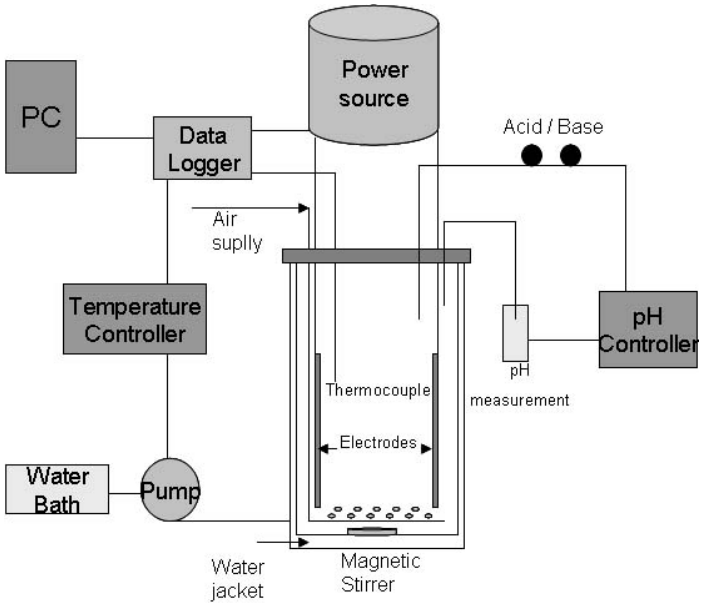

Figure 4.7: Schematic diagram of the experimental setup.

2.13. MEF treatments

The fermentations were performed under aerobic or anaerobic conditions and the different experimental conditions are represented in Figure 4.8.

The following treatments were comparatively investigated:

1. **Conventional treatment** - no electric field was applied and these conditions were considered the control
2. **Continuous MEF** - An electric field ranging from 0.5 to 2.0 V/cm was continuously applied during the entire fermentative process
3. **Partial MEF** (only aerobic conditions) – A MEF of 1 V/cm was applied only partially during the course of the fermentation. "Early MEF" was applied for 2.5 or 5.0 h from the beginning of the bioreactor operation; "Late MEF" was applied when the lactose concentration inside the bioreactor was lower than 10 g/l.
4. **Addition of ethanol** (only anaerobic conditions) – Ethanol was added to the fermentation broth and two sets of experiments were performed: a control (0 V/cm) and a MEF of 1 V/cm was applied during the course of the fermentation.

All these sets of experiments were conducted in duplicate in the bioreactor previously described. The growth parameters were calculated and the averaged values and respective standard deviation are presented further ahead in the chapter. Furthermore, data was analyzed statistically using an Analysis of Variance approach (ANOVA). When treatment factors were significant, Student's t-statistics were used for multiple comparisons of means.

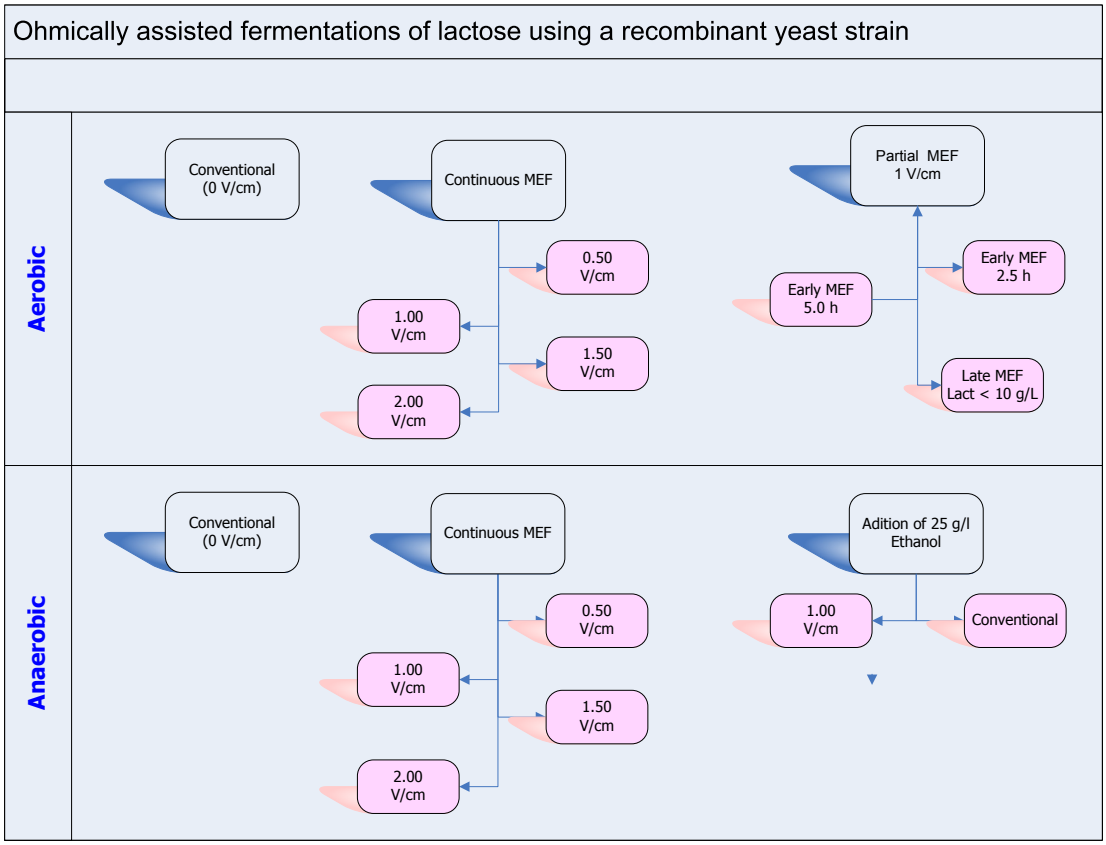

Figure 4.8: Depiction of the experimental conditions assayed

3. Results and Discussion

Some authors reported advantages of using moderate electric fields during fermentative processes. Those results pointed out to an effect of electric field in bacterial growth parameters and opened the possibility of further optimization of the process by applying an electric field.

Aiming at deeper investigating the effects of MEF during a fermentative process a set of experimental conditions was tested. The fermentations were conducted under aerobic and anaerobic conditions setting the initial lactose concentration to a value of 50 g/l. For both conditions, different electric fields (ranging from 0 to 2 V/cm) were applied.

The main fermentation conditions such as pH, aeration and temperature were previously optimized by Domingues (2001).

The effects on growth parameters such as lag phase and growth rate and also primary metabolites production namely ethanol and β-galactosidase were determined. Moreover the effect on the yeast flocculation capability and plasmid stability were addressed as well.

3.1. Aerobic fermentations

3.1.1. Continuous MEF experiments

In this part of the research the electric field was continuously applied during the whole course of the fermentation, at different field strenghts. The fermentation made at 0 V/cm was established as the control (optimal growth conditions, Domingues, 2001). Typical fermentation parameters' evolution with time is presented in Figure 4.9 and Figure 4.10.

Lactose is totally metabolized by the recombinant strain in less than 22 h, when an electric field of 2 V/cm is applied. This represents a reduction of about 8 hours in the fermentation time when comparing to the absence of electric field where the time needed to consume lactose is about 30 h. This reduction in the fermentation time is mainly attributed to two factors: the reduction of the lag phase (Figure 4.10) and the significant increase in the biomass production (Figure 4.14).

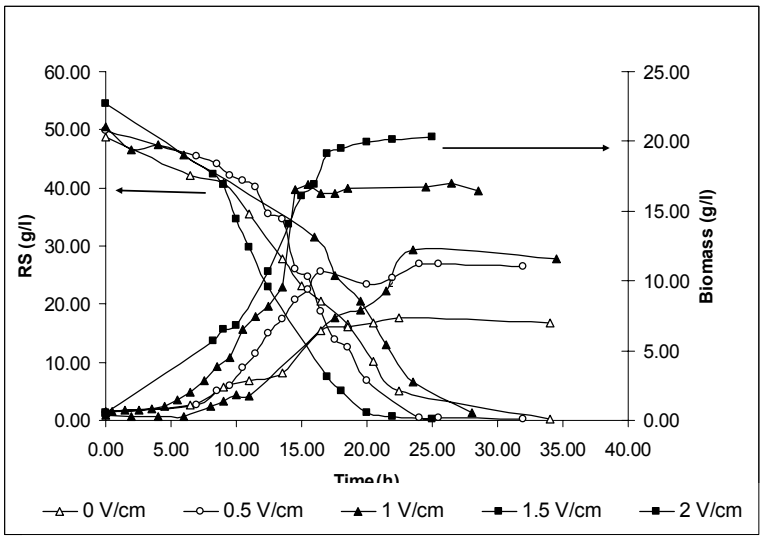

Figure 4.9: Variation of reducing sugars and biomass inside the bioreactor using SSLactose medium (50 g/l), for the different electrical fields

In fact, the lag phase length (Figure 4.10) decreases with the increase of the applied electric field from 0 to 2 V/cm. This observation is in line with the results obtained by Cho *et al.* (1996) and Loghavi *et al.* (2005) which also reported a decrease of the lag phase of *L. acidophilus* with increasing electric field strength. However the data from Cho *et al.* (1996), when using sub-optimal growth temperatures, referred that there were distinguished effects between 1.07 V/cm and 2.86 V/cm which were not visualized in this work. The influence of the cell size (bacterial cells are smaller than yeast cells) may help to explain this issue. The

study performed by Heinz *et al.*, (2002) regarding the determination of critical electroporative field strength as a function of cell dimensions, concluded that bigger cells are more affected by the electrical field thus having a lower critical field strength. In the present work all the electric fields applied led to a decrease of the lag phase consistent with the field intensity applied, therefore one may consider that for all the strengths used, that threshold electric field was overcome. Moreover, this work was conducted at the optimal growth conditions thus, under such scenario, the effects of MEF may be less pronounced.

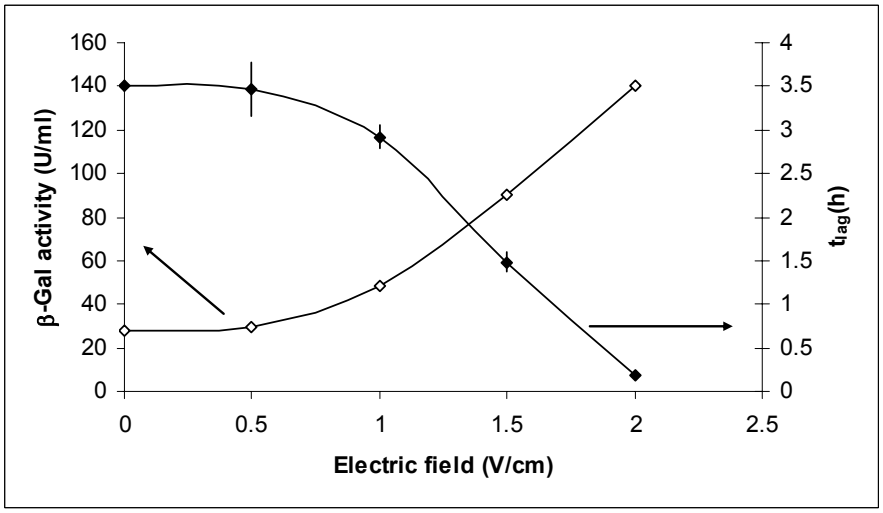

Figure 4.10: Relation between the lag phase and the activity of β-gal in the fermentation broth after 7 h of the start, as a function of electric field applied (aerobic fermentations)

The lag phase decreases sharply with the increase of the electric field and when using 2 V/cm the lag phase is almost inexistent. The lag phase when using the lower MEF (0.5 V/cm) is similar ($p > 0.05$) to the one obtain when no voltage is applied. The other results are all statistically different from each other ($p < 0.05$). This decrease in the lag period may be explained by several isolated factors or their combination. The external application of an electric field can affect the membrane properties in terms of selectivity or permeability Cho *et al.* (1996); consequently, the entrance of nutrients into the cell may be facilitated. It is also noteworthy that the formation of pores in the membrane due to the presence of an electric field was reported by Yoon *et al.* (2002). In fact, these authors stated that ohmic heating was found to translocate intracellular protein materials out of the cell wall, and the amount of exuded protein increased significantly as the electric field increased from 10 to 20 V/cm. Although the electric field used in the present work was 10 fold lower, if the electric field aids the excretion of β-gal in the early stages of the fermentation the yeast can start growing on the lactose hydrolyzed to glucose and galactose by β-gal instead of using

the nutrients present in the fermentation broth (e.g. yeast extract), consequently reducing the lag phase. It should be stressed that the bioreactor was inoculated using microorganisms in the exponential phase of growth which were already producing the enzyme. The production and excretion of the enzyme β-gal is associated with cell growth (Figure 4.13) increasing not only during the exponential phase but also during the lag and stationary phase. The analysis of β-gal activity in the fermentation broth leads to the conclusion that, until approximately 7 h after the fermentation starts (Figure 4.10), the activity increases with the increase of the electric field, which is coincident with the reduction of the lag phase. These results are in accordance with the conclusions obtained by Yoon *et al.* (2002).

Evidence for cell-cell communication in bacteria has been accumulating in recent years and numerous cases of coordinated activities of cells inside a colony have been described. Bacterial cells can communicate with each other through auto inducer (AI) molecules which function as signaling molecules. The process of coordinating gene expression via the production, release, and sensing of AI molecules by bacteria is known as "quorum sensing." Over the past decade, new information about the different quorum-sensing systems, the types of AI molecules, the genes influenced by quorum sensing, and their role in food spoilage and safety has been obtained (Waters and Bassler, 2005; Walters and Sperandio, 2006; Lu *et al.*, 2004; Rasch *et al.*, 2005). Moreover, auto inducers have been found to reduce the lag phase and increase the exponential growth rate of milk-spoilage organisms (Dunstall *et al.*, 2005). Nevertheless, little is known about communal behavior in eukaryotic unicellular organisms.

Although ammonia was suggested to be involved in long-distance communication between yeast colonies (Palkova *et al.*, 1997), the explanation of its growth-inhibitory effect may be trivial: production of ammonia causes a dramatic increase of the pH in the adjacent region thus inhibiting the growth of the neighboring colony. Alternative chemical, and/or physical signals are to be sought and their modes of action need to be resolved as it has been investigated for bacterial populations. Quorum sensing data in yeasts are scarce and not completely understood; however, in engineered yeasts cells, it was possible to detect quorum sensing. Weiss and Chen (2005) integrated *Arabidopsis thaliana* signal synthesis and receptor components with yeast endogenous protein phosphorylation elements and new response promoters. Engineered yeast 'sender' cells synthesize the plant hormone cytokinin, which diffuses into the environment and activates a hybrid exogenous/endogenous phosphorylation signaling pathway in nearby engineered yeast 'receiver' cells (Figure 4.11).

The sender-receiver network was integrated under positive-feedback regulation, resulting in population density-dependent gene expression (*quorum sensu*) (Figure 4.12). Varon and Choder (2000) found patterns of cell organization and cell-cell interactions during colony development in starvation conditions, namely the formation of one fibril between two neighboring cells. A signaling and sensing or transport function was attributed to the observed fibrils because the fibrils and the cell walls seem to form a continuous network that connects all the cells and fibrils size (180 ± 6 50 nm) is theoretically large enough to permit the passage of macromolecules.

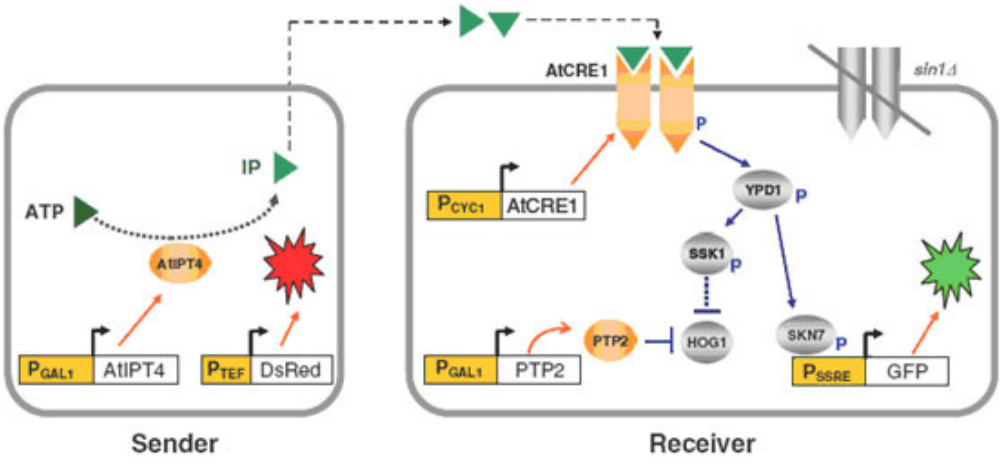

Figure 4.11: Engineered yeasts for sending and receiving cytokinin isopentenyladenine (IP) (from Weiss and Chen, 2005)

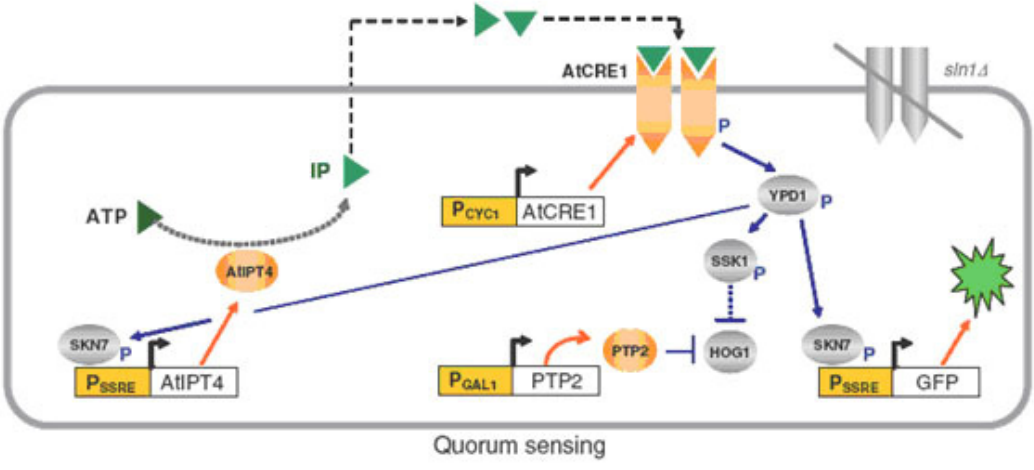

Figure 4.12: Integrated system with quorum sensing behaviour (from Weiss and Chen, 2005)

The review of the literature on this subject made clear that the reduction of the lag phase may also be related with mechanisms of cell-cell communication. Several hypotheses are herein advanced: 1) the electricity can be used by the cell as a communication

mechanism *per se*; 2) the formation of pore membranes facilitates the entrance of AI's thus activating growth; 3) the electricity stimulates the production of AI's as a consequence of electric stress; 4) the electric stress may induce mechanisms of signaling or transport such as the formation of fibrils. In the last case the mechanisms of transport might aid the passage of nutrients into the centre of the cell aggregates (flocs) where cells may experience nutrient depletion. All these hypotheses need further verification which was out of the scope of the current research.

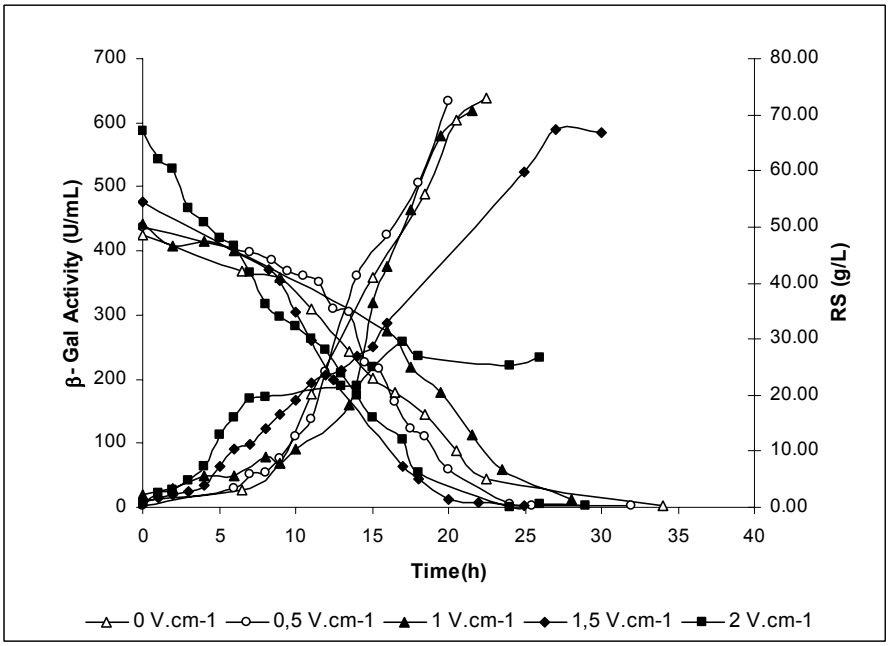

Figure 4.13: Variation of reducing sugars (RS) and β-galactosidase activity inside the bioreactor using SSLactose media (50 g/l), for the different electrical fields

The growth parameters and fermentation yields were calculated and are summarized in

Table 4.5.

The specific growth rate is significantly ($p < 0.05$) affected by the electric field, exception made for the experiments at 0.5 V/cm where it is similar ($p > 0.05$) to the control experiment. The results point out to a stimulatory effect of the electric field on growth until 1.5 V/cm and then presented a slight decrease for higher values of the electric field strength. The production of biomass, determined by the final biomass concentration within the reactor and also by the yield of biomass on substrate (Yx/s), seems to have a direct relation with the electric field and a linear relation between these parameters can be obtained (Figure 4.14). No data was found on the literature that could help explain this effect, however several mechanisms can be proposed: 1) the electric field may accelerate the cell cycle, thus increasing specific growth rate and biomass production; 2) the mass transfer limitations are reduced (e.g. via the mass transport by the fibrils) meaning that even the cells in the interior of the flocs receive nutrients and oxygen in sufficient amounts and continue to divide during the entire fermentation period.

Cell viability was monitored at the end of the fermentative process by two distinct techniques: staining and plating. The results obtained by the two methods were distinct when using an electric field and the staining method retrieved higher levels of mortality (> 40 %) when compared to the ones obtained by plating (< 20 %). This may be due to the possibility of pore formation which permit the entrance of the stain into the living cells. The results obtained when the electric field is absent and also by the plating technique were similar to the ones obtained by Domingues (2001) which reported viability levels over 80 % at the end of fermentations.

Table 4.5: Growth parameters and fermentation yields as a function of the electric field, for aerobic fermentations (P1 is ethanol and P2 is β-Gal)

	Electric field (V/cm)				
Kinetic parameters	0	0.5	1.0	1.5	2.0
μ (h^{-1})	0.158 ± 0.001	0.176 ± 0.008	0.198 ± 0.016	0.288 ± 0.003	0.264 ± 0.002
t_{lag}(h)	3.52 ± 0.06	3.47 ± 0.30	2.92 ± 0.13	1.49 ± 0.12	0.10 ± 0.01
t_D (h)	4.40 ± 0.01	3.94 ± 0.07	3.52 ± 0.13	2.41 ± 0.01	2.63± 0.01
Final biomass (g/l)	7.20 ± 0.25	10.50 ± /	12.68 ± 0.32	16.00 ± 1.81	21.30 ± 1.51
$Y_{x/s}$ ($g_{biomass}/g_{lactose}$)	0.149±0.003	0.211±/	0.251±/	0.347±0.008	0.439±0.011
$Y_{P1/s}$ ($g_{ethanol}/g_{lactose}$)	0.491± 0.009	0.493± 0.038	0.346 ±0.012	0.381± 0.023	0.322 ±0.011
$Y_{P2/s}$ ($U/g_{lactose}$)	2.16E+04±2.55 E+02	1.25E+04±3.44 E+02	1.45E+04±1.70 E+03	1.25E+04±5.4 3E+02	5.56E+03±/
$Y_{P2/x}$ ($U/g_{biomass}$)	1.45E+05±4.98 E+03	5.93E+04±1.63 E+03	5.52E+04±3.34 E+03	2.84E+04±1.1 4E+04	8.09E+03±5.7 2E+02
qs_{p1} ($g_{ethanol}/g_{lactose}.h^{-1}$)	0.077 ± 0.001	0.087 ± 0.003	0.068 ± 0.008	0.110 ± 0.008	0.085 ± 0.003
qs_{p2} ($U/g_{lactose}.h$)	2.28E+04 ± 8.86E+02	1.05E+04 ± 7.45E+02	1.09E+0 ± 2.49E+02	8.16E+03 ± 3.19E+03	2.14E+03 ± 1.64E+02

The ethanol conversion yields are higher then the ones reported by Domingues (2001) but tend to decrease with the increase of the electric field. Considering 5 % significance level, the ethanol yields are statistically equal in two groups being the first group 0 and 0.5 V/cm and the second 1.0, 1.5 and 2.0 V/cm meaning that ethanol yield is only affected when using electric fields above 0.5 V/cm.

On the contrary, β-gal conversion yields are higher than the ones obtained by Domingues (2001), however these yields also decrease with the increase of the electric field applied. Regarding enzyme yields, there are three groups of statistically different results: those for 0 V/cm, those for 0.5, 1.0 and 1.5 V/cm (which are statistically equal between them) and those for 2 V/cm. This means that the use of an electric field equal to or higher than 0.5 V/cm affects enzyme production but the increase of the field strength until 1.5 V/cm does not have significant influence on the production yields; when using higher electric fields (*e.g.* 2 V/cm) the β-gal production is again affected. The decrease of β-gal production with increasing electric fields will be discussed further ahead in the chapter (see section "Plasmid stability").

The existence of an electric field range where the enzyme production is not significantly affected may be extremely usefull for process optimization (batch operation) when aiming e.g. at maximizing productivity due to the decrease of lag phase when using higher electric fields.

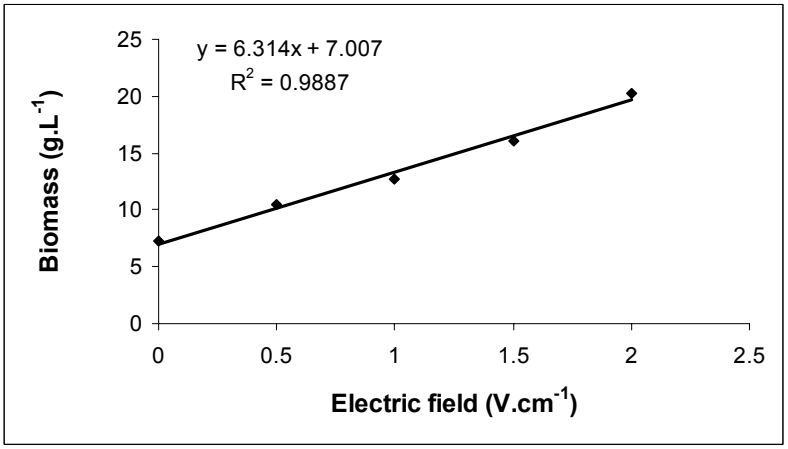

Figure 4.14: Biomass inside the bioreactor at the end of the aerobic fermentation for each electric field tested.

Considering the lactose fermentation, 4 mol of ethanol will be produced from 1 mol of lactose (Equation 4.1) and the yield as a function of the theoretical value can be calculated: using Equation 4.2.

$$C_{12}H_{22}O_{11} + H_2O \rightarrow 4C_2H_5O + CO_2 + 4ATP \qquad \textbf{(Eq. 4.1)}$$

$$\eta(\%) = \frac{Ethanol}{0.538 \times \left(Lactose_{t_0} - Lactose_t\right)} \times 100 \qquad \textbf{(Eq. 4.2)}$$

Ethanol yield as a percentage of the theoretical value was calculated and the results are displayed in Table 4.6. There is a decrease of ethanol production with the increase of the electric field; however, the obtained values are extremely promising for an industrial application of ethanol production.

Table 4.6: Percentage of the theoretic ethanol production yield, for the aerobic fermentations

Electric field (V/cm)	η (%)

0.0	91.26 ± 1.62
0.5	91.58 ± 7.07
1.0	64.27 ± 2.15
1.5	70.89 ± 4.23
2.0	59.78 ± 2.00

Although the yeasts are growing on lactose, the sugar is in fact hydrolyzed into glucose and galactose before entering the cells. Being so, the production of ethanol from lactose follows distinct pathways: glucose enters the Embden-Meyerhof-Parnas pathway followed by anaerobic reduction of piruvate to ethanol; the galactose enters the Leloir pathway where it is converted to glucose-phosphate prior to entering the Embden-Meyerhof-Parnas pathway.

The attained ethanol yields point out to a predominantly fermentative metabolism, even under aerobic conditions. However it tends to shift to a more respiratory metabolism as the electric field increases. The decrease of the ethanol yields and the significant rise in the biomass production support this hypothesis. The concentrations of galactose and glucose on the fermentation broth were monitored during the whole process and the maximum galactose concentration measured was 4.49 g/L while for glucose the maximum was 3.68 g/L, both measured when using 2 V/cm. The yeast *Saccharomyces cerevisiae* is known to display a respiratory bottleneck (Sonnleitner and Käppeli, 1986) when grown on glucose under aerobic conditions: if such bottleneck is attained, the sugar starts being fermented to ethanol in parallel with the ongoing respiratory metabolism. This explains the presence of ethanol in the medium even under aeration. However, the presence of the electric field seems to influence the metabolism resulting in an increase of the capacity of the yeast to metabolize the sugar oxidatively, this would explain the reduction in the yield of ethanol with the increase of the electric field.

3.1.2. Early and late MEF experiments

The application of a MEF during a limited time of a fermentative process may help to optimize the process either by the reduction of the lag phase either by aiding the excretion of metabolites of interest. Moreover, it can reduce some disadvantages of using a continuous electric field (*e.g.* plasmid losses in recombinant strains, which will be discuss further ahead in the chapter).

In order to make an initial assess of this issue, experiments using MEF just in the early stage of the fermentation (2.5 and 5 h after the inoculation) or exclusively in the later stages (Lactose < 10 g/l) were performed. In this section the electric field used was always of 1 V/cm.

The bioreactor operation was similar to previously described and the kinetic parameters are presented in Table 4.7 and the fermentation profile display in Figure 4.15 and Figure 4.16.

Table 4.7: Growth parameters and fermentation yields for the early and late MEF experiments using an electric field of 1 V/cm

	Early MEF 1 (V/cm)		**Late MEF 1 (V/cm)**
Kinetic Parameters	2.5 h	5.0 h	Lactose < 10 g/l
μ (h^{-1})	0.187 ±0.008	0.192 ± 0.027	0.189 ± -
t_{lag}(h)	2.66 ± 0.11	2.77 ± 0.33	3.82 ± -
t_D (h)	3.71 ± 0.15	3.65 ± 0.52	3.67 ± -
Final Biomass (g/l)	7.29 ± 0.28	7.28 ± 0.12	8.10 ± -
$Y_{x/s}$ ($g_{biomass}/g_{lactose}$)	0.146 ± 0.002	0.146 ± 0.005	0.144 ± -
$Y_{P1/s}$ ($g_{ethanol}/g_{lactose}$)	0.487±0.011	0.495±0.027	0.490± -
$Y_{P2/s}$ ($U/g_{lactose}$)	1.97E+04±2.01E+02	2.01E+4±1.85E+2	2.13E+4± -
η(%)	77.57±2.41	76.45±1.19	81.14± -

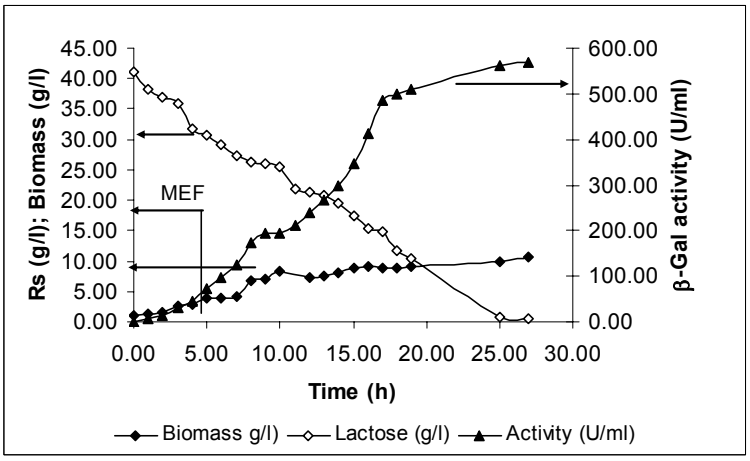

Figure 4.15: Variation of reducing sugars (RS) and biomass inside the bioreactor using late MEF of 1 V/cm during the first 5 h.

The comparison of the results obtained with early MEF and continuous MEF point out to the reduction of the lag phase (the desired effect) but increasing the production of β-gal whose yields are similar to the ones obtained when no voltage was applied. This fact is probably due to higher plasmid stability (see ahead in the chapter). As expected, no significant differences could be found between 2.5 and 5 h once the lag phase is reduced, in average, from 3.5 to 2.5 h when an electric field is present thus 2.5 h is enough time to stimulate earlier entrance of the cells in the exponential phase (shorter lag phase). The experimental data point out to potential advantageous applications of early MEF when the reduction of the lag phase is the main objective. However, it is noteworthy that these results should not be extrapolated to other strains which may be more/less sensible to "electric effects" thus need different conditions (*i.e.* electric field strength, MEF duration) to produce similar results.

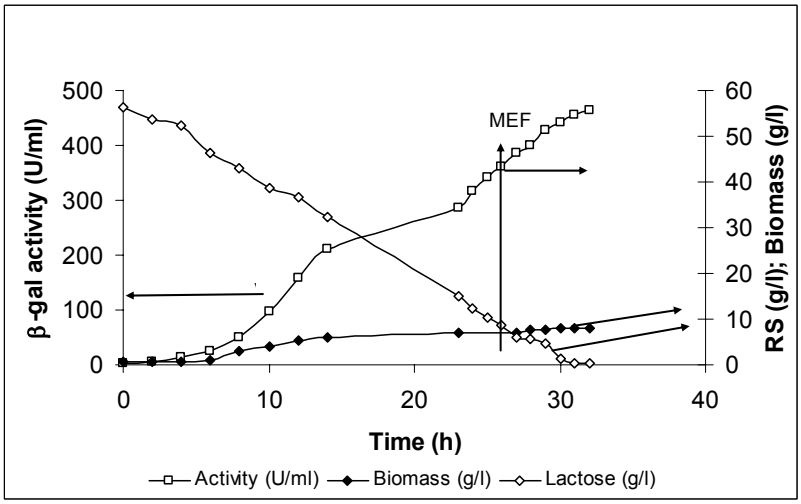

Figure 4.16: Variation of reducing sugars (RS), biomass β-Gal activity inside the bioreactor using late MEF of 1 V/cm.

Regarding the application of a late MEF (Figure 4.16) one could expect an increase of β-gal activity caused by enhanced excretion of the enzyme into the fermentation broth. The measured activity is the enzyme produced within the cells and afterward excreted into the media, thus the enzyme still remaining in the interior of the cell is not quantified. The application of an electric field could facilitate the excretion of the enzyme either by the formation of pores, permease activation or lysis induction (once the number of cells dead or more fragile increases in the late phase of a batch fermentative process) thus causing an increase in measured activity. However in the tested conditions this was not verified. These results, however, do not mean this hypothesis is not valid, just that further investigation is needed to verify it or not (e.g. using higher electric fields in the later stages of the fermentation, different time of application). Furthermore, the application of MEF in later stages may be very useful when secondary intracellular metabolites are produced thus difficult and expensive separation processes are needed to purify them.

3.2. Anaerobic fermentations

3.2.1. Continuous MEF experiments

In order to determine if the influence of the electric field is similar under aerobic and anaerobic conditions the previously described conditions were repeated in the absence of oxygen.

Figure 4.17 displays the fermentation profile for the several MEF's used in this set of experiments. In the absence of oxygen the lactose consumption is slower (time to complete consumption: approximately 35 h). Under these conditions the electric field does not seem to affect the fermentation time.

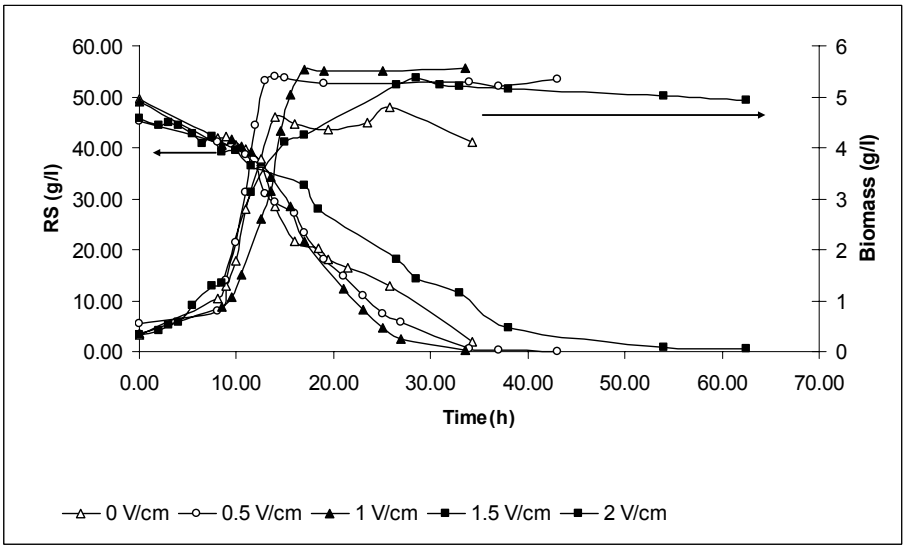

Figure 4.17: Variation of reducing sugars (RS) and biomass inside the bioreactor using SSLactose media (50 g/l), for the different electrical fields, anaerobic conditions

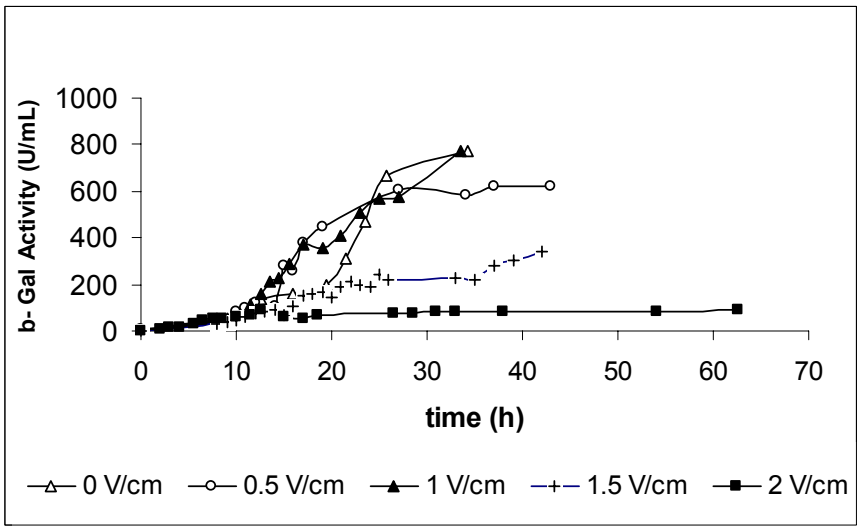

Figure 4.18: B-Gal production on the course of the anaerobic fermentations at different electric fields

The β-gal is produced mainly during the exponential phase but a detrimental effect of the increase of the electrical field is observed (Figure 4.18, Table 4.8) similarly to the one verified when oxygen was sparged into the broth. The kinetic parameters were calculated and are reported in Table 4.8. The b-gal yields from lactose and from biomass are significantly different when using MEF higher than 1.5 V/cm (inclusive). This fact is most probably related to plasmid stability as discussed further ahead in the chapter.

Table 4.8: Growth parameters and fermentation yields as a function of the electric field, for anaerobic fermentations

	Electric field (V/cm)				
Kinetic parameters	0	0.5	1.0	1.5	2.0
μ (h^{-1})	0.191 ± 0.001	0.220 ± 0.021	0.260 ± /	0.177 ± 0.011	0.168 ± 0.012
t_{lag}(h)	6.64 ± 0.32	6.55 ± 0.42	5.09 ± /	7.50 ± 0.54	6.88 ± 0.01
t_D (h)	3.62 ± 0.02	3.16 ± 0.30	2.66 ± /	3.92 ± 0.24	4.15 ± 0.30
Final biomass (g/l)	4.64 ± 0.74	5.38 ± 1.61	5.85 ± 0.94	5.62 ± 0.15	5.31 ± /
$Y_{x/s}$ ($g_{biomass}/g_{lactose}$)	0.092 ± 0.018	0.115 ± 0.042	0.119 ± 0.020	0.118 ± 0.008	0.116 ± /
$Y_{P1/s}$ ($g_{ethanol}/g_{lactose}$)	0.336 ± 0.014	0.416 ± 0.023	0.425 ± 0.049	0.462 ± 0.007	0.446 ± 0.026
$Y_{P2/s}$ ($U/g_{lactose}$)	1.24E+04 ± 4.51E+03	1.26E+04 ± 1.64E+03	1.56E+04 ± 1.04E+02	6.10E+03 ± 7.31E+02	1.47E+03 ± 5.91E+01
$Y_{P2/x}$ ($U/g_{biomass}$)	1.32E+05 ± 2.35E+04	1.15E+05 ± 2.84E+04	1.14E+05 ± 5.40E+03	2.95E+05 ± 8.76E+03	1.30E+04 ± /
qs_{p1} ($g_{ethanol}/g_{lactose}.h^{-1}$)	0.064 ± 0.002	0.092 ± 0.014	0.051 ± 0.072	0.082 ± 0.006	0.075 ± 0.010
qs_{p2} ($U/g_{lactose}.h$)	2.53E+04 ± 4.35E+03	2.57E+04 ± 8.65E+03	3.07E+04 ± 2.17E+04	5.23E+04 ± 4.80E+03	2.29E+03 ± /

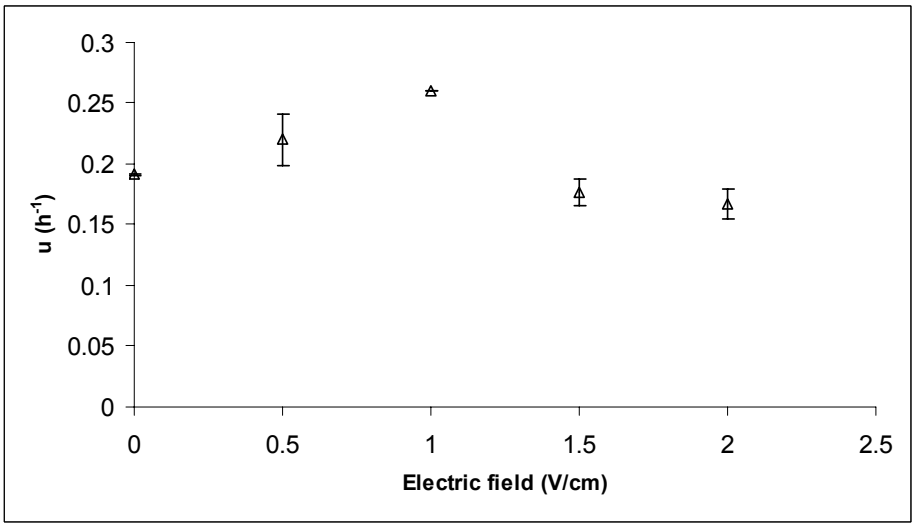

Figure 4.19: Specific growth rate as a function of the electric field for anaerobic fermentations

Regarding the specific growth rate (Figure 4.19) significant differences ($p < 0.05$) were only found for 1 V/cm which corresponds to the case where the yeast presents the highest growth rate. The length of the lag phase seems to show no significant differences ($p > 0.05$) between the fermentations performed under different electric field strength values (lag phase duration was of approximately 7 h). A reduction of the lag phase (Figure 4.20) similar to the one obtained for aerobic conditions might be expected but these results may lead to discard some of the hypotheses previously raised. The transport phenomena associated with improved mass transfer properties or pore formation accelerating nutrient transport into the cells should be similar under both situations. However the effect on membrane enzymes, namely on permease activity may be different or dependent on the oxgygen concentration. Although no stimulatory effect of moderate electric fields on enzymes activity was reported until now, MEF may affect enzyme activity as reported by Castro *et al.* (2004). Also as discussed in Chapter 2, MEF may influence transport mechanisms into the living cells. Advancing that the reduction of the lag phase was due to an effect on the membrane transport proteins the only variable is the electric current that is passing through the media. When oxygen is bubbled into the bioreactor the air bubbles act as insulators thus current does not pass through as easily in their vicinity. This environment may cause zones having different (higher) electric conductivity within the bioreactor because the current will flow through the more conductive areas. In fact, there is minimum current that will interfere with the enzyme activity which might not have been attained in the anaerobic experiments. This effect (zones with higher current passing through) might help to explain some of the differences observed once the increase of the electric field causes the reduction of the lag

phase. A new set of experiments using higher MEF's should be performed to verify this hypothesis.

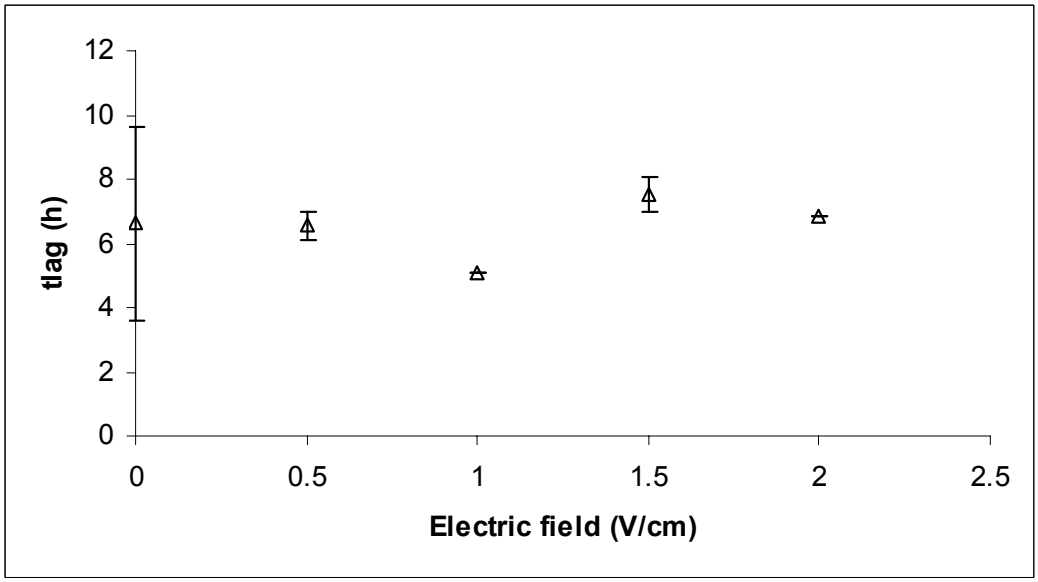

Figure 4.20: Relation between the lag phase duration and the electric field applied in the anaerobic fermentations

Furthermore, cell-cell communication namely the production of auto-inducers cannot be compared under different environmental conditions because the formation of these molecules is considered to be an adaptative response of the microbes to environment (Pillai and Jesudhasan, 2006). No references were found on the literature regarding stimulatory or inhibitory effect of oxygen concerning the production of AI's.

When analyzing the biomass production yields no statistically significant differences ($p < 0.05$) were found for this set of experiments. As expected (fermentative metabolism - Figure 4.21 - is usually predominant under anaerobic fermentations) the obtained biomass yields are considerably lower than those obtained under aerobic conditions, being the differences between two (at 0 and 0.5 V/cm) to four fold (at 2 V/cm).

The ethanol yied as a percentage of the theoretical value was determined and the results are presented in Table 4.9. The only statistically significant difference ($p < 0.05$) was observed for the control fermentation (0 V/cm) being the other values statistically equal denoting that there is no relevant effect of the electric field under these conditions.

Table 4.9: Percentage of the theoretical ethanol production yield obtained for the anaerobic fermentations

Electric field (V/cm)	η (%)
0.0	62.43± 2.69
0.5	77.32 ± 4.28
1.0	79.00 ± 9.19
1.5	85.90 ± 1.28
2.0	82.89 ± 4.84

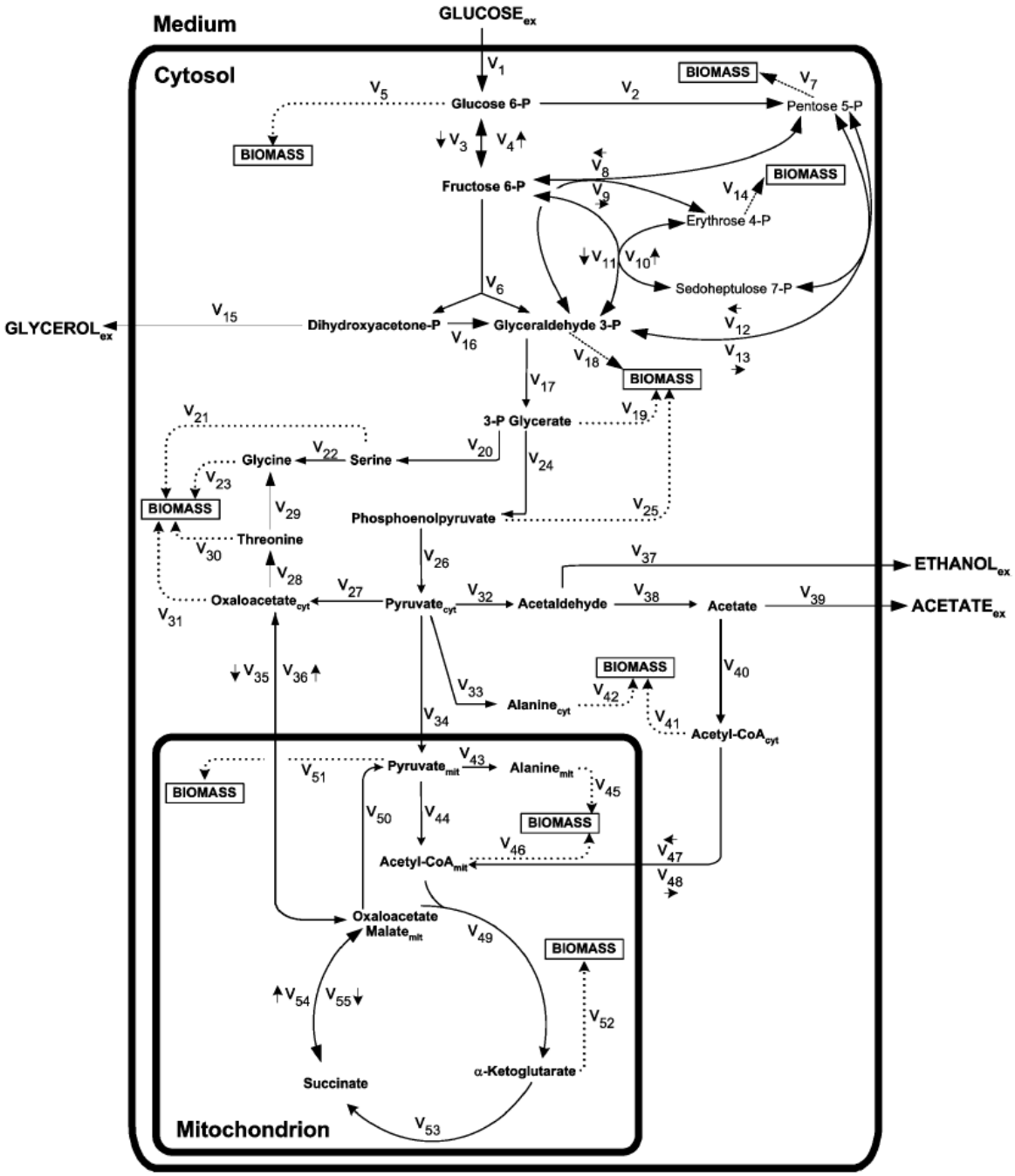

Figure 4.21: Metabolic network of the central cytosolic and mitochondrial metabolism of *S. cerevisiae*; the network comprises glycolysis, pentose phosphate pathway, anaplerotic carboxylation, fermentative pathways, inter-compartmental transport of acetyl-CoA, pyruvate, and oxaloacetate, respectively, TCA cycle, malic enzyme and anabolic reactions from intermediary metabolites into anabolism.

3.2.2. Addition of Ethanol to the fermentation broth

Ethanol is the major product of yeast sugar fermentation and yet, at certain concentrations, it is very toxic to yeast cells. The major targets for ethanol's toxicity are the plasma membrane and the cytosolic enzymes: ethanol alters membrane organization and permeability and inactivates and unfolds globular cytosolic enzymes (Lopes, Sola-Penna, 2001).

Moderate electric fields have also been reported to affect membrane permeability (Loghavi, 2005, Cho *et al.* 1996). Being so, it was relevant to test if ethanol has enhanced toxicity to the yeast cells when a moderate electric field is present during the course of the fermentation. A control was made using fermentation broth with additional 25 g/L of ethanol and the experiment was performed turning on a MEF of 1 V/cm.

A typical fermentation profile is presented in Figure 4.22

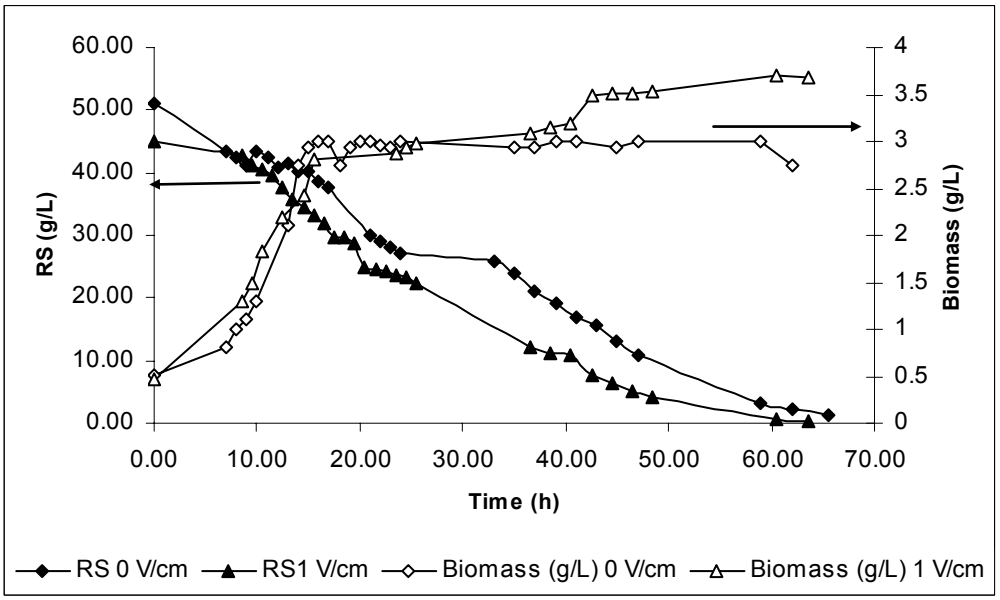

Figure 4.22: Variation of reducing sugars (RS) and biomass inside the bioreactor using SSLactose + Ethanol, with or without MEF

The lactose takes a considerably longer time to be consumed by the yeasts when ethanol is added to the media if compared to the same conditions without the addition of this compound. In fact, analyzing Figure 4.22 lactose complete metabolization takes more than 60 h which represents an increase in the fermentation time of over 50%, demonstrating the toxic effect of ethanol. Under such conditions, the growth rate (Table 4.10) significantly ($p < 0.05$) decreases even further when voltage is turned on. On the other hand, although in the

previously studied anaerobic conditions (whithout the addition of ethanol) there was no clear effect on the lag phase when an electric field was applied, in this case (when ethanol is added) a reduction of the lag phase was observed (Figure 4.24). In fact, the lag phase length is reduced to values identical to the ones obtained in the anaerobic fermentation where no ethanol was added. Probably the MEF induces pore formation accelerating the entrance of both nutrients and ethanol into the cell; the hypothesis raised here is that the effect of nutrient assimilation counterbalances the toxicity of ethanol in the early stages of the process (lag phase) but not when cells enter in the exponential growth phase. Interference of the electric field with membrane integrity and enzyme activity may be at stake here, but this is yet to be proven.

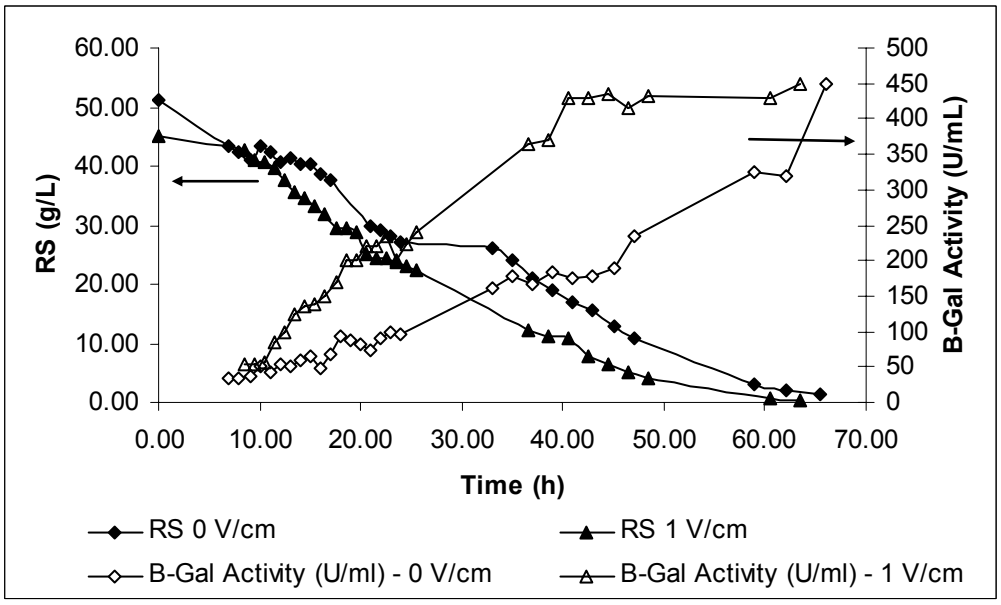

Figure 4.23: Variation of reducing sugars (RS) and β-galactosidase activity inside the bioreactor using SSLactose + Ethanol, with or without MEF.

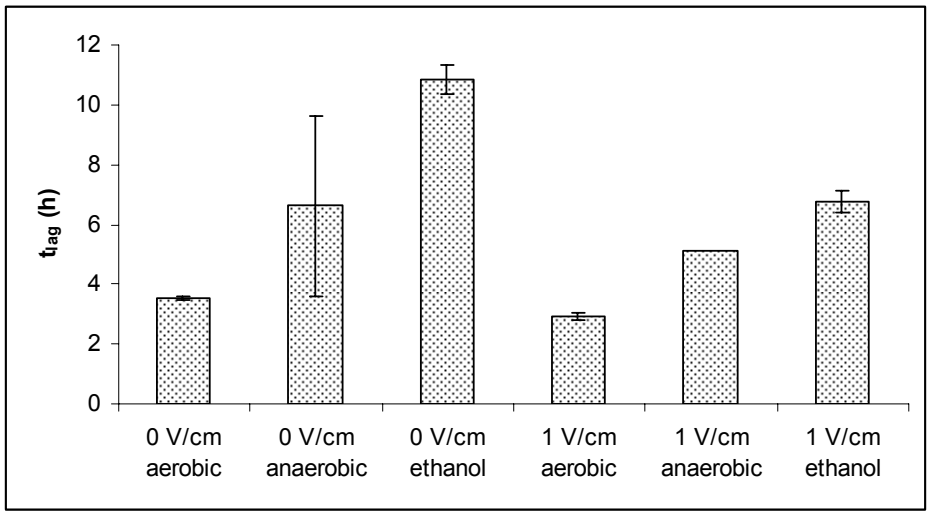

Figure 4.24: Effect of ethanol and electric field on the lag phase duration.

Table 4.10: Growth parameters and fermentation yields as a function of the electric field, for anaerobic fermentations with added ethanol

	Electric field (V/cm)	
Kinetic Parameters	0	1.0
μ (h^{-1})	0.141 ±0.021	0.073 ± 0.005
t_{lag}(h)	10.5 ± 0.49	6.75 ± 0.35
t_D (h)	4.96 ± 0.72	9.58 ± 0.67
Final Biomass (g/l)	2.46 ± 0.50	3.89 ± 0.07
$Y_{x/s}$ ($g_{biomass}/g_{lactose}$)	0.046±0.018	0.106±0.042
$Y_{P1/s}$ ($g_{ethanol}/g_{lactose}$)	0.317±0.026	0.278±0.003
$Y_{P2/s}$ (U/$g_{lactose}$)	7.63E+03±6.90E+02	7.67E+03±1.60E+03
$Y_{P2/x}$ (U/$g_{biomass}$)	1.67E+05±9.61E+03	9.65E+04±2.66E+04
η(%)	59.04 ± 4.82	51.71 ± 0.60

The ethanol production is significantly lower in the presence of an electric field and this decrease in accompanied by a raise in the biomass yield. These results point out to an

oxidative metabolism instead of a fermentative one suggesting that electric field may affect some enzymes of the fermentative pathways thus reinforcing the oxidative pathway were less ethanol and higher biomass levels are produced. This does not exclude, however, the possibility of the electrode replacing O_2 as the acceptor of electrons in the oxidative metabolism. Such hypotheses must be further investigated.

3.3. Effects on flocculation

Flocculation of yeast cells is of great importance in brewery and several other industrial processes (Stewart, 1975). Its mechanism is not yet completely understood and is still the subject of some controversy. Flocculation is a very complex process which depends on numerous factors: the yeast strain (genetics, physiological state, and metabolism), the composition of the culture medium, and the culture conditions (temperature, agitation and aeration). The involvement of all of these parameters in the flocculation process makes it very difficult to compare different studies and may thus explain the many conflicting data found in the literature. Cell flocculation can be controlled by specific (molecular recognition) and non-specific (double-layer interactions, Van der Waals forces, hydrophobic interactions, salt bridges, and steric (repulsion)) interactions. The most generally accepted mechanism is one mediated by lectins, which recognize mannan receptors on adjacent cells and require the presence of calcium (Figure 4.26) (Kihn *et al*., 1988; Masy *et al*., 1991,1992;33–Miki *et al*., 1982, Moradas-Ferreira *et al*., 1994, Stratford and Assinder. 1991). Van Hamersveld *et al.* (1994) found that the net interaction energy of flocculated brewer's yeast was much higher than could be expected on the basis of non-specific (van der Waals and electrostatic) interactions only. However, the involvement of a molecular recognition mechanism does not mean that non-specific interactions are negligible: the specific binding can be revealed only if there is a non-specific repulsion (Bell, 1988). The importance of physicochemical properties which are responsible for non-specific interactions has been investigated for brewer's yeast. Van Haecht *et al.* (1982) found a correlation between the isoelectric point of yeast cells and the N/P concentration ratio measured at the surface by X-ray photoelectron spectroscopy (XPS). Amory *et al.* (1988) reported that the influence of the culture conditions on the tendency of the cells to flocculate was related to the variation of the surface electrical properties.

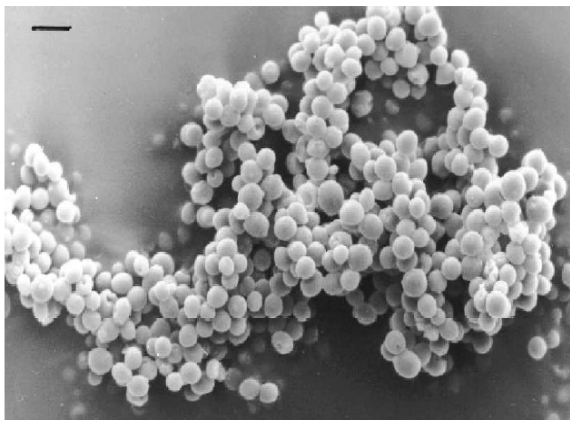

Figure 4.25: Flocculating cells of *S. cerevisiae* NCYC869-A3/pVK1.1 observed in SEM (Domingues *et al.*, 2000)

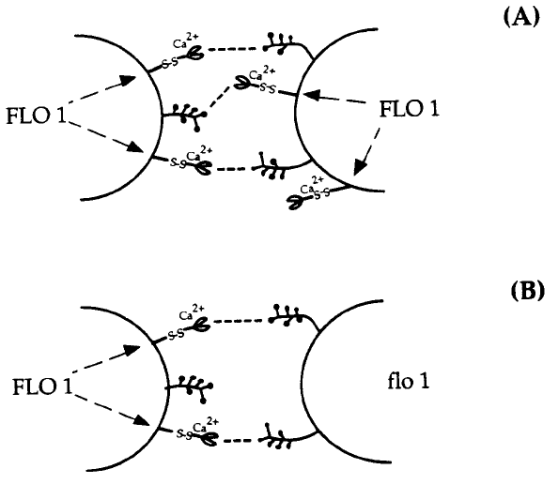

Figure 4.26: Schematic repreentation of the flocculating theory mechanism of lecticin interactions (Miki *et al.*, 1982); A – Interaction between two flocullating cells; B – Interaction between one flocculating and one non-flocculating cell.

The main objective of this part of the work was to assess the influence of moderate electric fields in the flocculation capacity of the studied yeast strain (Figure 4.25, Figure 4.26). This is of prime importance because the flocculation capacity largely determines whether the strain can be used in a continuous process (using high dilution rates for improved productivity) or not.

The results of sedimentation tests, performed at the end of each fermentation (reducing sugars concentration < 1 g/l), are presented in Figure 4.27. The results obtained for aerobic and anaerobic conditions are identical.

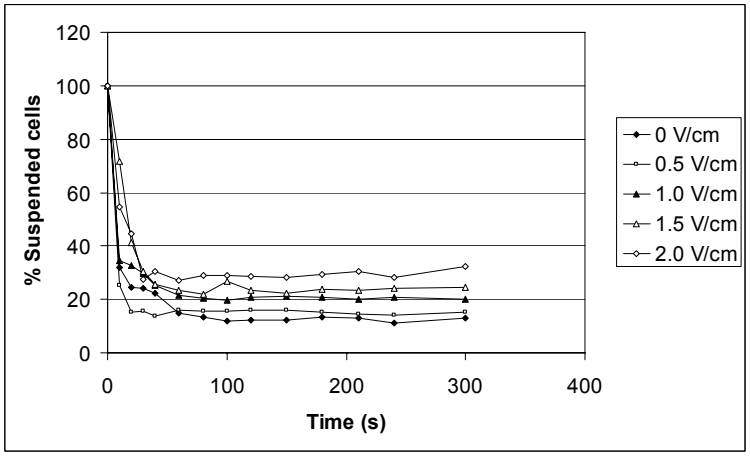

Figure 4.27: Flocculation profiles of the recombinant strain, at the end of the fermentation, when subjected to different electric fields, under aerobic conditions

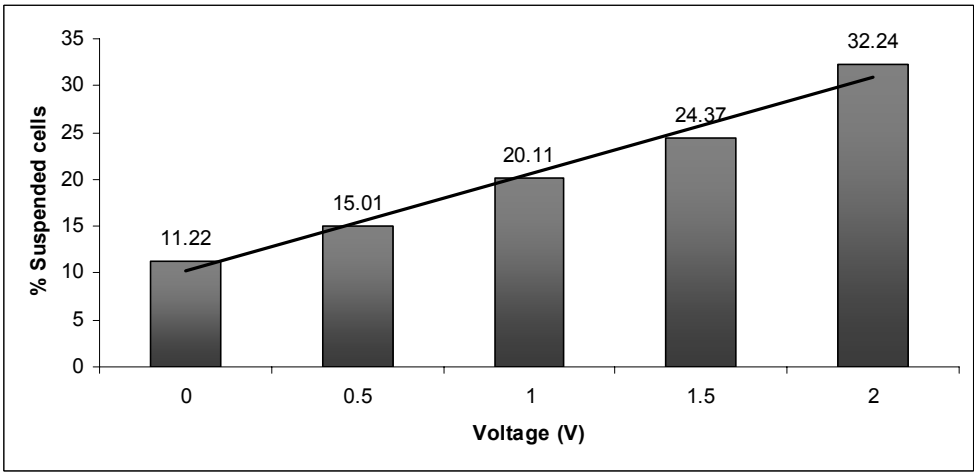

Figure 4.28: Percentage of suspended cells at the end of the fermentation, as a function of the applied electric field, under aerobic conditions (r^2 = 0.98)

The results clearly show that the increase of the electric field in the studied range (0-2 V/cm) decreases the flocculation capacity of the strain in approximately 20 %. In general, the decrease varies linearly with the increase of the electric field (r^2 > 0.98) in the range studied. The results seem to indicate that the use of higher electrical fields will favor deflocculation (Figure 4.28, Figure 4.29).

The influence of the electrical field should be expected because it may change the cell-cell electrical repulsion and it influences ionic movement thus having a direct impact on the formation of flocs.

Moreover, the electrical field may induce some conformational changes in the lectins and also help to create micro-environments around the cells or flocs, related to pH, electrical properties, ionic strength and organic solvents concentration (e.g. ethanol) which are all described as factors that influence the flocculation mechanism, as previously mentioned.

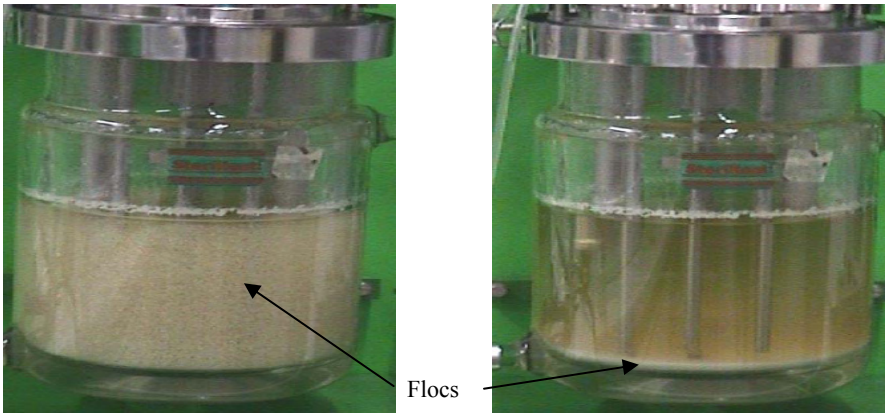

Figure 4.29: Flocs immediately after air and agitation are turned off (left) and after 5 min (right), 2 V/cm

Shimada and Shimahara (1985) reported that *E. coli* cells exposed to an alternating electric current (AC) of 50 Hz at a current density of 600 mA/cm^2 required a higher concentration of a cationic flocculant, poly (methacryloxyethyl-trimethyl-ammonium chloride), to form cell flocs than unexposed cells and also this need increases with exposure time. Furthermore, the electrophoretic mobility of the cells increased after AC-exposure. The author attributed these results to changes in the surface charge of the cells, namely enhancement of the negative charge on cell surface after AC-exposure.

3.4. Effects on plasmid stability

Plasmid stability is a major concern in industrial cultures using recombinant microorganisms to produce heterologous proteins. Segregational instability during cell division and changes in the plasmid structure, such as deletion, insertion, and rearrangement, are the main causes of plasmid instability.

Considering the use of a recombinant strain (transformed with a non integrative plasmid) this is one of the important issues to be addressed.

This strain was transformed with a 2 μm based plasmid (pVK1) which is a native plasmid present in several *Saccharomyces* strains in a number of 30-100 copies per cell (high copy number). The modified plasmids have, in general, lower stability then the original 2 μm but they are the most frequently used in yeast transformation (Futcher e Cox, 1984; Ludwig e Bruschi, 1991). The plasmid stability is defined as the number (or percentage) of cells containing the plasmid after several generations.

When the plasmid is lost the yeast is incapable of metabolizing lactose (the only existing carbon source) thus growth is affected and viability is lost.

The stability was only determined at the end of each fermentation and the results are shown in Table 4.11

The values obtained in the absence of the electric field are in accordance with the ones presented by Domingues *et al.* (2004) which reported, for the same yeast strain, when using a similar experimental setup and culture conditions, a plasmid stability of approximately 70 % under aerobic conditions and slightly less (68 %) when oxygen was absent.

Table 4.11: Plasmid stability as a function of electric field

Electric field (V/cm)	% Plasmid stability under aerobic conditions	% Plasmid stability under anaerobic conditions
0	72.00 ± 4.24	60.00 ± 2.83
0.5	57.10 ± 2.32	51.00 ± 2.83
1.0	40.24 ± 1.41	44.42 ± 2.00
1.5	31.07 ± 1.82	40.12 ± 3.46
2.0	31.43 ± 0.91	39.20 ± -
Early MEF 2.5 h	69.02 ± 2.23	-
Early MEF 5.0 h	63.15 ± 5.47	-
Late MEF	71.02 ± 3.18	-

However, it can be clearly concluded that the increase of electric field causes a significant decrease in stability. In the experiments performed under aerobic conditions the stability decreased more sharply (60 %) than in the experiments performed under anaerobic experiments (< 35 % decrease). Furthermore, a second-order model can be applied to both cases, as can be seen in Figure 4.30 and Figure 4.31.

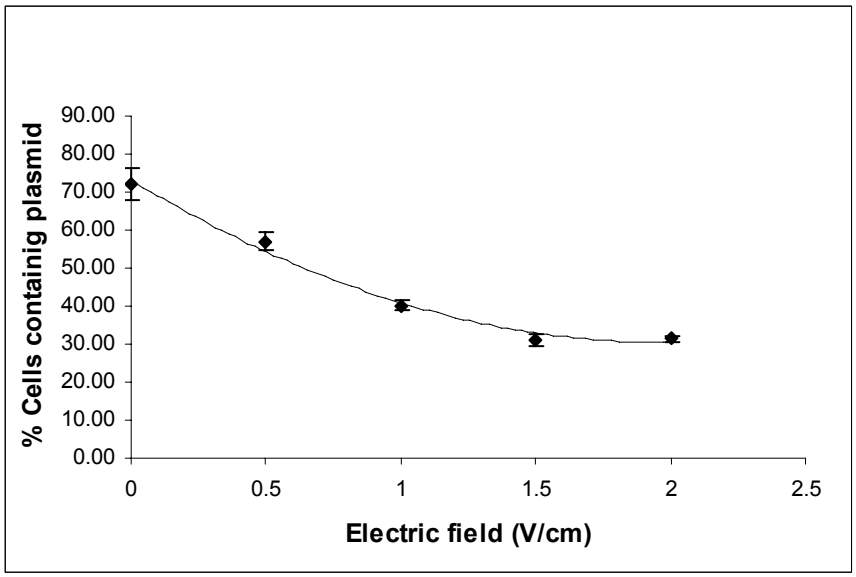

Figure 4.30: Plasmid stability as a function of the electric field for aerobic conditions

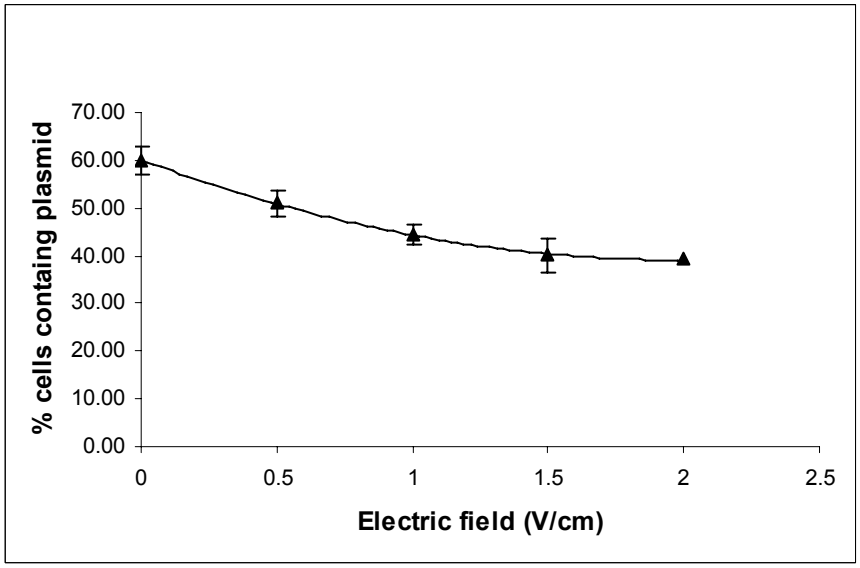

Figure 4.31: Plasmid stability as a function of the electric field for anaerobic conditions

Araújo *et al.* (2004) reported that the presence of an electric field in batch *S. cerevisiae* cultures induces electrochemical stress in the cells and affects the cellular cycle, cell size and also cell division synchrony. These results are in line with the ones obtained in this research regarding plasmid stability. Herein it is hypothesized that changes in the cell cycle and division, namely membrane instability and more fluidity of the lipid bi-layer, due to electrical interferences at the cellular micro-environment, contribute to an increased plasmid loss.

3.5. Characterization of the excreted enzyme

The enzyme applications largely depend on their characteristics in terms of stability over a wide range of temperatures, optimal activity temperature and pH. This particular enzyme was produced by a recombinant strain and excreted to the fermentation broth where it was subjected to moderate electric fields of intensities ranging from 0 (control) to 2 V/cm, applied continuously through all the fermentation time or just partially (during a few hours).

In order to verify if the electrical field influences the temperature and pH needed for optimal enzyme activity, both temperature and pH profiles were determined. A temperature range of 30 to 100 ºC was used and pH was varied from 3.5 to 6.0. The results obtained are presented in Figure 4.32 to Figure 4.39.

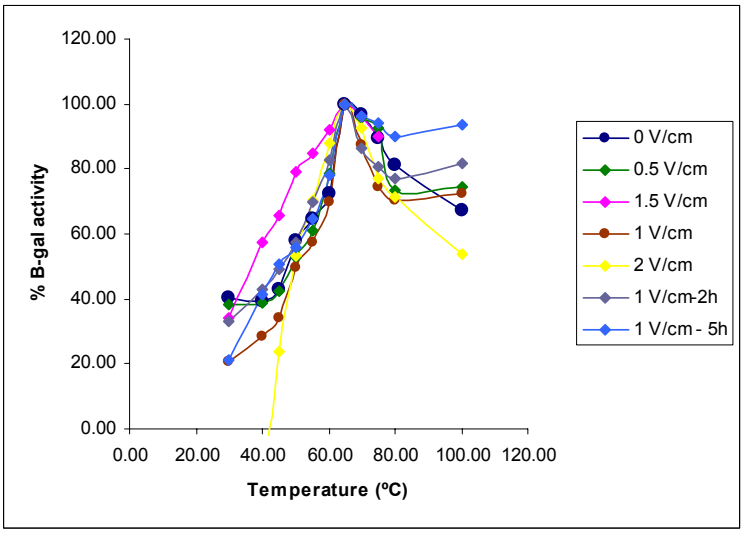

Figure 4.32: Temperature profile of the activity of the excreted enzyme when different electric fields were used under aerobic conditions.

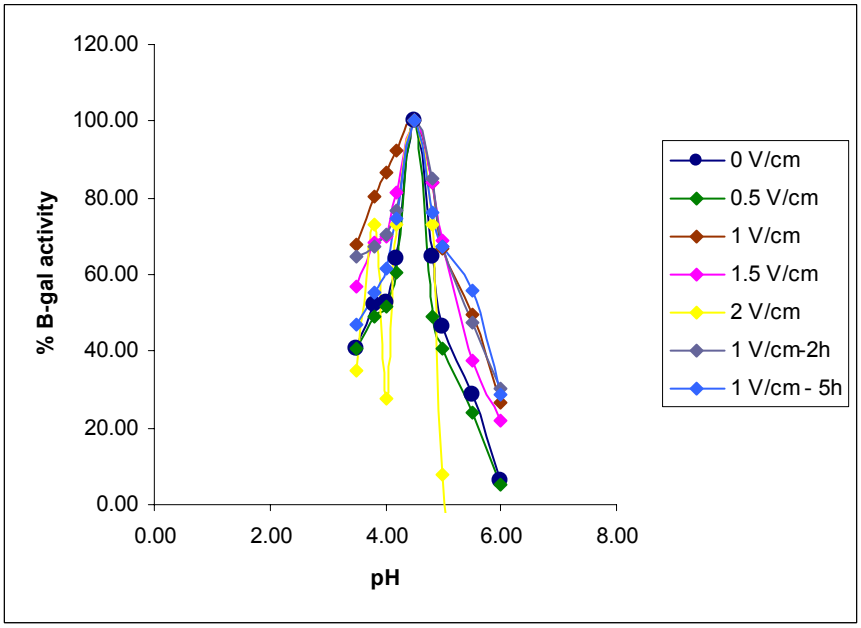

Figure 4.33: pH profile of the activity of the excreted enzyme when different electric fields were used under aerobic conditions.

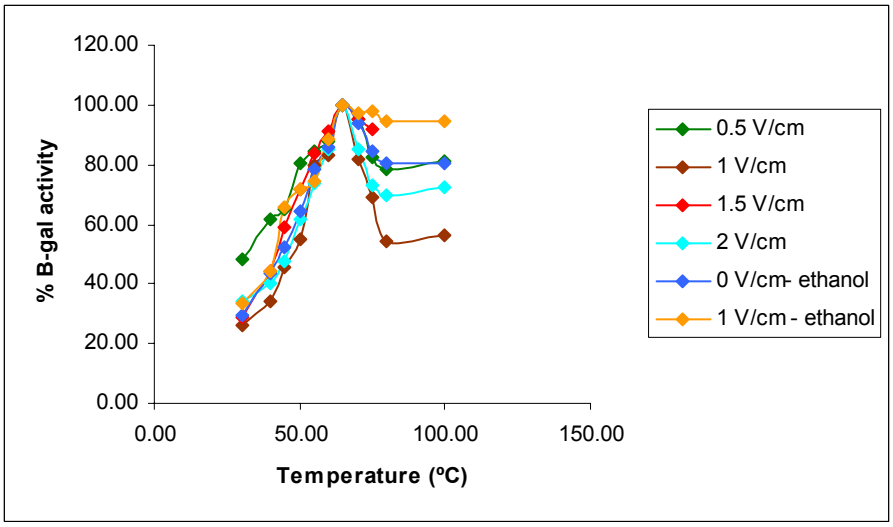

Figure 4.34: Temperature profile of the activity of the excreted enzyme when different electric fields were used under anaerobic conditions.

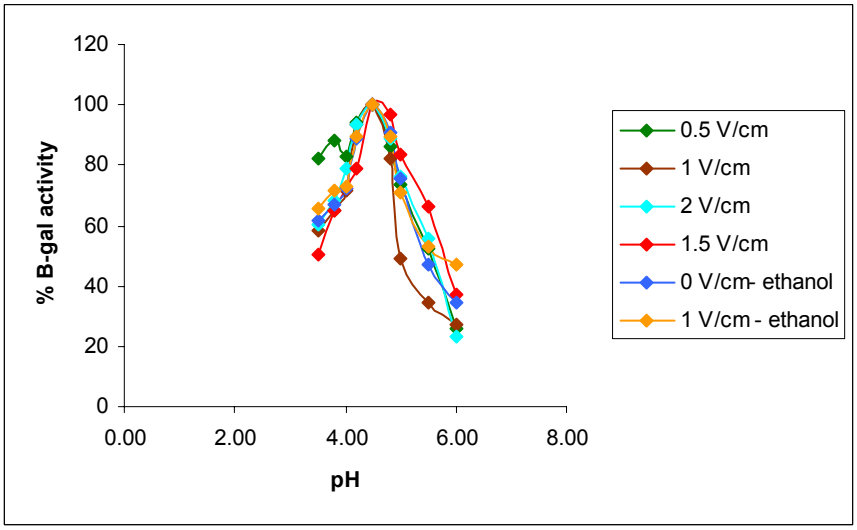

Figure 4.35: pH profile of the activity of the excreted enzyme when different electric fields were used under anaerobic conditions.

In both cases (aerobic and anaerobic) the profile for activity of the excreted enzyme is not affected by the presence of a continuous MEF. The analyses of the above figures evidences a maximum activity for 65 ºC and pH 4.5. These data is in accordance with the one reported by Domingues (2001) and also the values from the original enzyme produced by *A. niger* (Kumar, 1988) (

Table 4.12). Furthermore, it was reported by Castro *et al.* (2004) that MEF did not influence the inactivation kinetics of this enzyme.

Table 4.12: Possible sources of β-galactosidase and characterization of the produced enzyme

Microorganism	Optimal pH	Optimal temperature (ºC)
Aspergillus niger	3.0-4.0	55-60
Aspergillus orzyae	5.0	50-55
Kluyveromyces fragilis	6.6	37
Kluyveromyces lactis	6.9-7.3	35
Escherichia coli	7.2	40
Bacillus circulans	6.0	60-65
Bacillus sp	6.8	65
Lactobacillus bulgaricus	7.0	42-45
Lactobacillus thermophilus	6.2-7.1	55-57
Streptococcus thermophilus	6,5-7,5	55
Mucor pucillus	4,5-6,0	60
Thermus aquaticus	4.5 – 5.5	80
Saccharomyces cerevisiae NCYC869-A3/pVK1.1	4.0-4.5	65 ºC
Saccharomyces cerevisiae NCYC869-A3/pVK1.1 – using MEF	4.0-4.5	65 ºC

Regarding thermostability (Figure 4.36, Figure 4.37) the excreted enzyme is also not affected by the electric field present during the fermentative process and no differences were found at any temperature. When maintained at 30 or even 40 ºC the enzyme keeps more than 80% of the initial activity for 20 h. At higher temperatures, 65 and 80 ºC, the enzyme is obviously less stable and 90 % of its activity is lost after 10 h and 4 min, respectively.

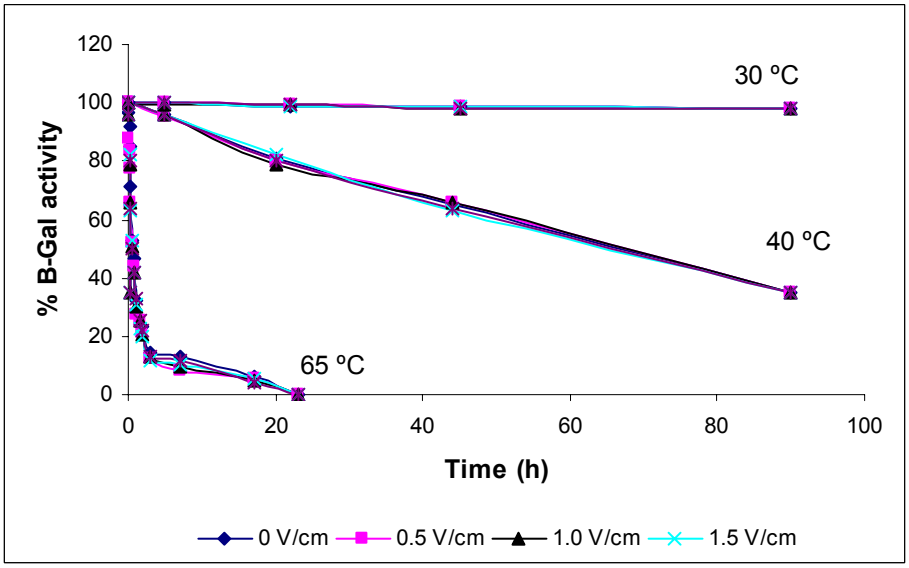

Figure 4.36: Thermostability of the β-gal excreted during the ohmically assisted fermentations, at different temperatures

When considering stability at different pH values, once again, the electric field applied during the fermentative process for the production of the enzyme apparently does not induce significant changes (Figure 4.38) and the results obtained are in line with the ones reported by Domingues (2001). It should be stressed that the enzyme is more stable at lower pH values (3.5 to 4.5) and can, therefore, be used in acid products. This is of extreme importance because acid environments prevent microbial contamination thus are often used in the food industry to help assuring food safety.

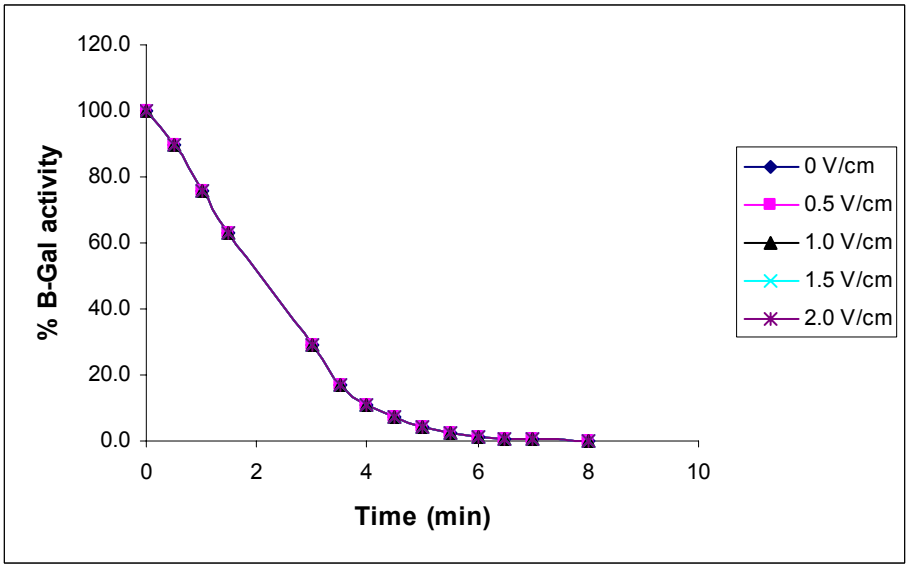

Figure 4.37: Thermostability of the β-gal excreted during the ohmically assisted fermentations, at 80 ºC

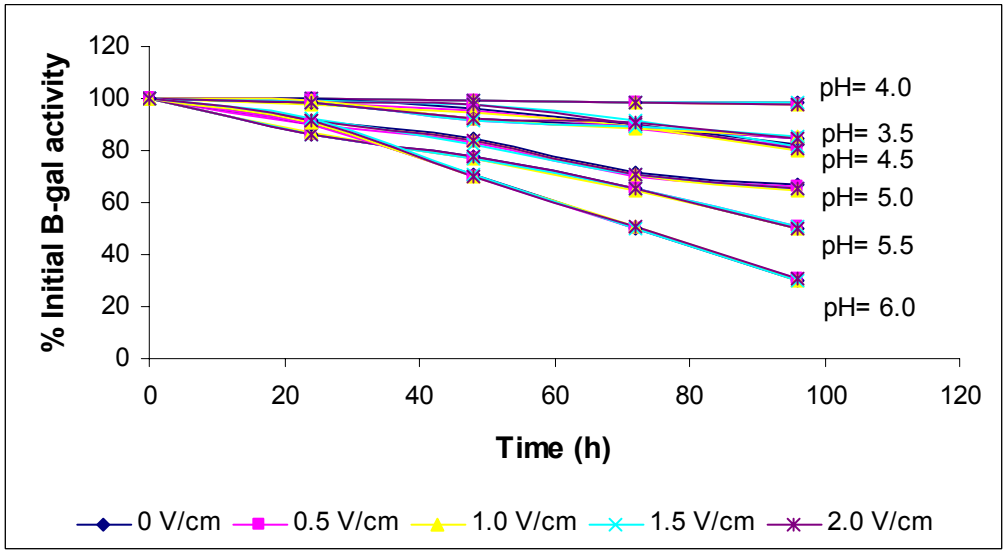

Figure 4.38: Stability of the enzyme when maintained at different pH values

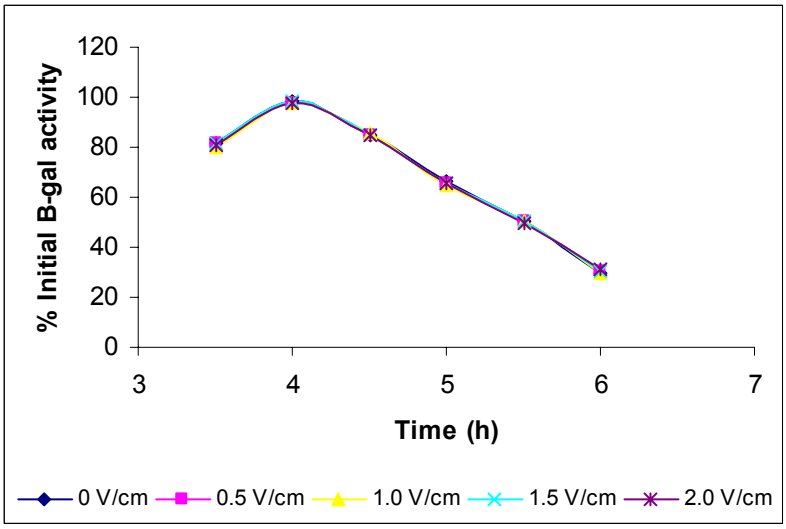

Figure 4.39: pH profile of β-gal as a function of the electric field applied during the fermentative process, after 96h

The pH profile (optimal pH) doe not shift when the enzyme is exposed to an electric field (Figure 4.39) thus maintains its advantageous properties for industrial used are not altered if an electric field is applied.

In conclusion, the presence of a moderate electric field (up to 2 V/cm) during the fermentative process does not affect the excreted b-gal neither in terms of activity, thermal stability or pH stability. These observations reinforce the conclusion that the loss of activity, when using higher electric fields, is mainly due to the loss of plasmid by the recombinant yeast and not to changes occurring in the enzyme.

4. Conclusions

The fermentation evolution, namely biomass growth, can be estimated by the measurement of the electrical conductivity as it is shown in Figure 4.40. In fact when biomass is in the exponential growth phase the addition of ammonia solution to the medium in order to control the pH value increases the medium electrical conductivity. Cho *et al.* (1996) drawn similar conclusions and reported the possibility of fermentations' monitoring by electrical conductivity measurements.

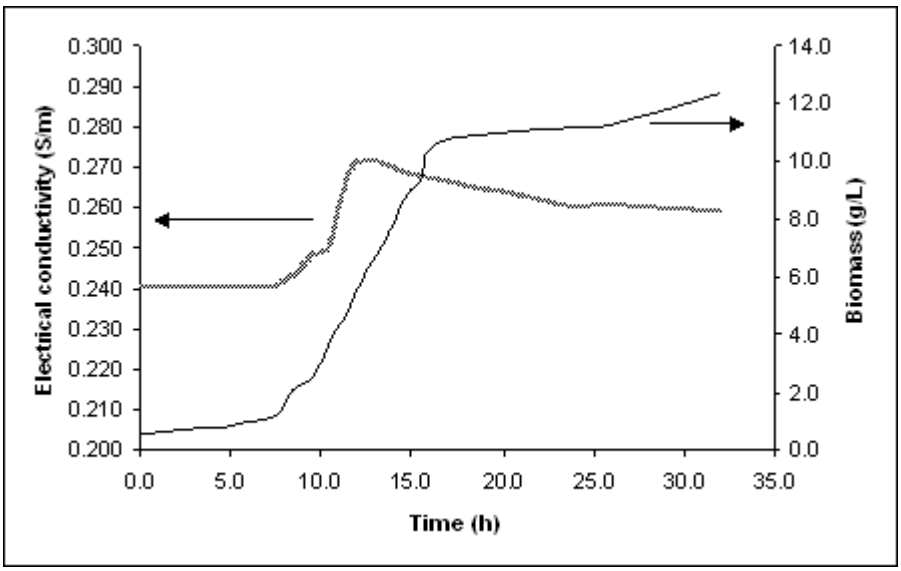

Figure 4.40: Electrical conductivity profile during the aerobic fermentation using 0.5 V/cm

Comparing the values of the obtained ethanol yields (Figure 4.41) it is clear that aerobic (O_2 concentration above 20 %) conditions using low electric fields (0.5 and 1.0 V/cm) are the most favorable for its production. On the contrary, if the biomass is the desired main product high electric fields (1.5 and 2.0 V/cm should be used. The absence of oxygen is not favorable in any case.

The results also showed that the lag phase of the fermentation, especially under aerobic conditions, can be reduced in more 50% when using an electric field (Figure 4.10). The results were similar when the electric field was only applied in the early stages of the fermentation (2.5 and 5 h). Being so, industrially the start-up time of fermentations can be reduced thus increasing annual productivity.

The use of continuous electric fields led to significant losses in plasmid stability and, consequently, to lower level of β-gal production. However, if the electric field is only

applied in the early stages of the process it was possible to reduce the lag phase without affecting plasmid stability. This results reinforces the potential advantages of using a MEF only in the beginning of the process (for recombinant strains).

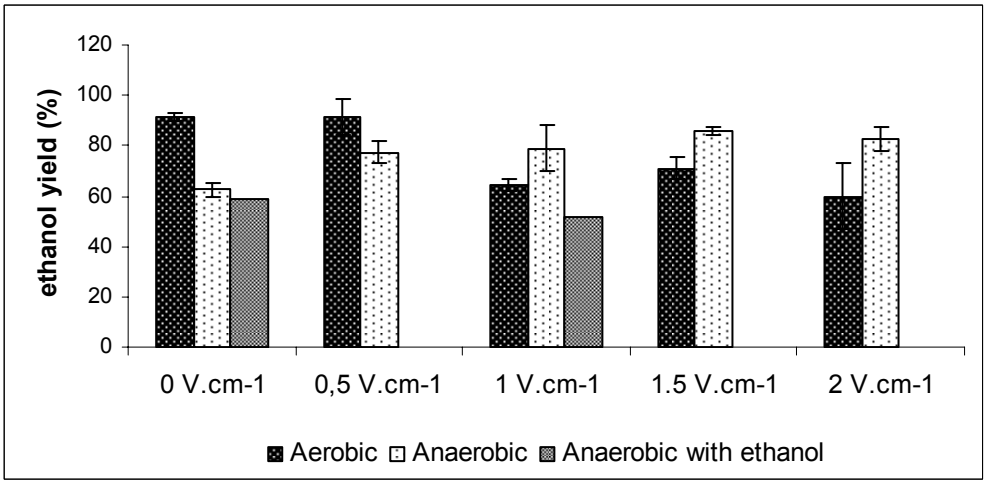

Figure 4.41: Comparison of ethanol yield as a function of theoretical yield for the several experimental assays

Furthermore, the electric field does not seem to affect flocculation of the cells thus it won't jeopardize the application of this technique to continuous fermentations.

However, although in the case under study this was not verified, it is important to assess the effect of the electric field on the desired metabolites (proteins, enzymes, aromatic compounds) because its application can have detrimental effects (see chapter 2 were effects on enzymes were shown).

Depending on the specific application, environmental conditions and microorganisms used the use of MEF must be optimized in terms of strength and length and also frequency and waveform (which were reported to affect growth on some strains – Loghavi, 2006).

Further research is needed to achieve a deeper understanding of the "electric effect" and clarify a number of issues raised during the chapter.

5. Future challenges: Using an electric field to assist fermentative processes

Biotechnology is a multidisciplinary field, which is in reality the networking of biological sciences with engineering principles. It has potential impact on virtually all domains of human welfare, ranging from food/feed processing, energy and environmental protection, to human health. In recent years, advances in fermentation technology have shown much promise in the development of several bioprocesses and products. Moreover, the use of fermentation technology for the production of new functional foods or ingredients (e.g. in soybean fermentation for manufacture of soy sauce several bioactive peptides are produced with anti-cancer and anti-thrombotic properties) challenges the food technologists to innovate. One of the possible innovations is the use of moderate electric fields during the fermentative process or, at least, during a part of the process.

As previously mentioned the available information on this subject is scarce reasoning the need to further investigate the possible applications of ohmically assisted fermentations. The potential application to bacteria, yeast and fungi must be explored considering physiological, economical and environmental factors. It is noteworthy that the application of this technique to recombinant microorganisms should not be forgotten considering their predominance in the pharmaceutical and food sectors.

In fact, some of the topics to conduct research on are:

- Evaluation of physiological functions and health benefit mechanisms of new/different metabolites obtained during fermentation processes
- Address the effects on cell-cell communication and growth
- Evaluation of safety for fermented products, using this new feature of fermentation technology
- Optimization of electric field intensity, frequency and waveform
- Optimization of the period and duration of electric field application (continuous, early stages of fermentation, late stages, pulsed)
- Design of innovative bioreactors with optimized electric field distribution (homogeneous)
- Use of electric field to aid separation processes for product recovery – this is of particular importance because often the optimal conditions for growth make the separation of final product a hard task. The use of moderate electric

fields was reported to have promising results when working at sub-optimal conditions, thus it may help achieving a good compromise between optimal growth and optimal separation process (or minimization of by-products).

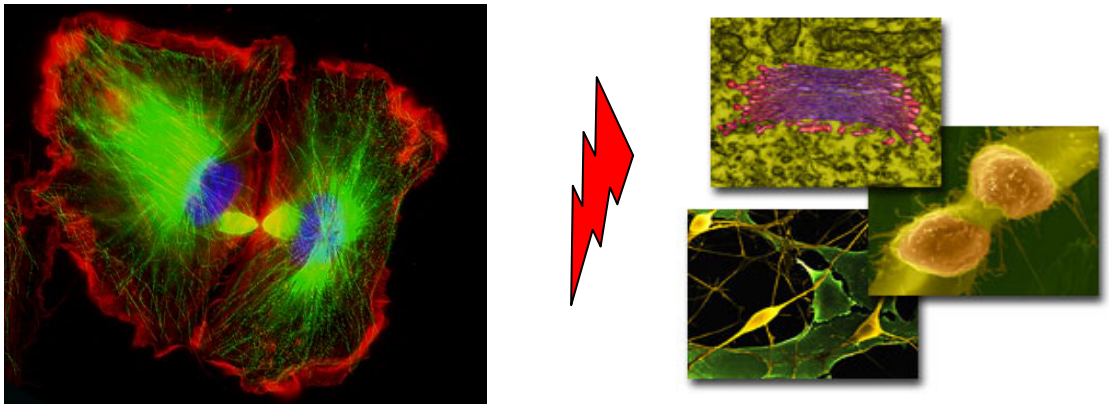

Figure 4.42: dividing cells in ohmically assisted bio-reactors?

Furthermore, this knowledge can be extended to several other bioreactors namely for the growth of animal cells or tissues, inducting differentiation of stem cells, facilitation of drug delivery and diffusing.

The mentioned examples are just the top of the iceberg and a wide range of new applications and new research topics can be exploited, thus contributing to relevant scientific advances in the food and health sector.

6. References

Alp, B. *et al.,* (2002). Formation of artificial, structured microbial consortia (ASMC) by dielectrophoresis. EnzymeMicrobiol. Technol. 31,35–43.

Amory, D. E., Dufour, J.-P. and Rouxhet, P. G., (1988). Flocculence of brewery yeasts and their surface properties: chemical composition, electrostatic charge and hydrophobicity. J. Inst. Brew. 94:79–84.

Bailey M.J. and Linko M, (1990). Production of β-galactosidase by *Aspergillus oryzae* in submerged bioreactor cultivation. J Biotechnol 16:57-66.

Bartlett, P.N., Pletcher, D., Zeng, J., (1997). Aprroaches to the integration of electrochemistry and biotechnology. J. Electrochem. Soc., 144 (11): 3705-370.

Bell, G. I., (1988). Models of cell adhesion involving specific binding, p. 227– 258. In P. Bongrand (ed.), Physical basis of cell-cell adhesion. CRC Press Inc., Boca Raton, Fla.

Biol. Med. 139(3), 929-934.

Biotechnology. 12(2), 183-188.

Carlson, V.S., (1954). Arch. Hyg. Bacteriol. 137, 86-95.

Chen, M. T., Weiss, R., (2005). Artificial cell-cell communication in yeast *Saccharomyces cerevisiae* using signaling elements from *Arabidopsis thaliana*. Nat Biotechnol 23(12):1551

Cho, H.Y., Yousef, A.E., Sastry S.K., (1996). Growth kinetics of *Lactobacillus acidophilus* under ohmic heating. Biotechnology and Bioengineering 49:334-340.

Domingues, L., (2001). Estirpes Floculantes de *Saccharomyces cerevisiae* Geneticamente Modificadas para a Utilização da Lactose: Construção e Aplicação Biotecnológica. PHD dissertation.

Domingues, L., Oliveira, C., Castro, I., Lima, N. and Teixeira, J. A., (2004). Production of β-galactosidase from recombinant Saccharomyces cerevisiae grown on lactose. J Chem Technol Biotechnol 79:809–815.

Dunstall, G., Rowe, M.T., Wisdom, G.B., and Kilpatrick, D., (2005). Effect of quorum sensing agents on the growth kinetics of Pseudomonas spp. of raw milk origin. J. Dairy Res. 72: 276-80.

Futcher, A. B., Cox, B. S., (1984). Copy number and the stability of 2-μm circle-based artificial plasmids of *Saccharomyces cerevisiae*. J Bacteriol 157: 283-290.

Godfrey, T., (2000). Developments in speciality enzymes. World Food Ingredients; February/March:30–5.

Grier, D. G., (2003). A revolution in optical manipulation. Nature 424, 810–816.

Kida K, Yamadaki M, Asano S-I, Nakata T, Sonoda Y (1989) The effect of aeration on stability of continuous ethanol fermentation by a flocculating yeast. J Ferm Bioeng 68: 107-111.

Kihn, J.-K., Masy, C. L., and Mestdagh, M. M., (1988). Yeast flocculation:competition between nonspecific repulsion and specific bonding in cell adhesion.Can. J. Microbiol. 34:773–778.

Kim, S. K. and Kaiser, D., (1990). Cell alignment required in differentiation of Myxococcus xanthus. Science 249, 926–928.

Kumar, V., (1988). Cloning and expression of the *Aspergillus niger* beta-galactosidase gene in *Saccharomyces cerevisiae*. PhD Thesis, London University, London.

Loghavi, L., Sastry, S. K. and Yousef, A. E., (2005). Moderate electric filed (MEF) treatment effect on growth kinetics of bacteriocin-producing *Lactobacillus acidophilus*. IFT proceedings.

Loghavi, L., Sastry, S. K. and Yousef, A. E., (2006). Effect of moderate electric field at different frequencies on the growth kinetics of *Lactobacillus acidophilus* . IFT proceedings.

Lopes DH, Sola-Penna M (2001). Urea increases tolerance of yeast inorganic pyrophosphatase activity to ethanol: the other side of urea interaction with proteins. Arch Biochem Biophys. 1;394(1):61-6.

Lu, L., Hume, M.E., and Pillai, S.D., (2004). Autoinducer-2-like activity associated with foods and its interaction with food additives. J. Food Protect. 67: 1457-1462.

Ludwig, D. L., Bruschi, C. V., (1991). The 2-μm plasmid as a nonselectable, stable, high copy number yeast vector. Plasmid 25: 81-95.

Masy, C. L., Henquinet, A., Mestdagh, M. M., (1992). Flocculation of *Saccharomyces cerevisiae*: inhibition by sugars. Can. J. Microbiol. 38:1298–1306.

Masy, C. L., Kockerols, M. and Mestdagh, M. M., (1991). Calcium activity versus ‘‘calcium threshold’’ as the key factor in the induction of yeast flocculation in simulated industrial fermentations. Can. J. Microbiol. 37:295–303.

Miki, B. L. A., Poon, N. H., James, A. P. and Seligy, V. L,. (1982). Possible mechanism for flocculation interactions governed by gene FLO1 in *Saccharomyces cerevisiae*. J. Bacteriol. 150:878–889.

Miller, G. L., (1959). Use of dinitrosalicilic acid reagent for determination of reducing sugar. Anal Chem 31:426-428.

Moradas-Ferreira, P., Fernandes, P. A. and Costa, M. J., (1994). Yeast flocculation—the role of cell wall proteins. Colloids Surf. B 2:159–164.

Neelakantan, S., Mohanty, A. K., Kaushik, J. K., (1999). Production and use of microbial enzymes for dairy processing. Curr Sci 77: 143–9.

Neelakantan, S., Mohanty, A. K., Kaushik, J. K., (1999). Production and use of microbial enzymes for dairy processing. Curr Sci 77:143–9.

Ozkan, A. *et al,.* (2003). Electro-optical platform for the manipulation of live cells. Langmuir 19, 1532–1538.

Ozkan, A. *et al.,* (2003). Electro-optical platform for the manipulation of live cells. Langmuir 19, 1532–1538.

Palkova, Z., Janderova, B., Gabriel, J., Zikanova, B., Pospisek, M., and Forstova, J. (1997). Ammonia mediates communication between yeast colonies. Nature 390: 532-536.

Pillai, S. D. and Jesudhasan, P. R., (2006). Quorum sensing: How bacteria communicate,

Pohl, H. A., (1972). Electrical forming of masses of living cells. J. Colloid Interface Sci. 32, 437–438.

Poortinga, A.T. *et al.,* (2000). Controlled electrophoretic deposition of bacteria to surfaces for the design of biofilms. Biotechnol. Bioeng. 67, 117–120.

Rasch, M., Andersen, J. B., Nielsen, K. F., Flodgaard, L. R., Christensen, H., Givskov,M., and Gram, L. (2005). Involvement of bacterial quorum sensing signals in spoilage of bean sprouts. Appl. Environ. Microbiol. 71: 3321-3330.

Rowley, B. A., (1972). Electrical current effects on *E. coli* growth rates. Proc. Soc. Exptl.

Rowley, B.A., (1972). Electricalcurrent effects on *E. coli* growth rates. Proc. Soc. Expl. Biol. Med. 139 (3):929-934.

Sarney, D. B., Hale, C., Frankel, G., Vulfson, E. N., (2000). A novel approach to the recovery of biologically active oligosaccharides from milk using a combination of enzymatic treatment and nanofiltration. Biotechnol Bioeng 69:461–7.

Shapiro, J. A. and Dworkin, M., (1997). Bacteria as Multicellular Organisms, Oxford University Press.

Shapiro, J. A., (1995). The significance of bacterial colony patterns. Bioessays 17, 597–607.

Shapiro, J.A., (1998). Thinking about bacterial populations as multicellular organisms. Annu. Rev. Microbiol. 52, 81–104.

Shimada and Kenzo Shimahara. (1985). Changes in Surface Charge, Respiratory Rate and Stainability with Crystal Violet of Resting *Escherichia coli* B Cell Agric. Biol. Chem., 49 (2), 405-411.

Shimada, K., and Shimahara, K., (1977). Effect of alternating current on growth lag in *Escherichia coli.* B. Journal of General and Applied Microbiology. 23, 127-136.

Spengler, J. F. *et al.,* (2000). Observation of yeast cell movement and aggregation in a small-scale MHz ultrasonic standing wave field. Bioseparation 9, 329–341.

Stacey, M., Stickley, J., Fox, P. V., Statler, K., Schoenbach, S. J., Beebe, S., Buescher, (2003). Differential effects in cells exposed to ultra-short, high intensity electric fields: cell survival, DNA damage, cell cycle analysis - Mut Res 542 65-75.

Stewart, G. G., (1975). Yeast flocculation—practical implications and experimental findings. Brew. Dig. 50:42–62.

Stratford, M., and Assinder, S., (1991). Yeast flocculation: Flo1 and NewFlophenotypes and receptor structure. Yeast 7:559–574.

Sonnleitner, B. e Käppeli, O., 1986. Growth of *Saccharomyces cerevisiae* Is Controlled by Its Limited Respiratory Capacity: Formulation and Verification of a Hipothesis. Biotechnol. Bioeng., 28, 927-937.

Van Haecht, J. L., Defosse, C., Van den Bogaert, B. and Rouxhet, P. G., (1982). Surface properties of yeast cells: chemical composition by XPS and isoelectric point. Colloids Surf. 4:343–358.

Van Hamersveld, E. H., Van Loosdrecht, M. C. M. and Luyben, K. C. A. M., (1994). How important is the physicochemical interaction in the flocculation of yeast cells? Colloids Surf. B 2:165–171.

Varon, M., Choder, M., (2000). Organization and Cell-Cell Interaction in Starved *Saccharomyces cerevisiae* Colonies. Journal of Bacteriology, p. 3877–3880 Vol. 182, No. 13.

Verduzco-Luque, C.E. *et al.,* (2003). Construction of biofilms with defined internal architecture using dielectrophoresis and flocculation. Biotechnol. Bioeng. 83, 34–44.

Walters, M. and Sperandio, V., (2006). Quorum sensing in *Escherichia coli* and Salmonella. Intl. J. Med. Microbiol. (in press)

Waters, C.M. and Bassler, B.L., (2005). Quorum sensing: Cell-to-cell communication in bacteria. Ann. Rev. Cell. Dev. Biol. 21:319-346.

Yoon, S.W., Lee, S.Y.J., Kim K.M., and Lee C.H. (2002). Leakage of cellular material from *Saccharomyces cerevisiae* by ohmic heating. Journal of Microbiology and Biotechnology. 12(2), 183-188.

Chapter 5.

HYDRODYNAMIC HARACTERIZATION OF PILOT SCALE OHMIC HEATING

APPLICATION TO AN INDUSTRIAL STRAWBERRY PULP

Abstract

A pilot ohmic heater was tested for the continuous aseptic processing of strawberry pulps and jams. The hydrodynamics and the fluid residence time distribution (RTD) were numerically simulated for Newtonian and non-Newtonian fluids (water and an industrial strawberry pulp, respectively), for several inlet mass flow rates and different operational temperatures. The results were obtained using Computational Fluid Dynamics (CFD) with a user-defined function (UDF) description of the fluid phase (pulp). For all of the conditions tested the fluid phase is described using a laminar flow model. For strawberry pulp simulations it was necessary to determine its rheological behaviour, which was best described by a Herschel-Bulkley model.

The results show that the RTD is affected by the inlet flow rate but not so significantly by the process temperature (in the studied temperature range). Shortcuts and dead zones were detected in the ohmic heater especially for Newtonian fluids. The heater behaves as a piston flow with longitudinal (axial) mixing.

The simulated results were validated using experimental data and, in general, a good match was found between the two sets of data.

Moreover, the RTD exclusively in the heating zone was used for the establishment of an equation relating the final temperature of the fluid fractions with the operational conditions (initial temperature, flow rate and applied voltage). This equation can be used to optimize the operational conditions (*e.g.* maximizing productivity and minimizing energy costs) of this ohmic heater, while assuring the microbiological safety of the processed products.

Keywords: Hydrodynamics; food processing; non-Newtonian fluids; safety; ohmic heating; strawberry pulp

1. Introduction

Especially interesting is the application of ohmic heating technology to foods containing solid particles and/or being viscous fluids (e.g. fruit purees and fruit pulps). When processing particulate foods, this technology allows heating solid and liquid phases uniformly and at the same rate (when they have the same electrical conductivity), eliminating the problem of overcooking the surrounding volume to ensure that the center of the solid particles is adequately processed (Castro *et al.*, 2006). When processing viscous foods, ohmic heating will also provide a uniform heating throughout all the volume thus eliminating the significant heat transfer resistances which are present when a conventional heating technique (e.g. scrapped surface heat exchanger) is used.

While reviewing the rheological models of fluid food products, Holdsworth (1993) underscored the importance of accurate rheological data for calculation of the volumetric flow rates, selection of pumps, determination of pressure drops for pipe sizing and power consumption for pumping systems and for prediction of heat transfer coefficients for heating, evaporation and sterilization processes.

Being able to demonstrate that the correct heat treatment is being applied to the products is a crucial step for the industrial application of ohmic heating. In order to validate this technology it is important to know some physical-chemical properties of the fluid being processed such as its rheological behavior and to fully characterize the hydrodynamic behavior of heater in order to determine the worst case scenario that can jeopardize the safety of foods being processed.

1.1. Newtonian and non-Newtonian Fluids

In a Newtonian fluid the relation between the shear stress (τ) is linearly proportional to the velocity gradient in the direction that is perpendicular to the plane of shear. The constant of proportionality is known as the viscosity.

The equation describing Newtonian fluid behaviour is:

$$\tau = \mu \frac{dv}{dx} \qquad \textbf{(Eq. 5.1)}$$

where:

τ is the shear stress exerted by the fluid "drag"

μ is the fluid viscosity (the constant of proportionality)

$\frac{dv}{dx}$ is the velocity gradient perpendicular to the direction of shear

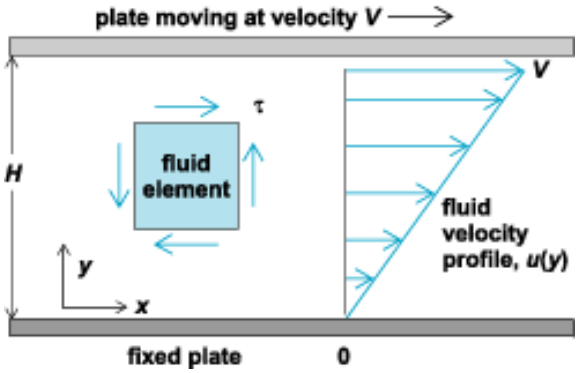

Figure 5.1: A fluid sheared between two plates.

This behavior is represented in Figure 5.1, being the resulting strain rate equal to V/H.

So it is possible to indicate that the fluid continues to flow, regardless of the forces acting on it. E.g. water is a Newtonian fluid because its behaviour can be described by equation 5.1 above. For Newtonian fluids the viscosity is dependent of the temperature, the pressure to which the fluid is exposed and also of the chemical composition, but not on the forces acting upon the fluid.

There are several fluids such as water, milk, air, gasoline which present a Newtonian behaviour, however many others do not obey this relation and are termed as non-Newtonian fluids.

A non-Newtonian fluid is a fluid that presents a non-linear relation between the shear stress and the velocity gradient. In consequence, non-Newtonian fluids may not have a well-defined viscosity. Common examples include toothpaste, liquid soaps, multigrade engine oils and several food products like mayonnaise, peanut butter and egg whites. According to Krokida *et al.* (2000), fruit and vegetable juices are assumed to behave as non-Newtonian fluids, following the power law model. However, if there is a considerable amount of fruit pulp (e.g. solids in suspension) there may be an additional resistance to flow represented by a yield stress (Gut *et al.*, 2005).

Although the concept of viscosity is commonly used to characterize a material, it can be inadequate to describe the mechanical behaviour of a substance, particularly in the case of non-Newtonian fluids. Being so, the relations between the stress and strain tensors under

many different flow conditions, such as oscillatory shear, or extensional flow are the most studied.

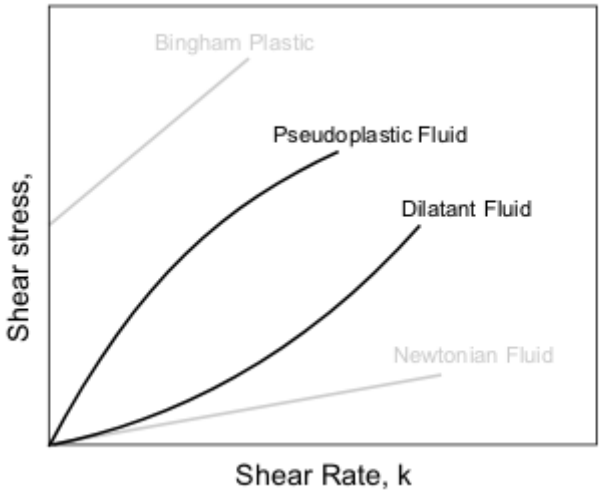

Figure 5.2: Relation of the shear rate and the shear stress in different fluids.

Figure 5.2 shows the relation of the shear rate and the shear stress in different fluids and what should be expected in terms of the behavior of the fluid according to its type.

1.2. Laminar Flow versus Turbulent Flow

Fluid flow is characterized as being either laminar or turbulent. In laminar flow the fluid moves in layers, with one sliding smoothly over the other. There is no mixing of fluid from layer to layer, since viscous shear forces damp out relative motions between layers. Since each layer of fluid is in effect flowing over the one adjacent to it, the fluid velocity increases with the distance from the pipe wall. The resulting velocity profile is approximately parabolic in shape (Figure 5.3).

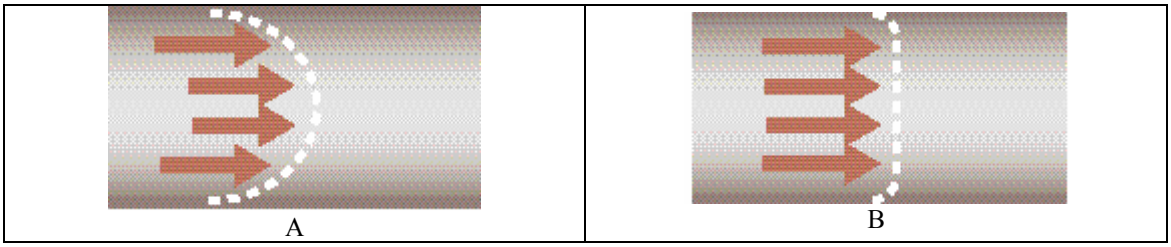

Figure 5.3: Laminar flow profile (A) and turbulent flow profile (B)

In turbulent flow, there are no discrete layers of flowing liquid. The momentum of the fluid overcomes the viscous shear forces, and there is extensive and continual mixing across the flow stream. This causes the velocity profile across a pipe to be nearly flat (Figure 5.3).

1.3. Tools in reactor engineering

Reactor engineering activity is related to the engineering of (chemical or biochemical) transformations. Such transformations can occur only if the reactant molecules are brought into short contact (mixed) under the appropriate environment (temperature and concentration fields, catalysts/biocatalysts) for an adequate time. The process vessel (reactor) must provide the necessary conditions to favour the desired reaction and allow the removal of products. To describe a reactor's behaviour it is necessary to characterise it in terms of flow patterns and mixing for the different phases present. Recently, Computational Fluid Dynamics (CFD) tools appear to make a substantial contribution in establishing the best way to carry out a desired transformation, as on accelerating the reactor engineering tasks (Ranade 2002).

The description and design of multiphase (gas–liquid, gas–liquid–solid and gas-liquid-liquid-solid) reactors still relies to a large extent on empirical rules and correlations, which, in turn, are based on measurements made under conditions that try to mimic the industrial conditions.

Some new approaches appeared in the last years to help in the design of multiphase reactors, of which CFD is an example. Even in this case, the physical models used require information on local and transient flow characteristics (e.g. turbulence characteristics, viscosity, etc.), since *ab initio* calculations are up to now impossible.

Reliable measuring techniques are, therefore, needed for the rational description and the design of multiphase reactors. Measurement techniques can be classified according to different criteria. A first classification distinguishes between 'time-averaged' and 'transient' measurements and between 'local' and 'global' measurements. Since the classification between local and global measurements is not always possible other classification has been preferred by Boyer (2002), relying on the physical basis of the measurement, thus distinguishing between 'invasive' and 'non-invasive' measuring techniques as follows:

a) Non-invasive techniques
    (a) Global techniques
        i. Time-averaged pressure drop

ii. Measurement and analysis of signal fluctuations
iii. Dynamic gas disengagement technique (DGD)
iv. Tracing techniques
    1. Tracing of the liquid
    2. Tracing of the gas-phase
    3. Tracing of the solid (coloured tracers, magnetic tracers, fluorescent tracers)
v. Conductimetry
vi. Radiation attenuation techniques
    1. *X*-ray, γ-ray or neutron absorption radiography
    2. Light attenuation
    3. Ultrasound techniques

(b) Techniques yielding local characteristics

i. Visualisation techniques
    1. Photographic techniques
    2. Radiographic techniques
    3. Particle image velocimetry
    4. NMR imaging
ii. Laser Doppler anemometry and derived techniques
iii. Polarographic technique
iv. Radioactive tracking of particles
v. Tomographic techniques
    1. Tomography by photon attenuation measurement
    2. Electrical tomographic system
    3. Ultrasonic tomography

b) Invasive techniques

(a) The so-called 'needle probes' (optical probes, resistive or conductive probes, or 'impedance probes')

(b) Heat transfer probes

(c) Ultrasound probes

vi. Ultra-sound transmittance technique (UTT)
vii. Pulse echo technique

(d) Pitot tubes.

1.4. Assessment of the non-ideal flow

The most widely used concept in reactor engineering is that of an "ideal" reactor. The simplest reactor, whose performance is governed by the so-called 'zero dimensional' equation, is the 'completely mixed reactor'. The key assumption is that mixing in the reactor is complete, so that the properties of the reaction mixture are uniform in all parts of the reactor and are, therefore, the same as those of the 'exit' stream. The other ideal reactor concept, known as 'plug flow reactor' is based on a 'one dimensional' approximation of the material and energy balance equations. In an ideal plug flow reactor, unidirectional flow through the reactor is assumed (similar to the flow through a pipe) (Ranade 2002).

It is of extreme importance to evaluate the consequences of the assumptions involved in the concepts of ideal reactors to estimate the behaviour of a "real reactor", as the mixing may deviate significantly from the ideal flow cases (Figure 5.4). This deviation can be caused by channelling of fluid, recycling of fluid or formation of stagnant regions within the reactor (e.g. Levenspiel 1972). The mixing of a phase may be experimentally characterised by tracing techniques (e.g. Boyer *et al.* 2002).

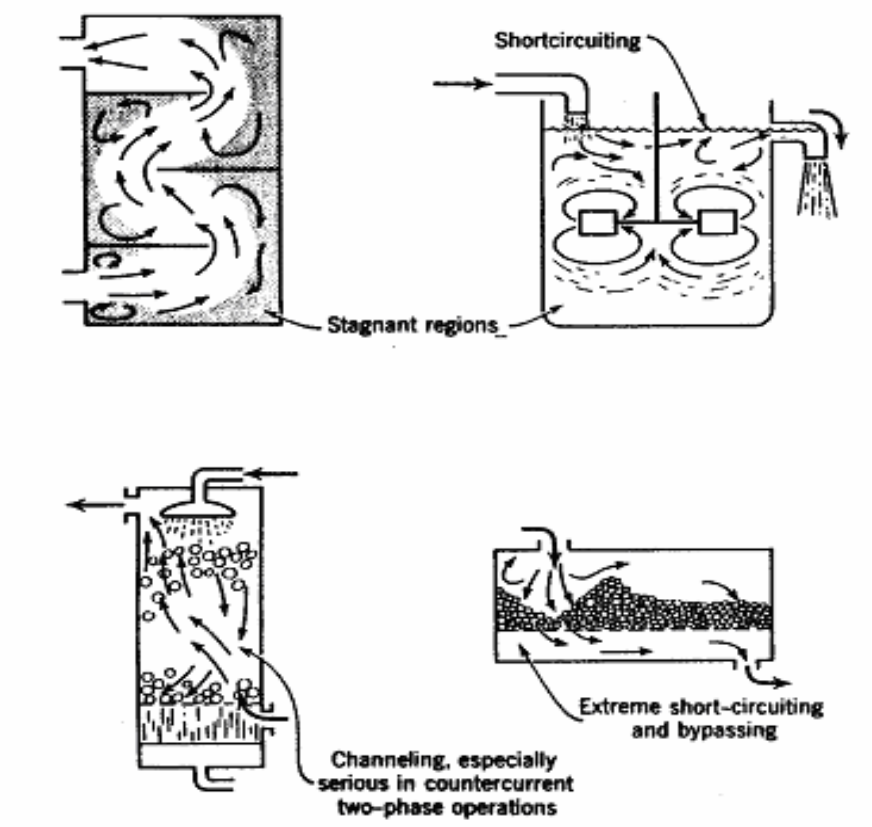

Figure 5.4: Non ideal flow patterns which may exist in process equipment.

1.5. Residence time distribution

The concept of residence time distribution (RTD) is fundamental for the design of reactors or industrial plants in which a continuous flow is present. RTD is the exit age distribution of fluid molecules leaving the system under study. The residence time is the total time spent by the fluid molecules within the system. The response data of a tracer at the system outlet may be used to estimate the RTD. The completely segregated (assuming no mixing between fluid elements of different ages) and completely mixed fluid elements constitute the two limiting solutions. Obtaining the RTD of an actual reactor and applying these two limiting assumptions to obtain the bounds of the performance of the reactor is a practical method for reaction engineering analysis (Ranade 2002). RTD affects heat transfer rates, interphase mass transfer rates and the conversion and selectivity of chemical and biochemical reactions (Briens *et al.* 1995).

Several sophisticated techniques and data analysis methodologies have been developed to measure the RTD of reactors. Measuring the RTD of a tracer dissolved in the liquid phase is a well-known methodology to assess the mixing of the liquid phase. This technique is simple but presents some disadvantages (Briens *et al.* 1995).

Several tracers can be used namely (Boyer *et al.* 2002):

a) Tracer dissolved in the liquid phase, e.g.:
    (a) Salt tracer
    (b) Coloured tracers
    (c) Radioactive isotope tracer
b) Particle tracking technique, i.e. neutrally buoyant solid particles followed by electromagnetic means.

Various different types of models have been developed to interpret RTD data (tracer concentration versus time) and to use it further to predict the influence of non-ideal behaviour on reactor performance. Most of these models use ideal reactors as building blocks. In a simple case, a two-parameter model (the mean residence time and the axial dispersion coefficient) may be sufficient to yield an adequate description of the global flow behaviour of a reactor: In more complex cases, models with more parameters must be used (Levenspiel 1972).

The physical boundaries of the reactor also play a role in the RTD studies. When the flow patterns are disturbed across a boundary (e.g. a measurement point), such boundary is

classified as being open. If flow patterns are not disturbed along the boundary it is classified as closed.

The "imperfect pulse method" is the most common technique found in the literature. A pulse of tracer is injected upstream of the reactor and the resulting tracer concentration peaks are detected at two different locations in the reactor. Then, the residence time distribution between these locations is obtained by deconvolution (Briens *et al.* 1995).

Care must be taken when measuring the RTDs in reactors with one or two open boundaries. In such cases tracer measurements do not provide RTD but a 'transient response function' from which RTD may only be obtained if separate experiments provide more information (Nauman and Buffham 1983). The measurement of the tracer concentration can be performed by three different techniques (Briens *et al.* 1995):

a) mixing-cup
b) local concentration (e.g. as the measured by an effective fibre-optical probe or a conductivity probe)
c) through-the-wall, along a diameter of a cross-section (e.g. conductivity meters or scintillation systems).

Only the mixing-cup concentration provides the true RTD (Nauman and Buffham 1983).

For a perfect pulse disturbance the RTD can be expressed (Nauman and Buffham 1983; Wen and Fan 1975) by means of the cumulative distribution function evaluated from the tracer response at the exit (x_{out}) of the reactor.

$$F_t = 1 - \frac{x_{out}(t)}{x_{in}} \qquad \textbf{(Eq. 5.2)}$$

$$F_\theta = 1 - \frac{x_{out}(\theta)}{x_{in}} \qquad \textbf{(Eq. 5.3)}$$

Where θ is the dimensionless residence time and is give by $t/\bar{t}$. The reduced distribution function results from derivation:

$$E_t = \frac{\mathrm{d}F_t}{\mathrm{d}t} \qquad \textbf{(Eq. 5.4)}$$

$$E_\theta = E_t\,\bar{t} \qquad \textbf{(Eq. 5.5)}$$

Moments are used to characterise RTD functions in terms of statistical parameters. The mean residence time ($\bar{t}$) is given by the first moment of the distribution function:

$$\bar{t} = \int_0^{x_{in}} t \frac{1}{x_{in}} \mathrm{d}x \qquad \textbf{(Eq. 5.6)}$$

and the spread in residence time (characterised by the variance, σ^2) is given by (Westerterp *et al.* 1963):

$$\sigma^2 = \int_0^{x_{in}} t^2 \frac{1}{x_{in}} \mathrm{d}x - \bar{t}^2 \qquad \textbf{(Eq. 5.7)}$$

Analytical solutions for RTD are simply derived from the mass balance equation in the Laplace domain.

1.6. Computational flow modelling

Computational Fluid Dynamics, commonly abbreviated as CFD, is a technique to model fluid flow using a computer simulation. Due to the recent rapid grow of powerful computer resources and the development of general purpose CFD software packages CFD can nowadays be applied to solve industrial flow problems. Today, CFD has already proven to be a valuable tool to complement experimental findings in flow structure studies. In a computational simulation the flow structure is computed by solving the mathematical equations that govern the flow dynamics. The result is a complete description of the three-dimensional flow in the entire flow domain in terms of the velocity field and pressure distribution, including profiles of temperature variations, density and other related physical quantities. Today's CFD codes include in their basic flow computations effects of heat and mass transfer and a range of physical and chemical models.

CFD has been extremely popular in the car and airspace industry but chemical engineers have only recently become aware of the large potential it bears for equipment design and process optimization. This is probably explained by the complexity of the processes in chemical engineer often involving two or more phase flows, making modelling an even harder task.

Bio-medical engineering is a rapidly growing field and uses CFD to study the circulatory and respiratory systems. The following figure shows pressure contours and a cutaway view that reveals velocity vectors in a blood pump that assumes the role of heart in open-heart surgery.

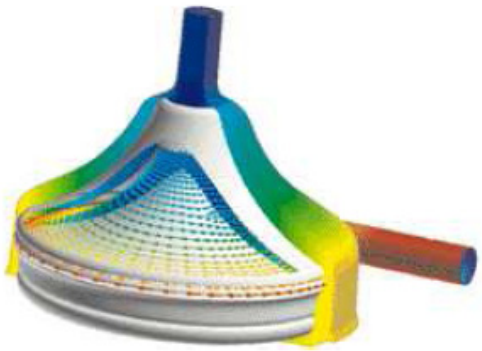

Figure 5.5: Velocity vectors in a blood pump

1.6.1. Model equations

In most of CFD packages (e.g. Fluent 5 – Fluent Inc., Paris, France) the governing equations are solved in cylindrical coordinates, as follows (Ni *et al.* 2002):

Momentum equations:

$$\rho\left(\frac{\partial V_r}{\partial t}+V_r\frac{\partial V_r}{\partial r}+\frac{V_\theta}{r}\frac{\partial V_r}{\partial \theta}-\frac{V_\theta^2}{r}+V_z\frac{\partial V_r}{\partial z}\right)=-\frac{\partial p}{\partial r}-\left[\frac{1}{r}\frac{\partial}{\partial r}\left(r\tau_{rr}\right)+\frac{1}{r}\frac{\partial \tau_{r\theta}}{\partial}-\frac{\tau_{\theta\theta}}{r}+\frac{\partial \tau_{rz}}{\partial z}\right] \quad \textbf{(Eq. 5.8)}$$

$$\rho\left(\frac{\partial V_\theta}{\partial t}+V_r\frac{\partial V_\theta}{\partial r}+\frac{V_\theta}{r}\frac{\partial V_\theta}{\partial \theta}-\frac{V_rV_\theta}{r}+V_z\frac{\partial V_\theta}{\partial z}\right)=-\frac{1}{r}\frac{\partial p}{\partial \theta}-\left[\frac{1}{r^2}\frac{\partial}{\partial r}\left(r^2\tau_{r\theta}\right)+\frac{1}{r}\frac{\partial \tau_{\theta\theta}}{\partial \theta}-\frac{\partial \tau_{\theta z}}{\partial z}\right] \quad \textbf{(Eq. 5.9)}$$

$$\rho\left(\frac{\partial V_z}{\partial t}+V_r\frac{\partial V_z}{\partial r}+\frac{V_\theta}{r}\frac{\partial V_z}{\partial \theta}+V_z\frac{\partial V_z}{\partial z}\right)=-\frac{\partial p}{\partial z}-\left[\frac{1}{r}\frac{\partial}{\partial r}\left(r\tau_{rz}\right)+\frac{1}{r}\frac{\partial \tau_{z\theta}}{\partial \theta}-\frac{\partial \tau_{zz}}{\partial z}\right] \quad \textbf{(Eq. 5.10)}$$

Continuity equations:

$$\frac{1}{r}\frac{\partial}{\partial r}\left(rV_r\right)+\frac{1}{r}\frac{\partial V_\theta}{\partial \theta}+\frac{\partial V_z}{\partial z}=0 \quad \textbf{(Eq. 5.11)}$$

where

$$\tau_{rr} = -\mu\left[2\frac{\partial V_r}{\partial r} - \frac{2}{3}(\nabla V)\right] \quad \textbf{(Eq. 5.12)}$$

$$\tau_{\theta\theta} = -\mu\left[2\left[\frac{1}{r}\frac{\partial V_\theta}{\partial \theta} + \frac{V_r}{r}\right] - \frac{2}{3}(\nabla V)\right] \quad \textbf{(Eq. 5.13)}$$

$$\tau_{zz} = -\mu\left[2\frac{\partial V_z}{\partial z} - \frac{2}{3}(\nabla V)\right] \quad \textbf{(Eq. 5.14)}$$

$$\tau_{r\theta} = \tau_{\theta r} = -\mu\left[\frac{1}{r}\frac{\partial V_r}{\partial \theta} + r\frac{\partial}{\partial r}\left(\frac{V_\theta}{r}\right)\right] \quad \textbf{(Eq. 5.15)}$$

$$\tau_{z\theta} = \tau_{\theta z} = -\mu\left[\frac{1}{r}\frac{\partial V_z}{\partial \theta} + \frac{\partial V_\theta}{\partial z}\right] \quad \textbf{(Eq. 5.16)}$$

$$\tau_{zr} = \tau_{rz} = -\mu\left[\frac{1}{r}\frac{\partial V_z}{\partial r} + \frac{\partial V_r}{\partial z}\right] \quad \textbf{(Eq. 5.17)}$$

where

$$(\nabla V) = \frac{1}{r}\frac{\partial}{\partial r}(rV_r) + \frac{1}{r}\frac{\partial V_\theta}{\partial \theta} + \frac{\partial V_z}{\partial z} \quad \textbf{(Eq. 5.18)}$$

where V_r, V_θ and Vz are the fluid velocities at r, θ and z coordinates respectively, p is the pressure drop (Pa). The viscous term in Eq.s 5.12 – 5.18 takes the form of $\mu = \mu_0 + \mu_t$, where μ_0 is the nominal laminar viscosity (kg m^{-1} s^{-1}) and μ_t the turbulent viscosity (kg m^{-1} s^{-1}). For laminar flow simulation, μ_t, = 0, and V_r, V_θ and V_z are the laminar velocity components. For turbulence simulation, μ_t, is included and V_r, V_θ and V_z are averaged velocities. For 2-D simulations, all variables in the third direction (θ) are treated as constants, thus simplifying the above equations accordingly.

This software package solves numerically the Navier-Stokes equations to determine the flow pattern in the heater. Three main steps are involved in numerical simulations with Fluent:

1. designing the geometry and meshing (discretisation of domain into finite elements)
2. defining the fluid properties
3. boundary conditions

For complex geometries, the design and mesh are generated using a Fluent's CAD tool, the 'Gambit' software package

In fact, the quality of the mesh plays a significant role in the accuracy and stability of the numerical computation and the effectiveness of the convergence. The attributes associated with mesh quality are node point distribution, smoothness, and skewness.

A numerical simulation can be considered to be an idealized experiment with well-defined boundary conditions, being perfectly reproducible with full control of the initial flow properties. The contributions of effects of heat and mass transfer and other physical or chemical processes that are included in the simulation can be studied individually just by changing or switching them on and off in a series of simulations. However, the results of the calculations represent a flow-model obeying the physics and boundary conditions imposed by the user. Proper physical modeling of the fluid flow investigated is therefore a very important step in preparing a CFD simulation, since it dominates the applicability of the results obtained later on. This requires solid knowledge and justification of the models of all physical and chemical processes taken into account in the computations.

2. Materials and Methods

2.1. The continuous ohmic heating

The pilot scale ohmic heater used in this study (EA Tecnology, Ltd., Chester, UK) is shown in Figure 5.6. With a volume of 2.2 L it was designed for the continuous aseptic process of food products, especially fruit pulps. A maximum flow rate of 2 L/min is allowed. The temperature range of the industrial aseptic processing of (strawberry) fruit pulps is between 40 ºC (pre-mixture temperature) and 90 ºC (pasteurization temperature). The maximum voltage that may be applied to the ohmic heater is 480 V.

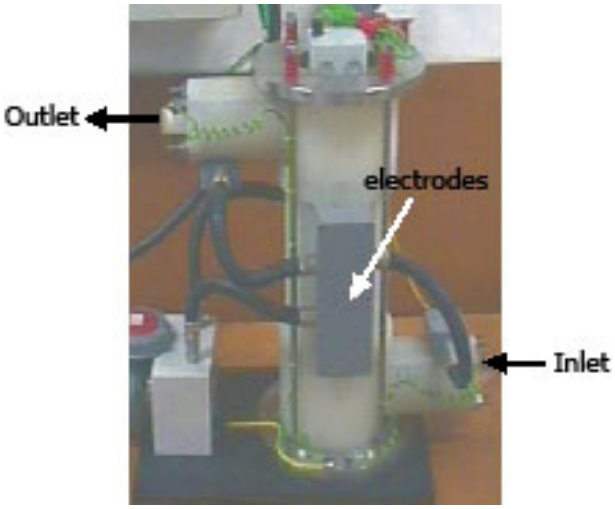

Figure 5.6: Continuous ohmic heater

2.2. The CFD model and the mesh

A 3D axisymmetric geometry was created using Gambit™ 2.1.6 reproducing the internal geometry of the ohmic heater (Figure 5.7). The hexagonal mesh (default mesh) consisted of 378348 cells and was created with an axial symmetry condition in order to minimize the total number of cells. The mesh independence was tested as shown further in the text.

The quality of the computation depends on the quality of the mesh and therefore the generation of a good mesh is another important stage in the preparation of a CFD simulation. Cells have to be distributed so that cells of small sizes are clustered in regions of interest with severe flow gradients, leaving larger cells where such gradients are not so

important. Therefore, an impression of the flow field to be computed is necessary in advance and the mesh has to be adjusted accordingly. Consequently, boundary layers were imposed in order to decrease the cell spacing near the walls.

Flow patterns at steady-state flow within the ohmic heater were simulated using Fluent™ 6.2.22 software for two different processing fluids: water (Newtonian fluid) and industrial strawberry pulp (non-Newtonian fluid).

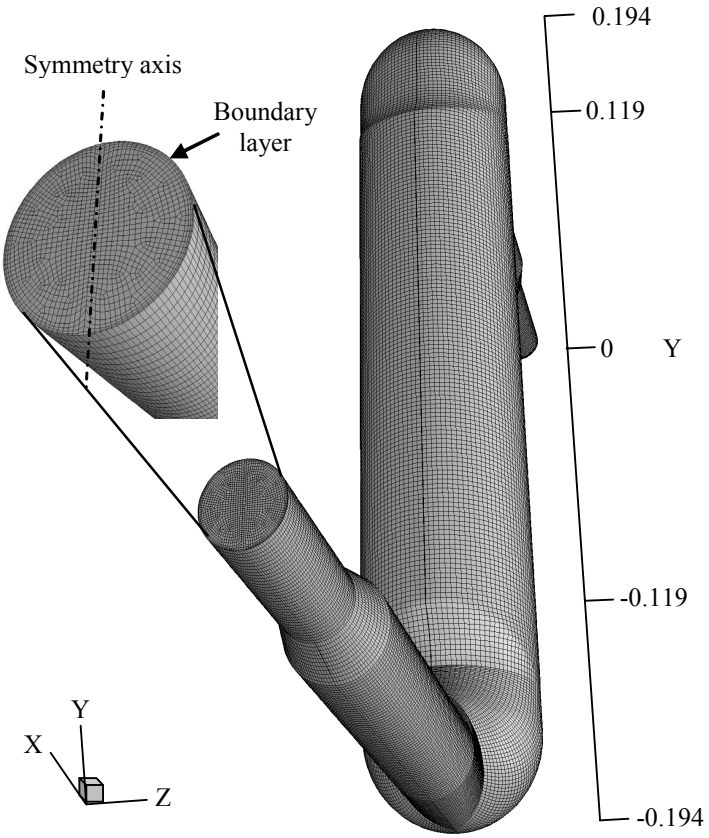

Figure 5.7: Mesh created for the ohmic heater and detail of the boundary layer

The domain determined for each mesh (i.e., the portion of the system that the fluid needs to cross from the inlet to the outlet) is quite important since, for each simulation, this domain can be changed and indicated by the user. In the present study, the dimensions (in mm) of the domain in the x and y directions are $-259 < x < 259$ and $-194 < y < 194$, respectively. In the case of the 3D mesh, the domain depth, z, varies between $0 < z < 37.5$.

Inlet boundary conditions (in this case velocities) were defined on Fluent's boundary conditions panel. Due to the flow mass limitations of the ohmic heater (maximum of 2 l/min) the Reynolds number (Re) at the inlet ($d1$ = 0.025 m) was lower than 2000 for all simulated flow conditions, thus a laminar model was considered in all cases (Table 5.1,

Table 5.2). Simulations were run for inlet mass flow rates of 0.5, 1.0 and 2.0 kg/min, converted into inlet velocity values. A flat velocity profile was considered at the inlet attending to the long entrance length, allowing for complete velocity profile development.

Table 5.1: Determination of *Re* when the operating fluid is water.

Velocity (m/s)	Density (kg/m3)	Viscosity (kg/m·s)	*Re1* (d1=0.025 m)	*Re2* (d2=0.082m)
0.0085			211	695
0.0170			423	1390
0.0340	998.2	0.0010	846	2780
0.0509			1266	4162
0.0679			1689	5552

Table 5.2: Determination of Re when the operating fluid is strawberry pulp.

Velocity (m/s)	Density (kg/m^3)	Viscosity (kg/m·s)	*Re1* (d1=0.025 m)	*Re2* (d2=0.082m)
0.0085			12	40
0.0170			24	80
0.0340	990.0	0.0172	49	161
0.0509			73	241
0.0679			98	321

The default under-relaxation parameters for all variables are set to values optimal for the largest possible number of cases. These values are suitable for many problems, but for some particular nonlinear problems it is prudent to reduce the under-relaxation factors initially. Occasionally, it is possible to make changes in the under-relaxation factors and resume the calculation, only to find that the residuals begin to increase. Solutions were considered converged when normalized residuals decreased to a value below $1x10^{-3}$. Most of the problems required less then 5,000 iterations for convergence. For *Re* above 400 some convergence problems occurred but they were solved by modifiying (decreasing) under-relaxation parameters. Discretization schemes to solve the coupled equations were the standard method for pressure equation, the SIMPLEC algorithm for pressure-velocity coupling and a first order model for the momentum equation.

Fluent software was also used to simulate the residence time distribution (RTD) functions in the whole volume of the heater, once the steady-state flow patterns' convergence was obtained.

2.3. Simulations of RTD

To simulate tracer injection, an user defined scalar (UDS) was used, setting the diffusivity at a very low value (e.g. $1x10^{-12}$ m/s^2) in order to avoid tracer dispersion. Then, momentum, velocity and pressure equations were turned off and the scalar (dimensionless) was initiated at a value of 1 at the inlet corresponding to a step tracer input. The simulations were then restarted at unsteady flow conditions. The scalar concentration was monitored at the outlet by using an area weighted average. A time step of $1/200^{th}$ of the mean residence time was used to ensure the independency of the results.

After the determination of flow patterns and in order to allow the estimation of temperature profiles of the pulp at the exit of the heating zone the mesh was divided into 3 zones: inlet zone, heating zone ($-119 < y < 119$, in mm) and outlet zone. The scalar concentration was initialized at the value of 1 at the inlet of the heating zone ($y = -119$ mm) and its concentration was monitored at the outlet of the heating zone ($y = 119$ mm). All the other parameters were kept constant.

2.4. Experimental determinations of RTD

RTD experiments in the ohmic heater were performed using step response experiments with a pH tracer. A schematic of the experimental setup is illustrated in Figure 5.8. A steady, continuous fluid flow rate was supplied with a peristaltic pump and flow rate was confirmed during the course of the experiments.

For both working fluids (water and strawberry pulp) a different pH fluid was prepared using a concentrated acid or base solution. The pH probes were installed at the inlet and outlet of the ohmic heater and data was continuously collected to a spreadsheet through a data acquisition system created in Labview Express (National Instruments) (Figure 5.8).

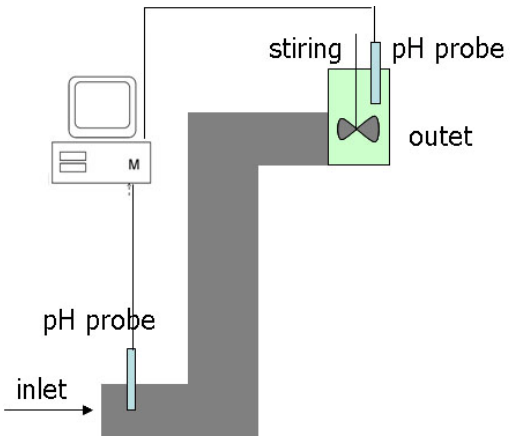

Figure 5.8: Experimental set-up used to determine RTD for the different fluids

The step input injection method was applied since it is relatively easy to generate experimentally. The step-down concentrations (Figure 5.9) were converted into a positive-step response by considering the linear relation between the cumulative washout probability function, *W(t)*, and the cumulative distribution function, *F(t)*, i.e. $W(t) = 1 - F(t)$, which simplified some of the mathematical manipulation of data (results not shown). All experiments were performed at room temperature (20 ºC) for water and different temperatures for strawberry pulp.

Experiments were made in duplicate (two concordant assays).

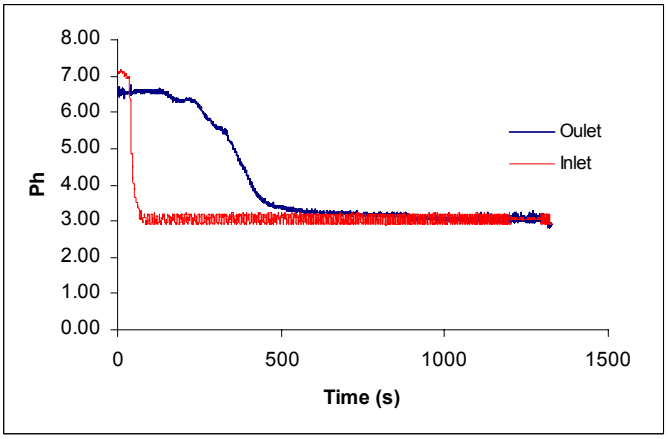

Figure 5.9: Negative step input using water at a flow rate of 0.5 kg/min

2.5. Determining the rheological properties of strawberry pulp

The rheology of an industrial strawberry pulp (pH = 4.0 and 14.5 ºBrix) was determined using a New TA Instruments AR-2000 Rheometer. A Peltier plate controlled Smart Swap™ temperature system was used along with a flat plate as the measuring system. A time controlled step flow procedure was used, applying successively higher shear rate values to the material. This procedure was repeated for eight different temperatures (ranging from 40 to 90 ºC). The rheology of the strawberry pulp was fitted by a Herschel-Bulkley model (Eq. 5.19), a three-parameter model that includes a yield stress (τ_0), a consistency index (K) and a flow behaviour index (n). This rheological model combines the effects of Bingham and power law in a fluid. For low strain rates ($\gamma < \tau_0/\mu_0$) the material acts like a very viscous fluid with viscosity μ_0. The increase of the strain rate increases the yield stress and the fluid behaves as a power law fluid. These parameters were introduced into Fluent to simulate the effect of temperature on strawberry pulp viscosity. Within the applied range of shear rates, it was evident from Figure ?? that the Herschel-Bulkley model provides a good representation of the shear-thining rheology of this pulp ($r^2 > 0.98$).

$$\eta = \frac{\tau_0 + K\left[\gamma^n - \left(\frac{\tau_0}{\mu_0}\right)^n\right]}{\gamma} \qquad \textbf{(Eq. 5.19)}$$

3. Results and Discussion

Food safety is always a concern for food manufacturers. To guarantee the safety of foods, the most used operations are pasteurization and sterilization by means of heat, and those processes imply heating, holding at a given temperature and eventually cooling for storage/packaging.

Flow modelling is being used as an analysis tool to ensure that food products meet the safety requirements of HACCP guidelines, e.g. aiding at the determination of the optimal lengths of the heating, holding and cooling sections in an industrial processing line. Using this tool it is possible to ensure proper microbial destruction while minimizing the thermal detrimental effects on food, thus contributing to obtain higher quality foodstuffs.

3.1. Rheological model of the strawberry pulp

The rheology of the strawberry pulp was experimentally determined at eigth different temperatures, ranging from 40 ºC to 90 ºC and experimental data was best-fitted to a Herschel-Bulkley model. These data are necessary for Fluent simulations. In Figure 5.10 and Figure 5.11 the experimentally determined rheological behavior of the strawberry pulp is shown and compared with the curves obtained from the best fitted parameters of the Herschel-Bulkley model. Analyzing these figures it is clear that the rheological behaviour of the strawberry pulp noticeably changes in the temperature range of 40 ºC to 60 ºC but the changes are not so evident when the temperature rises from 60 to 90 ºC. These differences are probably due to the destruction of the vegetable cells caused by the temperature increase until 60 ºC and also to the starch gelatinization occurring at 60 ºC (according to the starch manufacturer's technical specifications).

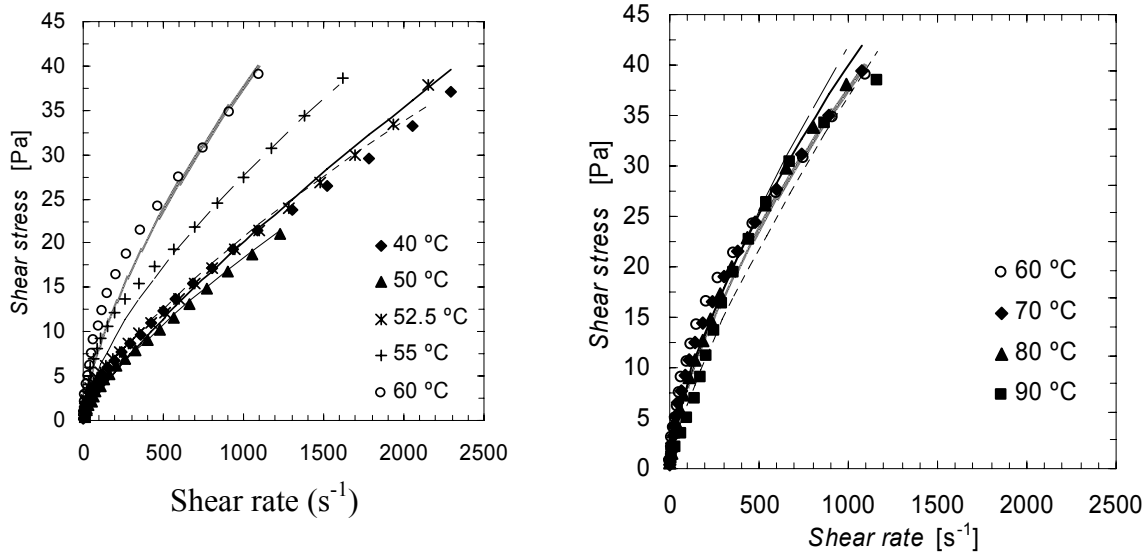

Figure 5.10: Comparison between the experimental values (data points) and the Herschel-Bulkley model fit (for shear rate values from 0.005 to 2500 s-1) for strawberry pulp in the temperature range under study.

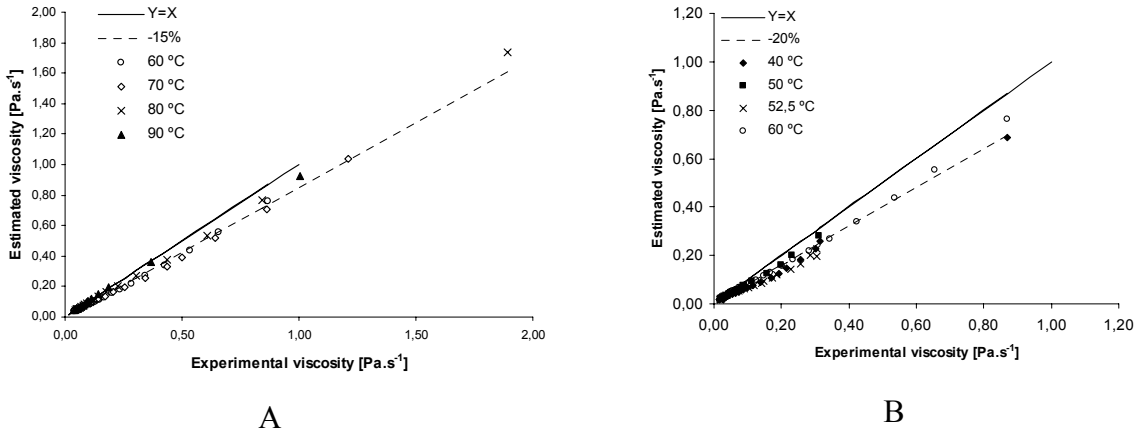

A B

Figure 5.11: Comparison of the experimental values of viscosity of strawberry pulp with those estimated using the Herschel-Bulkley model for the temperature ranges of a) 40 – 60 ºC and b) 60 - 90 ºC.

The observed differences in the rheological behavior of the pulp are reflected in the parameters of the model. displays the parameters of the Herschel-Bulkley model used for simulations of flow patterns at 40, 60 and 90 ºC.

Figure 5.11a clearly shows that the experimental values obtained below 60 ºC are deviated from those estimated by the model by a significant order of magnitude. This does not happen for temperatures above 60 ºC (Figure 5.11b). This is possibly explained by the

fact that the rheological model does not take into consideration the cell disruption which is important for temperatures below 60 ºC.

Table 5.3: Experimental parameters used to simulate flows pattern of strawberry pulp

Temperature	40 ºC	60 ºC	90 ºC
K [kg.s^{n-2}.m^{-1}]	0.08	0.42	0.20
n [-]	0.81	0.65	0.76
τ_0 [Pa]	1.48	5.19	9.42
μ_0 [Pa.s]	0.32	1.38	1.01

3.2. Independence of the mesh

Mesh influences the accuracy, convergence and speed of the solution. When testing mesh independence the objective is therefore to create meshes with different cell numbers, element types, amongst other parameters and, according to the associated energy that the mesh generates, to analyze which one is the most adequate option for continue working. One should consider not only the accuracy of the results but also the computational effort (and consequently time) to obtain a converged solution.

In this particular case, water having an inlet velocity of 0.0340m/s was the fluid chosen to perform the simulations using meshes having different number of cells. However the change of the cell number is not straightforward thus the number of cells was modified as summarized in Table 5.4.

Table 5.4: Different scenarios used to test mesh independence.

Scenario	Number of cells	Differences from the default mesh
Default mesh	29040	-
1	7260	Doubling the distance between cells in the x and y directions
2	16335	Doubling the distance between cells in the x and y directions and doubling the numbers of rows in the boundary layers
3	65340	Halving the distance between cells in the y direction

The simulation results confirmed that the default mesh guarantees the independence of the results and minimizes the computational time required for the simulations, thus the simulations were all made using this number and type of cells and geometry.

3.3. Hydrodynamic behavior of the ohmic heater

Simulations of steady-state flow patterns were performed for a Newtonian fluid (water) and a non-Newtonian fluid (an industrial strawberry pulp), at different flow rates and inlet temperatures. The main objective was to determine the effect of these two parameters (inlet mass flow rate and temperature) over the flow patterns within the continuous ohmic heater. Thus, six numerical simulations were initially run corresponding to two mass flow rates (0.5 and 2.0 kg/min) and three inlet temperatures (40, 60 and 90 ºC) (Figure 5.12).

Analysis of flow patterns within the ohmic heater lead to the conclusion that flow separation occurs within the ohmic heater when operating with water as main fluid, independently of the inlet mass flow rate (0.5 or 2.0 kg/min). Being so, when using Newtonian fluids with viscosity close to that of water the deviation from plug flow behavior is more pronounced. Crossing of fluid path lines means some extent of radial mixing which may be of interest in industrial processes. When operating with strawberry pulp under the same simulated conditions (0.5 and 2 kg/min) flow seems to approach a perfectly laminar behavior, with no flow separation or radial mixing.

The flow behavior within the ohmic heater may also be represented in terms of the - diagrams which result from simulations of RTD. In the *F*-diagrams the simulated results are compared with those obtained for both ideal PF and perfectly mixed (CSTR) behavior (Danckwerts, 1952) (Figure 5.13).

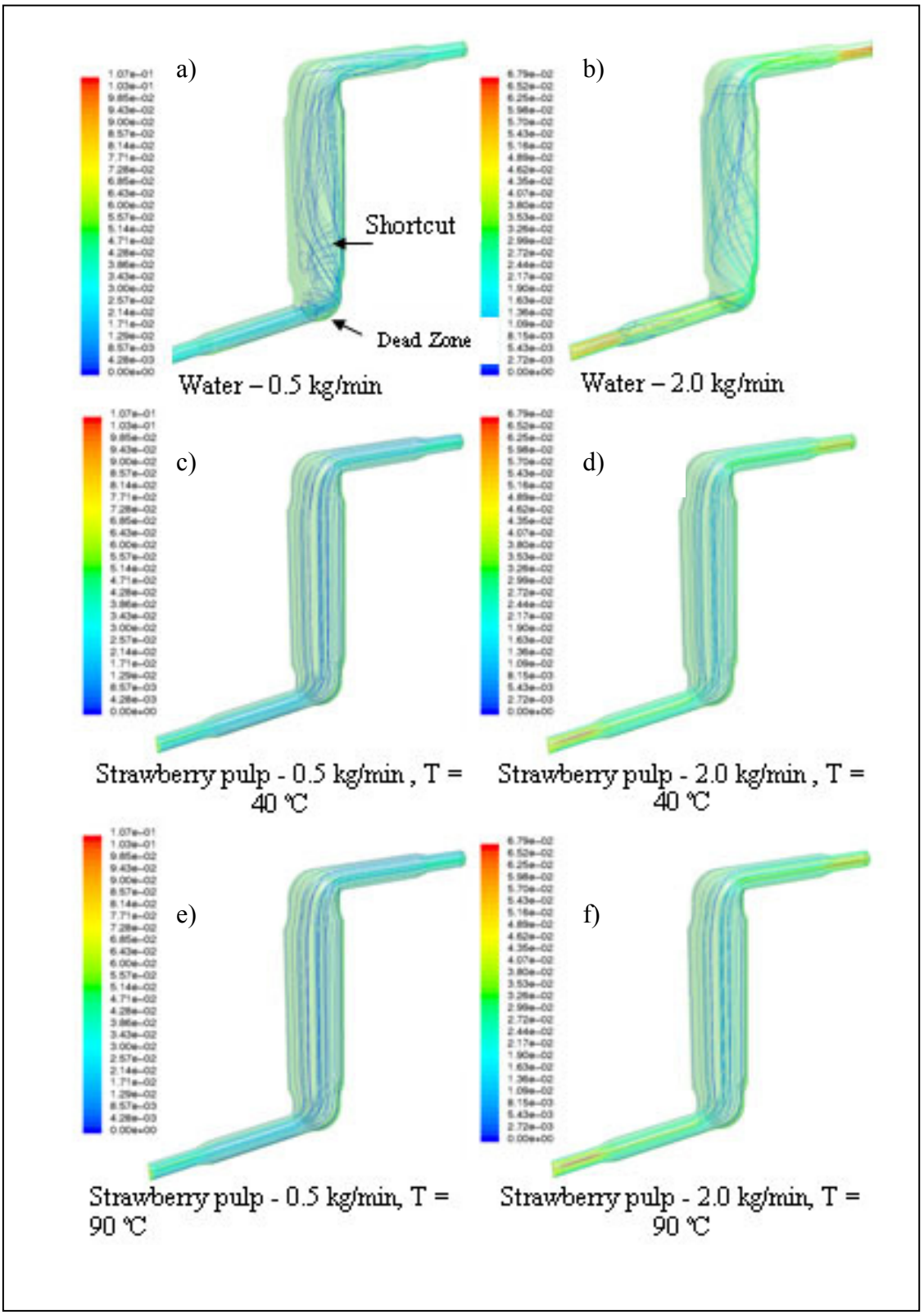

Figure 5.12: Simulated fluid path lines coloured by velocity magnitude (m/s) for: a) water at 0.5 kg/min and 20 ºC; b) water at 2.0 kg/min and 20 ºC; c) strawberry pulp at 0.5 kg/min and 40 ºC; d) strawberry pulp at 2.0 kg/min and 40 ºC; e) strawberry pulp at 0.5 kg/min and 90 ºC; f) strawberry pulp at 2.0 kg/min and 90 ºC.

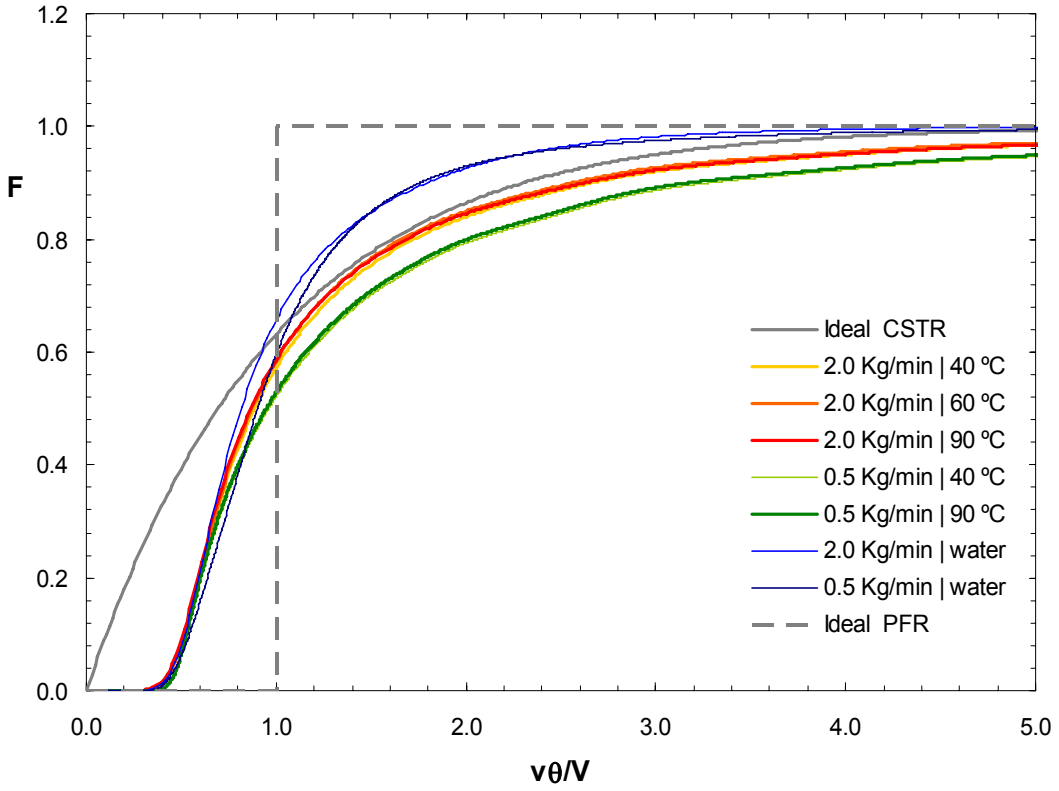

Figure 5.13: F diagrams for strawberry pulp and water, at several inflows and temperatures (v is the flow rate [$m^3.s^{-1}$], θ is the flow time [s] and V is the ohmic heater volume [m^3])

Table 5.5: Hold back (H) and segregation (S) calculations for several conditions tested with strawberry pulp and water

	Segregation (water)	Hold back			
Flow rate (Kg/min)	Water	Water	Temperature pulp (ºC)		
			40	60	90
0.5	0.204	0.205	0.185	0.188	0.193
2.0	0.164	0.167	0.162	-	0.170

Figure 5.13 and Table 5.5 clearly show the existing deviations of hydrodynamic behavior from plug flow. Such deviations can be measured by the hold-back (H) which varies from 0 (for plug-flow -PF) to 1 (when most of the reactor is occupied by dead zones). The value of H is equal to $1/e$ (0.368) for a CSTR (Danckwerts, 1952). The decrease of shortcuts is related to the decrease of H (Danckwerts, 1952) and the decrease of dead zones is related to the deviation from 1 of the values of F for $(v\theta/V) = 1$. The presence of shortcuts may risk food safety once parts of the food spend less time then required in the vessel and

consequently may be under-processed. In turn, dead zones affect food quality as their presence leads to overprocessed particles or volumes of fluid.

As previously determined (section 5.1), there is a clear influence of the temperature on the rheological behavior of the strawberry pulp. In the numerical simulations such influence was reflected in the variation of the parameters of the Herschel-Bulkley model adopted to describe the pulp rheology. However, by the analysis of Table 5.5 it was possible to observe that temperature (within the studied range) does not affect significantly the flow dynamic behavior of strawberry pulp within the ohmic heater when compared to the effect of inlet mass flow. This means that, for this fluid under the tested experimental conditions and for mentioned purpose, the viscosity dependence on temperature may be neglected when compared to the inlet velocity. In fact, differences in H values produced by the increase of pulp temperature from 40 to 90 ºC are below 5 % for both mass flow rates (Table 5.5).

Table 5.6 – Estimation of death zones for strawberry pulp and water at two different flow rates

	1-F (($v\theta/V$) = 1)			
Flow rate (Kg/min)	**Water**	**Temperature pulp (ºC)**		
		40	**60**	**90**
0.5	0.404	0.479	-	0.472
2.0	0.343	0.428	0.416	0.414

The strawberry pulp simulations show that increasing the flow rate from 0.5 to 2.0 kg/min (a four-fold increase) causes an average 13 % decrease in the deviation of F value from 1, meaning that operating at higher flow rates will minimize the existence of dead zones. Moreover, a 12 % reduction in H value (see Table 5.6) is observed for a similar increase in the flow rate, meaning that operating at higher flow rates will minimize the existence of shortcuts. However, when the operating fluid is water the hydrodynamic behavior is different. The same increase in the flow rates induces a 19 % diminution in the H value (less shortcuts), and a 15 % decrease in the deviation of F value from 1 (less dead zones).

Comparing the performance of the two fluids (water and strawberry pulp) it can be concluded that for the lower flow rate (0.5 kg/min) water (or other fluids with similar rheological characteristics) induces the formation of more shortcuts (10 % higher H value) then pulp. Therefore, pulp has a more favorable behavior for thermal processing in this

heater. However when the flow rate is higher (2 kg/min) the two fluids display a similar behavior (less than 3 % difference between *H* values).

A comparison between water and milk (also Newtonian fluid) was made in order to establish if, for newtonian fluids, a similar hydrodynamic behavior within this ohmic heater was to be expected (Figure 5.14)

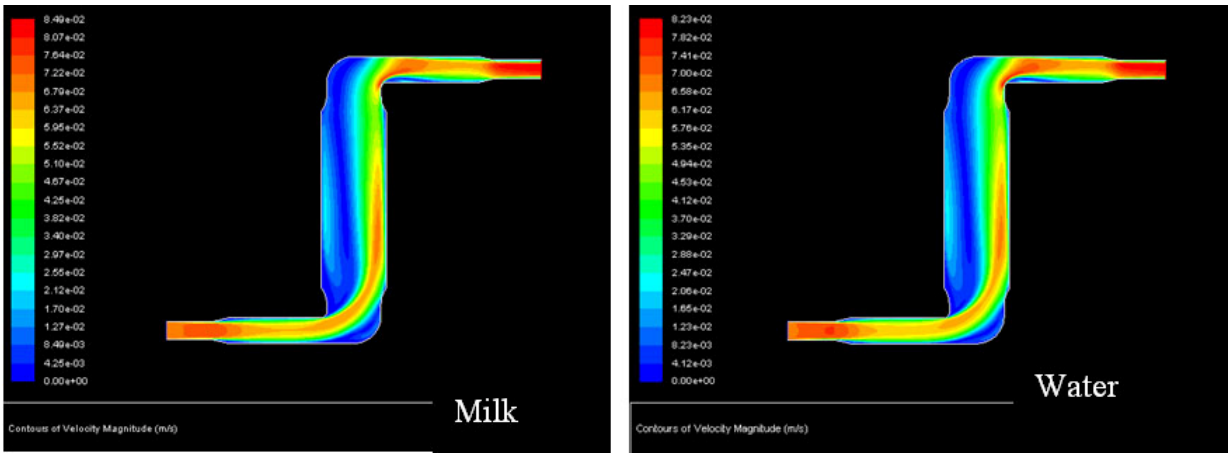

Figure 5.14: Velocity contours obtained after convergence using milk and water and an inlet velocity of 2 Kg /min

A similar behaviour was observed in the two fluids meaning that the results may be carefully extrapolated to other Newtonian fluids.

Efficiency of mixing can be expressed by a dimensionless parameter, *S* (segregation). It can be interpreted, in terms of the F-diagrams, as the departure from CSTR behavior. *S* may vary from -1 to 1/*e*, corresponding to a reactor completely occupied by dead zones or a PF, respectively. As previously discussed when water is the operational fluid, the path-lines show some degree of mixture, as represented by the helicoidal movement of some elements of the fluid (Figure 5.12). On the contrary, when operating with strawberry pulp there is no observable radial mixing, thus *S* was not calculated. The inexistence of mixing can be confirmed in *F*-diagrams (Figure 5.13), since none of the RTD curves for strawberry pulp intercepts the RTD curve for an ideal CSTR (Danckwerts, 1952).

The values of segregation have been calculated and clearly show that the reactor approaches a plug flow behavior (Table 5.5).

From the analysis performed to the flow patterns and also from the determined RTD of strawberry pulp in the ohmic heater it was concluded that no significant changes occur with the increase of temperature. This can be further observed in Figure 5.15, where it is clearly seen that the velocity profiles are coincident for all the temperatures tested.

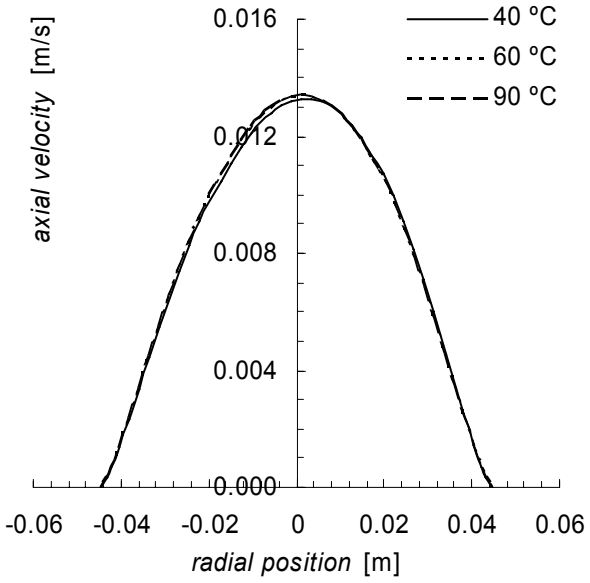

Figure 5.15: Simulated radial profile of axial velocity at y = 0.119 m and z = 0 m (over the symmetry axis, at the exit of the heating zone) for strawberry pulp flowing at 2.0 kg/min.

In the above analysis the whole volume of the reactor has been considered and no particular attention has been given to the flow patterns in the heating zone. Figure 5.15 indicates that the flow behavior of the strawberry pulp is laminar in that region. This is further demonstrated by the radial profile of the axial velocity at the outlet of the heating zone represented in Figure 5.16 a) for different flow rates.

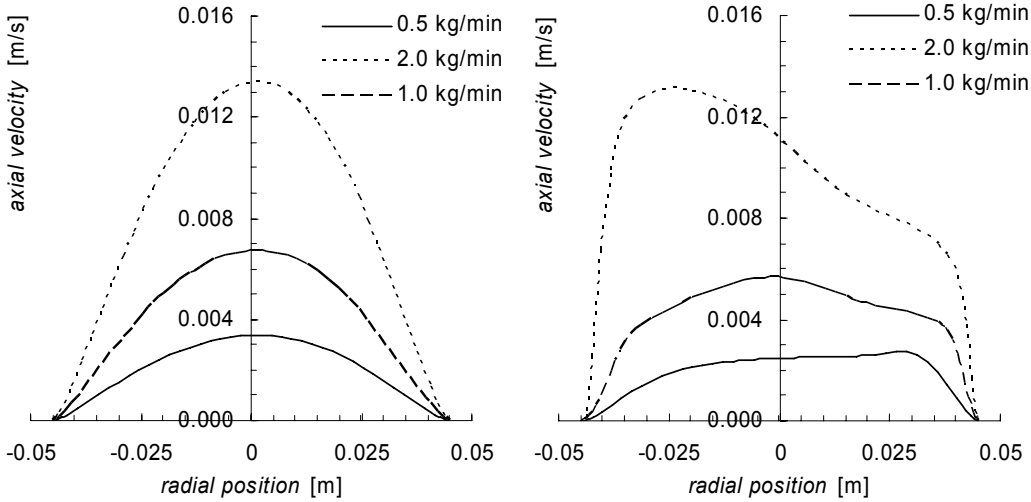

Figure 5.16: Simulated radial profiles of axial velocity at y = 0.119 m and z = 0 m (over the symmetry axis, at the exit of heating zone) at different inlet mass flow rates of: a) strawberry pulp at 90 ºC and b) water at 20 ºC.

In contrast, Figure 5.16 b) shows the radial profile of the axial velocity for water at the outlet of the heating zone, where the presence of turbulence can be clearly seen.

This information, especially that concerning strawberry pulp, will be crucially useful in the following section, where the outlet temperature is estimated as a function of the mass flow rate and of the applied voltage.

3.4. Experimental RTD determination and model validation

Experimental data obtained was analyzed and expressed in terms of *F*-diagrams. The results were compared with data from the CFD simulations (see previous sections) and ideal flow reactors (Figure 5.17).

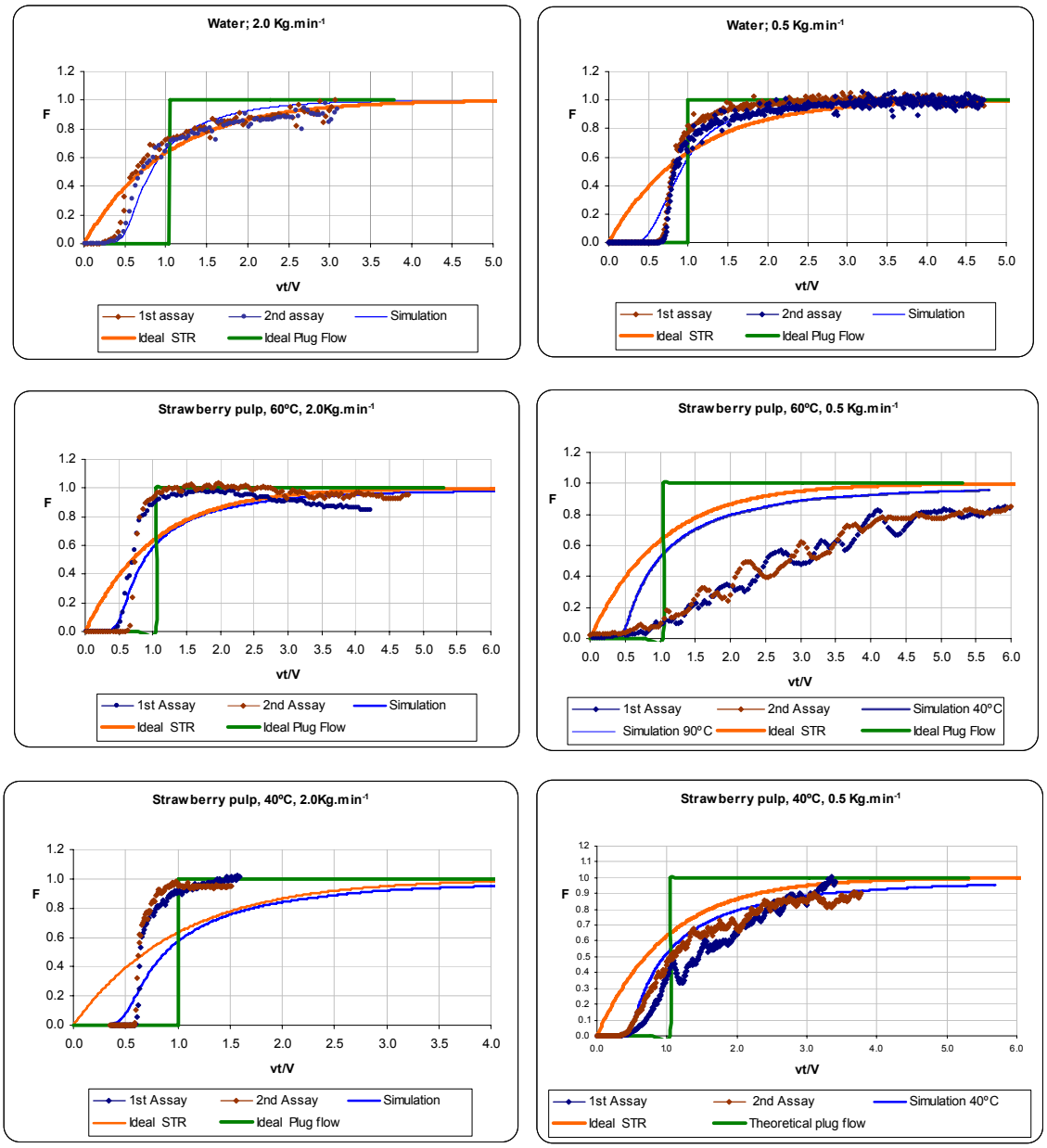

Figure 5.17: *F*-diagrams for the set of experiments performed

For the Newtonian fluid (water) the simulations made closely match the experimental data, for both flow rates. This means that the geometry of the reactor and the assumptions made in Fluent were correct, thus validating the conclusions made from the simulated results. It is clear that, when using water (and other Newtonian fluids such as milk), the reactor behavior approaches an ideal STR.

On the other hand, when operating with strawberry pulp major differences can be found between the simulated results and the ones obtained from the experimental data. This can probably due to several factors, namely: experimental difficulties when pumping the pulp and also slight differences between the pulps having different pH values (*e.g.* colour

changes were quite evident); variations between the lots of the pulp used in the several assays (including the ones used for determining the rheological model which was an input for Fluent) and a poor fit of the rheological model that was used in Fluent simulations. Variability between different lots is a known problem in the industry and the fact that industrial pulps have been used in this work is a very probable cause for many of the deviations found. Moreover, the pulp has several hydrocolloids such as pectin and starch, whose properties vary with pH and also with temperature thus affecting the rheological behavior of the pulp. In fact, according to the manufacturer specifications stach gelatinization occurs ar 58 ºC which may help to explain the profile obtained when operating at this temperature and at a low flow rate (Figure 5.17).

Despite of the deviations observed, it is possible to conclude from Figure 5.17 that when the operating fluid is the strawberry pulp the reactor behavior shifts from a plug flow at higher flow rates to a STR when using lower flow rates.

Summing up, the CFD simulations were a powerful and accurate tool to predict the behavior of this reactor and may be very useful to help optimizing the design of industrial ohmic heaters operating with fluids whose physical characteristics are known.

3.5. RTD simulations in the heating zone

Considering a potential industrial application for this ohmic heater, it is essential to assure that all fluid elements are heated up to a desired temperature (e.g. for strawberry pulp, a pasteurization temperature of 90 ºC). However, it must be stressed that, in ohmic heating, fluid heating only occurs in the zone between the electrodes. If a perfect plug flow is considered and knowing that heating by means of current dissipation only depends on the applied voltage and on the electrical conductivity of the fluid (Eq. 5.20), a linear correlation between fluid residence time in the heating zone and fluid final temperature can be determined. However, for a non-ideal flow with a given RTD (which is the case of the strawberry pulp flowing in the ohmic heater) a different approach is necessary.

The determination of the RTD exclusively in the heating zone allowed the prediction of the residence time of each pulp fraction (Figure 5.18).

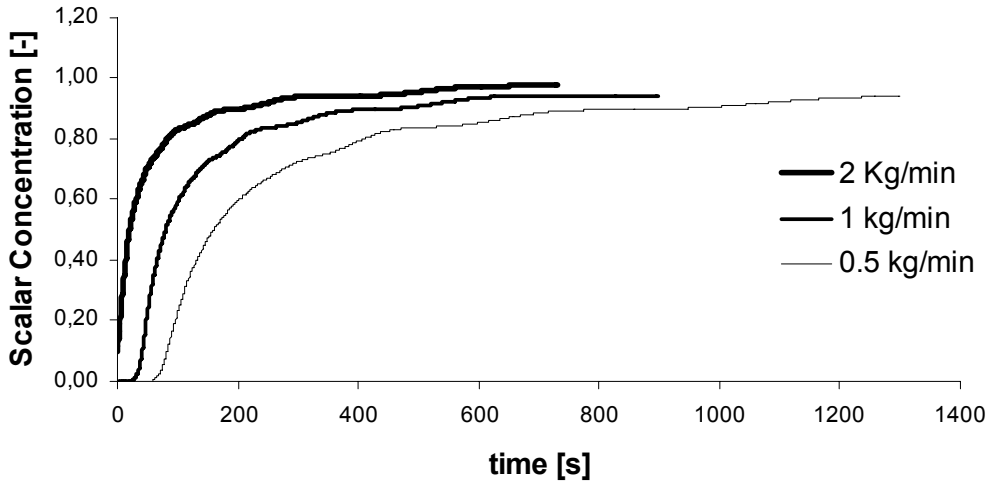

Figure 5.18: RTD in the heating zone for the different mass flow rates simulated.

Based on this information as well as on previously obtained data on electrical conductivity and its dependence on temperature ($\sigma = f(T)$) it was possible to estimate the temperature of the fluid at the end of the heating zone (T_f). In fact, the relation of σ with temperature (T) is usually well described by a straight line of the type:

$$\sigma = mT + b \qquad \textbf{(Eq. 5.20)}$$

where m is the temperature coefficient.

Further, heat generation ($\dot{Q}$) in foods is given by:

$$\dot{Q} = \left|\nabla V\right|^2 \cdot \sigma \qquad \textbf{(Eq. 5.21)}$$

Where $\left|\nabla V\right|$ is the applied voltage.

Replacing σ by equation 5.20, the following equation is obtained:

$$\dot{Q} = \left|\nabla V\right|^2 \cdot (mT + b) \qquad \textbf{(Eq. 5.22)}$$

Knowing that $\dot{Q} = cp\dfrac{dT}{d\tau}$ for a constant pressure process, where cp is the specific heat of the fluid, it is possible to write:

$$cp\frac{dT}{d\tau} = \left|\nabla V\right|^2 \cdot (mT + b) \qquad \textbf{(Eq. 5.23)}$$

Integrating and rearranging:

$$T_f = \frac{(mT_i + b)\exp\left(\frac{m\left|\Delta V\right|^2}{cp}\,\tau\right) - b}{m} \qquad \textbf{(Eq. 5.24)}$$

where T_i is the temperature before heating and T_f is the final temperature, after heating.

Using Eq. 6 and the RTD in the heating zone obtained for each flow rate, and setting operating voltage as a variable, it was possible to obtain the simulated final temperature of a fluid element (T_f). The electrical conductivity as a function of temperature (Eq. 5.20) was previously determined by Castro *et al* (2003). Being so, it is possible, for each electric field, to calculate the time needed to achive 90 ºC (Figure 5.19).

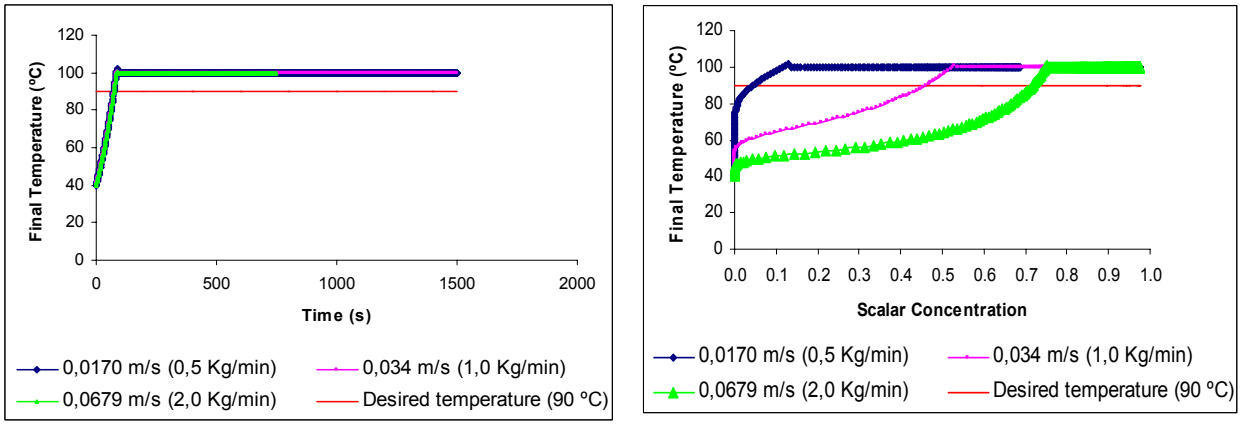

a) **b)**

Figure 5.19: Time to reach 90ºC when using strawberry pulp at different flow rates and operating voltage of 80 V (a); fraction of strawberry pulp that has left the heating zone before achieving 90 ºC (b)

The industrial pasteurization of this pulp occurs at 90 ºC, temperature at which the holding phase takes place. A fluid element was considered under-processed when its temperature (T_f) was lower than 90 ºC. Based on the RTD results, the percentage of under-processed fluid elements at 3 different flow rates and several applied voltages was determined. The results are summarized in Figure 5.20

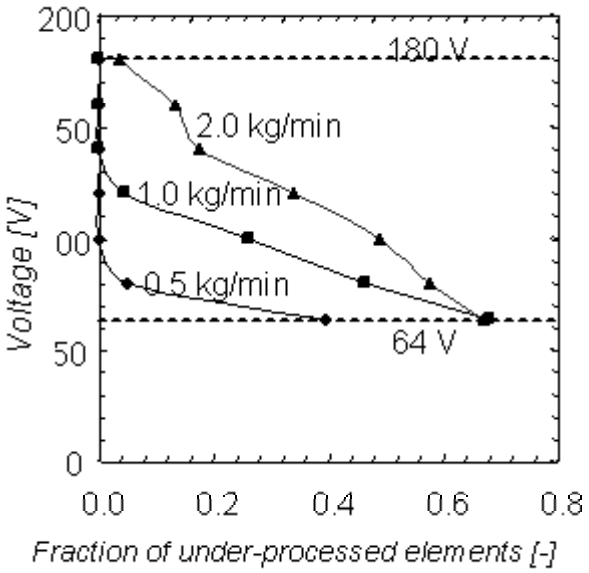

Figure 5.20: Fraction of under-processed elements of pulp as a function of the voltage applied to the electrodes, for different inlet mass flow rates

Figure 5.20 is the basis for the optimization of the operation conditions for the ohmic pasteurization of strawberry pulp. It should be pointed out that this optimization procedure must be performed individually for each product that is intended to be processed once flow patterns and heating rates are fully dependent on the rheological properties and its physical-chemical properties (Castro *et al.*, 2003).

As an example, if a criterion for accepting the product is fixed at 1 % of under-processed fluid elements (T_f < 90 ºC) at the end of the heating zone, in order to guarantee product safety, it can be concluded from Figure 5.20 that the minimal operation voltage that assures safety is 100 V for a mass flow rate of 0.5 kg/min, or 140 V, if a mass flow rate of 1.0 kg/min is used instead. Figure 5.20 also clearly shows that, when working with a mass flow rate of 2.0 kg/min it is not possible to assure food safety for this ohmic heater using voltages lower than 180 V. It is noteworthy that this criteria for under processed fluid elements should be determined considering the holding phase time in order that the fluid element could reach the desired temperature (90 ºC) thus not jeopardizing food safety.

Generically, operating at lower voltages reduces energy costs as well as over-processed volumes; at higher voltages the heating rate is usually higher (related to $\sigma = f(T)$,) thus leading to over-processing and consequently to an increased loss of organoleptic and nutritional properties.

4. Conclusions

Even though the ohmic heating process eliminates most of the conventional thermal gradients formed during heating, thus increasing the final product quality, the hydrodynamic behaviour of the heater could minimize this advantage. The increase of dead zones and shortcuts when using Newtonian fluids (such as water) may diminish significantly the productivity of this ohmic heater for continuous sterilization of food products. In fact, the existence of a distribution of the residence times of the fluid means that either the faster fraction will not be properly sterilized or the slowest will be over-processed. Thus the optimization of the heater should consider its hydrodynamic characteristics.

The CFD simulations of the hydrodynamic behavior were validated by experimental data with a fairly good match between the results for Newtonian fluids.

The use of this continuous ohmic heater to efficiently process strawberry pulps is possible if using voltages higher than 100 V and flow rates lower than 2.0 kg/min; otherwise there will be an unacceptable fraction of under-processed particles. To operate at higher flow rates (which are better from a hydrodynamic point of view) it will be necessary either to increase the electrical conductivity of the strawberry pulp (which can be achieved through the addition of salts or other ionic constituents - Castro *et al.*, 2003) or the voltage applied on of the heater. A highly conductive fluid will have higher heating rates and will need to spend less time in the heater to achieve the desired pasteurization temperature.

The main contributions of this section were the establishment of an equation which allows the prediction of the outlet temperature of the fluid subjected to a continuous ohmic heating process together with the corresponding methodology to obtain the correct parameters of that equation.

5. References

Boyer, C., Duquenne, A. M., Wild, G., (2002). Measuring techniques in gas-liquid and gas-liquid-solid reactors. Chemical Engineering Science 57(16):3185-3215.

Briens, C. L., Margaritis, A., Wild, G. (1995). A New Stochastic-Model and Measurement Errors in Residence Time Distributions of Multiphase Reactors. Chemical Engineering Science 50(2):279-287.

Castro, I., Teixeira, J. A., Vicente, A. A., (2003). The influence of field strength, sugar and solid content on electrical conductivity of strawberry products; Journal of Food Process Engineering 26, 17-29.

Castro, I., Teixeira, Vicente, A. A., (2006). Ohmic heating in food processing, In Thermal Food Processing:

Danckwerts, P. V., (1953). Continuous Flow Systems - Distribution of Residence Times. Chemical Engineering Science 2(1):1-13.

Gut, J. A. W., Pinto, J. M. Gabas, A. L., Telis-Romero, J., (2005). Continuous Pasteurization of Egg Yolk: Thermophysical Properties and Process Simulation, Journal of Food Process Engineering, 28(2), p.181-203.

Holdsworth, S. D. (1993). Rheological models used for the prediction of the flow properties of food products: a literature review. Transactions of the Institution of Chemical Engineers, Part C, 71, 139–179.

Krokida, M. K.; Karathanos, V. T.; Maroulis, Z. B.; Marinos-Kouris, D., (2000). Effect of osmotic dehydration on color and sorption characteristics of apple and banana. Drying Technology, New York, v. 18, p. 937-950.

Levenspiel, O., (1972). Chemical reaction engineering. New York: John Wiley & Sons, Inc.

Modeling, Quality Assurance and Innovations, CRC Press, a Taylor & Francis Company.

Nauman, E., Buffham, B., (1983). Dispersion, diffusion and open systems, in Mixing Continuous Flow Systems. Toronto: Wiley.

Ni, X. W., de Gelicourt, Y. S., Neil, J., Howes, T. (2002). On the effect of tracer density on axial dispersion in a batch oscillatory baffled column. Chemical Engineering Journal 85(1):17-25.

Ranade, V. V., (2002). Computational flow modeling for chemical reactor engineering: Academic Press, c2002. 452 p. p.

Wen, C. F., Fan, L. T., (1975). Models for flow systems and chemical reactors. New York: Marcel Dekker.

Westerterp, K. R., van Swaaij, W. P. M., Beenackers, A. A. C. M., (1963). Chemical Reactor Design and Operation. New York: John Wiley & Sons.